Diverse Roles of Protein S-acyl Transferases in Arabidopsis thaliana

Li, Yaxiao

Award date:
2017

Awarding institution:
University of Bath

Diverse Roles of Protein S-acyl Transferases in *Arabidopsis thaliana*

Yaxiao Li

A thesis submitted for the degree of Doctor of Philosophy

University of Bath

Department of Biology and Biochemistry

December 2016

Acknowledgement

My deep gratitude first goes to my supervisor Dr. Baoxiu Qi for her constant guidance and patience in my work, and caring in my life. I would like to thank my supervisors Prof. Rod Scott and Dr. James Doughty for all their suggestions to my project and endless encouragement. Without all their help, I won't have this opportunity to carry out my PhD project at University of Bath, where I have met and worked with so many excellent scientists from all over the world.

I also want to express my appreciation to Prof. Murray Grant (University of Warwick, UK) and Dr. Ondřej Novák (Palacký University and Institute of Experimental Botany ASCR, Czech Republic) for their technological support to measure phytohormone content, and also to Prof. Chris Hawes (Oxford Brookes University) and Ms. Ursula Potter (University of Bath) for their assistance on microscopy observation. Thanks Prof. Weicai Yang and Dr. Hongju Li (Institute of Genetics and Developmental Biology, CAS) for their guidance about gametogenesis in chapter 6. Thanks also goes to Dr. Taijoon Chung (Pusan National University, Korea) for sharing *atg9-2* mutant and the ProUBQ10-GFP-ATG8a construct and Dr. Piers Hemsley (University of Dundee, UK) for providing me with the pESC-AKRC-S construct.

Special thanks to all members who work in plant group in Biology and Biochemistry department at University of Bath. Your friendship makes me feel at ease and helps me to settle in the new work environment very quickly. And I also want to thank Society for Experimental Biology (SEB) and Biochemistry Society for funding the confernces. And of course, thanks Natural Science Foundation of China (NSFC) and University of Bath for funding this project

My most sincere appreciation goes to my family who gave me selfless love and encouragement. Thank my parents for all their help and support spiritually and financially, and my sister who is always so considerate. In the end but not least, I also want to thank my partner for always giving me energy when I feel depressed.

Abbreviations

ABA	abscisic acid
ABE	acyl-biotinyl exchange
Acyl-RAC	acyl- resin assisted capture
CK	cytokinin
DAP	day(s) after pollination
ER	endoplasmic reticulum
GA	gibberellic acid (gibberellin)
GUS	β-Glucuronidase
JA	jasmonic acid
LD	long day with 16h-light/8h-dark
MS	Murashige and Skoog
PAT	Protein S-acyl transferase
PLP	PAT-like Protein
PM	plasma membrane
SA	salicylic acid
SAM	shoot apical meristem
SEM	scanning electronic microscopy
SUC	sucrose
TAG	triacylglycerol
TMD	transmembrane domain
WT	wild type

Abstract

S-acylation, commonly known as S-palmitoylation, is a reversible posttranslational lipid modification in which fatty acid, usually palmitic acid, covalently attaches to specific cysteine residues of proteins via thioester bonds. Palmitoylation enhances the hydrophobicity of proteins and contributes to their membrane association. It plays roles in protein trafficking, signalling, protein-protein interaction, protein stability and other important cellular functions. A family of Protein S-acyl Transferases (PATs) is responsible for this reaction. PATs are multi-pass transmembrane proteins that possess a catalytic Asp-His-His-Cys cysteine rich domain (DHHC-CRD) of ~50 amino acids. In Arabidopsis there are at least 24 such DHHC-CRD containing PAT proteins and they are named as AtPAT01 to AtPAT24. The function of only 2 AtPATs, AtPAT10 and AtPAT24 were studied in some detail, and a recent survey showed the ubiquitous expression pattern and different membrane localization habit of all 24 AtPATs. However, the biological function of the remaining 22 AtPATs in Arabidopsis was not reported when I started my project. Therefore, we carried out an initial screen of all the available T-DNA insertion lines of the 22 Arabidopsis PATs and identified transcriptional null mutants of 18 of the AtPATs. Among them, the k/o mutant plants of only 3 genes showed significantly altered phenotypes compared to wild-type Arabidopsis, and the mutants are named as *atpat14*, *atpat21 and plp1(PAT-like Protein 1)*. This project aims to characterize these three putative PATs in details in terms of their PAT activities, catalytic domains, expression patterns, subcellular localizations and biological functions.

AtPAT14 was proved as a PAT by yeast complementary and *in vitro* auto-acylation assays. Mutagenesis studies clearly demonstrated that the cysteine residue in the DHHC motif is essential for the enzyme activity of AtPAT14. Transgenic Arabidopsis plants expressing AtPAT14-GFP were observed and it was shown that AtPAT14 is predominantly localized at the Trans-Golgi. The phenotype was observed in both *atpat14-1* and *atpat14-2* mutant lines and this showed that the leaves of both lines were aging much faster than the WT. Analysis of the levels of different phytohormones revealed that the mutant leaves contained much higher salicylic acid (SA) than the WT. This coincided with the increased transcript levels of genes involved in SA biosynthesis and signalling.

Therefore, AtPAT14 mediated protein S-acylation plays important roles in leaf senescence via the regulation of SA biosynthesis and signalling pathways.

AtPAT21 was also confirmed as a PAT and the DHHC its functional domain by similar approaches as for AtPAT14. The plasma membrane (PM) localized AtPAT21 plays essential roles in both male and female gametogenesis. As such, loss-of-function by T-DNA insertion in AtPAT21 leads to the plant being completely sterile. Therefore, AtPAT21-mediated S-acylation of proteins(s) plays important roles in the reproduction of Arabidopsis.

AtPLP1 (PAT-like Protein 1) contains the signature DHHC-CRD. However, it does not rescue the growth defects of *akr1*, *pfa3* and *swf1*, the 3 yeast PAT mutants used in enzyme activity assays of other known PATs from plant and animals. Further, the cysteine residue in the DHHC motif was not essential for the function of AtPLP1 as mutated variant containing serine in place of cysteine of the DHHC motif can still rescue the growth defects of *atplp1-1*. Seedling establishment of *atplp1-1* was impaired without external carbon source. This is because the efficiency in converting the seed storage lipid to sugar in the mutant is much lower than WT due to the defective β-oxidation process involved in the degradation of free fatty acids released from lipid during post-germinative growth. In addition, *atplp1-1* seedlings are also de-etiolated in the dark, and this was coincided with more cytokinin (CK) and less active gibberellin (GA) related pathway in the mutant. Other defects were also found in *atplp1-1*, such as hypersensitive to abscisic acid (ABA) and sugar during seed germination and abnormal shoot apical meristem (SAM) in older plants.

Therefore, protein S-acyltransferases play distinct and diverse roles throughout the life cycle, from seed germination, seedling growth to seed production in Arabidopsis. This is most likely through the palmitoylation of an array of proteins they modify. Hence, our results provide vital clues for future studies on the molecular mechanism as to how AtPATs operate in plant.

Table of Contents

Chapter 1 Introduction

Lipid modification is a common mechanism in organisms, in which a fatty acid was attached to specific amino acid residues, leading to increased hydrophobicity of proteins to help them anchor to membranes or specific lipid rafts (Levental et al., 2010). The three most commonly known lipid modifications are N-myristoylation, prenylation and S-acylation (Fig. 1-1). N-myristoylation is an irreversible, co-translational protein modification in which 14-carbon myristoyl group is covalently attached to N-terminal glycine residue via an amide bond. Prenylation is a post-translational lipid modification which involves the transfer of either a 15-carbon farnesyl or a 20-carbon geranyl-geranyl moiety to CaaX C-terminal cysteine of the target protein. The thioether linkages in prenylation are catalyzed by three types of enzymes, farnesyl transferase (PFT), geranylgeranyl transferase-I (PGGT-I) and Rab GTPase specific Rab geranylgeranyl transferase (Rab-GGT) (Casey and Seabra, 1996; Hemsley, 2009, 2015). S-acylation, more commonly known as S-palmitoylation, is a post-translational lipid modification in which saturated fatty acid, usually the 16-carbon palmitate, covalently attaches to the specific cysteine residue(s) throughout the protein via a thioester bond (Resh, 2006; Greaves and Chamberlain, 2011). Some other lipid modifications, such as Glycosylphosphatidylinositol (GPI) and glycosylinositolphosphorylceramide (GIPC) anchors can link the whole glycolipids to the protein instead of the simple fatty acid or polyisoprene group (Hemsley, 2015). GPI and GIPC anchors modify the proteins at the lumen side instead of the cytoplasm as the three lipid modifications do (Ganesan and Levental, 2015). There are also some lipid modifications which are only found in specific proteins, such as palmitate addition through an amide linkage at the N-terminal cysteine and cholesterol addition at the C-terminal glycine of proteins (Buglino and Resh, 2012). All these lipid modifications are widely present in eukaryotes, and they play important roles during growth and development.

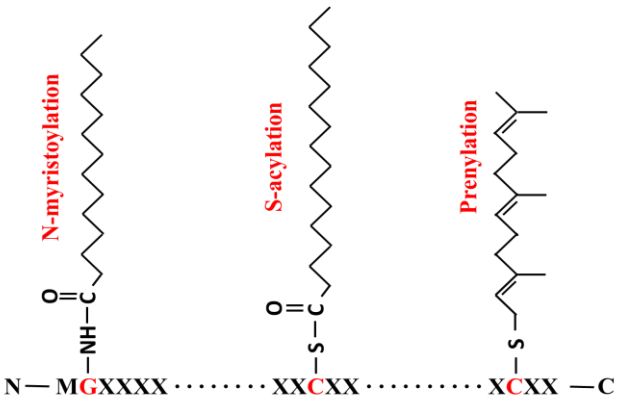

Figure 1-1. Formulae of N-myristoylation, S-acylation and prenylation.
For N- myristoylation, a 14-carbon myristoyl group was attached to glycine through amide bond; S-acylation is the attachment of 16-carbon palmitate to cysteine residue via thioester bond; and Prenylation makes a 15-carbon farnesyl link to the C-terminal cysteine residue.

1.1 S-acylation

There are two types of protein palmitoylation found so far, one is the S-palmitoylation in which the palmitate is attached via thioester bond as shown in Fig. 1-1 and another called N-palmitoylation is a stable lipid modification at the N-terminal cysteine through amide linkage. A small group of secreted proteins have been identified as N-palmitoylated proteins, including the epidermal growth factor (EGF) like ligand 'Spitz' and members of the Wnt/wingless family in Drosophila, Hedgehog family members in Drosophila and mammals (Miura et al., 2006; Resh, 2006; Kurayoshi et al., 2007; Greaves and Chamberlain, 2011; Buglino and Resh, 2012).

In S-palmitoylation (palmitoylation for short) palmitate is the most common acyl group found to attach to the cysteine residue, hence the term of palmitoylation. However, other acyl groups, such as stearate or oleate are also accepted in this lipid modification, therefore, S-acylation is a more representative term than palmitoylation (Jones et al., 1997; Sorek et al., 2007; Hurst and Hemsley, 2015). In contrast to other lipid modification such as myristoylation, prenylation or N-palmitoylation, S-acylation is a unique posttranslational modification that is usually reversible (Fukata and Fukata, 2010). It is

important for cellular protein sorting, vesicle trafficking, activation state control, protein stability, microdomain partitioning of protein and protein complex assembly (Baekkeskov and Kanaani, 2009; Greaves and Chamberlain, 2007; Charollais and Van Der Goot, 2009; Hemsley, 2009; Hemsley et al., 2013). Although all lipid modifications can facilitate the attachment of proteins to membranes, modification with palmitoyl groups provide more affinity, about 10 times stronger than myristoyl groups and 100 times than farnesyl groups (Silvius and l'Heureux, 1994).

S-acylation can occur in both soluble and transmembrane proteins (Roth et al., 2006; Blaskovic et al., 2013). S-acylation of soluble proteins allows their association with membranes, trafficking, regulation and signalling (Roth et al., 2006; Blaskovic et al., 2013). For example, a de/re-acylation of H- and N- Ras drive their subcellular localization from plasma membrane (PM) to Golgi which initiates RAS activation (Rocks et al., 2005). S-acylation of transmembrane proteins plays multiple roles in altering signalling capacity (Merrick et al., 2011), reducing activity (Huang et al., 2010), trafficking modification (Abrami et al., 2008; Flannery et al., 2010) and changing stability (Abrami et al., 2006; Maeda et al., 2010; Blaskovic et al., 2013) although the direct mechanism is not very clear. It is thought that S-acylation of transmembrane proteins, such as death receptor 4 (Oh et al., 2012), β-secretase BACE1 (Motoki et al., 2012), cannabinoid receptor (Oddi et al., 2012) and influenza virus M2 protein (Thaa et al., 2011), can promote their association with lipid rafts. However, for transferrin receptor both of its palmitoylated sites are localized to non-raft domains (Charollais and Van Der Goot, 2009), and for tumor endothelial marker 8 (TEM8) palmitoylation was actually found to negatively regulate its raft association (Abrami et al., 2006). Therefore, it seems that the roles of palmitoylation of transmembrane proteins are more complex than that of soluble proteins.

1.1.1 S-acylation in yeast

A proteomic method using the acyl-biotinyl exchange (ABE) chemistry combining with the traditional [^{3}H] palmitate *in vivo* labeling protocol identified about 50 S-acylated proteins in *Saccharomyces cerevisiae* (Roth et al., 2006), which demonstrated proteins

that span a wide range of cellular functions are S-acylated in yeast. These include many SNAREs (soluble N-ethylmaleimide-sensitive fusion protein-attachmentprotein receptor) that are involved in vesicle fusion. The redundant SNAREs, such as plasma membrane localized synaptobrevin homologs Snc1 and Snc2, were the first identified S-acylated proteins in 1995 (Couve et al., 1995). This was subsequently confirmed independently by other research groups (Valdez-Taubas and Pelham, 2005; Roth et al., 2006). Another commonly known S-acylated SNARE is Ykt6, which is different from other single transmembrane domain (TMD) SNAREs, requires both C-terminal prenylation and palmitoylation to target to the membrane (Fukasawa et al., 2004). Interestingly, Tlg1 lacking S-acylation undergoes ubiquitination, implying S-acylation can protect proteins from degradation (Valdez-Taubas and Pelham, 2005). Other SNAREs that have been confirmed to be S-acylated are Sso1, Sso2, Vam3, Tlg2 and Syn8 (Valdez-Taubas and Pelham, 2005; Roth et al., 2006).

S-acylation is also very common in many important signalling proteins, such as the heterotrimeric G protein subunits Gpa1 (Song and Dohlman, 1996; Song et al., 1996), Gpa2 (Harashima and Heitman, 2005) and Ste18 (Gγ, Hirschman and Jenness, 1999); small monomeric G proteins (GTPases) such as Rho1, Rho2 (Roth et al., 2006) and Rho3 (Zhang et al., 2013), Ras1 and Ras2 (Deschenes et al., 1990; Mitchell et al., 1994; Bartels et al., 1999). A recent study shows that the pathogenesis, morphogenesis and sexual differentiation of an encapsulated yeast *Cryptococcus neoformans* is achieved through the important roles S-acylation plays in modulating the localization of Ras1 (Nichols et al., 2015). Interestingly, all of these proteins require prenylation or myristoylation before S-acylation occurs (Roth et al., 2006).

In addition, many amino acid permeases (AAP) were proved to be S-acylated (Roth et al., 2006). The yeast type I casein kinases, Yck1, Yck2, and Yck3, which play important roles in cellular morphology, bud emergence and mating pheromone receptor endocytosis, are membrane localized via S-acylation for function (Roth et al., 2006; Roth et al., 2011). ENV7 (late endosome and vacuole interface) encodes a protein kinase and play important

roles in vacuole morphology, and S-acylation of its N-terminal triple cysteine motif ($C^{13}C^{14}C^{15}$) is required for proper localization and function of Env7 (Cocca, 2014). S-acylation of telomere-binding protein Rif1 enhances the formation of budding-yeast heterochromatin (Park et al., 2011). Mutagenesis of cysteine in different positions of arsenite permease Acr3p can cause its completely or partially functional defects as a low affinity As(III)/H^+ and Sb(III)/H^+ antiporter, and Cys90 which localizes in the cytosolic loop but in close proximity to transmembrane regions has the high possibility to be S-acylated (Maciaszczyk-Dziubinska et al., 2013). Chitin synthase 3 (Chs3) plays important roles in chitin synthesis which is regarded as an excellent target for pharmaceutical and agricultural pathogen management (Cohen, 1993; Gaughran et al., 1994). It was found that S-acylation status of Chs3 is necessary for its export from the ER (Lam et al., 2006). Table 1-1 lists the main S-acylated proteins that were confirmed in yeast.

Table 1-1. Commonly known S-acylated proteins in yeast

Groups	Specific proteins	References
SNAREs	Snc1/2, Ykt6,Tlg1/2, Sso1/2,Vam3, Syn8	Couve et al., 1995; Valdez-Taubas and Pelham, 2005; Roth et al., 2006; Fukasawa et al., 2004
G proteins	Gpa1/2, Ste18, Rho1/2/3, Ras1/2	Song and Dohlman, 1996; Song et al., 1996; Hirschman and Jenness, 1999; Harashima and Heitman, 2005; Roth et al., 2006; Zhang et al., 2013; Deschenes et al., 1990; Bartels et al., 1999; Mitchell et al., 2012; Nichols et al., 2015
AAPs	Tat1/2, Gnp1, Sam3, Hip1, Bap2, Agp1, Gap1	Roth et al., 2006
Protein kinases	Yck1/2/3, Env7	Roth et al., 2006; Roth et al., 2011; Cocca, 2014
Other proteins	Rif1, Acr3p, Chs3	Park et al., 2011; Maciaszczyk-Dziubinska et al., 2013; Lam et al., 2006

1.1.2 S-acylation in mammals

S-acylation is also a common lipid modification of many proteins in mammalian cells. Followed by the study of S-acylation in yeast research has extended to the mammalian system and considerable knowledge has been gained in recent years, revealing the involvement of protein S-acylation in the regulation of disease status, growth and development. For example, using the ABE method about 300 S-acylated proteins were identified from a global rat neural palmitoyl-proteome (Kang et al., 2008). Similarly, 331 S-acylated proteins were found in human prostate cancer cells (Yang et al., 2010), 57 from human B lymphoid cells (Ivaldi et al., 2012) and 150 from endothelial cells (Marin et al., 2012). By bio-orthogonal labeling of S-acylated proteins with 17-octadecynoic acid (ODYA) about 125 and over 400 S-acylated proteins were identified from human Jurkat T-cells and mouse T-cell hybridoma cells, respectively (Martin and Cravatt, 2009; Martin et al., 2012).

It is noteworthy that proteins that have been proved to be S-acylated in yeast, their homologous proteins in mammals tend to be also S-acylated. For instance, many human SNAREs were also S-acylated (Greaves et al., 2010), S-acylation of α subunits of G proteins is necessary for their membrane localization and function (Wedegaertner et al., 1993; Grassie et al., 1994; Ponimaskin et al., 1998; Ponimaskin et al., 2000; Kleuss and Krause, 2003). Many G-protein-coupled receptors (GPCRs) (Blaskovic et al., 2013), small rat sarcoma (Ras) GTPase (Rocks et al., 2005) and phospholipid scramblase 3 (Merrick et al., 2011) are also S-acylated. However, G-protein γ subunits were not S-acylated in mammals. Some S-acylated proteins in mammals can also make themselves avoid to be degraded. For instance, LRP6 (lipoprotein-receptor-related protein 6) is S-acylated and the removal of acyl group leads to destabilization or ubiquitination (Abrami et al., 2008). Similarly, the palmitoylation of TEM8 (Abrami et al., 2006), CCR5 (chemokine and HIV receptor) (Percherancier et al., 2001) and Rhodopsis (Maeda et al., 2010) prevents the degradation of these proteins. S-acylation can also play opposite role for some proteins. For example, a cancer-promoting protein CDCP1 (CUB domain-

containing protein 1) is degraded upon S-acylation, leading to a decrease of ovarian cancer cell migration (Adams et al., 2015).

Many signalling proteins involved in keeping T-cell homeostasis are S-acylated, such as T-cell co-receptors CD4 and CD8, tyrosine kinases Lck and Fyn, and adaptor proteins LAT (linker for activation of T cells) and Cbp/PAG (Bijlmakers, 2009; Hundt et al., 2009; Akimzhanov and Boehning, 2015). S-acylation of Lck is essential for propagating T-cell receptor signaling and releasing apoptotic calcium. Lck is S-acylated at both Cys3 and Cys5, and the S-acylations of these two cysteines are redundant for the function of Lck (Akimzhanov and Boehning, 2015). Same as Lck, LAT is also a dual (Cys26 and Cys29) S-acylated protein which is required for T cell development and activation. S-acylation of Cys26 alone is enough for LAT to target lipid rafts, but not Cys29 (Hundt et al., 2009).

The importance of S-acylation of synaptic proteins is well recognized for synaptic plasticity. The key S-acylated synaptic proteins include postsynaptic density protein PSD-95, δ-catenin, gephyrin, A-kinase anchoring protein AKAP79 and 150, the small GTPase Cdc42. Lack of S-acylation impairs the performance on learning and memory tasks (Brigidi et al., 2015). Huntington's disease is a neurodegenerative disorder caused by defects of the huntingtin (HTT) gene, and the function of HTT relies on its S-acylation (Butland et al., 2014). Defects of S-acylation can also cause mental problems such as schizophrenia and X-linked mental retardation (XLMR) although the specific S-acylated target proteins have not been identified (Mukai et al., 2004; Raymond et al., 2007). Alzheimer's disease (AD) is a type of neurodegenerative dementia which accounts for 60% to 70% of all cases of dementia. Many studies have demonstrated that S-acylation plays very important roles in the pathogenesis of AD, and the related S-acylated proteins include β- and γ-secretases, such as the major APP (amyloid precursor protein) cleaving enzyme BACE1 which are S-acylated at four sites (Benjannet et al 2001; Hornemann, 2015).

Autophagic protein light chain-3B (LC3B) is a positive regulator of chronic

obstructive pulmonary diseases such as emphysema. LC3B associated with the extrinsic apoptotic factor Fas, and their interaction is mediated by caveolin-1 (Cav-1). Both Fas and Cav-1 are S-acylated proteins (Chen et al., 2010). S-acylation of the bone developmental regulator membrane type1-metalloprotease (MT1-MMP) is a key modulator of bone homeostasis (Song et al., 2014). Goltz syndrome is an X-linked dominant form of ectodermal dysplasia, which is primarily characterized by skin manifestations as atrophic and hypoplastic areas and results in osseous defects and dental anomalies later (Wang et al., 2007). Porcupine is an S-acylated protein, its loss of function causes the Goltz syndrome (Galli et al., 2007; Hornemann, 2015).

An increasing number of studies have reported the involvement of S-acylation in cancer in recent years. For instance, Ras, the negative regulator of cell proliferation, is found to be S-acyled. This lipid modification of Ras helps to maintain its steady state of plasma membrane (PM) localization which is essential for the transduction of extracellular proliferative signals (Rocks et al., 2005; Schmick et al., 2015). S-acylation of the neurotensin receptor 1 (NTSR-1), a key mediator in breast, pancreas, prostate, colon and lung cancers, is essential for its localization and efficient signaling (Heakal et al., 2011). The induction of apoptosis is an efficient way to stop the tumor to develop further. Many proteins involved in apoptosis are S-acylated including FasL (Fas Ligand) (Guardiola-Serrano et al., 2010), FasR (Fas receptor) (Chakrabandhu et al., 2007), DR4 (a receptor of the tumor necrosis factor-related apoptosis-inducing ligand) (Rossin et al., 2009), DCC (deleted in colorectal cancer) (Furne et al., 2006), UNC5H (Maisse et al., 2008), BAX (BCL-2-associated X) (Fröhlich et al., 2014). Metastasis makes cancer spread from the original site to other parts of the body. Importantly, it was reported that S-acylation of metastasis associated proteins KAT1/CD82, CD9 and CD151 is essential for their function in suppressing metastasis or inhibiting tumor cell adhesion and migration (Zhou et al., 2004; Hemler, 2014; Termini et al., 2014). S-acylation of Integrin β4 (ITGβ4) is required for its lipid raft localization and signaling. ITGβ4 can interact with growth factor receptors and enhance the invasive potential of cancer cells (Soung and Chung, 2011). It was found that the level of ITG β4 S-acylation was correlated with the

Table 1-2. S-acylated proteins individually verified in mammalian cells

Groups	Examples	References
SNAREs	SNAP23, SNAP25, SNAP25b	Greaves and Chamberlain, 2010; Greaves et al., 2010
G Proteins	Go1α, $G\alpha_{12}$, $G\alpha_{13}$, GPCRs, GTPase	Wedegaertner et al., 1993; Grassie et al., 1994; Ponimaskin et al., 1998; Ponimaskin et al., 2000; Rocks et al., 2005
T-cell specific proteins	CD4/8, Lck, Fyn, LAT, Cbp/PAG	Bijlmakers, 2009; Hundt et al., 2009; Akimzhanov and Boehning, 2015
B-cell specific proteins	CD20/23	Ivaldi et al., 2012
Synaptic proteins	PSD-95, δ-catenin, gephyrin, AKAP79/150, Cdc42, HTT, β- and γ-secretases, BACE1	Brigidi et al., 2015; Butland et al., 2014; Benjannet et al 2001; Hornemann, 2015
Cancer related proteins	CDCP1, Ras, NTSR-1, FasL, FasR, DR4, DCC, UNC5H, BAX, CD82/9/151/44, ITGβ4, Enos	Adams et al., 2015; Schmick et al., 2015; Heakal et al., 2011; Guardiola-Serrano et al., 2010; Chakrabandhu et al., 2007; Rossin et al., 2009; Furne et al., 2006; Maisse et al., 2008; Fröhlich et al., 2014; Zhou et al., 2004; Termini et al., 2014; Hemler, 2014; Soung and Chung, 2011; Coleman et al., 2015; Xie et al., 2009; Fernandez-Hernand et al., 2006; Wei et al., 2011
Other Proteins	Plscr3, LRP6, Fas, Cav-1, MT1-MMP; Porcupine, TEM8, CCR5	Merrick et al., 2011; Abrami et al., 2008; Abrami et al., 2006; Percherancier et al., 2001; Chen et al., 2010; Song et al., 2014; Galli et al., 2007

invasive potential of breast cancer cells (Coleman et al., 2015). Another S-acylated protein related to breast cancer is CD44 which negatively regulates cell migration (Xie et

al., 2009). Endothelial nitric oxide synthase (eNOS), which localizes in the Golgi complex and cholesterol-rich microdomains of the plasma membrane through S-acylation, promotes angiogenesis and tumorigenesis (Fernandez-Hernand et al., 2006; Wei et al., 2011). The identified S-acylated proteins in mammals are summarized in Table 1-2.

All these studies clearly demonstrate that S-acylation is involved in a wide range of human diseases including mal-development, infectious diseases, autoimmune diseases, neuropsychiatric disorders, dermatosis, osteoporosis and cancer (Ivaldi et al., 2012; Chavda et al., 2014; Hornemann, 2015; Yeste-velasco et al., 2015). Therefore, understanding S-acylation will provide invaluable information to the insight of disease processes which in turn will aid the development of drugs to control and target these various diseases. As such, protein S-acylation and disease in human becomes a hot research topic in the medical field in recent years.

1.1.3 S-acylation in plants

Knowledge on S-acylation in plants is poor compared to that in yeast and mammals. D1, a chloroplast herbicide-binding protein in Spirodela oligorrhiza, is the first S-acylated protein identified in plant (Mattoo and Eldelman, 1987), but its function was not very clear at that time. In the past 15 years, more and more S-acylated proteins have been identified in plants. Some homologous proteins of S-acylated proteins in yeast and mammals are also identified to be S-acylated in plants, such as SNAREs and G proteins. In Arabidopsis, three SNAREs were confirmed to be S-acylated including Syntaxin of plants 71 (SYP71), SYP122 and Novel plant snare 11 (NPSN11), however the function of their S-acylations have not been studied in details (Hemsley et al., 2013). The α subunit GPA1 and γ subunit AGG2 of plant heterotrimeric G protein were confirmed to be S-acylated. GPA1 has dual lipid modification with a myristoylation site at the G^2 position and an adjacent S-acylation site at the C^5 position, ensuring its localization to the PM (Adjobo-Hermans et al., 2006). Apart from promoting PM localization, S-acylation of GPA1 may also stabilize the newly formed heterotrimer. AGG2 is S-acylated at the Golgi before being delivered to the PM and its membrane localization is dependent on the dual

lipid modification of prenylation and S-acylation where S-acylation acts as a membrane targeting signal to guide AGG2 shuttling in and out of the PM (Zeng et al., 2007; Hemsley, 2009). Some small GTPases are also known to be S-acylated. For instance, S-acylation of AtROP6 is responsible for its targeting to detergent-resistant membrane (DRM) domains, which is coupled with its GTP binding and activation (Sorek et al., 2007). AtROP9 and AtROP10, which are involved in ABA signalling, contain 3 and 2 S-acylation sites respectively, and their plasma membrane (PM) localizations rely on S-acylation (Lavy et al., 2002; Hemsley, 2009). For AtRABF1 (ARA6), S-acylation is essential for its prevacuolar compartment localization (Ueda et al., 2001).

Proteins involved in Ca^{2+} signalling such as calcineurin B-Like proteins AtCBL1, AtCBL2, AtCBL3 and AtCBL6 (Batistic et al., 2008; Batistic et al., 2012; Zhou et al., 2013); calcium dependent protein kinases OsCPK2 in rice (Martin and Busconi, 2000), LeCPK1 in tomato (Leclercq et al., 2005), MtCPK3 in *Medicago truncatula* (Gargantini et al., 2006) and StCDPK1 in *Solanum tuberosum* (Raices et al., 2003) were all S-acylated. AtCBL1 is a dually lipid modified protein, in which myristoylation targets it to the ER and then the trafficking from ER to PM and the PM anchoring depends on its S-acylation.

Recently, Kumar and his coworkers found many catalytic subunits of cellulose synthase complex (CSC) in Arabidopsis are S-acylated, such as cellulose synthase A 1 (CESA1), CESA4, CESA6, CESA7 and CESA8. And up to 6 S-acylation sites in each of these proteins (Kumar et al., 2016). Other known S-acylated proteins are: the pathogenesis related proteins such as RPM1 interacting protein 4 (RIN4) and leucine-rich repeat receptor like kinase flagellin sensitive 2 (FLS2) (Kim et al., 2005; Hemsley et al., 2013; Running, 2014); POLTERGEIST (POL) and POLTERGEIST LIKE 1 (PLL1) (their PM localization is depended on both myristoylation and S-acylation at their N-termini) (Gagne and Clark, 2010); the Lost In Pollen tube guidance 1 (LIP1) and 2 (LIP2) (mutations of their S-acylation sites abolished PM localization. Although individual knockout mutant of LIP1 and LIP2 did not have any defects the double mutant is sterile due to loss of pollen tube guidance) (Liu et al., 2013). All the above mentioned proteins

are listed in Table 1-3.

Table 1-3. S-acylated proteins individually identified in plants

Groups	Examples	References
SNAREs	AtSYP71, AtSYP122, AtNPSN11	Hemsley et al., 2013
G-proteins	AtGPA1, AtAGG2, AtROP6/9/10, AtRABF1	Adjobo-Hermans et al., 2006; Zeng et al., 2007; Sorek et al., 2007; Hemsley, 2009; Ueda et al., 2001
Proteins in Ca^{2+} signalling	AtCBL1/2/3/6, OsCPK2, LeCPK1, MtCPK3, StCDPK1	Batistic et al., 2008; Batistic et al., 2012; Zhou et al., 2013; Martin and Busconi, 2000; Leclercq et al., 2005; Gargantini et al., 2006; Raices et al., 2003
Cellulose Synthase complex	AtCESA1, AtCESA4, AtCESA6, AtCESA7, AtCESA8	Kumar et al., 2016
Others	D1, RIN4, FLS2, POL, PLL1, LIP1, LIP2	Mattoo and Edelman, 1987; Kim et al., 2005; Hemsley et al., 2013; Running, 2014; Gagne and Clark, 2010; Liu et al., 2013

More putative and confirmed S-acylated proteins have been identified by large scale proteomics from Arabidopsis and poplar (Hemsley et al, 2013; Srivastava et al., 2016). The 600 plus putative S-acylated proteins isolated from Arabidopsis involve in many processes across plant growth and development, which greatly expanded the range of functions of protein S-acylation involves in plants. They include the mitogen-activated protein kinases (MAPKs), leucine-rich repeat receptor-like kinases (LRR-RLKs) and

RLK superfamily members, integral membrane transporters, ATPases, SNAREs and others. Similarly, about 450 S-acylated proteins were identified from poplar cell suspension with the same method. Except for the commonly known intracellular trafficking related proteins such as protein kinases, SNAREs, band 7 family proteins and tetraspanins, some cell wall related proteins were also found to be S-acylated (Srivastava et al., 2016).

1.1.4 S-acylation in other organisms

S-acylated proteins were also identified from other organisms. For example, more than 400 putative S-acylated proteins were isolated from the most severe human malaria causing parasite *Plasmodium falciparum*. These proteins are involved in almost all the stages of the life cycle of this parasite (Hodson et al., 2015). It's noteworthy that a number of S-acylated proteins are localized in the inner membrane complex (IMC) as it is known that IMC plays central roles in invasion and cytokinesis in *P. falciparum* (Wetzel et al., 2014). In another parasite *Toxoplasma gondii*, S-acylated proteins were also proved to be involved in many physiological processes including motility, invasion and division (Beck et al., 2010; Frénal et al., 2010; Frénal et al., 2014). In *Aspergillus fumigatus*, one of the most common species that cause the invasive aspergillosis in individuals with an immunodeficiency, Ras pathway signaling is its critical virulence determinant and the properly localized and activated Ras is dependent on a series of posttranslational lipid modification including S-acylation (Al Abdallah and Fortwendel, 2015). Study also showed that S-acylation is essential for spermatogenesis of *Caenorhabditis elegans* (Gleason et al., 2006).

S-acylation not only occurs in eukaryotes but also in prokaryotic bacteria and viruses. In Gram-negative bacteria S-acylated Lipid A, which is a structural component of cell membrane and a hydrophobic anchor of lipopolysaccharide (LPS), can protect the bacterium from host immune defenses (Bishop et al., 2005). *Legionella* and other bacterial pathogens can secrete effectors that mimic the substrates of host lipid transferases, which can help them target the proper host membranes after different lipid

modification (Ivanov and Roy, 2013).

S-acylation can also happen in viral proteins and in fact the first S-acylated protein was found in *vesicular stomatitis virus* where a palmitate was added to the glycoprotein (Schmidt and Schlesinger, 1979; Hurst and Hemsley, 2015). The hemagglutinin of *Influenza virus* are S-acylated at three cysteine residues, which is essential for virus replication (Zurcher et al., 1994; Wagner et al., 2005; Brett et al., 2014).

1.2 Protein S-acyl transferases (PATs)

S-acylation of proteins was initially thought to be a non-enzymatic process and happens spontaneously in the cells. However, it is now generally accepted that a family of proteins, the protein S-acyl transferases (PATs for short) are the enzymes that catalyze this reaction. This is because research on PATs was much delayed compared to the S-acylation. The first PAT, Akr1 was identified from *Saccharomyces cerevisiae*, in 2002 which is 20 years later than S-acylation first reported (Schmidt and Schlesinger, 1979; Bartels et al., 1999; Roth et al., 2002). Since then, the significance of this family of enzymes has been gradually realized. This is particularly noticeable for the last 10 years that an increasing number of studies were carried out in this field, leading to the great enrichment of our knowledge of PATs, largely from studies in yeast and mammals.

1.2.1 The structure and functional domains of PATs

Comparing to the numbers of enzymes that catalyze the N-myristoylation or prenylation, there are much more DHHC-containing PATs existing in eukaryotes (Hemsley et al., 2013). Also, different from the cytoplasmic catalyzing enzymes for S-prenylation and N-myristoylation, PATs are multi pass transmembrane proteins containing 4-6 membrane spanning domains (Fig. 1-2). Most importantly, PATs also have a highly conserved catalytic Asp-His-His-Cys Cysteine Rich Domain (DHHC-CRD) of ~50 amino acids with a structure of Cx2Cx9HCx2Cx4DHHCx5Cx4Nx3F, usually residing on the cytoplasmic face of membranes between transmembrane domains (TMD) 2 and 3 (Mitchell et al., 2006; Gottlieb et al., 2015). The DHHC motif is the functional

domain of PATs, in which the cysteine residue links with a fatty acid to form an acyl intermediate. This acyl chain is then transferred to the specific cysteine of the target protein (Roth, et al., 2002). Mutation of cysteine to a different amino acid in the DHHC domain inhibits both acyl intermediate formation and acyl chain transfer activity of PATs (Mitchell et al., 2006; Gottlieb et al., 2015). Indeed, when the cysteine residue in the DHHC motif of AtPAT24, AtPAT10 and AtPAT14 from Arabidopsis was mutated to alanine or serine all these three PATs lost their ability to rescue the growth defects of yeast *akr1* and their respective loss-of-function mutant plant, indicating that their PAT activities rely on the cysteine residue in the DHHC domain (Hemsley et al., 2005; Qi et al., 2013; Li et al., 2015).

Study on human DHHC3 showed the acyl intermediate happened to the cysteine residue in the DHHC motif, but mutations of other conserved cysteines in the CRD also decrease its activity (Gottlieb et al., 2015). Cysteine residues within a novel $CCX_{7-13}C$(S/T) motif downstream of the conserved DHHC-CRD of human PATs DHHC5, DHHC6 and DHHC8 were also proved to be S-acylated (Yang et al., 2010). The PAT activities of all 22 human DHHC-PAT proteins were tested in both mammalian cells and yeast expression system, and interestingly, not all of them exhibited PAT activities (Ohno et al., 2012). Further details will be given later. Even though we usually think the DHHC domain is mainly responsible for PAT catalytic role, it was also reported many residues in this domain determine its substrate specificity, such as A145 and K148 in Swf1 (Montoro et al., 2011).

Some PATs also has a N-terminal ankyrin repeat (AR) domain. Usually two AR containing PATs or DHHC proteins are found in per genome, such as in mammals (Fukata et al., 2004), yeast (Roth et al., 2006), fly (Bannan et al., 2008), apicomplexan parasite (Frenal et al., 2013), nematode (Edmonds and Morgan, 2014) and Arabidopsis (Batistic, 2012). It is thought that AR can help the PAT to recognize its specific targets for S-acylation (Lemonidis et al., 2015). However, other functions of AR that are independent from S-acylation were also found in some such PATs (Harada et al., 2003; Yang and

Cynader, 2011; Hemsley and Grierson, 2011). For example, ARs are required to suppress yeast pheromone response by sequestration of the Gβγ dimer (Hemsley and Grierson, 2011).

Both the N- and C-termini of all PATs characterized so far are highly variable and cytosolic which is believed to be essential for substrate specificity of PATs (Huang et al., 2009; Greaves et al., 2010; Montoro et al., 2011). A recent study reported the finding of a 16-amino-acid motif, which is conserved in 70% eukaryotic PATs and named as PaCCT (Palmitoyltransferase Conserved C-Terminus). Absence of the PaCCT motif abolished Pfa3's function in yeast. And tyrosine residue within this motif of Swf1 is essential for its PAT activity to Tlg1 in yeast (Gonzalez et al., 2009).

Many PATs also have a conserved aspartate-proline-glycine (DPG) motif which is close to the second TMD, and a threonine-threonine-asparagine-glutamate (TTxE) motif which is adjacent to the last TMD (Fig. 1-2). Both of them are cytosolic, however, their roles in the function of PATs are waiting to be explored. Different regions of PATs interact to carry out PAT function, which can't be replaced between the PATs (Montoro et al., 2011).

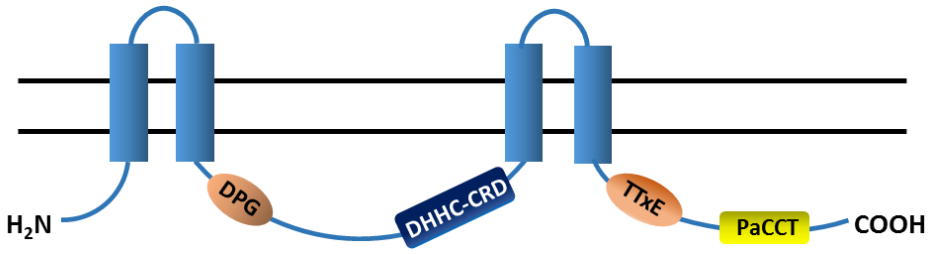

Figure 1-2. Topology structure and conserved domains of PATs.
Most PATs have 4 transmembrane domains and their N- and C-termini are in the cytoplasm. A highly conserved catalytic DHHC-CRD (Asp-His-His-Cys Cysteine Rich Domain) resides between the 2- and 3- TMDs. The majority of PATs also have the DPG (aspartate-proline-glycine), TTxE (threonine-threonine-asparagine-glutamate) and PaCCT (Palmitoyltransferase Conserved C-Terminus) domains and all of them are cytosolic.

1.2.2 DHHC proteins are commonly found in eukaryotes

Since the first DHHC protein was found and proved to be a PAT from yeast, significant advances have been made in the understanding of DHHC-PAT protein family in yeast, mammals, worm and plants. Different numbers of PATs were found in different organisms and the common features of them is that all the identified PATs have a highly conserved DHHC-CRD. The only exception is Ykt6 in yeast, a PAT that has PAT activity but with no DHHC-CRD domain (Dietrich et al., 2004)

At present, 6 of the 7 yeast DHHC proteins have been confirmed to be PATs, and they are Akr1 (Roth et al., 2002; Lobo et al., 2002), Erf2 (Valdez-Taudas and Pelham, 2005), Swf1 (Smotrys et al., 2005), Pfa3 (Hou et al., 2005), Pfa4 (Smotrys et al., 2005) and Pfa5 (Roth et al., 2006). Akr2 is highly homologous to Akr1 with a typical DHHC-CRD and two ARs, however, *akr2* mutant didn't show any remarkable phenotype and there is no direct evidence to show whether it has PAT catalytic activity or not. (Kihara et al., 2005; Linder and Deschenes, 2007).

Among the 22 human DHHC proteins (DHHC1-22), 17 were proved to have PAT activities excluding DHHC 4, 11, 13, 19 and 22 (Ohno et al., 2012). An extra DHHC protein, DHHC23, was found in mice but its homologue cannot be found in human (Ohno et al., 2006; Greaves and Chamberlain, 2010). 22 DHHC containing proteins were found in Drosophila, and all of them show expression throughout Drosophila development with some of them highly expressed in neural (Bannan et al., 2008). *Caenorhabditis elegans* has 15 DHHC-PATs, but so far only 1, SPE10 (spermatogenesis 10), was characterized in some detail and found that it has an essential role in membranous organelles to deliver fibrous bodies to the spermatid (Gleason et al., 2006).

Plant genomes also possess various numbers of DHHC proteins. A recent survey from 31 plant species with complete sequenced genomes, including Arabidopsis, identified 804 DHHC proteins. The number of DHHC proteins was up to 52 in *Panicum virgatum*. Expression pattern of DHHC proteins in *Zea mays* and their response to

phytohormones and abiotic stress showed that DHHC proteins play important roles in plant growth and development as well as stress responses (Yuan et al., 2013). Arabidopsis has 24 DHHC-containing proteins, named as ATPAT1-24 (Hemsley et al, 2005; Batistic, 2012). The expression patterns, PAT activity and subcellular localization were surveyed recently (Batistic, 2012). The biological functions of only 2 AtPATs have been characterized in some detail and they are AtPAT24 (TIP1, Hemsley et al., 2005) and AtPAT10 (Qi et al., 2013; Zhou et al., 2013).

Many DHHC proteins were also found in species of Apicomplexan, including 18 DHHC proteins in *Toxoplasma gondii*, 17 in *Neospora caninum*, 12 in *Trypanosome brucei*, 12 in *Plasmodium falciparum*, 11 in *Plasmodium bergbei*, 10 in *Cryptosporidium* species, 9 in *Theileria parva*, 8 in *Babesia bovis* and 6 in *Eimeria tenella* (Frenal et al., 2013). It was reported that TgDHHC7 from *Toxoplasma gondii* is essential for rhoptry organelles localization and parasite invasion.

1.2.3 Expression pattern and subcellular localization of PATs

The spatial and temporal expression patterns of genes are very important for their cellular functions. It was shown that the human DHHC-1, 3-10, 12-14, 16-18 and 20-22, are ubiquitously expressed in different tissues. DHHC-19 had very high expression level in testis with weak expression in thymus and small intestine while DHHC-11 was only expressed in testis. In addition, only very low level of *DHHC-2* transcript was present in kidney and testis, and similar low levels of *DHHC-15* transcript were also very low in heart, brain, lung, kidney, thymus, and small intestine (Ohno et al., 2006).

The expression patterns of DHHC proteins in Drosophila were also analyzed. Among them, CG1407, CG5620, CG6017, CG6627, CG17257 and CG18815 exhibited maternal expression and were enriched in neural tissues, with transcripts of all of them except for CG1407 also detected in larval brains. Some DHHC proteins were only expressed in testis, including CG4483, CG4956, CG13029, CG17075, CG17195-17198, CG17287 and CG18810. There are also some proteins expressed only in ovary, such as

CG5880, CG6017 and CG34449 (Bannan et al., 2008).

A recent survey reported that nineteen of the 24 AtPATs in Arabidopsis expressed in a broad and constant pattern with transcripts detected in most tissues at different developmental stages (Batistič, 2012). For example, AtPAT1, 2, 3, 11 and 21 had relatively low expression than other AtPATs. AtPAT2 and 3 also exhibited stronger expression in pollen (Batistič, 2012; Yuan et al., 2013). In *Oryza sative*, the transcripts of 26 out of the 30 OsPATs were detected in more than one type of tissue while that of OsPAT29 was only detected during germination stage, OsPAT21 and OsPAT26 only in the internode and stamen respectively. The transcripts of OsPAT13 and OsPAT28 were in very low levels and barely detectable (Yuan et al., 2013). In *Zea mays* 28 of 38 ZmPATs have extensive expression in different developmental stages and tissues with ZmPAT13 and ZmPAT22 having higher expression in anther than in other tissues. However, in *Glycine max*, specific, rather than broad expression patterns were found where 7 GmPATs were specifically expressed in the flowering stage and 11 GmPATs expressed in the other developmental stages except for flowering stage.

Study of the expression patterns of PATs in parasite also showed that most of them have ubiquitous expression patterns with a few being more tissue or developmental stage specific. For instance, TgDHHC18 is specially expressed in bradyzoites, TgDHHC10 at oocyst stage, PfDHHC6 and PfDHHC10 at gametocyte stage (Frenal et al., 2013; López-Barragán et al., 2011). Therefore, it seems that most PATs exhibit a broad expression pattern in different developmental stages and tissues with few PATs being stage or tissue specific, suggesting that most PATs have multiple functions in any given organisms.

1.2.4 Subcellular localization of PATs

PATs are membrane proteins with multiple TMDs and are localized in different endomembranes. This locality nature of PATs may determine the specific set of proteins they modify. For example, the plasma membrane-localized Pfa5 in yeast and DHHC-5, 20 and 21 in human are the PATs involved in S-acylation mediated signal transduction of

PM localized heterotrimeric G protein alpha subunit Gsα, the β2-adrenergic receptor and endothelial nitric oxide synthase (Mumby et al., 1994; Robinson et al., 1995; Loisel et al., 1996; Ohno et al., 2006). The ER- and Golgi- localized DHHC proteins may be responsible for palmitoylation of de novo synthesized proteins during the processes of membrane localization and delivery to other organelles (Ohno et al., 2006). The tonoplast-localized Pfa3 in yeast palmitoylates Vac8p for its vacuolar membrane targeting (Hou et al., 2005; Smotrys et al., 2005). Therefore, to determine the subcellular localization of individual PAT is very important in order to understand its function by identifying the substrate proteins it modifies and signaling pathways it is involved.

As mentioned above that PATs are found in all endomembrane systems in the cell. However, in different species they have different preference as to which endomembrane compartment(s) it is localized. For instance, in yeast, 3 PATs including Swf1, Pfa4 and Erf2 are localized at ER; Akr1 and Akr2 are localized at Golgi; Pfa3 and Pfa5 are localized at vacuole and PM respectively (Valdez-Taubas and Pelham, 2005; Ohno et al., 2006). In human, 8 PATs are localized at ER (DHHC-1, 6, 10, 11, 13, 14, 16, 19), 7 at Golgi (DHHC-3, 4, 7, 8, 15, 17, 18, 21), 4 localized at both ER and Golgi (DHHC-2, 9, 12 and 22) and 3 PATs localized in PM (DHHC-5, 20, 21) (Ohno et al., 2006).

Similar to the mammalian PATs, DHHC-PATs in Drosophila also are mainly localized at ER (CG4483, CG4676, CG4956, CG5196, CG5620, CG6627, CG10344, CG13029, CG17075, CG17195, CG17196, CG17197, CG17198 and CG17287) and Golgi (CG5880, CG6017, CG6618, CG8314, CG17257 and CG18810). There are two exceptions, CG1407 localizes at PM and CG18815 localizes in cytoplasm (Bannan et al., 2008).

In Arabidopsis, transiently expressed GFP-tagged AtPATs in tobacco showed that nearly half of them were localized on PM, such as AtPAT04-09, 12, 19 and 21. Therefore, it was proposed that PM is the main site for S-acylation in Arabidopsis (Batistic, 2012). This is different from mammalian PATs where most PATs localized on ER, therefore ER is thought to be the major S-acylation machineries (Ohno et al., 2006). It is also interesting

to note that many AtPATs are localized on ER or PM and the vesicles associated with them, such as AtPAT3, 15, 17 and 18 at ER and vesicles, AtPAT13, 20 and 22 at PM and vesicles (Batistic, 2012). AtPAT10, 14, 16, 23 and 24 are mainly localized at Golgi, and the Golgi-localization of AtPAT10 and AtPAT14 were further confirmed by stably transformed Arabidopsis plants later (Qi et al, 2013; Li et al, 2015). AtPAT01 and AtPAT02 are localized in some endosomal compartments (Batistic, 2012). Tonoplast localization was found with AtPAT10 and AtPAT11 (Batistic, 2012; Qi et al, 2013; Zhou et al, 2013). It is noteworthy that similar to mammalian PATs, many AtPATs also have dual subcellular localizations, such as AtPAT10 in Golgi and Tonoplast, AtPAT13/20/22 in PM and vesicles (Batistic, 2012; Qi et al., 2013). However, the significance of this dual-localization of PATs is currently unknown.

In Apicomplexan, such as *Toxoplasma gondii*, TgDHHCs are not only localized on the common organelles like Golgi (TgDHHC1, 5, 6, 9, 11, 12, 15 and 17), ER (TgDHHC3, 8 and 16), PM (TgDHHC4 and 13), but also the Apicomplexan-specific organelles like IMC (TgDHHC2 and 14) and rhoptries (TgDHHC7).

Little is known about how the PAT proteins achieve their respective localization in the cell. A recent study show that the lysine-based sorting signals KXX and KKXX (the second X means the terminal residue of a protein sequence) are present in the mammalian DHHC4 and DHHC6, respectively, and it is these motifs that restrict their localization to the ER (Gorleku et al., 2011). It is also revealed that the C-terminal 68 amino acids of the mammalian DHHC2 plays an important role to define its subcellular localization to the ER and Golgi (Fukata et al., 2013).

1.2.5 The identified PAT/substrate pairs

As an enzyme PAT carries out its function mainly through palmitoylating their substrate proteins. Therefore, to understand how PATs operate it is important to identify the target proteins they modify. However, to match an individual PAT and its S-acylated substrate proteins is proved to be a very difficult task so far. This is because: 1) The

number of potential S-acylated proteins are far exceeded the number of their modifying PATs. For example, there are 7 PATs in yeast, however, at least 50 S-acylated proteins were identified by a proteomic approach (Roth et al., 2006). Similarly, more S-acylated proteins were isolated than their PATs in mammals and Arabidopsis (Martin and Cravatt, 2009; Hemsley et al., 2013). Therefore, it seems most likely that at least some if not all PATs can S-acylate multiple substrate proteins, i.e., PATs do not have strict substrate specificity; 2) Many substrate proteins can be modified by more than one PAT. For instance, in yeast, the S-acylation of Vac8 is only partially reduced in the yeast PAT knock-out strain *pfa3*, thus it is most likely that Vac8 is S-acylated by Pfa3 as well as one another or other PATs (Smotrys et al., 2005). Similarly, Ras2 S-acylation is partially suppressed in the absence of Erf2 (Roth et al., 2006; Gonzalez Montoro et al., 2011). Therefore, some PATs have specific yet overlapping substrate specificity. For some peripheral membrane proteins in mammalian cells, their S-acylation is devoid of specificity altogether (Rocks et al., 2010). However, reports show that some PATs do have their preferentially modified proteins. For example, Swf1 in yeast prefers to function on transmembrane proteins that have cysteines close to TMDs (Roth et al., 2006). In human, integrin α4β6 is strictly modified by DHHC-3 (Sharma et al., 2012); 3) No consensus sequences in S-acylated proteins. Although lots of S-acylated proteins have been identified and some of them are S-acylated by the same PAT, there are no consensus sequences characterised in these proteins (Gonzalez Montoro et al., 2011).

1.2.5.1 PATs and their substrate proteins in yeast

In yeast, five PATs have been mapped to one or more substrate proteins of their own. However, the total number of these individual substrate proteins are far less than the >50 S-acylated proteins identified via a proteomic approach (Roth et al, 2006). Akr1 S-acylates casein kinase Yck1, Yck2 and Yck3 (Roth et al., 2002). Sphingosine kinase Lcb4 S-acylation was reduced by 60%-80% in *akr1* mutant (Kihara et al., 2005), and Meh1, Sna4 and some unknown function proteins such as Ypl199c, Ykl047w and Ypl236c were reported to be the substrates of Akr1 (Roth et al., 2006). In addition, Meh1 was also S-

acylated by Pfa3 with a slightly lower efficiency than Akr1 (Greaves and Chamberlain, 2011). Therefore, Akr1 alone can S-acylate at least 9 protein substrate proteins in yeast.

Table 1-4. Substrates of Yeast PATs

PATs	Substrates	References
Akr1	Lcb4, Yck1, Yck2, Yck3, Meh1, Sna4, Ypl199c, Ykl047w , Ypl236c, Vac8	Roth et al., 2002; Kihara et al., 2005; Roth et al., 2006; Roth et al., 2011; Babu et al., 2004
Erf2 (shr5)	Ras1, Ras2, Rho2, Rho3, Gpa1, Gpa2, Ste18, Ycp4, Psr1, Yg1108	Bartels et al., 1999; Lobo et al., 2002; Roth et al., 2006; Ohno et al., 2006; Zhang et al., 2013; Greaves and Chamberlain, 2011
Swf1	Many SNAREs, Mnn1, Mnn10 , Mnn11, Pin2	Valdez-Taubas and Pelham, 2005; Roth et al., 2006
Pfa3	Vac8, Meh1	Hou et al., 2005; Smotrys et al., 2005; Roth et al., 2006
Pfa4	APPs, Lcb4, Ras1,Yg1108	Roth et al., 2006; Ohno et al., 2006; Nichols et al., 2015; Greaves and Chamberlain, 2011
Pfa5	Gpa2	Greaves and Chamberlain, 2011

It seems that Ark1 prefers hydrophilic proteins that tether to membranes solely through N- or C-terminal palmitoyl modifications (Roth et al., 2006). Erf2 is responsible for S-acylation of Ras protein (Bartels et al., 1999; Lobo et al., 2002), also other signalling proteins such as Rho2, Rho3, Gpa1, Gpa2 and Ste18, all of which seem to be heterolipidated (Roth et al., 2006; Zhang et al., 2013). An unknown protein Yg1108 was S-acylated equally by Erf2 and Pfa4 (Greaves and Chamberlain, 2011). Swf1 tends to S-acylate proteins that have juxta-TMD mapping cysteines (Roth et al., 2006), such as SNAREs (Valdez-Taubas and Pelham, 2005), mannosyltransferases including Mnn1, Mnn10 and Mnn11 and prion induction protein Pin2 (Roth et al., 2006). Pfa4, devoted to palmitoylation of a group of Amino Acid Permeases (AAPs). AAPs is a family of plasma

membrane transporters with 12 TMDs and a conserved C-terminal Phe-Trp-Cys palmitoylation site. Experiments in *Cryptococcus neoformans* showed Pfa4 is responsible for PM localization of Ras1 (Merino et al., 2014). Pfa5 prefer lipidated substrates, such as Gpa2 which is pre-myristoylated before S-acylation (Greaves and Chamberlain, 2011). However, so far the substrates of Akr2 has not been identified. A summary of PATs and their substrate proteins in yeast is shown in Table 1-4.

1.2.5.2 PATs and their substrate proteins in mammals

Similarly, the substrate proteins of some mammalian PATs have also been identified in recent years. These include GTP-binding proteins, cytoskeletal proteins, enzymes, neurotransmitter receptors and synaptic scaffolding proteins (Table 1- 2). Similar to what is found in yeast, some proteins can be modified by more than one PAT. For instance, PSD-95, a protein that scaffolds receptors and signaling enzymes at the postsynapse (Topinka and Bredt, 1998), can be S-acylated by DHHC-2, -3, -7, -8, -15 and -17 (Fukata et al., 2004; Fukata et al., 2006; Greaves and Chamberlain, 2011; Butland et al., 2014). A t-SNARE protein that regulates neurotransmitter release, SNAP-25, is the substrate of DHHC-2, -3, -7, -8, -15 and -17 (Greaves et al., 2009). S-acylation of a tyrosine kinase Fyn is mediated by DHHC-2, -3, -7, -15, -20 and -21 (Mill et al., 2009). Another tyrosine kinase Lck can be S-acylated by DHHC-17, -18 and -21 (Fukata et al., 2004; Butland et al., 2014). Endothelial nitric oxide synthase (eNOS) is modified by DHHC-2, -3, -7, -8 and -21 (Fernández-Hernando et al., 2006). Multiple PATs are required for S-acylation-dependent regulation of large conductance calcium- and voltage-activated potassium channel (STREX), such as DHHC-3, -5, -7, -9 and -17 (Tian et al., 2010; Butland et al., 2014). S-acylation-dependent targeting of BACE1 (β-site APP-cleaving enzyme 1) to lipid raft required DHHC-3, -4, -7, -15 and -20 (Vetrivel et al., 2009). Glutamate decarboxylase GAD65 is S-acylated by DHHC-3, -8, -13 and -17 (Saleem et al., 2010; Butland et al., 2014). Different type of Ras proteins can be modified by different PATs including DHHC-9, -17, -18 and -19 (Fukata et al., 2004; Baumgart et al., 2010; Butland et al., 2014). Transport and function of ATP-binding cassette transporter (ABC) A1 is

mediated by many PATs including DHHC-2, -12, -20 and -21 (Singaraja et al., 2009). DHHC-17 is required for the targeting of CSP (cysteine string protein) to synaptic vesicles which is also enhanced by other PATs including DHHC-3, -7 and -15 (Ohyama et al., 2007; Greaves et al., 2008). The γ2 subunit of gaminobutyric acid ($GABA_A\gamma2$) was first reported to be S-acylated by DHHC-3 (Keller et al., 2004), and further study showed that it was also modified by DHHC-7 and -15 (Fang et al., 2006). Nuclear distribution factor E homolog-1 (NDE1) and NDE-like 1 (NDEL1), proteins that are involved in the regulation of the retrograde motor cytoplasmic dynein, are S-acylated by DHHC-2, -3 and -7. S-acylation of a group of proteins have been identified to be mainly catalysed by two PATs, such as Gα, AMPA-selective glutamate receptor 1 and 2 (GLUR1/2), neuronal cell adhesion molecule of 140 kDa (NCAM140), CD9/151, phosphodiesterase isoform 10A2 (PDE10A2), sortillin, Phosphatidylinositol 4-kinase (PI4KII), the sex steroid estrogen, progesterone and androgen receptors (ER, PR and AR) (Tsutsumi et al., 2009; Huang et al., 2009; Butland et al., 2014; Charych, et al., 2010; Yeste-Velasco et al., 2015).

Some proteins are modified by a specific PAT, such as cytoskeleton-associated protein 4 (CKAP4) and AKAP79/150 by DHHC-2 (Chavda et al., 2014; Keith et al., 2012); integrin α6β4, Calmodulin-dependent protein kinase isoform 1γ (CaMKIγ), NMDA receptor subunits 2A and 2B (NR2A/B) and DR4 by DHHC-3 (Takemoto-Kimura et al., 2007; Hayashi, et al., 2009; Sharma et al., 2012; Yeste-Velasco et al., 2015); Grip1b, δ-catenin, Flotillin-2, somatostatin receptor 5 and Ankyrin-G by DHHC-5 (Brigidi et al., 2015); Chaperone calnexin by DHHC-6 (Lakkaraju et al., 2012); paralemmin-1 by DHHC-8 (Huang et al., 2009); membrane type 1- metalloprotease (MT1-MMP) by DHHC-13 (Song et al., 2014); Cation-independent mannose-6-phosphate receptor (CI-MPR) by DHHC-15 (McCormick et al., 2008); GPM6A, JNK3, , SYT1 and SPRED1/3 by DHHC-17 (Butland et al., 2014); platelet endothelial cell adhesion molecule-1 (PECAM1) (Yeste-Velasco et al., 2015) and SOD1 by DHHC-21 (Antinone et al., 2013).

Table 1-5. Mammalian PATs and their (regulated) target proteins

PATs	Targets	References
DHHC-2	PSD-95, CKAP4, SNAP23/25, eNOS, Fyn, NDE1, NDEL1, CD9/151, ABCA1, AKAP79/150	Huang et al., 2004; Fukata et al., 2004; Shmueli et al., 2010; Fernandez-Hernando et al., 2006; Sharma et al., 2008; Zhang et al., 2008; Singaraja et al., 2009; Greaves et al., 2010; Chavda et al., 2014
DHHC-3 (GODZ)	PSD-95, SNAP23/25/25b, Gα, CSP, Integrin α6β4, $GABA_A$γ2, eNOS, GluR1/2, GAD65, STREX, Fyn, BACE1, NDE1, NDEL1, NCAM140, CaMKIγ, NR2A/B, DR4, PI4KII	Hayashi et al., 2005; Fukata et al., 2004; Greaves et al., 2010; Mill et al., 2009; Huang et al., 2009; Tian et al., 2010; Fang et al., 2006; Shmueli et al., 2010; Fernández-Hernando et al., 2006; Greaves et al., 2008; Vetrivel et al., 2009; Takemoto-Kimura et al., 2007; Tsutsumi et al., 2009; Yeste-Velasco et al., 2015
DHHC-4	BACE1	Vetrivel et al., 2009
DHHC-5	Grip1b, δ-catenin, Flotillin-2, somatostatin receptor 5, Ankyrin-G, STREX	Brigidi et al., 2015; Thomas et al., 2012; Brigidi et al., 2014; Li et al., 2012; Kokkola et al., 2011; Tian et al., 2010
DHHC-6	Chaperone calnexin	Lakkaraju et al., 2012
DHHC-7	PSD-95, Gα, CSP, Fyn, eNOS, SNAP25/23/25b, GABAAγ2, STREX, BACE1, NDE1, NDEL1, NCAM140, sortillin, PDE10A2, CD9, ER, PR, AR, PI4KII	Fukata et al., 2004; Fukata et al., 2006; Greaves et al., 2009; Greaves et al., 2010; Tian et al., 2010; Ohno et al., 2012; Fang et al., 2006; Shmueli et al., 2009; Fernández-Hernando et al., 2006; Greaves et al., 2008; Vetrivel et al.,

		2009; Ponimaskin et al., 2008; Tsutsumi et al., 2009; McCormick et al., 2008; Charych et al., 2010
DHHC-8	eNOS, SNAP25, paralemmin-1, GAD65, PSD95, PSD93	Fernández-Hernando et al., 2006; Mukai et al., 2008; Huang et al., 2009
DHHC-9	H- and N-Ras, STREX	Swarthout et al., 2005; Tian et al., 2010
DHHC-12	ABCA1	Chavda et al., 2014; Singaraja et al., 2009
DHHC-13 (HIP14L)	MT1-MMP, HTT, GAD65	Song et al., 2014; Huang et al., 2009; Saleem et al., 2010
DHHC-15	PSD95, GAP43, SNAP25b, CSP, $GABA_A\gamma2$, Fyn, BACE1, CD151, CI-MPR, sortillin	Fukata et al., 2004; Greaves et al., 2010; Mill et al., 2009; Fang et al., 2006; Sharma etal., 2008; Greaves et al., 2008; Vetrivel et al., 2009; McCormick et al., 2008
DHHC-17 (HIP14)	PSD95, CLIP3, CSP, GAD65, GAP43, GLUR1/2, GPM6A, HTT, JNK3, Lck, SNAP25/23/25b, STREX, SYT1, SPRED1/3, Ras	Ohno et al., 2012; Butland et al., 2014; Fukata et al., 2004; Greaves et al., 2010; Mill et al., 2009; Huang et al., 2009; Tian et al., 2010; Greaves et al., 2008
DHHC-18	H- and N-Ras, Lck	Fukata et al., 2004
DHHC-19	R-Ras, PDE10A2	Charych et al., 2010; Baumgart et al., 2010
DHHC-20	Fyn, BACE1, ABCA1	Mill et al., 2009; Singaraja et al., 2009; Vetrivel et al., 2009
DHHC-21	PECAM1, SOD1, Lck, eNOS, Fyn, ABCA1, ER, PR, AR	Antinone et al., 2013; Yeste-Velasco et al., 2015; Akimzhanov and Boehning, 2015; Mill et al., 2009; Vetrivel et al., 2009; Fernández-Hernando et al., 2006; Takemoto-Kimura et al., 2007

Most DHHC proteins in mammals can catalyse S-acylation independently, however, DHHC-9 needs a Golgi-localized protein GCP16 to specially palmitoylate H- and N-Ras (Swarthout et al., 2005). Most PATs can modify multiple proteins such as DHHC-2, -3, -5, -7, -8, -13, -15, -17 and -21 (Table 1-5). Some DHHC proteins have been indicated to be involved in certain diseases, such as DHHC-8 in schizophrenia, DHHC-9 and -15 in X-linked mental retardation, DHHC17 in Huntington's disease and many PATs are involved in different types of cancer including DHHC-2, -3, -7, -9, -11, -14, -17, -20 and -21 (Chavda et al., 2014; Yeste-Velasco et al., 2015). However, for some of them, their specific substrate proteins have not been identified.

1.2.5.3 PATs and their substrate proteins in other organisms

In other organisms very little information is available for PAT/substrate pairs. Parasite inner membrane complex (IMC), a membranous structure consisting of two layers located underneath the plasma membrane, which is important for host cell invasion (Cavalier-Smith, 1993; Wetzel et al., 2014). PfDHHC1, an apicomplexan-specific and IMC-localized PAT in *P. falciparum*, has identical distribution to two S-acylated proteins PfISP1 and PfISP3 (Wetzel et al., 2015). And this is the only PAT/substrate pair characterized in this organism. In plant the only PAT/substrates pairing identified is ATPAT10/AtCBL2, 3, 6. This was achieved by transient expression of AtCBL2, AtCBL3 and AtCBL6 in Arabidopsis protoplast, showing the tonoplast localization of AtCBLs is lost in protoplast prepared from AtPAT10 loss-of-function mutant (Zhou et al., 2013). The targeting of AtCBL2, 3 to tonoplast by AtPAT10 was further confirmed *in vivo* by stably expressing AtCBL2, 3-GFP in *atpat10* mutant (Li et al, unpublished).

Therefore, although thousands of S-acylated proteins were isolated from different species so far and many more to come in the future due to the readily available proteomics facilities in large institutions, a framework for characterizing PAT/substrate selectivity need to be set out to match individual PATs and their S-acylated substrate proteins in order to understand the functionality of protein S-acylation in the biological context.

1.3 De-S-acylation

Similar to phosphorylation and ubiquitiation, S-acylation process is reversible, which makes it a very important lipid modification of proteins (Hemsley, 2009). S-acylation turnover by de-S-acylation, can be constitutive or stimulated (Smotrys and Linder, 2004). Ras proteins were the first proteins to be reported to have dynamic S-acylation with different H-Ras has different de-S-acylation rates (Baker et al., 2003). S-acylation/ de-S-acylation of Fyn, a member of the Src kinase family, happens with a half-life of 1.5-2 hours (Wolven, et al., 1997; Zeidman et al., 2009). Neuronal activity can enhance the de-S-acylation process of PSD-95 (El-Husseini et al., 2002).

At present four protein thioesterases have been identified to catalyze the de-S-acylation process, including acyl protein thioesterases 1 (APT1) and 2 (APT2), palmitoyl thioesterases 1 (PPT1) and 2 (PPT2) (Tomatis et al., 2010; Hornemann, 2015). APTs carry out the de-S-acylation step in which it remove the palmitate from the palmitoylated proteins (Linder and Deschenes, 2007). APT1 was first found in rat liver as a lysophospholipase and its substrates include Ras, GPA1, RGS4, SNAP-23 and eNOS (Toyoda et al., 1999; Akimzhanov and Boehning, 2015). APT2 was reported to de-S-acylate the growth-associated protein 43 (GAP43) (Tomatis et al., 2010). PPT1 is responsible for degradation of S-acylated proteins (Linder and Deschenes, 2007; Chavda et al., 2014). It is a soluble lipase which is localized in lysosomes. Its loss-of-function resulted in severe infantile neuronal ceroid lipofuscinosis (Vesa et al., 1995). PPT2 has very limited acyl protein thioesterase activity, which prefers de-S-acylating short-chain lipid substrate. Study showed that it is up-regulated in obesity (Burger et al., 2012; Fox et al., 2012).

It is surprising that only four thioesterases have been identified so far yet many hundreds of S-acylated proteins were isolated from different genomes. The explanations for this could be: 1) thioesterases are broad specificity enzymes, each of which can de-S-acylate a wide range of substrates; 2) not all S-acylated proteins undergo de-S-acylation;

3) of course, it could be because many more thioesterases have not been found (Chavda et al., 2014).

1.4 Mechanism of Protein S-acylation

DHHC proteins transfer acyl group via a two-step catalytic mechanism in which the enzyme first modifies itself with palmitate in a process termed autoacylation. The enzyme then transfers the acyl group from itself onto its substrate proteins. The number and location of the S-acylated cysteines in the autoacylated intermediate is unknown. Generally, it was well known that the cysteine in the DHHC motif is the auto-S-acylation site, but cysteines in other positions of PATs domains may also be auto-S-acylated. It was found 6 auto-S-acylation sites in DHHC3, including Cys-132, Cys-133, Cys-146, Cys-157 and Cys-163 in CRD, Cys-24 in N-terminal domain (Gottlieb et al., 2015).

1.4.1 Protein S-acylation sites prediction and confirmation

Currently, there is no consensus sequences in the S-acylated proteins despite many such proteins have been isolated through proteomics approach or individually confirmed via radioactive labelling or/and mutation studies. This is the main reason slowing down the research in the protein S-acylation field. Nevertheless, it is noted that: 1) in some soluble proteins, the S-acylated cysteines are frequently surrounded by basic or hydrophobic amino acids, such as GAP-43 (Liu et al., 1993), Yck2 (Roth et al., 2002) and SNAP-25b (Lane and Liu, 1997; Smotrys and Linder, 2004); 2) in other S-acylated soluble proteins the Cys residue is located near the prenylated or myristoylated residues, resulting in the dual lipidition. These proteins include α (GPA1) and γ (AGG2) subunits of heterotrimeric G protein (Adjobo-Hermans et al., 2006; Zeng et al., 2007), small GTPases (Deschenes et al., 1990; Bartels et al., 1999; Roth et al., 2006; Zhang et al., 2013); 3) for transmembrane proteins, the Cys residues are often situated in the cytoplasmic regions of membrane-spanning regions (Roth et al., 2006; Ohno et al., 2012). For instance, the S-acylation of death receptor 4 (Oh et al., 2012) and β-secretase BACE1 (Motoki et al., 2012) promotes their association with lipid raft.

Based on the above information several softwares have been developed to predict the S-acylated cysteines of proteins, such as a clustering and scoring strategy known as CSS-Palm, which has been updated to the latest version CSS-Palm4.0 (Zhou et al., 2006; Xue et al., 2011), incremental feature selection (IFS)-Palm (Hu et al., 2011), weight, amino acid composition and position specific scoring (WAP)-Palm (Shi et al., 2013) and PalmPred (Kumari et al., 2014). All of them are on-line so that one can input the protein sequence of interest to predict the possibility of its S-acylation and where the Cys residues are located within the sequence. The prediction data from these platforms can then be confirmed experimentally.

The related experiments include: 1) PAT inhibitors. For example, the palmitate analog, 2-bromopalmitate (2-BP) is the most commonly used inhibitor of S-acylation, which inhibits palmitoylation in cells and PAT activity of DHHC proteins *in vitro* (Webb et al., 2000; Fukata et al., 2004; Jennings et al., 2009). However, it lacks specificity and can also inhibit other enzymes involved in lipid metabolism such as myristoylation (Webb et al., 2000). Tunicamycin and cerulenin are also used to inhibit S-acylation, but similar effect was found (Patterson and Skene, 1995; Lawrence et al., 1999). Recently, a compound, 2-(2-hydroxy-5-nitro-benzylidene)-benzo[*b*]thiophen-3-one, was shown to have more specificity, but it does not have selectivity for specific PAT, i.e., it inhibits all PATs (Jennings et al., 2009). Therefore, results obtained from these inhibitors should be further validated by mutational or biochemical analysis; 2) Mutational analysis to change the potential S-acylated Cysteine to alanine or serine. Both alanine and serine were frequently used to replace the cysteine to achieve similar results (Hemsley et al., 2005; Qi et al., 2013; Li et al., 2015). However, because cysteine and serine have very similar structure, when the cysteine is mutated to serine it can maintain the size and the properties of the putative S-acylated protein. Therefore, serine is more preferred amino acid to use in mutagenesis studies. This is followed by comparing the effect on the differences of functions or the subcellular localizations to native protein. If a difference was found the proteins were most likely to be S-acylated at the cysteine residues that were mutated; 3) Biochemical assays to analyze the attachment of fatty acids of the individual proteins,

including traditionally feeding experiment with tritiated fatty acids followed by exposures to X-ray film (Lavy et al., 2002); azido-alkyne CLICK-chemistry (Martin and Cravatt, 2009); Acyl-exchange, or Biotin-switch assay (Wan et al., 2007; Hemsley et al., 2008); and direct resin immobilisation (Forrester et al., 2011). 4) Direct detection of the S-acyl group by gas chromatography–mass spectrometry (GC-MS) analysis. The identification of lipid groups attached to proteins can help to understand the biophysical properties of such proteins. This method has been successfully used to demonstrate the S-acylation of CBL1 (Batistic et al., 2008) and CBL2 (Batistic et al., 2012) in Arabidopsis.

1.4.2 Specificities of PAT-substrate interaction

Studies in yeast showed that some PATs exhibit substrate specificities. For instance, Akr1 prefers to S-acylate soluble proteins at their N- or C- terminus, such as Ypl236c S-acylted at N-terminal cysteine and Yck1 S-acylated at C-terminal cysteine. Erf2 and Pfa5 show preference for pre-lipidated substrates, such as prenylated Ras1 and Ras2, myristoylated Gpa1 and Gpa2. Swf1 and Pfa4, on the other hand, prefer single and multiple transmembrane proteins such as SNAREs and AAPs (Roth et al., 2006; Ohno et al., 2012). Similar conclusion was made from studies of mammalian DHHC proteins where Ohno and co-workers (2012) found that DHHC-3, -7, -8 and 14-17 had high PAT activities towards soluble proteins, while DHHC-2, -20 and -21 were highly active to S-acylate integral membrane proteins. However, it was also noted that most DHHC proteins in both yeast and mammals had overlap activity to modify pre-lipidated substrates, such as 4 yeast PATs and 16 PATs can S-acylate Gpa2 in different levels (Ohno et al., 2012).

The question is how PATs and their substrates recognize each other? To address this studies were carried out on some PATs and their S-acylated proteins in mammalian system. For example, the AR domain of the two Ankyrin repeating containing PATs DHHC-13 and -17 in mammals can act as S-acylation substrate-recruiting molecule and recognizes the [VIAP][VIT]XXQP motif that is shared between some S-acylated proteins including SNAP25/23, CSP, HTT and CLIP3 (Lemonidis et al., 2015). Fusing the AR domain of DHHC-17 to the N-terminus of DHHC-3, which lacks an AR domain, can make DHHC-

3 a PAT for the DHHC-17 substrate protein HTT. Therefore, this result supports the notion that the AR domain contributes to the substrate specificity of DHHC-17 (Huang et al., 2009). The N-terminal 13 amino acids of PSD-95 is required for the recognition and S-acylation of PSD95 by DHHC-17 (Huang et al., 2009). DHHC-7 has two splicing isoforms, the longer one has additional 111bp compare to the shorter one, which might possess its tissue-specific function since it expresses specifically in placenta, lung, liver, thymus and small intestine (Ohno et al., 2006). The cysteine rich 'CCPCC' motif of PI4KII is required for its S-acylation by DHHC-3 and DHHC-7 (Lu et al., 2012). DHHC-3 and -7 also interact with $GABA_A\gamma2$ through a 14-amino acid cysteine rich domain (Fang et al., 2006). Subtle changes in the S-acylation domains of proteins can alter their PAT specificity, which were proved from SNAP23/25 (Greaves et al., 2010). For instance, a SNAP25 mutant which lacks a proline located 25 residues downstream of the S-acylated domain can only be modified by DHHC-3 but not by DHHC-17 (Greaves et al., 2009).

DHHC-PATs are integral membrane proteins containing multiple transmembrane domains. Individual PAT resides in a specific endomembrane compartment. This can have a profound effect on the type of proteins it can S-acylate (Greaves and Chamberlain, 2011). A transmembrane proteins might only have the access to be S-acylated by the PATs localized on the same membrane. For example, PM-localized Pfa5 in yeast is responsible for Gpa1 PM-localization (Ohno et al., 2006); the tonoplast-localization of AtCBL2 rely on AtPAT10 which is also localized on tonoplast (Zhou et al., 2013).

For S-acylation of a protein to occur its prior membrane attachment via TMD or another lipid modification is acquired (Hemsley, 2015). S-acylation of transmembrane protein TEM8 negatively regulated its raft association (Abrami et al., 2006). Some proteins need another lipid modification such as myristoylation prior to S-acylation. AtCBL1 is one such protein which targets to the ER first by myristoylation. And then some unknown ER-localized PATs can S-acylate the pre-lipidated AtCBL1 to confer its PM targeting. Similarly other AtCBLs also go through this dual lipidation for their final membrane targeting process (Batistics et al., 2008). Therefore, it seems that the

localization of proteins after the first lipid modification has selectivity to their corresponding PATs. It was also reported that the N-terminal 12–amino acid peptide of AtCBLs is sufficient to mediate its dual lipid modification and target it to the specific membranes (Batistic et al., 2008).

1.4.3 Important molecules that are involved in S-acylation

Special molecules have positive or negative effect on S-acylation of certain proteins. These molecules could be another protein, hormone, ions or protein inhibitors etc. For instance, Selenoprotein K (SelK), an 11-kDa endoplasmic reticulum (ER) protein of unknown function (Shchedrina et al, 2011), is required for the S-acylation of both IP3R (inositol-1, 4, 5-triphosphate receptor) and CD36 (Fredericks and Hoffmann, 2015). S-acylation of PI4KII is cholesterol-dependent (Lu et al., 2012). Zinc ion is tightly bound to the cysteine rich domain of the DHHC-3, which is essential for its structural integrity and PAT activity (Gottlieb et al., 2015). Some compounds might have negative effect to specific S-acylation, such as curcumin can prevent S-acylation of integrin β4 by DHHC-3 in breast cancer cells (Coleman et al., 2015). These might supply important information for developing new targets to inhibit S-acylation.

1.5 Perspectives and Aims

1.5.1 Protein S-acylation and S-acyl transferases in plant

As mentioned earlier plant genomes contain multiple PATs ranging from 6 to 52 (Yuan et al, 2013). Large scale proteomics approach identified many putative S-acylated proteins from Arabidodsis and poplar recently (Hemsley et al, 2013; Srivastava et al., 2016). In addition, many S-acylated proteins have also been individually characterized since the first S-acylation was found to assist CDPK membrane localization in rice (reviewed by Hemsley 2009, 2013, 2015), demonstrating the important roles of S-acylation of proteins plays in growth, development, fertility and stress signalling.

The information we gained is primarily from studies carried out in the model plant

Arabidopsis thaliana. At least 24 putative AtPATs were predicted in the genome of Arabidopsis (Hemsley et al, 2005, Batistic, 2012). All these putative PATs have 4 TMDs except for AtPAT15 and AtPAT17 which has 3 and 6 TMDs, respectively. Similar to what was found in yeast and mammals, Arabidopsis genome also has 2 ankyrin repeats containing PATs, AtPAT23 and AtPAT24 that are highly homologous. Being the first PAT identified in higher plant, AtPAT24 was confirmed to be an S-acyl transferase because it can rescue the yeast PAT AKR1 knockout mutant *akr1* for its morphological and temperature sensitive defects. AtPAT24 can also restore the correct localization of one of the AKR1 palmitoylating proteins, the yeast casein kinase 2 (Yck2). The loss-of-function mutant *tip1* (*atpat24*) of Arabidopsis plants exhibited defects in cell size control, pollen tube and root hair growth, as well as cell polarity (Hemsley et al., 2005). However, the substrate proteins it modifies have not been identified despite a proteomic approach was carried out (Hemsley et al, 2013). The second plant PAT characterized, again in Arabidopsis, is AtPAT10. Its enzyme activity was experimentally confirmed *in vitro* and *in vivo* (Qi et al, 2013). AtPAT10 is expressed ubiquitously in all tissues and throughout the growth and development stages. It is predominately localized in Golgi and tonoplast (Batistic, 2012; Qi et al, 2013; Zhou et al, 2013). Three T-DNA insertion mutant alleles were identified for *AtPAT10* and all showed pleiotropic defects, including cell expansion, cell division, vascular patterning, fertility and salt stress in Arabidopsis (Qi et al., 2013; Zhou et al., 2013). An *in vitro* study showed that the tonoplast-localization of CBL2, 3 and 6 was lost in protoplast prepared from *atpat10* mutant cells, indicating AtPAT10 could be the PAT for these 3 CBL proteins (Zhou et al., 2013).

1.5.2 S-acylation is more common than expected in Arabidopsis

As we mentioned above, 582 S-acylated proteins were isolated in Arabidopsis through ABE-dependent proteomics (Hemsley et al., 2013). However, the real number of S-acylated proteins can be much more than that. All PATs must be S-acylated proteins since they auto-acylate themselves first. From the dataset done by Hemsley and his co-workers, there were only 4 DHHC-proteins (AtPAT10, 13, 19 and 24) isolated instead of

the total 24 putative AtPATs (Batistic, 2012; Hemsley et al., 2013), which means the sensitivity of the experiment not very reliable. Similar case also happened for cellulose synthase complex (CSC). There are totally 18 catalytic subunits in CSC, all of which are supposed to be S-acylated proteins, although only 5 of them were confirmed through individual experiment (Kumar et al., 2016). There were only 2 subunits (AtCESA1 and AtCESA2) were found in the dataset (Hemsley et al., 2013). Based on these ratio (4:24 and 2:18), there are over 3000 S-acylated proteins in Arabidopsis. This makes the journey to map the PATs/substrates more challengeable.

1.5.3 Aim of this project

Despite the characterization of many S-acylated proteins in plants the PATs that carry out their S-acylation are largely unknown. To further our understanding of PAT and protein S-acylation in plants we obtained T-DNA insertion lines for 18 of the remaining 22 putative AtPATs in Arabidopsis. Homozygous T-DNA insertion lines were identified by PCR-based genotyping. Among these lines, loss-of-function mutant plants of three putative PATs, name as AtPAT14, AtPAT21 and AtPLP1 (PAT-like Protein), exhibited dramatic phenotypic alteration compared to the wild-type Arabidopsis plant. For example, *atpat14* mutant plants show semi-dwarf and precocious leaf senescence phenotype; plants lacking AtPAT21 have smaller stature and completely fail to produce seeds; while AtPLP1 loss-of-function mutant *atplp1-1* are sugar dependent for seedling growth, highly sensitive to abscisic acid (ABA) and strongly de-etiolated in the dark.

The aim of this project is to work out the mode of action of these three selected putative PATs in Arabidopsis. To achieve this aim, we first verified their PAT activities *in vitro* and *in vivo,* studied their spatial and temporal expression profiles by RT-PCR and GUS reporter, determined their subcellular localization and studied their biological functions by further characterizing the T-DNA knockout mutant lines of these 3 AtPAT candidates in seedling establishment, growth and development, leaf senescence, and reproduction. Our work supplies important clues for future study to characterize their potential target proteins.

Chapter 2 Materials and Methods

2.1 Plant materials and growth conditions

Arabidopsis thaliana Wild-type, T-DNA insertion and point mutation lines in the Columbia 0 (Col-0) background were obtained from the Arabidopsis Biological Resources Centre (ABRC, http://www.arabidopsis.org/abrc/).

Seeds were surface sterilized by soaking in 70% ethanol for 1 minute followed by 50% thin bleach for 4 minutes, the bleach was removed by washing the seeds with autoclaved MilliQ water (water of Resistivity of 18.2 MΩ•cm at 25 °C) for 4 times.

For plate growth assays, the surface-sterilized seeds were placed on solid half-strength Murashige and Skoog (1/2 MS) containing 0.8% phytoagar (both from Melford, UK). Plates were kept at 4°C in darkness for 3 days to stratify before being transferred to a growth room and grown under long days (LD) with 16h-light (120 μm m^{-2} s^{-1})/8h-dark at 21°C and 60% relative humidity. For growth of Arabidopsis in soil, 7-day-old-plate-grown seedlings were transferred to Levington F2 compost that was surface drenched with 0.02% pesticide (Intercept, Scotts). Seedlings were covered with a transparent plastic lid for 3 days. The lid was subsequently removed and plants were grown to maturity under the same LD conditions.

Seeds were harvested and stored in a cool and dry place for at least 2 weeks before use.

2.2 Genotyping of different mutant lines

2.2.1 DNA extraction

Genomic DNA was extracted by grinding plant tissue in the CTAB extraction buffer. Briefly, approximately 0.1g of fresh leaf tissue was removed and transferred to a 1.5ml microfuge tube, 100μl of CTAB extraction buffer containing 0.14M d-Sorbitol, 0.22M

Tris-HCl pH 8.0, 0.022M Ethylenediaminetetraacetic acid (EDTA) pH 8.0, 0.8M NaCl, 0.8% hexadecyltrimethylammonium bromide (CTAB) and 0.1% n-Laurylsarcosine, was added and the plant material was homogenized with a plastic pestle (SIGMA-ALDRICH, UK) fitted on an electric drill. The homogenate was heated to 65°C for 5 minutes following which 100µl of chloroform was added. The contents were then mixed by vortexing and centrifuged at 12,000 x *g* for 5 minutes. The supernatant (about 80µl) was transferred into a fresh microfuge tube and 100µl of isopropanol was added. The solution was mixed by inverting the tube 5 times and incubated at room temperature for 15 minutes to allow DNA to precipitate. This was followed by centrifugation at 13,000 x *g* for 20 minutes to pellet the DNA and the supernatant was carefully removed using a pipette to avoid disturbing the pellet. The DNA pellet was then washed with 1ml of 70% ethanol and the ethanol was removed followed by centrifugation at 13,000 x *g* for 5minutes. The pellet was dried at 37°C for 10 minutes to remove any trace of ethanol. Finally, the DNA was resuspended in 50µl of sterilized MilliQ water and stored at -20°C for subsequent experiments.

2.2.2 PCR genotyping of T-DNA insertion lines

PCR-based genotyping was carried out to detect the presence of the T-DNA in all T-DNA insertion lines utilising three primers (Fig. 2-1). Gene specific primers LP and RP were used to amplify the wild-type allele of the gene of interest which gives a product of ~ 900bps. Primers BP and RP were used to amplify the T-DNA insertion allele of the gene of interest, generating a product of 410-710 bps. To determine the genotype of a plant both primer pairs were used in two separate PCR reactions. If an amplicon was produced with LP and RP primer pair but not with BP and RP primer pair the line genotyped must be wild-type (WT). Alternatively if an amplification product only appears with BP and RP primers, the genotyped line must be homozygous (HM) for the T-DNA insertion. Plants heterozygous (HZ) for the insertion will produce amplification products with both pairs of primers being used (Fig. 2-1).

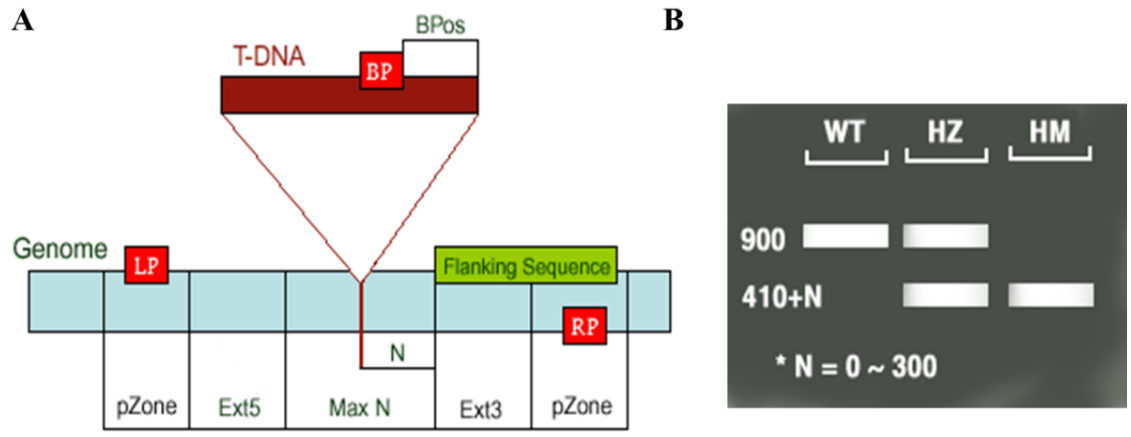

Figure 2-1. PCR-based genetyping for identification of SALK T-DNA insertion plants.
A. Diagram of T-DNA inserted gene. LP, RP - Left, Right genomic primer of gene of interest; BP - T-DNA border primer LB (the left T-DNA border primer); BPos - The distance from BP to the insertion site. Sequences of LP and RP primers are designed using the online tool on SALK website, and several different BP primers (LBb1, LBb1.3 and LBa1) are also listed.
B. Diagram of gel image of fragments amplified from WT, HZ or HM with LP+BP and LB+BP. WT, wild-type, HZ, heterozygous, HM, homozygous, N, Difference of the actual insertion site and the flanking sequence position, usually 0 - 300 bases.
Picture adapted from http://signal.salk.edu/tdnaprimers.2.html

Power Taq DNA Polymerase (Bioteke, China) was used for all PCR reactions. PCR conditions were as follows: step 1, denaturation at 95 °C for 3 minutes; step 2, 95 °C for 30 seconds; step 3, annealing at 50-60 °C (dependent on the primer pairs used) for 30 seconds; step 4, elongation at 72 °C for 1 minute (based on the length of PCR product, ~1000bps/min); steps 2 to 4 were then repeated for 34 times; step 5, final elongation at 72 °C for 10 minutes to make sure DNA is fully extended.

The PCR products were verified on 1% agrose gel by gel electrophoresis and visualised under UV after stained with ethidium bromide.

2.2.3 Sequencing to identify point mutation lines

To identify the point mutation in the lines ordered from ABRC, PCR was carried out using genomic DNA as template and primers crossing the mutation site of each gene. The PCR products were sequenced and compared to sequences in TAIR database. For

heterozygotes, two peaks were present at the mutation site, with one from the wild type allele and another from mutant allele. Only homozygous mutant plants with both mutated alleles were selected to use in the subsequent crossing.

2.2.4 Isolation of double or triple mutants

F1 seeds, generated from crossing two single homozygous mutant parent lines were planted and grown to maturity to obtain F2 seeds. These were germinated and grown to 4-true leaf stage for genotyping. If it is a single T-DNA insertion or point mutation event in both single mutant, there should be 1/16 in the F2 progeny that are homozygous double mutants. The double homozygous mutant plants were identified following genotyping about 50 plants by the method used for identifying single homozygous plants for T-DNA insertion or point mutation in each gene. After the double mutant was acquired, it was again crossed with the single T-DNA or point mutation mutant of the third gene. Similar method was carried out to isolate the triple mutant by confirming homozygosity for T-DNA insertion or point mutation of all three genes.

2.3 Semi-quantitative PCR and real-time PCR

2.3.1 Semi-quantitative reverse transcription PCR (RT-PCR)

Total RNAs were isolated from fresh young leaves of 3-week old wild type and each T-DNA insertion homozygous lines using Trizol (Invitrogen) according to the manufacturer's instructions. RNA integrity was checked by agrose gel electrophoresis. The concentration and RNA purity was analysed by NanoVue 4282 V2.0.3. The ratio of OD260/OD280 was used to determine RNA purity with high quality samples falling in the range 1.7 to 2.0; ratios outside these limits represent RNA contaminated by proteins or organic reagents. RNA was diluted to 100ng/µl with RNase free water and stored at -80°C for later use. Oligo (dT)-primed cDNAs were synthesized from 1µg RNA (10µl) using First-Strand cDNA Synthesis Kit (Transgen, China). Each component of the reaction mix was added as described in the manufacturer's instructions. Samples were heated to 65°C for 5 min to remove the RNA secondary structure, and the reaction mix

was incubated at 42°C for 30 minutes followed by 85°C for 5 minutes. These synthesised cDNA products were stored at -20°C for later use.

PCR was carried out with 2 µl of the cDNA in 20 µl reaction using DreamTaq Green PCR Master Mix (2X) (Thermo Fisher). The reaction was run for 30 cycles under the conditions showed in the protocol of the product. Sequences of all the primers used in RT-PCR are shown in Table S1 in the appendix. The house keeping gene *GAPc* was used as internal control.

2.3.2 Relative quantitative real-time PCR

First strand cDNA was synthesized as described in section 2.3.1. UltraSYBR PCR Mixture (With ROX) (CWBIO, China) was used and the real-time PCR reactions were run on a Stepone Plus real-time PCR system (Applied Biosystems). The relative transcript levels were calculated by the $2^{-\Delta\Delta t}$ method with the *AtEF-1α* gene as an internal control (Livak et al., 2001). At least three replicates were included in each run and the experiments were repeated 3 times. All primers of tested genes are shown in Table S2 in the appendix.

2.4 Plasmid construction

The Gateway System was used to make all the plasmid constructs used in this project. For example, to make the *AtPAT14* construct the attB-flanked coding region (without stop codon) of *AtPAT14* was PCR-amplified using KOD high fidelity polymerase (Novagen) from a construct obtained from Oliver Batistic (Institut für Biologie und Biotechnologie der Pflanzen). Two rounds of PCR reactions with 2 sets of PCR primers were used, one set for gene-specific amplification, (3g60800B1Beg and 3g60800B1EndNS) which includes 14 bases of the attB1 and attB2 sites on the 5' and 3' end of each primer respectively; and a second set to install the complete attB sequences using attB1 and attB2 primers (Table S1). For the first round PCR, a 50 µl PCR reaction containing 10 pmoles of gene-specific primer and appropriate template DNA was carried out and the reaction was carried out following the conditions listed below:

Steps	Temperature (℃)	Time	No. of cycles
Step 1	95	2 minutes	1
Step 2	94	15 seconds	10
Step 3	55	30 seconds	
Step 4	68	1 minute	

In the second round of PCR, 10µl of the 1st round PCR product was added to a 40µl PCR mixture containing 40 pmoles each of attB1 and attB2 and KOD polymerase to amplify the attB-flanked gene product. The following PCR conditions were utilised:

Steps	Temperature (℃)	Time	No. of cycles
Step 1	95	1 minutes	1
Step 2	94	15 seconds	5
Step 3	45	30 seconds	
Step 4	68	1 minute	
Step 5	94	15 seconds	20
Step 6	55	30 seconds	
Step 7	68	1 minute	

To create the *AtPAT14DHHC*^{157}*S* point mutant PCR-based mutagenesis with point mutant primers PAT14DHHC-SFor and PAT14DHHC-SRev were used. For this, two separate PCR reactions (10µl each) were set up, one with the primer pair PAT14DHHC-SFor and 3g60800B1EndNS, and the other with 3g60800B1Beg and PAT14DHHC-SRev. The reactions were run for 10 cycles as described above to generate 2 overlapping DNA fragments. Subsequently, 5µl of each PCR reaction mix was added to a 40µl PCR mixture containing 40 pmoles each of attB1 and attB2 primers and the reaction was run as for the amplification of *AtPAT14*.

Both attB-flanked products of *AtPAT14* and *AtPAT14DHHC*^{157}*S* were purified and

recombined into the attP-containing donor vector pDONR™/Zeo with BP Clonase™ to generate entry clones pDONR-*AtPAT14* and pDONR-*AtPAT14DHHC*^{157}*S* following standard protocols of the manufacturer (Gateway technology). The sequence of *AtPAT14* and its point mutation in *AtPAT14DHHS* were verified by sequencing.

For expression in yeast, they were re-combined into the Gateway^{TM} destination vectors pYES-DEST52 with LR Clonase™ (Figure 2-2) to generate C-terminal V5 tagged *AtPAT14* and *AtPAT14 DHHC*^{157}*S* to facilitate protein detection in Western blot. In the same way, the C-terminal GFP tagged AtPAT14-GFP and AtPAT14 DHHC^{157}S-GFP were created in the plant binary vector pEarlyGate103 vectors (Earley et al., 2006) for expression in plant. This binary vector contains a CaMV35S promoter and the nos terminator.

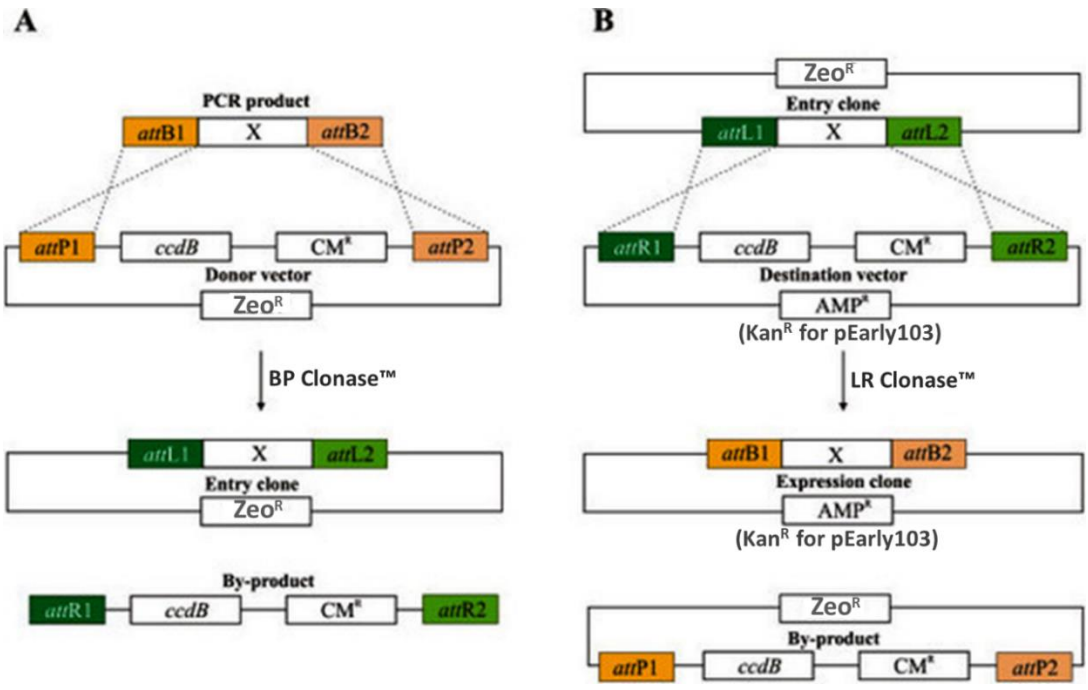

Figure 2-2. Gateway BP and LR reactions.
A. BP recombination of a PCR product "X" flanked by attB sites with a Gateway donor vector with Zeocin resistance.
B. LR recombination of an entry clone bearing a DNA fragment "X" with a Gateway destination vector (Magnani et al., 2006).

Yeast and plant expression vectors for *AtPLP1, PLP1DHHS, AtPAT21 and*

PAT21DHHS were also constructed using the same method as for *AtPAT14* and *AtPAT14DHHS*. Empty vector pESC-Leu and the construct containing AKR1C-S were gifted by Dr. Piers Hemsley from University of Dundee, UK.

For PAT promoter and Gus fusion constructs, each PAT promoter, which was around 1000bp from up stream of its start code, was amplified with a pair of primers pPAT21attB1/ pPAT21attB2 (Table S1). Then the fragment was re-combined to pMDC162 vector (Curtis and Grossniklaus, 2003) through gateway system as described above. The pMDC162 vector was ordered from TAIR.

2.5 *E.coli* transformation

Recombination products were transformed into *E. coli* competent cells (BIOLINE, UK) and the transformed cells were selected (overnight) on solid LB medium containing 1% tryptone, 0.5% yeast extract, 1% NaCl and 1.5% agar with 50 μg/ml Zeocin (for pDONR vector), 50 μg/ml Kanamycin (for pEarlyGate vector) or 100μg/ml Ampicillin (for pYES-DEST52 vector). Positive colonies were screened by PCR with M13F (for pDONR vector), 35S (for pEarlyGate vector), or T7 (for pYES-DEST52 vector) forward primers and gene specific reverse primers.

2.6 Preparation and transformation of competent *Agrobacterium tumefaciens* cell

A single colony of *A. tumefaciens*, strain GV3101 was cultured in 5ml 2xYT medium containing 1.6% Triptone, 1% Yeast extract and 0.5% Nacl with 50μg/ml Rifampin, 100μg/ml Ampicillin and 25μg/ml Gentamicin at 28°C, shaken at 220 rpm for overnight. 1ml culture was transferred into in a 250ml conical flask containing100ml of fresh sterilized 2xYT supplemented with antibiotics as described above and cultured at 28°C, with shaking at 220 rpm until OD600 between 0.6-0.8. The conical flask was cooled down on ice for 30 minutes. The culture was distributed into two 50ml centrifuge tubes equally and the tubes were centrifuged at 4°C, 4,500 x *g* for 10 minutes. The supernatant was discarded and the pellet was re-suspended in 20ml of ice-cold sterile MilliQ water by gently pipetting with a Pasteur's pipette. Following centrifugation at 4°C, 4,500 x *g* for

10 minutes and the supernatant was removed carefully. Again, the pellet was re-suspended with 10ml pre-chilled 10% glycerol and centrifuged as before. The supernatant was removed and the pellet was re-suspended in 1ml of ice-cold 10% glycerol. The cells were then distributed into ice-cold 1.5ml microfuge tubes as 50ul aliquots, immediately frozen in liquid nitrogen, and stored at -80°C for later use.

The plasmid DNA containing the relevant plant binary expression constructs were transformed into *A. tumefaciens* competent cells by electroporation. For this, a 50µl aliquot of competent cells were defrosted on ice and transferred to a 0.1cm electroporation cuvette and gently mixed with 2µl ultraclean plasmid DNA. The MicroPulser (Bio-Rad) was set to "Ec1" and the cuvette was placed between the contacts in the base of the chamber slide. After pulsing once the cuvette was removed from the chamber and 1ml of 2xYT medium was added immediately. The cells were quickly but gently resuspended by inverting 5 times and left at 28°C for 3 hours. The culture was then transferred to a microfuge tube and spun at 6000 x *g* for 1 minute. The supernatant was removed leaving approximately 80µl to re-suspend the pellet. This was spread on a 2xYT agar plate containing 25µg/ml Gentamicin, 50µg/ml Rifampicin, 50µg/ml Kanamycin, 100µg/ml Ampicillin. The plate was incubated at 28°C for 2-3 days until large colonies could be seen.

2.7 Complementation and Auto-Acylation in yeast

2.7.1 Yeast transformation

Wild type yeast stain BY4741 (MATa his3Δ1 leu2Δ0 met15Δ0 ura3Δ0) and their knock-out mutant *akr1*, *pfa3* or *swf1* were obtained from EUROScarf (http://www.euroscarf.de/search.php?name=Order). Single colonies of BY4741 or akr1 (pfa3 or swf1) were picked or 10µl of their frozen glycerol stock culture was transferred to 3ml of YPD medium (1% yeast extract, 2% peptone and 2% D-glucose) and cultured at 25°C overnight with shaking at 220 rpm. 1ml of culture was harvested by centrifugation at 1,000 x *g* for 5min and the supernatant was discarded. 10µl of 10µg/µl ssDNA (Sigma,

heated at 95°C for 5min and cooled down on ice before use) was added to the cell pellet and the mixture was vortexed. Following this 10µl of plasmid (empty vectors or constructs containing the target gene) was added and the mixture was vortexed. Next, 0.5ml of LiPEG (0.1M LiAc/TE and 40% PEG) was added and the content was mixed by vortexing. The mixture was left on bench at room temperature overnight and centrifuged at 1,000 x *g* for 5 minutes. The cells were re-suspended with 100µl of 1M sorbitol and 50µl of the cells were transferred and spread evenly on solid basic yeast selective media: 1.0% agar, 0.17% YNB, 0.5% (NH4)2SO4 and 2% D-glucose with 50µg/ml histidine, leucine and methionine respectively for pYES-DEST52 constructs selection; 50µg/ml histidine, methionine and 100µg/ml uracil respectively for pESC-Leu constructs selection; 50µg/ml histidine and methionine for transgenic strains with both above constructs. The plate was incubated at 25°C for approximately 3 days until colonies appeared.

2.7.2 Growth complementary test of yeast *pat* mutants

One colony of each BY4741 and *akr1* that harbour the empty vectors pYES-DEST52 and pESC-Leu as positive and negative controls (BY4741 and akr1), and colonies harbouring the pYES-DEST52:AKR1C-S, PAT14:pESC-Leu, PAT14:AKR1C-S, PAT14C-S: pESC-Leu, PAT14C-S:AKR1C-S respectively in the *akr1* background (*akr1*, akr1-PAT14 and akr1-PAT14C157S) were picked. These were cultured in 3 ml of liquid basic yeast media with 2% D-raffinose added instead of D-glucose, at 25°C for two days with shaking at 220 rpm. For growth tests, all four samples were diluted with sterile water to OD600=1.0. Following this, a series of dilutions including 1/5, 1/10, 1/20, 1/40 were made. 8µl of each dilution was spotted onto two identical solid basic yeast media plates with 2% galactose instead of D-glucose to induce protein expression. One of the plates was incubated at 25°C and another one at 37°C. Images of the plates were obtained on the 4th day after scanning with an Epson flatbed scanner.

For observation of cell morphology, 20µl of culture was transferred into a 3ml of basic yeast media containing 2% galactose instead of D-glucose and grown at 37°C for 2 more days. 1ml of cells from each sample was stained with 2.5 µg/ml DAPI (final

concentration) at room temperature for 30 minutes on a rotating mixer. The cells were observed by DIC light microscopy and under UV using a 90i Eclipse microscope, and images were captured using a Nikon C1 LSCM camera.

Same method was used for the yeast growth assays of AtPLP1 or AtPLP1DHHS harbouring yeast cells (BY4741:pYES-DEST52, *akr1*:pYES-DEST52, *akr1*:PLP1, *akr1*:PLP1DHHS), and AtPAT21 or AtPAT21DHHS containing cells (BY4741:pYES-DEST52, *akr1*:pYES-DEST52, *akr1*:PAT21, *akr1*:PAT21DHHS). BY4741:pYES-DEST52, *akr1*:pYES-DEST52 acted as positive and negative control, resctively.

For complementation studies in *pfa3* and *swf1*, the transgenic strains of the diluted cultures of BY4741:pYES-DEST52, *pfa3* or *swf1*:pYES-DEST52, *pfa3* or *swf1*:PLP1, *pfa3* or *swf1*:PLP1DHHS were spotted on the same yeast selective media containing 0.85M NaCl. They were cultured at 28°C for 3 days and the phenotypes were visualised and captured with the scanner.

2.7.3 Auto-acylation test in yeast

Auto-acylation test in yeast was carried out by Acyl-RAC (resin-assisted capture) (Forrester et al., 2011). With AtPAT14 as an example, total proteins were extracted from *akr1* yeast cells expressing AtPAT14 and AtPAT14DHHC^{157}S. Free thiols were first blocked with methyl methanethiosulfonate (MMTS), and thioesters were then cleaved with neutral hydroxylamine (NH_2OH). The newly formed thiols were captured on thiopropyl sepharose beads (Sigma). After being washed for at least five times with binding buffer, captured proteins are eluted with reductant and analyzed by SDS-PAGE. AtPAT14 and ATPAT14DHHC^{157}S were detected by western blotting with anti-V5 primary and HRP-conjugated secondary antibodies (Bethyl).

2.8 Plant transformation and selection

Agrobacterium tumefaciens harbouring the specific gene constructs were transformed to *Arabidopsis thaliana* ecotype Columbia 0 by the floral dipping method of

Clough and Bent (1998) with two rounds of dipping at 5-day intervals. To select transformants approximately 10,000 seeds collected from the dipped plants were surface sterilized, germinated and grown on the 1/2MS media containing 100μg/ml Cephalosporins (kill the Agrobacteria) and 5μg/ml of active ingredient phosphinothricin (PPT) present in the Basta® herbicide for 7 days. Positive transgenic lines could grow normally and developed true leaves, however the non-transgenic wild-type Arabidopsis plants became yellow and no true leaves appeared. Transgenic seedlings were then transferred to the soil and grown in the growth-room under the LD conditions as described before. Randomly selected transgenics were also screened by PCR with primers based on the vector (35S) and gene-specific reverse primers.

2.9 Microscopy

2.9.1 Subcellular localization

For the subcellular localization of AtPAT14 transgenic *pat14-1* plants complemented by 35S:AtPAT14-GFP were crossed with mCherry tagged marker Wavelines (Geldner et al., 2009). Primary roots and cotyledons of 7-day-old seedlings from the crossed F1 progeny were observed with the excitation/emission at 488nm/530nm for GFP and excitation/emission at 559nm/570nm for mCherry using 90i Eclipse microscope and imaged with EZ-C1 software, and/or Leica (for PAT14, was done in Oxford Brookes University). Images were processed and merged by using the Image J software.

2.9.2 Visualization and imaging of Pollen tubes

2.9.2.1 Aniline blue staining of in vivo pollen tubes

Pistils of 5 and 15 hours after being pollinated were excised and submerged in fixing solution (10% acetic acid, 30% chloroform, 60% ethanol) overnight. The fixative was then removed and pistils were rinsed in 50mM potassium phosphate buffer (pH7.0) twice for 5 minutes each. 4M NaOH was added and incubated for 15 minutes at room temperature to soften the tissue. NaOH was removed and again the tissue was rinsed in

50mM potassium phosphate buffer twice. The pistils were stained in Aniline Blue buffer (0.05% Aniline Blue in 0.15M K2HPO4) for 1 hour and the stained pistils were washed in 50 mM potassium phosphate as before. The potassium phosphate buffer was then carefully removed and a drop of mounting media (50% glycerol made by 50 mM potassium phosphate pH7.0 buffer) was applied. The pistils with some mounting media was transferred onto a glass slide and covered with a coverslip. The pistils were gently squashed to expose the pollen tubes. Visualization was carried out under UV light using a 90i Eclipse microscope and the images were captured by Nikon C1 LSCM (Nikon, Tokyo, Japan).

2.9.2.2 Semi-in vivo pollen tube guidance assay

For semi-*in vivo* pollen tube guidance assay, WT pollen grains were deposited on both WT and *atpat21* stigma. After 30 minutes the pollinated stigmas including the styles were carefully cut with a sharp scalpel and transferred to pollen tube growth media containing 18% sucrose, 0.8% agarose, 0.01% boric acid, 0.03% casein enzymatic hydrolysate, 1mM CaCl2, 1mM Ca(NO3)2, 1mM KCl, 0.25mM spermidine, 0.01% myo-inositol and 0.01% ferric ammonium citrate (adapted from Rodriguez-Enriquez, 2013). The ovules from fully opened flowers of wild-type and homozygous *atpat21* mutant plants were extracted and placed on the media within 1-2 cm away from the style. These were cultured at 24ºC for 16h. The pollen tubes were then observed under the dissecting microscope and images were taken as before.

2.9.2.3 In vitro pollen germination

Mature pollen grains from WT and heterozygous AtPAT21/atpat21 were collected and placed on freshly made pollen growth media as described above and incubated at 24℃ for overnight. Pollen tube growth was checked under the dissecting microscope. The number of germinated pollen grains were counted and calculated as percentage of total pollen grains placed on the media.

2.9.3 Microscopy of anthers, ovules and pollen grains

Anthers or ovules (both unfertilized and fertilized) were submerged in clearing solution (Chloral hydrate (g): Glycerol (mL):ddH2O (mL) = 8:1:3) for several hours (vary depending on the tissues used), then observed using a 90i Eclipse microscope as above. Freshly collected pollen grains were suspended in distilled water and directly observed under microscope; or stained for about 10 minutes in DAPI staining solution (0.1 M sodium phosphate, pH 7.0, 1 mM EDTA, 0.1% Triton X-100, and 0.5 μg/mL DAPI) and observed under UV light using 90i Eclipse microscope and images were captured.

2.9.4 Scanning electronic microscopy (SEM)

For SEM of shoot apical meristem (SAM), tissues were fixed with 4% paraformaldehyde, and 5% glutaraldehyde, in 0.1M CaC12 and 0.1M cacodylate buffer (pH 7.2) at 4°C for 16 h. The samples were rinsed with 0.1M cacodylate buffer (pH 7.2), and post-fixed 1% osmium tetroxide in the same buffer for 2h at room temperature. They were then freeze-dried, coated with gold and observed by a JOEL scanning electron microscope (JSM-6480-LV). For observing the pollen grains, the fully opened flowers were directly freeze-dried, coated with gold and observed.

2.9.5 Visualization and imaging of lipid droplets

5-day etiolated seedlings were immersed in 10μg/mL Nile Red for 5 minutes (Chen et al., 2009), the stained hypocotyls were observed under 530 nm and 583 nm excitation and emission laser using 90i Eclipse microscope (Nikon).

2.10 Chlorophyll content measurement

To estimate chlorophyll content, the methods in Porra et al (1989) and Katsiarimpa et al (2013) were followed. Briefly, seedlings (10 mg) or fresh rosette leaves (20 mg) were homogenised in 500 μl of 96% ethanol in pre-weighed 1.5 ml microfuge tubes. After centrifugation the supernatant was transferred to a fresh tube and the OD at 470, 649 and

665nm was recorded. The chlorophyll content is the sum of chlorophyll a (13.95 x OD665)-(6.88 x OD649) plus chlorophyll b (24.96 x OD649)-(7.32 x OD665), which is expressed as μg/mg fresh weight.

2.11 GUS staining

Tissues from AtPAT21promoter:GUS transgenic plants were stained in the staining buffer (100mM Sodium phosphate buffer, pH7.0; 10mM EDTA; 0.1% triton X-100; 1mM K3Fe(CN)6; 2mM X-Gluc) at 37°C for overnight, then the samples were cleared with 100% alcohol for 12 hours for several times (Jefferson, 1987).

2.12 Carbon deficiency and phytohormone treatment

2.12.1 Carbon deficiency treatment

The carbon deficiency assay was carried out according to Hanaoka et al (2002). Briefly, seeds of WT, pat14-1 and pat14-2, atg5-1 and atg9-2 were germinated and cultured vertically on ½ MS plus 1% sucrose under LD for 7 days. They were then transferred to ½ MS only and incubated in the dark for a further 7 days.

2.12.2 SA, JA and ABA treatment

Seeds were germinated and grown on ½ MS plus 1% sucrose under LD for 4 days. The seedlings were transferred to ½ MS without or with ABA, JA and SA and left to grow for up to 3 weeks before being scanned and weighed.

2.12.3 GA and cytokinin treatment

For GA treatment, WT and *atplp1* seeds were germinated and grown in the dark on the ½ MS+1% sucrose media with 0, 50 μM GA3 or 1 μM PAC (paclobutrazol) for 9 days. For cytokinin treatment, WT and *atplp1* were grown on the ½ MS+1% sucrose media with 0, 1, 5 and 10 μM 6-BA (6-Benzylaminopurine) in the dark for 11 days or in the LD condition for 8 days.

2.12.4 Germination sensitivity test to ABA

Surface sterilized WT and *atplp1* seeds were spread on ½ MS (+ 1% sucrose) containing 0 or 1 μM ABA, then they were grown in the dark or LD condition. After 4 days, the germination rates of WT and *atpa15* in each condition were calculated.

2.13 Phytohormone analysis

2.13.1 ABA, JA, OPDA and SA analysis

Each hormone determination was measured in triplicate using samples derived from 7-day-old seedlings and the 7th and 8th leaves of 30-day-old plants. ABA, JA and SA extractions were performed on 3mg of powdered, freeze-dried tissue exactly as detailed in Forcat et al (2008). OPDA (12-oxophytodienoic acid) was measured according to Dave et al (2011) using OPDA (Larodan) as a standard. All the measurements were carried out by Prof. Murray Grant in University of Exerter.

2.13.2 Cytokinin (CK) analysis

Different types of cytokinins were measured in 9-day and 11-day old seedlings grown in the dark by Dr. Ondřej Novák (Palacký University and Institute of Experimental Botany ASCR, Czech Republic). The method was described in Novák et al., 2008.

2.14 Fatty acids analysis

Fatty acids were extracted and methylated as follows. 40 etiolated seedlings (5-day old) for each sample were collected and homogenated in a 1.5ml eppendorf tube then the sample were freeze dried to constant weight. This was transferred to a 3ml glass vial with 1ml methylation solution (10% H_2SO4 in methanol). 10μl 0.5mM heptadecanoic acid (as internal standard) was added into the vial followed by heat treatment at 85°C for 1 hour and then the vial was cooled down to room temperature. After that, 1ml 1% NaCl and 0.5ml hexane were added and mixed well by vortexing, and leave the vial on the bench for 10 minutes or longer. The sample will separate into 2 phases at 5000rpm for 10min

and the upper hexane phase was transferred to a small GC vial (concentrate the sample by drying under a stream of N2 gas if necessary). The fatty acid methyl esters were analyzed by gas chromatography as described by Qi et al. (2004). Triacylglycerol (TAG) was quantified with C20:1 as a marker (Thazar-Poulot et al., 2015).

2.15 Secondary structures and conserved domains analysis of PATs

TMDs were analysed through TMHMM 2.0 (http://www.cbs.dtu.dk/services/TMHMM/). Multiple sequence alignments were performed using Clustal Omega (http://www.ebi.ac.uk/Tools/msa/clustalo/). All programmes were used in default settings.

2.16 Statistic analysis

One-way ANOVA and Tukey's HSD test were applied to compare three or more series of data with Minitab, where different letters mean significantly different to each other, $p<0.05$. Student's *t*-test was used to compare two series of data with Excel, where * shows the significant difference, p values were given in each figure legends. All the graphs were edited in Excel

Chapter 3 AtPAT14: A Specific Role for Palmitoylation in Leaf Senescence in Arabidopsis

3.1 Introduction

Plant senescence is the process by which the whole individual for annual plants, or individual organs for perennials are programmed to die (Rogers, 2015). An important characteristic of senescence is that the nutrients from organs which are no longer needed are removed to other parts of the plants where they can be re-utilized for growth or storage (Guiboileau et al., 2010). In Arabidopsis, leaf senescence, during which the nutrients in leaves are transferred to the young leaves or reproductive organs, is important for optimal growth, fruit and seeds development. Different from the floral senescence which is closely related to pollination (Rogers, 2013), leaf senescence is easily induced by abiotic and biotic stress signals in the environment including dark, cold, heat, osmotic and oxidative stress, wounding, heavy metal stress and pathogens (Guo and Gan, 2006; Lim et al., 2007). Senescence can also be regulated by many phytohormones which include positive regulators abscisic acid (ABA), salicylic acid (SA), jasmonic acid (JA), ethylene and brassinosteroids, and negative regulators cytokinins (CKs), gibberellins (GAs) and auxins (Rogers, 2015; Schippers, 2007; Richmond and Lang 1957). It has been demonstrated recently that autophagy also plays important roles in chloroplast degradation and nutrient remobilization (Avila-Ospina et al., 2014) as evidenced by early leaf senescence phenotype exhibited by autophagy gene-disrupted mutants (Hanaoka et al., 2002; Li et al., 2014).

As the major photosynthetic organs the green leaves in plants are the nutrient provider for plant growth, development and seed production (Bleecker and Patterson, 1997). Leaf senescence is the final stage of leaf development, during which cellular structures are gradually degenerated started from chloroplast and ended with mitochondria and nucleus (Lim et al., 2003; Noodén, 2012). It is an important process during the plant life cycle which allows for nutrient re-distribution to support new growth

(Guiboileau et al., 2010; Avila-Ospina et al., 2014). However, the molecular mechanism of leaf senescence is largely unknown. Studies show that during leaf senescence many genes encoding proteases are up-regulated including serine proteases, cysteine proteases, aspartic proteases metalloproteases and threonine proteases (Feller et al., 1977; Roberts et al., 2012). For example, SAG12, a cysteine protease, commonly used as a leaf senescence reference gene is induced at the onset of leaf senescence. Others, such as aspartic protease CND41 that might be involved in Rubisco degradation (Kato et al., 2004), FtsH metalloprotease family that are involved in the degradation of chloroplast (Wagner et al., 2011) are up-regulated. On the other hand, leaf senescence is also accompanied by down-regulation of protein synthesis and photosynthesis related genes (Lim et al., 2007). A recent genome-wide analysis showed that senescence-associated genes are functionally conserved in different plant species, indicating a similar pathway is commonly used in all plants (Breeze et al., 2011).

SA is a critical signal that regulates many different aspects of plant growth and development. Perhaps most importantly it is well known for its roles in pathogen response and pathogen-mediated cell death (Delaney et al., 1994; Dempsey et al., 2012). Because senescence also results in cell death it is not surprising that SA is also involved in age-dependent senescence and senescence-associated cell death (Morris et al., 2000). The fact that the expression of some senescence associated genes, such as *PR1a* and *SAG12*, were hugely decreased in the SA signalling defective mutant *npr1* and the SA biosynthesis defective *NahG* transgenic line clearly demonstrate that leaf senescence is closely associated with SA signalling pathways (Wu et al., 2012).

To investigate the pre-mature leaf senescence phenotype exhibited in the AtPAT14 loss-of-function mutant plants we first measured the chlorophyll content and monitored the expression levels of the senescence related genes *SAG12*, *SAG101* and *PR1*. Next, we carried out experiments to establish the involvement of SA, ABA, JA and autophagy pathways. We found that early senescence in *atpat14* was caused by the over-production of SA and enhanced response to SA signalling. Our results revealed a new mechanism of

protein palmitoylation that is involved in leaf senescence via its negative regulation of SA pathways.

3.2 Published data is attached

Protein *S*-Acyltransferase 14: A Specific Role for Palmitoylation in Leaf Senescence in Arabidopsis[1][OPEN]

Yaxiao Li, Rod Scott, James Doughty, Murray Grant, and Baoxiu Qi*

Department of Biology and Biochemistry, University of Bath, Claverton Down, Bath BA2 7AY, United Kingdom (Y.L., R.S., J.D., B.Q.); and College of Life and Environmental Sciences, University of Exeter, Stocker Road, Exeter EX4 4QD, United Kingdom (M.G.)

ORCID ID: 0000-0002-9425-935X (B.Q.)

The Asp-His-His-Cys-Cys-rich domain-containing Protein *S*-Acyl Transferases (PATs) are multipass transmembrane proteins that catalyze *S*-acylation (commonly known as *S*-palmitoylation), the reversible posttranslational lipid modification of proteins. Palmitoylation enhances the hydrophobicity of proteins, contributes to their membrane association, and plays roles in protein trafficking and signaling. In Arabidopsis (*Arabidopsis thaliana*), there are at least 24 PATs; previous studies on two PATs established important roles in growth, development, and stress responses. In this study, we identified a, to our knowledge, novel PAT, AtPAT14, in Arabidopsis. Complementation studies in yeast (*Saccharomyces cerevisiae*) and Arabidopsis demonstrate that AtPAT14 possesses PAT enzyme activity. Disruption of *AtPAT14* by T-DNA insertion resulted in an accelerated senescence phenotype. This coincided with increased transcript levels of some senescence-specific and pathogen-resistant marker genes. We show that early senescence of *pat14* does not involve the signaling molecules jasmonic acid and abscisic acid, or autophagy, but associates with salicylic acid homeostasis and signaling. This strongly suggests that AtPAT14 plays a pivotal role in regulating senescence via salicylic acid pathways. Senescence is a complex process required for normal plant growth and development and requires the coordination of many genes and signaling pathways. However, precocious senescence results in loss of biomass and seed production. The negative regulation of leaf senescence by AtPAT14 in Arabidopsis highlights, to our knowledge for the first time, a specific role for palmitoylation in leaf senescence.

Protein *S*-Acyl Transferases (PATs), which were initially identified from yeast (*Saccharomyces cerevisiae*; Lobo et al., 2002; Roth et al., 2002), catalyze protein *S*-acylation. Protein *S*-acylation, commonly known as *S*-palmitoylation, is a posttranslational lipid modification in which long chain fatty acids, usually palmitate, attach reversibly to cysteines (Resh, 2006; Greaves and Chamberlain, 2011). *S*-acylation, often coupled with myristoylation or prenylation, is important for cellular protein sorting, vesicle trafficking, activation state control, protein stability, microdomain partitioning of proteins, and protein complex assembly (Greaves and Chamberlain, 2007; Baekkeskov and Kanaani, 2009; Charollais and Van Der Goot, 2009; Hemsley, 2009; Fukata and Fukata, 2010; Hemsley et al., 2013). Recent large-scale proteomics studies indicate that many proteins are palmitoylated in eukaryotic organisms, with at least 50 occurring in yeast (Roth et al., 2006), more than 700 in mammals (Martin and Cravatt, 2009), and more than 500 in Arabidopsis (*Arabidopsis thaliana*; Hemsley et al., 2013).

PATs are eukaryote-specific proteins with a highly conserved "signature" catalytic Asp-His-His-Cys (DHHC)-Cys-rich domain (CRD) of approximately 50 amino acids. PATs are transmembrane proteins containing 4-6 membrane spanning domains and possess highly variable N- and C-terminal cytosolic domains that are essential for their substrate specificity (Huang et al., 2009; Greaves et al., 2010; González Montoro et al., 2011; Howie et al., 2014). Different numbers of DHHC-CRD PATs have been found in various species, such as seven in yeast (Putilina et al., 1999), 23 in mammals (Fukata et al., 2006), and 24 in Arabidopsis (Hemsley and Grierson, 2008; Batistic, 2012).

To date, research on plant PATs has been very limited compared to humans and yeast. Analysis of the 24 Arabidopsis PATs shows that most of them have a broad and constant expression pattern at different developmental stages (Batistic, 2012). Transient expression of AtPAT-GFP in tobacco (*Nicotiana benthamiana*) showed that Arabidopsis PATs have very complex cellular membrane localization patterns where half of them reside in the plasma membrane and others in the endoplasmic reticulum, Golgi, vesicles, and tonoplast (Batistic, 2012), indicating that the plasma membrane is the main palmitoylation site in higher plants. This contrasts with mammals where the Golgi is the main site for the palmitoylation machinery (Ohno et al., 2006).

At present, the biological functions of only two Arabidopsis PATs, TIP1/AtPAT24 (Hemsley et al.,

[1] This work was supported by the National Natural Science Foundation of China (grant no. 31170233 to B.Q.).

* Address correspondence to bssbq@bath.ac.uk.

The author responsible for distribution of materials integral to the findings presented in this article in accordance with the policy described in the Instructions for Authors (www.plantphysiol.org) is: Baoxiu Qi (bssbq@bath.ac.uk).

B.Q. designed the research; Y.L., B.Q., and M.G. performed research and analyzed the data; B.Q., R.S., and J.D. supervised Y.L.; B.Q. and Y.L. wrote the article with input from all the authors.

[OPEN] This article can be viewed without a subscription.

www.plantphysiol.org/cgi/doi/10.1104/pp.15.00448

2005) and AtPAT10 (Qi et al., 2013; Zhou et al., 2013), have been studied in any detail. AtPAT24 was confirmed as an *S*-acyltransferase based on rescue of both morphological and temperature sensitive defects in the yeast PAT knockout mutant *akr1*. The loss-of-function mutants exhibited defects in control of cell size, pollen tube and root hair growth, and cell polarity (Hemsley et al., 2005). Transient expression in tobacco localized AtPAT24 to the Golgi (Batistic, 2012). Functional characterization of AtPAT10 confirmed enzyme activity in vitro and in vivo (Qi et al., 2013). *AtPAT10* expression appears ubiquitous, being detectable in all tissues tested throughout growth and development, with the protein predominately localizing to the Golgi and tonoplast (Batistic, 2012; Qi et al., 2013; Zhou et al., 2013). Three T-DNA insertion mutant alleles for AtPAT10 were identified and all exhibited very similar pleiotropic phenotypes, including defects in cell expansion and cell division, vascular patterning, fertility, and also hypersensitivity to salt stress (Qi et al., 2013; Zhou et al., 2013).

Here, we report the identification and characterization of a further PAT, AtPAT14, in Arabidopsis. Two independent transcriptionally null T-DNA insertion lines of *AtPAT14* were found to exhibit dramatically reduced stature and early senescence. Leaf senescence is a highly integrated and indispensable feature of the plant life cycle. During senescence, cells undergo orderly changes that mobilize and export valuable nutrient resources to the plant body before the leaf dies or is shed. Senescence is a complex process involving the expression of thousands of genes and multiple signaling pathways (Buchanan-Wollaston et al., 2005; van der Graaff et al., 2006). Many external or internal cues, such as drought, salinity, nutrient deficiency, pathogen attack, imbalance in phytohormones, and defects in autophagy, can trigger precocious leaf senescence, resulting in reduced yield and crop quality. However, the precise mechanisms regulating leaf senescence remain unclear.

We found that the early senescence phenotype displayed by *AtPAT14* loss-of-function mutants is not related to abscisic acid (ABA), jasmonic acid (JA), or autophagy, but is associated with a role for PAT14 in the regulation of leaf senescence operating through salicylic acid (SA). Our results provide new insights into the mechanism of leaf senescence highlighting protein palmitoylation as a prominent regulatory component in this pathway.

RESULTS

Arabidopsis PAT14 Shares Homology with Other Known DHHC-PATs

The *AtPAT14* (At3g60800) gene is 2,420 nucleotide bp long, consisting of seven exons and six introns. It contains an open reading frame of 924 nucleotides, encoding a putative protein of 307 amino acids, which has a predicted M_r of 34.7 kD. *AtPAT14* is most similar to *AtPAT13*, sharing 66% amino acid identity (Batistic, 2012; data not shown). Protein sequence alignments with other DHHC-PATs from Arabidopsis, yeast, and humans show that *AtPAT14* shares high identity only within the DHHC-CRD domain (Supplemental Fig. S1). The TMHMM2.0 online software predicts that AtPAT14 has four transmembrane domains between the 21st to 43rd, 58th to 80th, 173rd to 195th, and 210th to 232nd amino acids, respectively. The conserved DHHC-CRD domain lies between the third and fourth transmembrane domains and is essential for *S*-acyltransferase activity in other PATs. This domain and the N and C termini are predicted to be cytosolic (Supplemental Fig. S1).

AtPAT14 Is Expressed Ubiquitously Throughout Growth and Development

Reverse transcription (RT)-PCR on total RNA isolated from seedlings and various parts of the mature plant revealed *AtPAT14* expression at high levels in all tissues (Supplemental Fig. S2). This is in agreement with publicly available gene expression data analyzed using Genevestigator software and previous reports (Batistic, 2012; data not shown).

Identification of AtPAT14 T-DNA Insertion Knockout Lines

Previous studies on two of the 24 members of the Arabidopsis PAT family revealed their diverse and important functions (Hemsley et al., 2005; Qi et al., 2013; Zhou et al., 2013). To expand our understanding of *S*-acylation in plants, we searched the available Arabidopsis mutant collections and identified two Arabidopsis T-DNA insertion lines, SALK_026159 and GK-153A10, for *AtPAT14*. Sequencing of the PCR products amplified from the junction of the T-DNA insertion sites confirmed the position of the T-DNA at nt467 and nt389 near the end of the first exon of *AtPAT14* for SALK_026521 and GK-153A10, respectively (Fig. 1A). No transcript was detected for the full coding region and the region across the T-DNA insertion sites in both lines of the homozygous mutant plants, although truncated transcripts were detected upstream and downstream of the T-DNA insertion sites (Fig. 1B), indicating they are most likely transcriptionally null. They were hence named *atpat14-1* for SALK_026159 and *atpat14-2* for GK-153A10, respectively. Both lines were back-crossed to wild type for two generations, and the mutants recovered were used for subsequent analysis.

Characterization of AtPAT14 Loss-of-Function Mutants

The most striking phenotype of both mutant lines is that they exhibited early senescence. At 4 weeks after sowing, when all the rosette leaves of wild type were still green and healthy, the first pairs of true leaves of

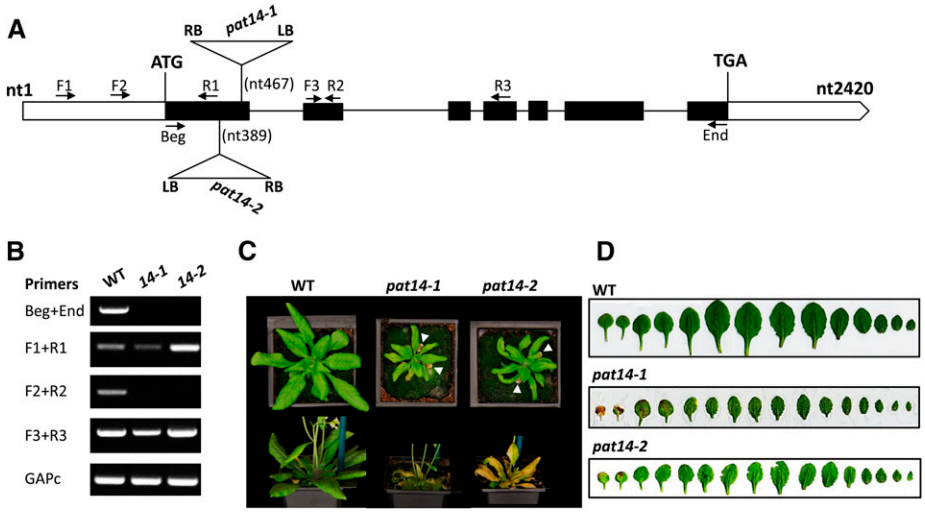

Figure 1. Molecular characterization of the *atpat14-1* (SALK_026159) and *atpat14-2* (GK-153A10) alleles. A, Schematic presentation of the *AtPAT14* gene (solid boxes, exons; empty boxes, untranslated regions; lines, introns) and the positions of the T-DNA in *atpat14-1* and *atpat14-2*. Arrows, Primers used for RT-PCR; RB, right border; LB, left border. B, Amplification of different regions of the *AtPAT14* transcript in wild-type, *atpat14-1*, and *atpat14-2* plants using primers according to A. The *GAPc* transcript served as a control. C, Four- (top) and 6-week-old (bottom) plants of wild-type Columbia-0, *atpat14-1*, and *atpat14-2*. White arrowheads highlight leaf senescence in mutants. D, Leaf line-ups of 5-week-old wild-type Columbia-0, *atpat14-1*, and *atpat14-2* plants.

both mutants were already yellow (Fig. 1, C and D). *atpat14-1* aged earlier than *atpat14-2*. The yellowing of the leaves progressed rapidly in the mutants, and the majority of them become completely yellow at 5 weeks. At this stage, wild-type plants only just started to show signs of aging with the first pair of true leaves turning yellow.

Both *atpat14-1* and *atpat14-2* plants are much smaller (*atpat14-1* is even smaller than *atpat14-2*) than wild type with smaller leaves, shorter and fewer branches in the primary inflorescence, and fewer siliques on the main inflorescence stem (Fig. 1; Supplemental Table S1). The appearance of *atpat14* flowers is similar to wild type, although the petals are smaller. The siliques are shorter with fewer seeds in both *atpat14* mutant lines (Supplemental Fig. S3). The mutants have smaller cells in the leaves and petals than wild type (Supplemental Fig. S4; Supplemental Table S1). However, the cell number in the petals is similar between the wild type and the mutants (Supplemental Table S1), indicating that the smaller stature of *atpat14* is due to smaller cells.

AtPAT14 Is an *S*-Acyltransferase

To confirm whether AtPAT14 is an *S*-acyltransferase and whether DHHC is the catalytic domain, we expressed *AtPAT14* and a version carrying a point mutation in the DHHC domain (*AtPAT14DHHC*^{157}*S*) in the yeast PAT knockout mutant *akr1*. Previous studies show that *akr1* is sensitive to high temperature (37°C) and grows poorly, having elongated multinucleate cells (Feng and Davis, 2000). Our observations showed that the majority of *akr1*-AtPAT14 transgenic cells were similar to wild type being round with one nucleus, although they were typically much larger. However, *akr1* cells carrying AtPAT14DHHC^{157}S were elongated with multiple nuclei (arrows in bottom right panel, Fig. 2A) and resembled *akr1*. The growth assay revealed that AtPAT14 can partially rescue the growth defect of *akr1* as more growth (though less than wild type) was observed when it was expressed in *akr1* compared to *akr1* alone. However, transgenic *akr1* expressing AtPAT14DHHC^{157}S failed to grow (Fig. 2B).

A recent study has shown that the restoration of temperature sensitivity of *akr1* requires both the ankyrin repeats and *S*-acyltransferase function of the AKR1 protein (Hemsley and Grierson, 2011). PAT14 does not have ankyrin repeats and, as such, cannot complement the ankyrin repeat mediated phenotypes. To see if the incomplete complementation of *akr1* by PAT14 was due to the lack of ankyrin repeats at its N terminus, we cotransformed PAT14 with a construct containing the *S*-acyl transferase null form of AKR1 (AKR1C-S), thereby providing the AKR1 ankyrin repeat function (Hemsley and Grierson, 2011). As demonstrated in Supplemental Figure S6, more growth was observed compared to *akr1* cells expressing AtPAT14 alone (PAT14/*akr1*). However, the growth was still less than that found for wild type. A small and comparable amount of growth was also found when expressing AKR1C-S (ANK), or coexpressing AtPAT14C^{157}S and AKR1C-S (ANK+PAT14C^{157}S) in *akr1* cells, indicating that this growth was due to the ankrin repeats of AKR1 as there was no rescue at all when expressing

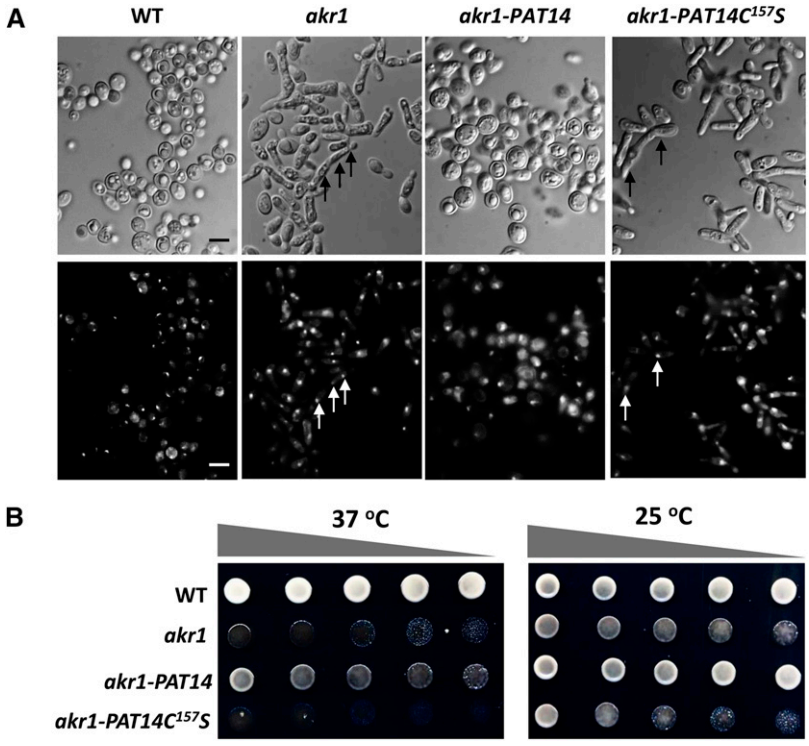

Figure 2. Arabidopsis AtPAT14 has *S*-acyltransferase activity. AtPAT14, but not AtPAT14C^{157}S, can partially rescue growth defects of the yeast temperature sensitive *akr1* mutant that lacks the DHHC-PAT AKR1. A, DIC light (top) and UV microscopy of DAPI (1 μg/mL)-stained cells (bottom) of all four genotypes grown at 37˚C. Arrows indicate multiple nuclei. B, Growth test. At nonpermissive temperature 37˚C (left), wild-type (WT) yeast grew well but *akr1* did not. This growth defect was less obvious at 25˚C because all genotypes grew well (right). Expressing AtPAT14 in *akr1* (PAT14/*akr1*) largely restored the growth inhibition by 37˚C, but expressing AtPAT14C^{157}S (PAT14C^{157}S/*akr1*) did not. Five microliters of 10-fold serial dilutions from 1 OD_{600} cells were spotted on solid medium supplemented with 2% Gal and grown at 25˚C or 37˚C for 3 d. Bars, 10 μm. Cells were transformed with empty vector pYES2 (wild type and *akr1*) or with AtPAT14 and AtPAT14C^{157}S (PAT14/*akr1*, PAT14C^{157}S/*akr1*).

AtPAT14C^{157}S alone in *akr1* cells. Therefore, this further confirms that the partial rescue of *akr1* at 37°C by AtPAT14 was largely dependent on its *S*-acyltransferase activity.

In summary, this yeast complementation data clearly demonstrates that AtPAT14 can partially complement the function of AKR1 and that this requires the Cys residue in the DHHC-CRD domain, which is essential for *S*-acyltransferase activity.

AtPAT14 Is Auto-Acylated in Vitro

One of the important characteristics of all PATs is that they can bind palmitic acid to form an intermediate complex, i.e. they are auto-acylated (Roth et al., 2002). To see if AtPAT14 also has this property, we carried out the Acyl-RAC (for resin-assisted capture) assay (Forrester et al., 2011), to capture on thiopropyl Sepharose beads all *S*-acylated proteins from transgenic *akr1* yeast cells. Because AtPAT14 and AtPAT14DHHC^{157}S are fused to the V5 epitope tag at their C termini, their presence on the beads can be detected via western blot using an anti-V5 antibody. As shown in Figure 3, AtPAT14 could be detected among the captured *S*-acylated proteins, but AtPAT14DHHC^{157}S could not, indicating that AtPAT14 is auto-acylated while AtPAT14DHHC^{157}S is not. This further proves that AtPAT14 is an *S*-acyltransferase and its activity relies on the Cys residue in the DHHC domain.

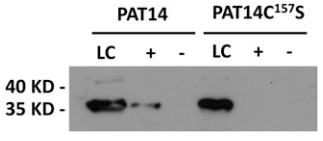

Figure 3. Arabidopsis AtPAT14 is auto-acylated. AtPAT14 (PAT14) and AtPAT14C^{157}S (PAT14C^{157}S) were detected by western blotting with an anti-V5 antibody using the ECL method. The molecular weight of AtPAT14 and AtPAT14C^{157}S is approximately 35 kD. A band corresponding to AtPAT14-V5 was detected in the +NH_2OH treated sample, indicating that it is bound to an acyl group via a labile thioester linkage confirming that it is autoacylated. However, no signal was detected for AtPAT14C^{157}S, indicating that it is not autoacyated. LC, Loading control; lane +, NH_2OH is present; lane −, no NH_2OH.

AtPAT14 Predominantly Localizes to Golgi

To see where AtPAT14 is localized, we stably transformed 35S:AtPAT14-GFP into *atpat14-1* and observed the cotyledons and primary roots of 10-d-old plate-grown seedlings of the complemented plants. We found that AtPAT14-GFP was present as many discrete fluorescent foci in cotyledons and root cells in the elongation and growth terminating zones (Fig. 4, left; Supplemental Fig. S8). To determine the identity of these structures, we crossed the AtPAT14-GFP line with mCherry-labeled marker Wavelines that carry different endomembrane markers (Geldner et al., 2009). Strong colocalization was visualized in the progeny of crosses with the R127 line, which contains a cis-Golgi marker (MEMB12, At5g50440; Uemura et al., 2004; Fig. 4A, middle and right). The highly motile structures of AtPAT14-GFP were seen moving together with this

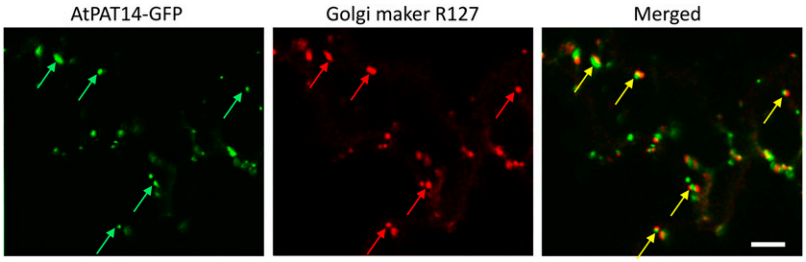

Figure 4. AtPAT14 is predominantly localized to the Golgi in Arabidopsis. Confocal microscopy observation of *atpat14-1* cotyledon of 10-d-old seedlings complemented with the 35S:ATPAT14-GFP construct and crossed with the Golgi marker line R127. Green arrows, AtPAT14-GFP; red arrows, R127; yellow arrows, colocalization. Bar, 5 μm.

Golgi marker (Supplemental Movie S1). The colocalization was not a complete "overlap," but instead, the GFP and mCherry appeared next to each other. High magnification views of the PAT14-GFP labeled structures in cotyledon epidermal cells revealed a doughnut-shaped Golgi apparatus that is very similar to the pattern observed by Boevink et al. (1998) using a trans-Golgi marker (STtmd-GFP) in tobacco leaf cells (Supplemental Fig. S7). This indicates that AtPAT14 is localized to the trans face of the Golgi stack. Due to very weak signals from other marker lines, we were unable to determine in which other compartment(s) AtPAT14 may reside. Nevertheless, our data indicate that a large proportion of AtPAT14, if not all, is localized in the trans-Golgi. This is similar to the observation made for transiently expressed AtPAT14-GFP in tobacco leaves (Batistic, 2012).

To see if mutation of the Cys within the DHHC motif has an effect on AtPAT14 localization, we observed transgenic Arabidopsis that carried the AtPAT14DHHC^{157}S-GFP construct. Similar florescent structures were seen in these plants as for AtPAT14-GFP, indicating that the mutation has no observable effect on the localization of the protein (Supplemental Fig. S8). Observation of AtPAT10 (Qi et al., 2013) and the mammalian DHHC2 (Greaves et al., 2011) resulted in the same conclusion that mutation of the Cys in the DHHC domain to an Ala residue blocks autopalmitoylation but does not have a gross effect on protein localization. This suggests that intramolecular autopalmitoylation of PATs is not having a major impact on targeting of the protein.

Expression of Senescence-Associated Genes and Defense-Related Genes Is Accelerated in *pat14* Mutants

Senescence involves degradation of leaf chlorophyll, resulting in yellow or brown leaves. Measurement of the chlorophyll content of the first pair of true leaves of 29-d-old plants showed a 3- and 2-fold reduction in *pat14-1* and *pat14-2*, respectively, compared to wild type (Fig. 5A). The *pat14* null mutation is responsible for this early senescence phenotype as a construct carrying AtPAT14 restored both *pat14-1* and *pat14-2* to wild type (Supplemental Fig. S5; data not shown).

Next, using real-time PCR, we compared the expression levels of two commonly used senescence marker genes, *senescence association genes 12* (*SAG12*) and *101* (*SAG101*; Vogelmann et al., 2012), in wild-type and mutant plants in the early and later developmental stages. A similar low-level expression was found in

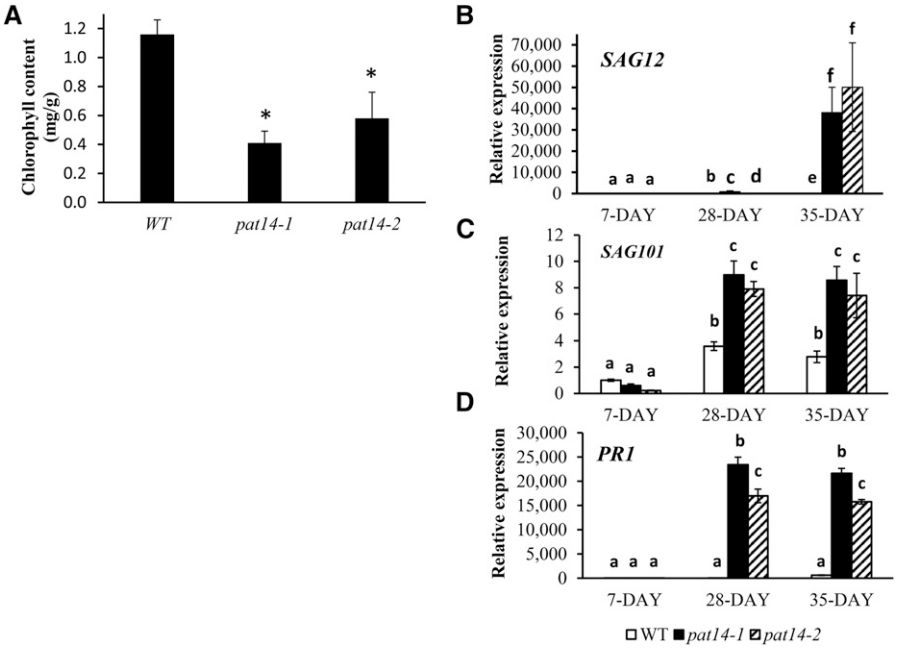

Figure 5. AtPAT14 is involved in early senescence. A, Chlorophyll content analysis. Left, The first pair of true leaves from 28-d plants were used to measure the chlorophyll content. B, Transcript level of *SAG12*. C, Transcript level of *SAG101*. D, Transcript level of the pathogen related gene 1, *PR1*. Seven-day-old plate-grown seedlings and the sixth and seventh rosette leaves of 28-d- and 35-d-old soil-grown plants were collected and used for RNA extraction followed by RT and real-time PCR. The gene expression level in the seedlings of 7-d-old wild type (WT) is regarded as 1, and the relative expression level of all four genes was calculated. *$P < 0.05$ in Student's t test in A, and the different letters above the columns in B to D indicate statistically different values analyzed by one-way ANOVA.

7-d-old seedlings in wild type and *pat14*. However, at 28 and 35 d, their expression levels were significantly upregulated in mutant lines compared to wild type (Fig. 5, B and C). Although the transcript level of *SAG12* was increased by 7- and 14-fold in the 28- and 35-d-old wild-type plants compared to 7-d-old seedlings, it was increased by 1,594- and 70,594-fold in *pat14-1*, and 251- and 67,676-fold in *pat14-2* for the same aged plants, respectively (Fig. 5B). Similarly, *SAG101* was increased by 3.6 fold in wild type, while 15- and 36-fold increases were found in *pat14-1* and *pat14-2* mutant leaves of 28-d-old plants (Fig. 5C). For Pathogenesis-related gene 1 (*PR1*), which is also regarded as an SA signaling gene and is readily inducible by SA (Zhang et al., 2013), a massive increase in transcript level of 212,815- and 121,357-fold was found in 28-d-old *pat14-1* and *pat14-2* plants compared to only a 14-fold increase in wild type (Fig. 5D). Likewise, the transcript levels of *SAG101* and *PR1* were much higher in 35-d-old mutant plants compared to wild type. This clearly demonstrates that *AtPAT14* regulates the expression of genes related to senescence and defense.

The Early Senescence Phenotype in *pat14* Is Not Caused by Defects in Autophagy

The importance of autophagy in the regulation of leaf senescence in Arabidopsis has been demonstrated by the characterization of many autophagy genes (*ATG* for short), where their loss-of-function mutants, such as *atg*2, *atg*5, *atg7*, *atg9*, and *atg11*, all exhibited early senescence (Hanaoka et al., 2002; Thompson et al., 2005; Farmer et al., 2013; Avila-Ospina et al., 2014; Li and Vierstra, 2014). To see if early senescence in *pat14* mutants is caused by defects in autophagy, we carried out carbon starvation assays on plate-grown seedlings. Seedlings of both *atg5-1* and *atg9-2* became yellow after this treatment, whereas wild-type, *pat14-1*, and *pat14-2* mutant seedlings remained green (Supplemental Fig. S9A). Seedlings of *pat14* contained a similar amount of chlorophyll as wild type, whereas *atg9-2* had much less chlorophyll (Supplemental Fig. S9B)—therefore, *pat14* mutants do not share the same phenotype as *atg5* and *atg9* under these conditions.

To confirm this notion, we utilized the autophagy molecular marker ATG8-GFP to determine if autophagic bodies were absent in the *pat14* mutant background. ATG8 proteins are useful molecular markers of autophagosomes in plants and can be used to define *atg* mutants defective in the autophagic processes (Yoshimoto et al., 2004; Contento et al., 2005; Thompson et al., 2005; Chung et al., 2010; Li and Vierstra, 2014). As shown in Supplemental Figure S10, many fluorescent foci were seen in primary root tips when ATG8-GFP was expressed in wild-type plants, while virtually no such structures were seen in the transgenic *atg9-2* root, indicating autophagy bodies are lacking in *atg9-2* as

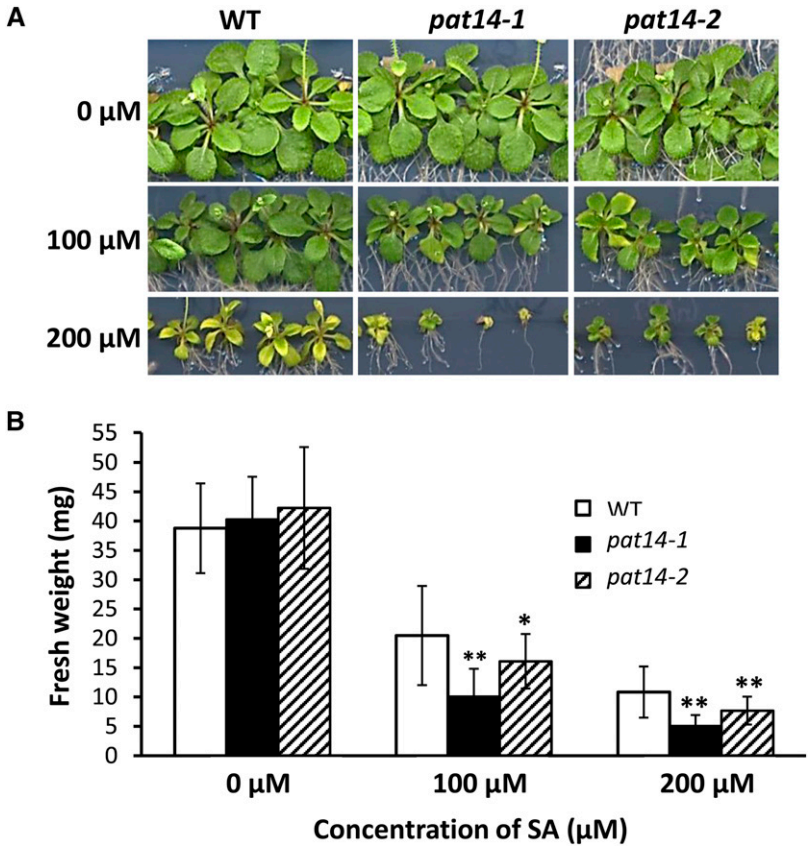

Figure 6. PAT14 knockout mutants are hypersensitive to exogenous SA treatment during early seedling growth. A, Images of seedlings. B, Fresh weight of seedlings. Seeds were geminated and grown on half-strength MS plus 1% Suc medium for 4 d. They were then transferred to the same fresh medium supplemented with 0 (control), 100, and 200 μM SA and grown for a further 15 d before being scanned, and the shoot weight of each seedling was recorded ($n = 20$). $^{*}P < 0.05$ and $^{**}P < 0.01$ in Student's t test.

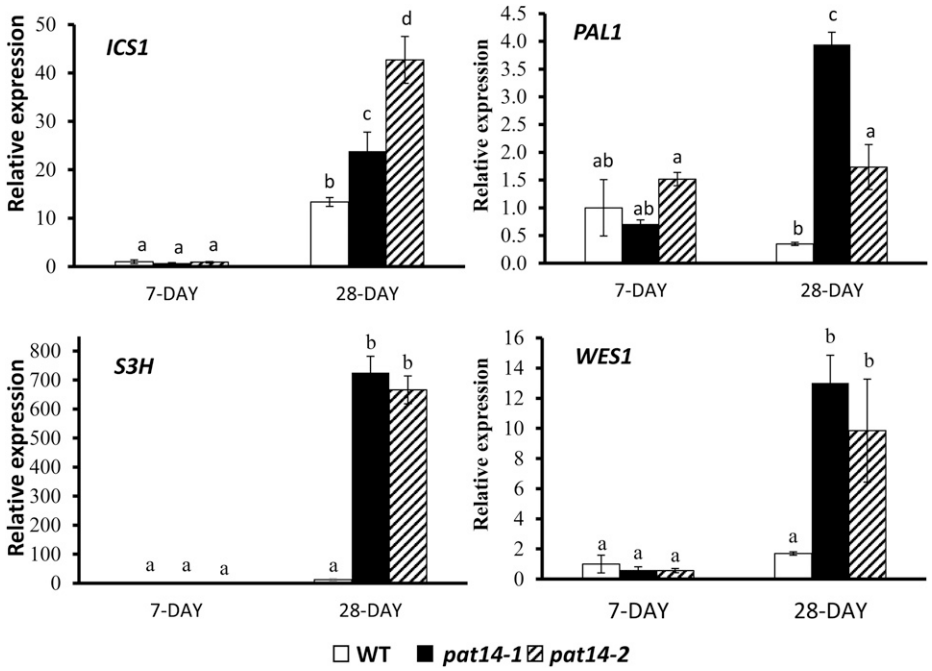

Figure 7. Transcript levels of several SA metabolic genes monitored by real-time PCR. Seven-day-old plate-grown seedlings and the sixth and seventh rosette leaves of 28-d-old soil-grown plants were collected for RNA extraction and reverse transcription followed by real-time PCR. The gene expression level in the 7-d-old wild-type (WT) seedlings is regarded as 1, and the relative expression level in 28-d-old leaves was calculated. The experiments were repeated three times. Each bar represents the mean ± SE (n = 3). Different letters above the columns indicate statistically different values analyzed by one-way ANOVA.

reported by Li and Vierstra (2014). However, in the roots of *pat14-1* and *pat14-2* seedlings expressing ATG8-GFP, the number and size of fluorescent foci were similar to those in the wild-type background, indicating that autophagy is normal in *pat14* mutants. Therefore, early senescence in AtPAT14 loss-of-function mutants is very unlikely due to defect in autophagy, i.e. AtPAT14 is not involved in autophagy-mediated senescence.

pat14 Mutants Are Hypersensitive to SA but Insensitive to ABA and JA Treatment

High levels of phytohormones, such as SA, ABA, and JA, can cause senescence in plants (Schippers et al., 2007). To see the effect of these phytohormones on *pat14* mutants, we first treated seedlings of wild-type, *pat14-1*, and *pat14-2* with SA. The seedlings of *pat14* were indistinguishable from wild type when grown on media lacking SA (Fig. 6A, top). However, when 100 μM of SA was added, a significant reduction in the growth of mutant lines was observed compared to wild type (Fig. 6A, middle). The shoot fresh weight was 52.8%, 25.1%, and 38.2% of untreated seedlings for wild type, *pat14-1*, and *pat14-2*, respectively (Fig. 6B). A similar effect was found for seedlings treated with 200 μM of SA (Fig. 6A, bottom; Fig. 6B). We next tested the effect of ABA and JA on seedling growth using the same method. *pat14* and wild-type seedlings treated with 0.5 and 1 μM ABA had a similar phenotype and reduction in shoot fresh weight (Supplemental Fig. S11, A and B). Likewise, no observable differences were found between *pat14* and wild-type seedlings treated with 15 and 30 μM of JA (Supplemental Fig. S12, A and B).

Therefore, AtPAT14 loss-of-function mutants are hypersensitive to SA, but respond to ABA and JA in a similar manner as wild type.

SA Pathway Related Genes Are Upregulated in *pat14* Mutants

To further confirm the involvement of the SA pathway in early senescence in the *pat14* mutants, we carried out real-time PCR to compare the expression levels of some SA metabolic and signaling genes in wild type and *pat14* mutants. SA is synthesized by two major pathways, with 90% being derived from the isochorismate synthase (ICS) pathway, and 10% from the Phe ammonia-lyase (PAL) pathway (Dempsey et al., 2011). As shown in Figure 7, low levels of *ICS1* transcript was present in both mutants and wild type in the 7-d-old seedlings. However, *ICS1* transcript increased significantly in the fifth and sixth leaves of 28-d-old soil-grown plants for wild type and *pat14* mutants. Strikingly, much higher transcript levels were found in the mutants than wild type: 32- and 47-fold for *pat14-1* and *pat14-2*, compared to a 13-fold increase for wild type (Fig. 7). For *PAL1*, the transcript level in wild type was unchanged between the 7-d-old seedlings and mature plants, whereas in the mutant lines it was upregulated in mature plants with 10- and 3-fold increases for *pat14-1* and *pat14-2*, respectively (Fig. 7). Therefore, at maturity, the SA biosynthetic genes are much more active in *pat14* mutants than wild-type plants.

Accumulation of SA to high levels in plants can induce the expression of SA modification genes, which can inactivate SA to maintain homeostasis in the cell. Arabidopsis plants lacking two of the most important

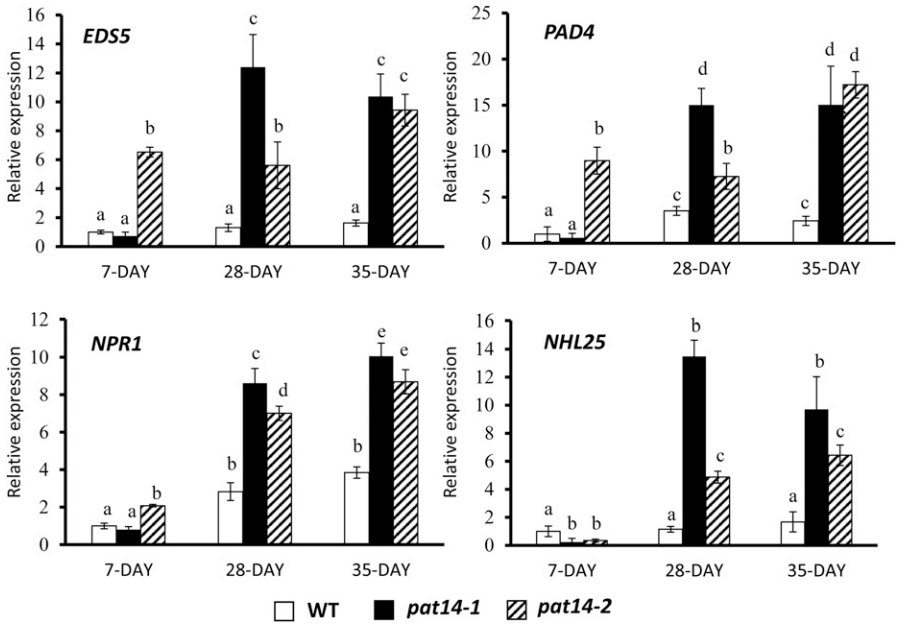

Figure 8. Transcript levels of SA signaling genes monitored by real-time PCR. The gene expression level in the 7-d-old wild-type (WT) seedlings is regarded as 1, and their relative expression levels in 28-d-old leaves were calculated. The experiments were repeated three times. Each bar represents the mean ± SE ($n = 3$). Different letters above the columns indicate statistically different values analyzed by one-way ANOVA.

SA modifying genes, SA 3-hydroxylase (*S3H*) and GH3 acyl adenylase family member 3.5 (*GH3.5/WES1*), show an early senescence phenotype due to the accumulation of high levels of SA (Dempsey et al., 2011; Zhang et al., 2013). Our results showed that the *S3H* transcript increased 12-fold in the 28-d-old wild-type leaves compared to 7-d-old seedlings. However, a surge to 1,728- and 925-fold increases of *S3H* transcript was found in mature *pat14-1* and *pat14-2* plants (Fig. 7). Similarly, the transcript level of *WES1* in mature *pat14-1* and *pat14-2* plants was much higher than wild type, although to a lesser extent (2-, 21-, and 17-fold increase for wild type, *pat14-1*, and *pat14-2*, respectively; Fig. 7). This demonstrates that both SA modification genes, *S3H* and *WES1*, are significantly upregulated in the *pat14* mutants compared to wild-type mature plants.

We next measured the transcript levels of SA signaling genes, such as enhanced disease susceptibility 5 (*EDS5*), phytoalexin deficient 4 (*PAD4*), Nonexpresser of Pathogenesis-Related genes 1 (*NPR1*), and NDR1/HIN1-LIKE 25 (*NHL25*; van der Graaff et al., 2006). Consistent with the SA metabolic genes, these signaling genes also showed higher expression levels in the mature *pat14* mutants than in wild type. Interestingly, higher expression levels of *EDS5*, *PAD4*, and *NPR1*, but not *NHL25*, were also found in the 7-d-old seedlings of *pat14-2*, but not *pat14-1*, compared to wild type (7-, 9-, and 2-fold more than wild type). All the signaling genes showed greater upregulation in 28- and 35-d-old plants of both *pat14-1* and *pat14-2* compared to wild type (10- and 9-fold compared to 2-fold for *EDS5*; 15- and 17-fold compared to 2-fold for *PAD4*; 10- and 9-fold compared to 4-fold for *NPR1* in 35-d-old plants; Fig. 8). For *NHL25*, very low-level expression was found in the 7-d-old seedlings in wild type and both mutant lines. However, in the 35-d-old plants, while *NHL25* accumulation in wild type was comparable to the seedlings, in the *pat14-1* and *pat14-2* lines, expression was increased by 10- and 6-fold. These data clearly show that the SA signaling genes were upregulated to a significantly greater extent in the mutants than in wild-type mature plants.

Therefore, the combined quantitative PCR data suggests that AtPAT14 is involved in leaf senescence via the regulation of genes involved in SA metabolism and signaling.

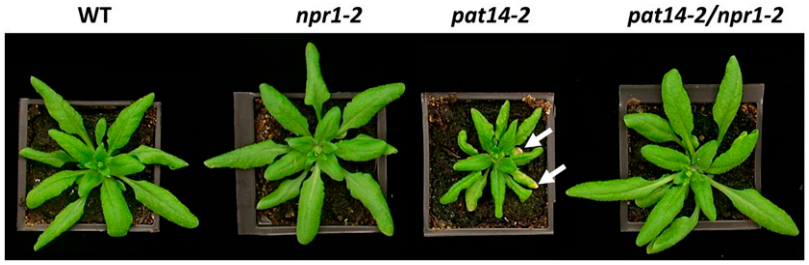

Figure 9. Blocking SA signaling in *pat14* can rescue its early senescence phenotype. Four-week-old plants of wild type (WT), *npr1-2*, *pat14-2*, and *pat14-2/npr1-2* double mutants are shown. Arrows indicate yellow leaf tips in *pat14-2*. No such phenotype was observed in wild type, *npr1-2*, and the double mutant *pat14-2/npr1-2*.

Table I. *Phytohormone analysis of 7-d-old seedlings and 30-d-old leaves of wild-type and pat14 mutants*

7 d, Shoots of 7-d-old plate grown seedlings; 30 d, the seventh and eighth leaves of 30-d-old soil-grown plants. SA, ABA, and JA are expressed as μg per g of dry weight, while SA-glycoside and OPDA are peak areas. Values are means ± SD of three replicates.

	SA	SA-Glycoside	OPDA	ABA	JA
Wild type					
7 d	4.10 ± 0.51	455.9 ± 41.5	235.9 ± 71.8	0.23 ± 0.05	0.17 ± 0.04
30 d	4.49 ± 1.11	9,348.5 ± 1,386.5	4,759.6 ± 1,204.3	0.39 ± 0.11	0.13 ± 0.02
pat14-1					
7 d	3.87 ± 0.23	546.7 ± 88.5	226.0 ± 125.8	0.19 ± 0.01	0.12 ± 0.02
30 d	19.49 ± 1.05	45,788.0 ± 4,289.3	11,856.0 ± 1,710.7	0.34 ± 0.07	0.40 ± 0.02
pat14-2					
7 d	4.22 ± 0.21	369.4 ± 9.2	182.1 ± 46.8	0.35 ± 0.10	0.15 ± 0.02
30 d	25.58 ± 1.59	44,581.4 ± 2,997.5	11,711.9 ± 3,384.2	0.29 ± 0.11	0.11 ± 0.02

Early Senescence of *pat14* Is Partially Rescued by Preventing SA Signaling

NPR1 has been shown to be a receptor for SA and it functions as a central activator of SA responses (Wu et al., 2012). Mutants defective in NPR1 (*npr1*) exhibit altered SAG expression patterns and delayed senescence (Morris et al., 2000). To further confirm the involvement of SA in early senescence of *pat14* plants, we crossed both *pat14-1* and *pat14-2* with *npr1-2* (Cao et al., 1997). The double mutant *pat14/npr1* plants, which largely resemble the wild type, had much delayed senescence compared to the *pat14* single mutants (Fig. 9; Supplemental Fig. S13). Therefore, this clearly demonstrates that the early senescence of Arabidopsis PAT14 loss-of-function mutants is caused by a defect in SA signaling pathway.

SA, OPDA, ABA, and JA Levels during Leaf Senescence

The data described above strongly supports the hypothesis that altered SA levels in the *pat14* mutants may be contributing to the enhanced senescence phenotype. To confirm this, we measured SA levels in seedlings and in the seventh and eighth green healthy leaves of 30-d-old wild type and *pat14* mutant lines. As shown in Table I, the total amount of SA in 7-d-old seedlings is very low and similar between *pat14* and wild type. These data are consistent with the low levels of the key SA biosynthetic gene transcripts, *ICS1* and *PAL1*, detected in seedlings (Fig. 7). However, in the leaves of 30-d-old plants, the SA content increased by 5- and 6-fold in *pat14-1* and *pat14-2*, respectively, while it remained unchanged in wild type. In addition, the SA glycoside content increased by 84- and 120-fold in the 30-d-old *pat14-1* and *pat14-2* plants, compared to only 20-fold in wild type, representing a 4- and 6-fold difference between the 30-d-old wild-type and *pat14-1* and *pat14-2* plants, broadly similar to the SA ratios at 30 d (Table I).

Consistent with the ABA treatment studies, ABA did not show significant differences between wild type and the *pat14* mutants (Table I). We also monitored changes in the phytohormones JA and the related jasmonate metabolite cis-(+; cis)-12-oxo-phytodienoic acid (OPDA). In wild type, OPDA levels increased from 7-d-old seedlings to 30-d-old leaves. Strikingly, OPDA levels were 3-fold greater in both mutants compared to wild type, at 30 d (representing increases in OPDA levels from days 7-30 of 50-60 fold in the mutants compared 20-fold for wild type). Interestingly, these differences between mutant and wild type were not reflected in JA abundances (OPDA is a precursor of JA). All samples, with the exception of *pat14-1* had similar JA levels. *pat14-1* had twice the level of JA, and this may be a consequence of its more severe growth defects (Fig. 1).

DISCUSSION

Loss of Enzyme Activity of AtPAT14 Causes Growth Defects

In this study, we identified, to our knowledge, a novel protein *S*-acyltransferase, AtPAT14, from Arabidopsis. To study its biological function, we first isolated two T-DNA knockout mutant alleles, *atpat14-1* and *atpat14-2* (Fig. 1). The mutant plants exhibited altered patterns of growth and development, with smaller stature and early leaf senescence being the most obvious. Interestingly, *atpat14-1* showed more severe growth defects than *atpat14-2* throughout. *atpat14-1* and *atpat14-2* lines expressing 35S:AtPAT14 show a wild-type phenotype, clearly demonstrating that the phenotypes observed in the mutants were caused by AtPAT14 being rendered nonfunctional (Supplemental Fig. S5).

Although AtPAT14 contains the characteristic DHHC-CRD domain (Supplemental Fig. S1), in order to confirm it is indeed an *S*-acyl transferase, we first carried out in vitro and in vivo studies on its enzyme activity in yeast and Arabidopsis. The fact that AtPAT14 can partially rescue the morphological and growth defects of yeast *akr1* mutant lacking the PAT AKR1, that it undergoes auto-palmitoylation, demonstrates that AtPAT14 can indeed function as an *S*-acyltransferase (Figs. 2 and 3). Importantly, the Cys to

Ser mutation in the DHHC catalytic domain of AtPAT14 failed to restore the growth defect of yeast *akr1* lines carrying this mutant polypeptide and no AtPAT14DHHC^{157}S auto-acylation was detected. Further, 35S:AtPAT14DHHC^{157}S is unable to rescue the growth defects of Arabidopsis *pat14* mutant lines. Collectively, these data confirm that, as for other characterized PATs, AtPAT14 functions as a PAT through its enzymatic catalytic DHHC domain.

Early Senescence in AtPAT14 Loss-of-Function Mutants Is Not Caused by Defects in ABA and JA

Disruption of the *AtPAT14* gene results in early senescence in Arabidopsis (Fig. 1). This coincides with a loss of more than half of the chlorophyll (Fig. 5A) and massive upregulation of senescence marker genes *SAG12*, *SAG101*, and *PR1* (Fig. 5, B–D). Senescence results in activation of signaling pathways involving the stress-related plant hormones SA, ABA, and JA (Weaver et al., 1998; Morris et al., 2000; He et al., 2002). However, the absence of obvious phenotypic differences between ABA-treated seedlings of *pat14* and wild type suggests that early senescence was not due to a defect in ABA signaling (Supplemental Fig. S9). Consistent with this conclusion, no differences in ABA accumulation were observed between mutant and wild-type seedlings or mature leaves (Table I). Application of JA had a similar effect on the growth behavior of wild-type and mutant seedlings (Supplemental Fig. S10). JA accumulation was identical between mutant and wild-type seedlings and leaves. Only *pat14-1*, with the more severe growth phenotype, showed twice the JA content (Table I). Therefore, the early senescence phenotype in AtPAT14 loss-of-function mutants is unlikely to be caused by defective ABA and JA signaling pathways.

Early Senescence in AtPAT14 Loss-of-Function Mutants Is Not Caused by Defects in Autophagy

Senescence involves nutrient recycling and remobilization, which is believed to be partially carried out by autophagy (Chung et al., 2010). Indeed, in higher plants, defects in autophagy lead to inefficient recycling of carbon and nitrogen, which is manifested in an enhanced senescence phenotype (Thompson et al., 2005; Bassham et al., 2006; Yoshimoto et al., 2009; Chung et al., 2010; Li and Vierstra, 2014). However, we found that early senescence of *atpat14* is not caused by defects in autophagy. We conclude this as (1) under carbon starvation and dark treatment, *pat14* seedlings were as green as wild type, while the two autophagy defective mutants, *atg5-1* (Thompson et al., 2005; Chung et al., 2010) and *atg9-2* (Li and Vierstra, 2014), became chlorotic (Supplemental Fig. S8). Thus, loss-of-function of AtPAT14 does not block autophagy-mediated nutrient remobilization under these conditions; (2) observation of autophagosomes in roots of *pat14* mutants shows that a large number of autophagic bodies were labeled by the autophagy molecular marker GFP-ATG8 as was the case in wild type (Supplemental Fig. S8). In contrast, very few fluorescent foci were observed in the *atg9* root. This clearly demonstrates that the starvation- and dark-induced senescence in *atg5* and *atg9* mutants is not found in AtPAT14 loss-of-function mutants, and hence, the autophagy process seems to be normal in *pat14*.

Taken together, these data clearly demonstrate that there is no direct involvement of ABA, JA, and autophagy in the early senescence phenotype of *pat14* mutants, i.e. AtPAT14 is unlikely to be involved in ABA and JA signaling or autophagy-regulated leaf senescence in Arabidopsis.

Early Senescence in AtPAT14 Loss-of-Function Mutants Is Caused by Defects in the SA Signaling Pathway

The plant hormone SA is best known for its role in response to pathogen attacks. The accumulation of SA during different plant resistance responses is the basis of systemic acquired resistance. Plants are hypersensitive to SA produced by pathogen invasion, causing rapid programmed cell death (Kapulnik et al., 1992; Vlot et al., 2009). Leaf senescence is a slow form of programmed cell death that allows plants to mobilize nutrients released from senescing cells to sink and actively growing tissues (Gan and Amasino, 1997; Zhang et al., 2012). Although the role of SA in leaf senescence and its underlying molecular mechanism have been less studied, there is some evidence that both disease defense and leaf senescence share SA signaling and regulatory components (Morris et al., 2000; Love et al., 2008; Rivas-San Vicente and Plasencia, 2011). Senescing leaves of Arabidopsis contain approximately 3-fold more SA than green leaves (Morris et al., 2000). The Arabidopsis mutant *npr1* lacking the SA signal transducer NPR1 shows delayed leaf senescence. Likewise, introducing a bacterial salicylate hydroxylase (encoded by *NahG*) results in very low levels of SA, and these plants display a significant delay in leaf senescence (Morris et al., 2000). These results are corroborated by studies of the recently identified equivalent plant enzyme, a SA 3-hydroxylase (S3H) from Arabidopsis. S3H converts SA to 2,3-dihydroxybenzoic acid, rendering SA inactive. Leaf senescence can be accelerated or delayed by blocking or overexpressing *S3H* due to the increased or decreased levels of active SA in these plants (Zhang et al., 2013).

To see if the senescence-like phenotype of *pat14* plants was related to SA, we monitored the transcript levels of some of the SA synthetic, catabolic, and signaling genes. The results revealed that both the SA synthetic genes *ICS1* and *PAL1* showed much higher transcript levels in leaves derived from the *pat14* mutant than wild type (Fig. 7). This could lead to a hyperaccumulation of SA in the mutants, and indeed, the mutant leaves were found to contain 6 times more SA than wild type (Table I). SA can induce the expression

of the SA catabolic gene *S3H*, and the induced S3H enzyme in turn hydrolyses SA to its inactive form (2,3-dihydroxybenzoic acid) to prevent over accumulation of SA (Zhang et al., 2013). Thus, a positive feed-forward mechanism may account for the higher transcript levels of *S3H* and *WES1* seen in the *pat14* mutant leaves (Fig. 7). The over accumulation of SA in the mutants can induce the expression of SA signaling genes that were readily detected by quantitative PCR (Fig. 8).

Consistent with a role for AtPAT14 in the negative regulation of SA during senescence, the transcript levels of the senescence-specific marker genes *SAG12* and *PR1* are massively upregulated in *pat14* mutant leaves (Fig. 6). Studies have shown that the expression of both *SAG12* and *PR1* rely on the presence of SA, since very low levels of SA were present in the SA signaling defective mutants *npr1* and *pad4* and in *NahG* overexpressing plants (Morris et al., 2000). However, increasing SA levels by blocking S3H or by spraying healthy green leaves with SA can induce the expression of *PR1* in wild type (Morris et al., 2000; Zhang et al., 2013). The fact that both *SAG12* and *PR1* were found to be highly expressed in the *pat14* mutants suggests that AtPAT14 can regulate SA levels by either blocking SA synthesis, signaling, or both. Loss-of-function *pat14* mutants may thus relieve this repression with the concomitant loss of SA homeostasis by over-accumulation of SA and/or heightened perception, resulting in precocious leaf senescence. This scenario is supported by the much higher SA levels detected in mature *pat14* leaves compared to wild type (Table I) and delayed leaf senescence in *pat14/npr1* double mutant plants (Fig. 9; Supplemental Fig. S13). Taken together, our data suggest that AtPAT14 plays very important roles in leaf senescence via the fine-tuning of SA biosynthesis and/or perception.

SA and OPDA in Early Senescence of *pat14*

Analysis of the phytohormones in the leaves of 30-d-old plants revealed that both SA and OPDA accumulated to much higher levels in *pat14* mutants than wild type (Table I). The accumulation of OPDA in the *pat14* mutants may be due to a metabolic feedback mechanism resulting from accumulation of the palmitate C16:3 substrate (Dave and Graham, 2012). OPDA is emerging as a phytohormone in its own right (Dave et al., 2011; Goetz et al., 2012). Unlike the antagonistic effect of JA and SA in plant-microbe interactions, it functions through a synergistic effect with SA, which is independent of the JA signaling cascade (Dave and Graham, 2012; Montillet et al., 2013; Schenk and Schikora, 2014). The idea that OPDA can act as an independent signaling molecule is supported by a transcriptional analysis of Arabidopsis following application of OPDA. More than 150 genes related to detoxification, stress responses, and secondary metabolism were found to respond specifically to OPDA treatment, but not to JA or methyl jasmonate (Taki et al., 2005; Mueller et al., 2008).

Although the role of OPDA in leaf senescence is less understood, there is some evidence to show its involvement in this process. For instance, Arabidopsis leaves undergoing natural or stress-induced senescence accumulate high levels of JA and OPDA (Seltmann et al., 2010). Application of Arabidopside A and OPDA can cause senescence of oat leaves (Hisamatsu et al., 2006). Arabidopsides are OPDA esterified galactolipids that are found in Arabidopsis and all members of the Brassicaceae (Stelmach et al., 2001; Buseman et al., 2006). They are thought to provide a rapidly available source of cis-OPDA. The fact that *pat14* leaves accumulated much more OPDA than wild type yet the JA levels were similar suggests that OPDA, but not JA, plays a role in early senescence in *pat14*. Furthermore, because *pat14* leaves also produced more SA, together with OPDA these two phytohormones could act synergistically (as is the case in plant defense) to accelerate senescence in the mutant.

In summary, we have shown for the first time, to our knowledge, that protein palmitoylation is involved in leaf senescence in Arabidopsis. We identify AtPAT14 as a negative regulator of leaf senescence in Arabidopsis that likely acts by altering SA homeostasis and perception in concert with OPDA, in a process that is independent of ABA, JA, and autophagy.

MATERIALS AND METHODS

Plant Material and Growth Conditions

Wild-type Arabidopsis (*Arabidopsis thaliana*), the two T-DNA insertion lines SALK_026159 (Alonso et al., 2003), and GK-153A10 (Kleinboelting et al., 2012) in the background of Columbia-0 were obtained from the Arabidopsis Biological Resource Center (ABRC; http://www.arabidopsis.org/abrc/). For *npr1-2* (N3801), seeds were obtained from the Nottingham Arabidopsis Stock Centre (NASC). Seeds were surface sterilized and germinate, and seedlings grown under long days (LD) as described previously (Qi et al., 2013).

Identification of AtPAT14 T-DNA Insertion Mutants

PCR-based genotyping was carried out to isolate homozygous T-DNA mutants from SALK_026159 and GK-153A10 lines using primers LBb1/SALK026159RP and SALK026159LP/SALK026521RP, and GABILBb1/GABI_153A10LP and GABI_153A10LP/GABI_153A10RP (Supplemental Table S1), respectively. PCR products amplified from the junction of the T-DNA insertion sites were sequenced to confirm their location in both lines as described previously (Qi et al., 2013).

RT-PCR and Real-Time PCR

Total RNA was extracted using Trizol (Invitrogen) according to the manufacturer's instructions. Oligo(dT)-primed cDNAs were synthesized from 1 μg RNA using the First-Strand cDNA Synthesis Kit (Transgen). To detect transcripts in wild type and both T-DNA homozygous lines, four pairs of gene specific primers were used to amplify the *AtPAT14* full coding region (Beg+End), upstream (F1+R1), across (F2+R2), and downstream (F3+R3) of the T-DNA insertion sites. For real-time PCR to detect transcripts of genes in the SA pathway, UltraSYBR PCR Mixture (With ROX; CWBIO) was used and the programs were run on a Stepone Plus real-time PCR system (Applied Biosystems). The relative transcript levels were calculated by the $2^{-\Delta\Delta t}$ method with the AtEF-1α gene as an internal control (Livak and Schmittgen, 2001). At least three replicates were included in each experiment, and the experiments were repeated three times. The sequences of all primers used are shown in Supplemental Tables S2 and S3.

Generating the *pat14/npr1* Double Mutant

The newly isolated *pat14-1* and *pat14-2* homozygous plants were crossed with *npr1-2* (Cao et al., 1997). The F2 progenies were genotyped for *pat14* by PCR as above. To identify *npr1-2*, PCR was carried out with the NPR1For and NPR1Rev primer pair (Supplemental Table S2), and the products were sequenced to detect the point mutation in the *NPR1* gene as described by Cao et al. (1997).

Complementation and Auto-Acylation in Yeast

The coding region of *AtPAT14* was PCR-amplifed without a stop codon with primers 3g60800Beg/3g60800End (Supplemental Table S2) using KOD high fidelity polymerase (Novagen) from first-strand cDNAs prepared from leaf total RNA. The *AtPAT14DHHC*^{157}*S* point mutant was made by PCR-based mutagenesis with primers PAT14DHHC-SFor and PAT14DHHC-SRev (Supplemental Table S2). Both *AtPAT14* and *AtPAT14DHHC*^{157}*S* were cloned into the Gateway donor vector pDONR/Zeo to generate entry clones pDONR-AtPAT14 and pDONR-AtPAT14DHHC^{157}S following protocols of the manufacturer (Gateway Technology). They were then recombined into the Gateway destination vector pYES-DEST52 (C-terminal V5 tagged). Both pYES-AtPAT14 and pYES-AtPAT14DHHC^{157}S were expressed in wild-type BY4741 and *akr1* yeast (*Saccharomyces cerevisiae*), respectively. AKR1C-S was cloned in the yeast expression vector pESC-Leu (Stratagene) and was a gift from Dr. Pier Hemsley (Hemsley and Grierson, 2011). It was cotransformed with empty pYES2 vector, pYES-AtPAT14, or pYES-AtPAT14DHHC^{157}S in *akr1* cells. Growth and observation of the transgenic yeast were according to the method by Qi et al. (2013). For the auto-acylation assay by Acyl-RAC (Forrester et al., 2011), total proteins were extracted from *akr1* yeast cells expressing AtPAT14 and AtPAT14DHHC^{157}S. The *S*-acylated proteins were captured on thiopropyl sepharose beads (Sigma), and AtPAT14 and ATPAT14DHHC^{157}S were detected by western blotting with anti-V5 primary and HRP-conjugated secondary antibodies (Bethyl).

Complementation of *pat14* and Subcellular Localization of AtPAT14

For complementation of the *pat14-1* and *pat14-2*, the C-terminal GFP tagged AtPAT14 and AtPAT14DHHC^{157}S were cloned into pEarlyGate103 (Earley et al., 2006). Transgenics were created and selected as described previously (Qi et al., 2004).

For the subcellular localization of AtPAT14 transgenic *pat14-1* plants complemented by 35S:AtPAT14-GFP were crossed with mCherry tagged marker Wavelines (Geldner et al., 2009). Primary roots and cotyledons of 10-d-old seedlings from the crossed F1 progeny were observed. Images were taken with a Zeiss LSM 510 inverted confocal microscope using a 488 nm argon ion laser with 505 to 530 nm band pass filter for detection of GFP and a 543 nm HeNe laser with a 560 to 615 nm band pass filter for detection of mCherry.

Chlorophyll Content Measurement

To estimate chlorophyll content, the methods described by Porra et al. (1998) and Katsiarimpa et al. (2013) were followed. Briefly, seedlings (10 mg) or fresh rosette leaves (20 mg) were homogenized in 500 μL of 96% ethanol in preweighed 1.5 mL microfuge tubes. After centrifugation, the supernatant was transferred to a fresh tube, and the OD at 470, 649, and 665 nm was recorded. The chlorophyll content is the sum of chlorophyll a $(13.95 \times OD_{665}) - (6.88 \times OD_{649})$ plus chlorophyll b $(24.96 \times OD_{649}) - (7.32 \times OD_{665})$, which is expressed as μg/mg fresh weight.

Carbon Deficiency and Phytohormone Treatment

The carbon deficiency assay was carried out according to Hanaoka et al. (2002). Briefly, seeds of wild type, *pat14-1* and *pat14-2*, *atg5-1*, and *atg9-2* were germinated and cultured vertically on half-strength Murashige and Skoog (MS) plus 1% Suc under LD for 7 d. They were then transferred to half-strength MS only and incubated in the dark for a further 7 d. For hormone treatment, seeds were germinated and grown on half-strength MS plus 1% Suc under LD for 4 d. The seedlings were transferred to half-strength MS without or with ABA, JA, and SA and left to grow for up to 3 weeks before being scanned and weighed.

Phytohormone Analysis

Each hormone determination was measured in triplicate using samples derived from 7-d-old seedlings and the seventh and eighth leaves of 30-d-old plants. Hormone extractions were performed on 3 mg of powdered, freeze-dried tissue exactly as detailed in Forcat et al. (2008). OPDA was measured according to Dave et al. (2011) using OPDA (Larodan) as a standard.

Accession Numbers

Sequence data from this article can be found in the GenBank/EMBL data libraries under accession numbers AtPAT14, NM_115944; AKR1, NM_001180572; MEMB12, NM_124426; SAG12, NM_123957; SAG101, NM_121497; PR1, NM_127025; ATG5, NM_121735; ATG9, NM_179833; ATG8, NM_001198362; ICS1, NM_202414; PAL1, NM_129260; WES1, NM_118860; EDS5, NM_120063; PAD4, NM_115103; NPR1, NM_105102; and NHL25, NM_123055.

Supplemental Data

The following supplemental materials are available.

Supplemental Figure S1. Protein sequence alignment and secondary structure prediction of AtPAT14.

Supplemental Figure S2. Expression level of *AtPAT14* in seedlings and various tissues of mature Arabidopsis plants.

Supplemental Figure S3. Comparison of Arabidopsis reproductive organs and seed development from wild-type Columbia-0 and AtPAT14 mutant lines *atpat14-1* and *atpat14-2*.

Supplemental Figure S4. The *pat14* mutant has smaller cells than wild type.

Supplemental Figure S5. Loss of AtPAT14 PAT activity causes the phenotypic defects of the *atpat14* mutant Arabidopsis plant.

Supplemental Figure S6. Restoration of *akr1*growth defects by PAT14 at the nonpermissive high temperature of 37°C was enhanced by the ankrin repeats of AKR1.

Supplemental Figure S7. AtPAT14 is predominantly localized in Golgi.

Supplemental Figure S8. Mutation in Cys-157 of the DHHC motif has no effect on AtPAT14 localization.

Supplemental Figure S9. Early senescence in *atpat14* is not caused by autophagy deficiency.

Supplemental Figure S10. The subcellular localization of ATG8-GFP is not changed in *pat14* mutant roots.

Supplemental Figure S11. PAT14 mutants are not sensitive to exogenous ABA treatment during early seedling growth.

Supplemental Figure S12. PAT14 mutants are not sensitive to exogenous JA treatment during early seedling growth.

Supplemental Figure S13. The early senescence phenotype of *pat14* is rescued by blocking SA signaling in the mutant.

Supplemental Movie S1. AtPAT14 colocalizes with the Golgi marker R127.

Supplemental Table S1. Phenotypic analysis of wild type, *pat14-1*, and *pat14-2*.

Supplemental Table S2. Sequence of primers used for cloning and standard PCR.

Supplemental Table S3. Sequence of primers used for real-time PCR.

ACKNOWLEDGMENTS

We thank the ABRC and NASC for providing Arabidopsis T-DNA insertion lines for *AtPAT14*, *ATG5* (*atg5-1*), and *npr1-2*. Thanks also go to Dr. Taijoon Chung for sharing *atg9-2* and the ProUBQ10-GFP-ATG8a construct. We thank Ms. Debbie Salmon for help with hormone analyses. We are very grateful for the kind help of Professor Chris Hawes with confocal scanning microscopy

observation. We would also like to thank Dr. Piers Hemsley for providing us with the pESC-AKRC-S construct. Lastly, we would like to thank the editor and the reviewers for their constructive comments.

Received March 23, 2015; accepted November 3, 2015; published November 4, 2015.

LITERATURE CITED

Alonso JM, Stepanova AN, Leisse TJ, Kim CJ, Chen H, Shinn P, Stevenson DK, Zimmerman J, Barajas P, Cheuk R, Gadrinab C, Heller C, et al (2003) Genome-wide insertional mutagenesis of *Arabidopsis thaliana*. Science **301:** 653–657

Avila-Ospina L, Moison M, Yoshimoto K, Masclaux-Daubresse C (2014) Autophagy, plant senescence, and nutrient recycling. J Exp Bot **65:** 3799–3811

Baekkeskov S, Kanaani J (2009) Palmitoylation cycles and regulation of protein function (Review). Mol Membr Biol **26:** 42–54

Bassham DC, Laporte M, Marty F, Moriyasu Y, Ohsumi Y, Olsen L, Yoshimoto K (2006) Autophagy in development and stress responses of plants. Autophagy **2:** 2–11

Batistic O (2012) Genomics and localization of the Arabidopsis DHHC-cysteine-rich domain S-acyltransferase protein family. Plant Physiol **160:** 1597–1612

Batistic O, Rehers M, Akerman A, Schlücking K, Steinhorst L, Yalovsky S, Kudla J (2012) S-Acylation-dependent association of the calcium sensor CBL2 with the vacuolar membrane is essential for proper abscisic acid responses. Cell Res **22:** 1155–1168

Boevink P, Oparka K, Santa Cruz S, Martin B, Betteridge A, Hawes C (1998) Stacks on tracks: the plant Golgi apparatus traffics on an actin/ER network. Plant J **15:** 441–447

Buchanan-Wollaston V, Page T, Harrison E, Breeze E, Lim PO, Nam HG, Lin JF, Wu SH, Swidzinski J, Ishizaki K, Leaver CJ (2005) Comparative transcriptome analysis reveals significant differences in gene expression and signalling pathways between developmental and dark/starvation-induced senescence in Arabidopsis. Plant J **42:** 567–585

Buseman CM, Tamura P, Sparks AA, Baughman EJ, Maatta S, Zhao J, Roth MR, Esch SW, Shah J, Williams TD, Welti R (2006) Wounding stimulates the accumulation of glycerolipids containing oxophytodienoic acid and dinor-oxophytodienoic acid in Arabidopsis leaves. Plant Physiol **142:** 28–39

Cao H, Glazebrook J, Clarke JD, Volko S, Dong X (1997) The Arabidopsis NPR1 gene that controls systemic acquired resistance encodes a novel protein containing ankyrin repeats. Cell **88:** 57–63

Charollais J, Van Der Goot FG (2009) Palmitoylation of membrane proteins (Review). Mol Membr Biol **26:** 55–66

Chung T, Phillips AR, Vierstra RD (2010) ATG8 lipidation and ATG8-mediated autophagy in Arabidopsis require ATG12 expressed from the differentially controlled ATG12A and ATG12B loci. Plant J **62:** 483–493

Contento AL, Xiong Y, Bassham DC (2005) Visualization of autophagy in Arabidopsis using the fluorescent dye monodansylcadaverine and a GFP-AtATG8e fusion protein. Plant J **42:** 598–608

Dave A, Graham IA (2012) Oxylipin signaling: a distinct role for the jasmonic acid precursor cis-(+)-12-oxo-phytodienoic acid (cis-OPDA). Front Plant Sci **3:** 42

Dave A, Hernández ML, He Z, Andriotis VME, Vaistij FE, Larson TR, Graham IA (2011) 12-Oxo-phytodienoic acid accumulation during seed development represses seed germination in Arabidopsis. Plant Cell **23:** 583–599

Dempsey DA, Vlot AC, Wildermuth MC, Klessig DF (2011) Salicylic acid biosynthesis and metabolism. Arabidopsis Book **9:** e0156

Earley KW, Haag JR, Pontes O, Opper K, Juehne T, Song K, Pikaard CS (2006) Gateway-compatible vectors for plant functional genomics and proteomics. Plant J **45:** 616–629

Farmer LM, Rinaldi MA, Young PG, Danan CH, Burkhart SE, Bartel B (2013) Disrupting autophagy restores peroxisome function to an Arabidopsis lon2 mutant and reveals a role for the LON2 protease in peroxisomal matrix protein degradation. Plant Cell **25:** 4085–4100

Feng Y, Davis NG (2000) Akr1p and the type I casein kinases act prior to the ubiquitination step of yeast endocytosis: Akr1p is required for kinase localization to the plasma membrane. Mol Cell Biol **20:** 5350–5359

Forcat S, Bennett MH, Mansfield JW, Grant MR (2008) A rapid and robust method for simultaneously measuring changes in the phytohormones ABA, JA and SA in plants following biotic and abiotic stress. Plant Methods **4:** 16

Forrester MT, Hess DT, Thompson JW, Hultman R, Moseley MA, Stamler JS, Casey PJ (2011) Site-specific analysis of protein S-acylation by resin-assisted capture. J Lipid Res **52:** 393–398

Fukata Y, Fukata M (2010) Protein palmitoylation in neuronal development and synaptic plasticity. Nat Rev Neurosci **11:** 161–175

Fukata Y, Iwanaga T, Fukata M (2006) Systematic screening for palmitoyl transferase activity of the DHHC protein family in mammalian cells. Methods **40:** 177–182

Gan S, Amasino RM (1997) Making sense of senescence (molecular genetic regulation and manipulation of leaf senescence). Plant Physiol **113:** 313–319

Geldner N, Dénervaud-Tendon V, Hyman DL, Mayer U, Stierhof YD, Chory J (2009) Rapid, combinatorial analysis of membrane compartments in intact plants with a multicolor marker set. Plant J **59:** 169–178

Goetz S, Hellwege A, Stenzel I, Kutter C, Hauptmann V, Forner S, McCaig B, Hause G, Miersch O, Wasternack C, Hause B (2012) Role of cis-12-oxo-phytodienoic acid in tomato embryo development. Plant Physiol **158:** 1715–1727

Greaves J, Carmichael JA, Chamberlain LH (2011) The palmitoyl transferase DHHC2 targets a dynamic membrane cycling pathway: regulation by a C-terminal domain. Mol Biol Cell **22:** 1887–1895

Greaves J, Chamberlain LH (2007) Palmitoylation-dependent protein sorting. J Cell Biol **176:** 249–254

Greaves J, Chamberlain LH (2011) DHHC palmitoyl transferases: substrate interactions and (patho)physiology. Trends Biochem Sci **36:** 245–253

Greaves J, Gorleku OA, Salaun C, Chamberlain LH (2010) Palmitoylation of the SNAP25 protein family: specificity and regulation by DHHC palmitoyl transferases. J Biol Chem **285:** 24629–24638

Hanaoka H, Noda T, Shirano Y, Kato T, Hayashi H, Shibata D, Tabata S, Ohsumi Y (2002) Leaf senescence and starvation-induced chlorosis are accelerated by the disruption of an Arabidopsis autophagy gene. Plant Physiol **129:** 1181–1193

He Y, Fukushige H, Hildebrand DF, Gan S (2002) Evidence supporting a role of jasmonic acid in Arabidopsis leaf senescence. Plant Physiol **128:** 876–884

Hemsley PA (2009) Protein S-acylation in plants (Review). Mol Membr Biol **26:** 114–125

Hemsley PA, Grierson CS (2008) Multiple roles for protein palmitoylation in plants. Trends Plant Sci **13:** 295–302

Hemsley PA, Grierson CS (2011) The ankyrin repeats and DHHC S-acyl transferase domain of AKR1 act independently to regulate switching from vegetative to mating states in yeast. PLoS One **6:** e28799

Hemsley PA, Kemp AC, Grierson CS (2005) The TIP GROWTH DEFECTIVE1 S-acyl transferase regulates plant cell growth in Arabidopsis. Plant Cell **17:** 2554–2563

Hemsley PA, Weimar T, Lilley KS, Dupree P, Grierson CS (2013) A proteomic approach identifies many novel palmitoylated proteins in Arabidopsis. New Phytol **197:** 805–814

Hisamatsu Y, Goto N, Hasegawa K, Shigemori H (2006) Senescence-promoting effect of arabidopside A. Z Naturforsch C Biosci **61:** 363–366

Howie J, Reilly L, Fraser NJ, Vlachaki Walker JM, Wypijewski KJ, Ashford ML, Calaghan SC, McClafferty H, Tian L, Shipston MJ, Boguslavskyi A, Shattock MJ, et al (2014) Substrate recognition by the cell surface palmitoyl transferase DHHC5. Proc Natl Acad Sci USA **111:** 17534–17539

Huang K, Sanders S, Singaraja R, Orban P, Cijsouw T, Arstikaitis P, Yanai A, Hayden MR, El-Husseini A (2009) Neuronal palmitoyl acyl transferases exhibit distinct substrate specificity. FASEB J **23:** 2605–2615

Kapulnik Y, Yalpani N, Raskin I (1992) Salicylic acid induces cyanide-resistant respiration in tobacco cell-suspension cultures. Plant Physiol **100:** 1921–1926

Katsiarimpa A, Kalinowska K, Anzenberger F, Weis C, Ostertag M, Tsutsumi C, Schwechheimer C, Brunner F, Hückelhoven R, Isono E (2013) The deubiquitinating enzyme AMSH1 and the ESCRT-III subunit VPS2.1 are required for autophagic degradation in Arabidopsis. Plant Cell **25:** 2236–2252

Kleinboelting N, Huep G, Kloetgen A, Viehoever P, Weisshaar B (2012) GABI-Kat SimpleSearch: new features of the Arabidopsis thaliana T-DNA mutant database. Nucleic Acids Res **40:** D1211–D1215

Li F, Vierstra RD (2014) Arabidopsis ATG11, a scaffold that links the ATG1-ATG13 kinase complex to general autophagy and selective mitophagy. Autophagy **10:** 1466–1467

Lobo S, Greentree WK, Linder ME, Deschenes RJ (2002) Identification of a Ras palmitoyltransferase in Saccharomyces cerevisiae. J Biol Chem **277:** 41268–41273

Love A, Geri C, Laird J, Yuri B, Loake G, Sadanandom A, Milner J (2008) An effector protein encoded by cauliflower mosaic virus inhibits SA-dependent defence responses in Arabidopsis via an NPR1-dependent mechanism. Ann Meet Soc Exp Biol Marseille **150:** S193–S193

Martin BR, Cravatt BF (2009) Large-scale profiling of protein palmitoylation in mammalian cells. Nat Methods **6:** 135–138

Montillet JL, Leonhardt N, Mondy S, Tranchimand S, Rumeau D, Boudsocq M, Garcia AV, Douki T, Bigeard J, Laurière C, Chevalier A, Castresana C, et al (2013) An abscisic acid-independent oxylipin pathway controls stomatal closure and immune defense in Arabidopsis. PLoS Biol **11:** e1001513

González Montoro A, Chumpen Ramirez S, Quiroga R, Valdez Taubas J (2011) Specificity of transmembrane protein palmitoylation in yeast. PLoS One **6:** e16969

Morris K, MacKerness SAH, Page T, John CF, Murphy AM, Carr JP, Buchanan-Wollaston V (2000) Salicylic acid has a role in regulating gene expression during leaf senescence. Plant J **23:** 677–685

Mueller S, Hilbert B, Dueckershoff K, Roitsch T, Krischke M, Mueller MJ, Berger S (2008) General detoxification and stress responses are mediated by oxidized lipids through TGA transcription factors in Arabidopsis. Plant Cell **20:** 768–785

Ohno Y, Kihara A, Sano T, Igarashi Y (2006) Intracellular localization and tissue-specific distribution of human and yeast DHHC cysteine-rich domain-containing proteins. Biochim Biophys Acta **1761:** 474–483

Porra RJ, Urzinger M, Winkler J, Bubenzer C, Scheer H (1998) Biosynthesis of the 3-acetyl and 13(1)-oxo groups of bacteriochlorophyll a in the facultative aerobic bacterium, *Rhodovulum sulfidophilum*–the presence of both oxygenase and hydratase pathways for isocyclic ring formation. Eur J Biochem **257:** 185–191

Putilina T, Wong P, Gentleman S (1999) The DHHC domain: a new highly conserved cysteine-rich motif. Mol Cell Biochem **195:** 219–226

Qi B, Doughty J, Hooley R (2013) A Golgi and tonoplast localized S-acyl transferase is involved in cell expansion, cell division, vascular patterning and fertility in Arabidopsis. New Phytol **200:** 444–456

Qi B, Fraser T, Mugford S, Dobson G, Sayanova O, Butler J, Napier JA, Stobart AK, Lazarus CM (2004) Production of very long chain polyunsaturated omega-3 and omega-6 fatty acids in plants. Nat Biotechnol **22:** 739–745

Resh MD (2006) Palmitoylation of ligands, receptors, and intracellular signaling molecules. Science STKE **2006:** re14

Rivas-San Vicente M, Plasencia J (2011) Salicylic acid beyond defence: its role in plant growth and development. J Exp Bot **62:** 3321–3338

Roth AF, Feng Y, Chen L, Davis NG (2002) The yeast DHHC cysteine-rich domain protein Akr1p is a palmitoyl transferase. J Cell Biol **159:** 23–28

Roth AF, Wan J, Bailey AO, Sun B, Kuchar JA, Green WN, Phinney BS, Yates JR III, Davis NG (2006) Global analysis of protein palmitoylation in yeast. Cell **125:** 1003–1013

Schippers JHM, Jing H, Hille J, Dijkwel PP (2007) Developmental and hormonal control of leaf senescence. Ann Plant Rev **26:** 145–170

Seltmann MA, Stingl NE, Lautenschlaeger JK, Krischke M, Mueller MJ, Berger S (2010) Differential impact of lipoxygenase 2 and jasmonates on natural and stress-induced senescence in Arabidopsis. Plant Physiol **152:** 1940–1950

Stelmach BA, Müller A, Hennig P, Gebhardt S, Schubert-Zsilavecz M, Weiler EW (2001) A novel class of oxylipins, *sn*1-*O*-(12-oxophytodienoyl)-*sn*2-*O*-(hexadecatrienoyl)-monogalactosyl Diglyceride, from *Arabidopsis thaliana*. J Biol Chem **276:** 12832–12838

Taki N, Sasaki-Sekimoto Y, Obayashi T, Kikuta A, Kobayashi K, Ainai T, Yagi K, Sakurai N, Suzuki H, Masuda T, Takamiya K, Shibata D, et al (2005) 12-Oxo-phytodienoic acid triggers expression of a distinct set of genes and plays a role in wound-induced gene expression in Arabidopsis. Plant Physiol **139:** 1268–1283

Thompson AR, Doelling JH, Suttangkakul A, Vierstra RD (2005) Autophagic nutrient recycling in Arabidopsis directed by the ATG8 and ATG12 conjugation pathways. Plant Physiol **138:** 2097–2110

Uemura T, Ueda T, Ohniwa RL, Nakano A, Takeyasu K, Sato MH (2004) Systematic analysis of SNARE molecules in Arabidopsis: dissection of the post-Golgi network in plant cells. Cell Struct Funct **29:** 49–65

van der Graaff E, Schwacke R, Schneider A, Desimone M, Flügge UI, Kunze R (2006) Transcription analysis of arabidopsis membrane transporters and hormone pathways during developmental and induced leaf senescence. Plant Physiol **141:** 776–792

Vlot AC, Dempsey DA, Klessig DF (2009) Salicylic acid, a multifaceted hormone to combat disease. Annu Rev Phytopathol **47:** 177–206

Vogelmann K, Drechsel G, Bergler J, Subert C, Philippar K, Soll J, Engelmann JC, Engelsdorf T, Voll LM, Hoth S (2012) Early senescence and cell death in Arabidopsis saul1 mutants involves the PAD4-dependent salicylic acid pathway. Plant Physiol **159:** 1477–1487

Weaver LM, Gan S, Quirino B, Amasino RM (1998) A comparison of the expression patterns of several senescence-associated genes in response to stress and hormone treatment. Plant Mol Biol **37:** 455–469

Wu Y, Zhang D, Chu JY, Boyle P, Wang Y, Brindle ID, De Luca V, Després C (2012) The Arabidopsis NPR1 protein is a receptor for the plant defense hormone salicylic acid. Cell Reports **1:** 639–647

Yoshimoto K, Hanaoka H, Sato S, Kato T, Tabata S, Noda T, Ohsumi Y (2004) Processing of ATG8s, ubiquitin-like proteins, and their deconjugation by ATG4s are essential for plant autophagy. Plant Cell **16:** 2967–2983

Yoshimoto K, Jikumaru Y, Kamiya Y, Kusano M, Consonni C, Panstruga R, Ohsumi Y, Shirasu K (2009) Autophagy negatively regulates cell death by controlling NPR1-dependent salicylic acid signaling during senescence and the innate immune response in Arabidopsis. Plant Cell **21:** 2914–2927

Zhang K, Halitschke R, Yin C, Liu CJ, Gan SS (2013) Salicylic acid 3-hydroxylase regulates Arabidopsis leaf longevity by mediating salicylic acid catabolism. Proc Natl Acad Sci USA **110:** 14807–14812

Zhang K, Xia X, Zhang Y, Gan SS (2012) An ABA-regulated and Golgi-localized protein phosphatase controls water loss during leaf senescence in Arabidopsis. Plant J **69:** 667–678

Zhou L, Li S, Feng Q, Zhang Y, Zhao X, Zeng Y, Wang H, Jiang L, Zhang Y (2013) Protein S-ACYL Transferase10 is critical for development and salt tolerance in Arabidopsis. Plant Cell **25:** 1093–1107

A

```
AtPAT14   KCNQLKPSRCHHCSVCGRCVLKMDHHCVWVVNCVGALNYKYFLLFLFYTFLETTLVTLVL 190
AtPAT10   YCHVEQPPRTKHCHDCDRCVLQFDHHCVWLGTCIGQKNHSKFWWYICEETTLCIWTLIMY 225
AtPAT24   TCKIIRPLRAKHCSTCDRCVEQFDHHCPWVSNCVGKKNKWEFFLFLLLEVLAMLITGGVT 434
Akr1p     ETWIRKPLRSKFSPLNNAVVARFDHYCPWIFNDVGLKNHKAFIFFITLMESGIFTFLALC 533
Akr2p     ETLERKPLRSKYSFFSGALVARYDHYCPWIYNDVGLKNHKLFVFFAVTVQYHMFLFMWLC 509
Swf1p     TCRIVKPARSKHCSICNRCVLVADHHCIWINNCIGKGNYLQFYLFLISNIFSMCYAFLRL 197
Erf2p     SCRIWRPPRSSHCSTCNVCVMVHDHHCIWVNNCIGKRNYRFFLIFLLGAILSSVILLTNC 236
Pfa3      VCHVWKPDRCHHCSSCDVCILKMDHHCPWFAECTGFRNQKFFIQFLMYTTLYAFLVLIYT 167
Pfa4      KCQSYKPERSHHCKTCNQCVLMMDHHCPWTMNCVGFANYPHFLRFLFWIIVTTSVLFCIQ 141
Pfa5      ECQSLKMERTHHSSELGHCIPRFDHYCMWIGTVIGRDNYRLFVQFAAYFSTLLLIMWVSI 192
HIP14     TCLIRKPVRSKHCGVCNRCIAKFDHHCPWVGNCVGAGNHRYFMGYLFFLLFMICWMIYGC 500
GODZ      KCCSIKPDRAHHCSVCKRCIRKMDHHCPWVNNCVGENNQKYFVLFTMYIALISLHALIMV 190
                : *  ..     :  ****.*    *  *   *  :
```

B

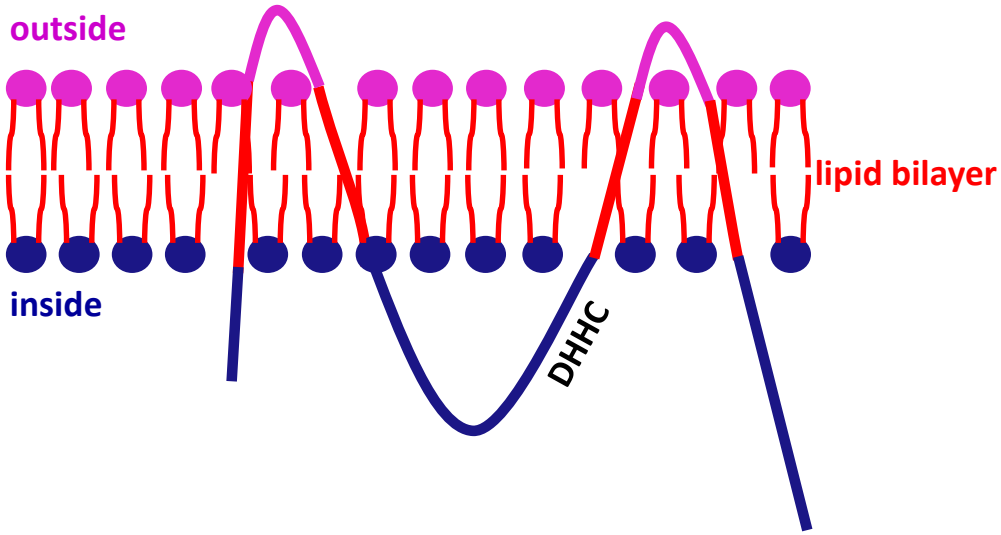

Supplemental Figure S1. Protein sequence alignment and secondary structure prediction of AtPAT14. A, AtPAT14 shares sequence homology around the DHHC-CRD region with other known PATs from Arabidopsis, yeast and mammals. The DHHC motif is boxed. AtPAT10, ACCESSION NP_566950.1, AtPAT24 (TIP1), ACCESSION NP_197535, HIP14, ACCESSION AAH50324, ERF2, ACCESSION Q06551, PFA3, ACCESSION NP_014073), SWF1, ACCESSION NP_010411, PFA5, ACCESSION NP_010747, PFA4, ACCESSION NP_014640, AKR1, ACCESSION NP_010550, AKR2, ACCESSION NP_014677. B, Secondary structure prediction of AtPAT14 shows that it has 4 transmembrane domains, and DHHC-CRD as well as both the C- and N-termini are localised in the cytosol.

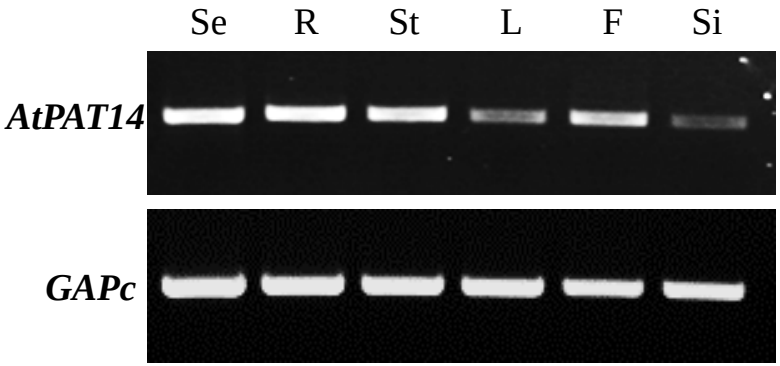

Supplemental Figure S2.. Expression level of AtPAT14 in seedlings and various tissues of mature Arabidopsis plants. RT-PCR was carried out on total RNA isolated form wild-type Col-0 whole seedlings and different parts of the plant. Se, 7-day old seedlings; R, roots of 2-week old seedlings grown on the 1/2 MS plate; St, stem of the first node of 35-day old soil-grown plants; L, the 5^{th} and 6^{th} rosette leaves of 4-week old soil-grown plants; F, fully-opened flowers; Si, 3-day-old siliques after pollination.

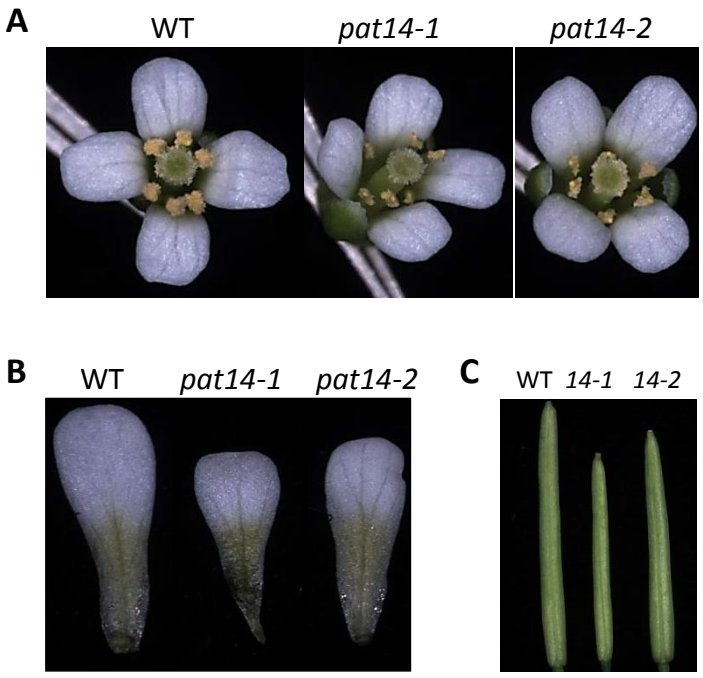

Supplemental Figure S3. Comparison of Arabidopsis reproductive organs and seed development from WT Col-0 and AtPAT14 mutant lines *atpat14-1* and *atpat14-2*. . A, flowers. B, petals. C, siliques at 5-days after pollination

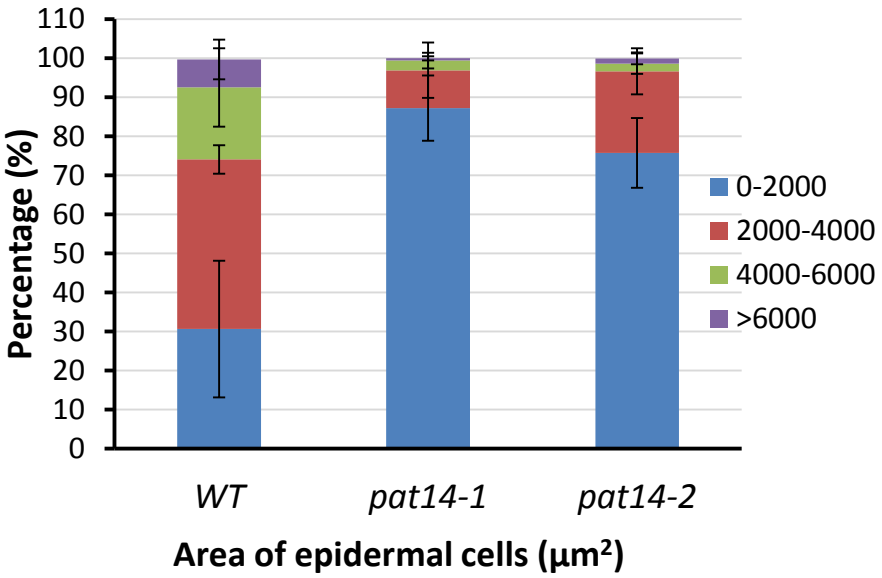

Supplemental Figure S4. *pat14* mutant has smaller cells than WT. The epidermal cells from fully expanded leaves of 28-day old WT, *pat14-1* and *pat14-2* were measured and put into 4 groups depending on their size ranges. The percentage of each size range out of 100 cells was calculated. Error bars are means ± SD of 3 replicates.

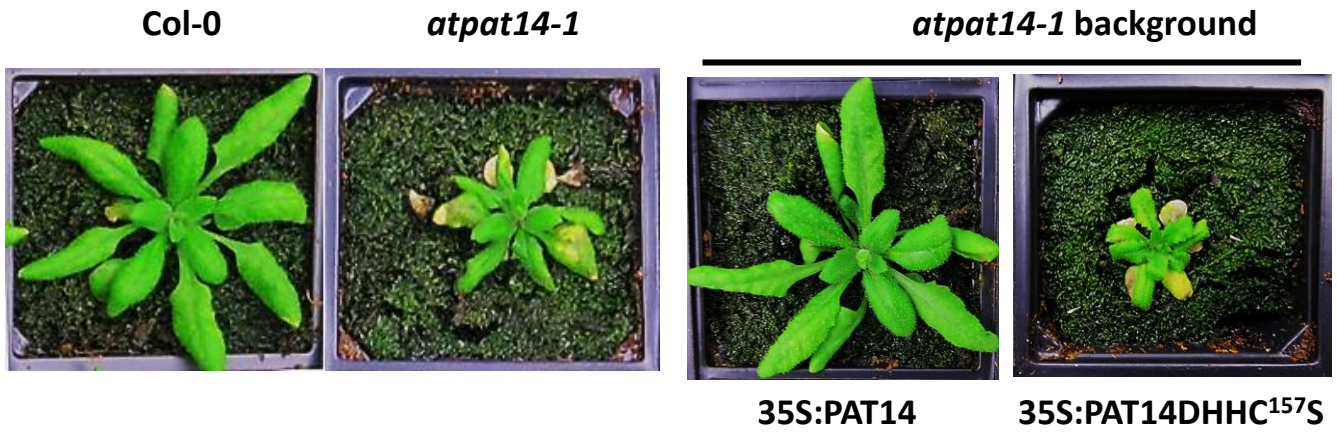

Supplemental Figure S5. Loss of AtPAT14 PAT activity causes the phenotypic defects of the *atpat14* mutant Arabidopsis plant. The mutant *atpat14-1* plants were transformed with 35S:PAT14 and 35S:PAT14DHHC^{157}S constructs and transgenic plants were recovered from selection on *Basta* herbicide.

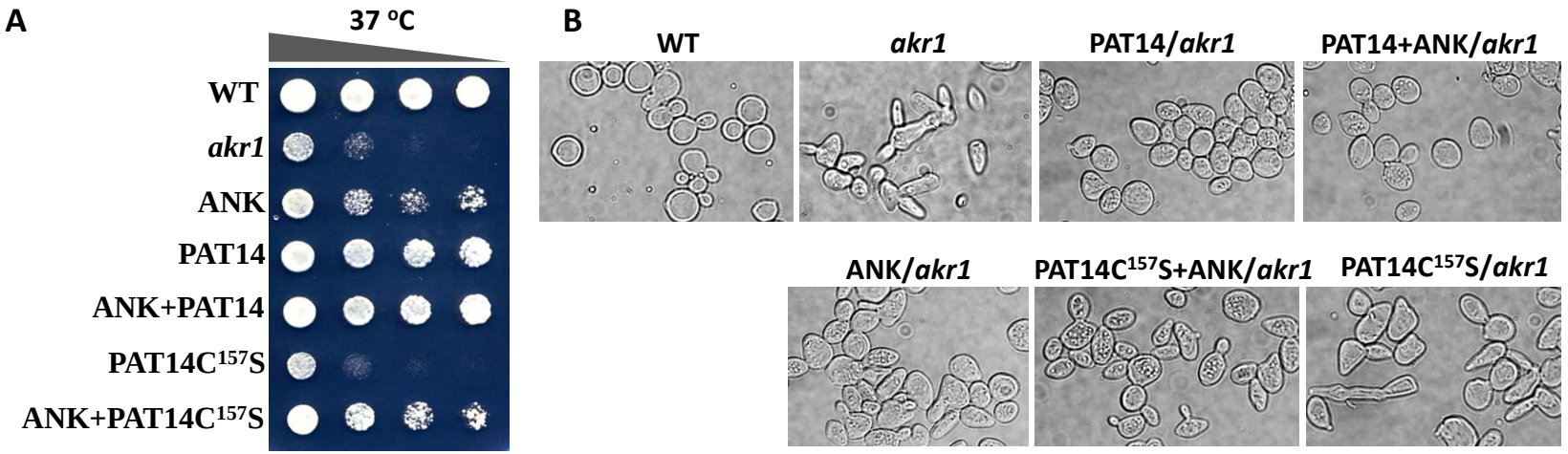

Supplemental Figure S6.. Restoration of akr1growth defects by PAT14 at the non-permissive high temperature of 37ºC was enhanced by the ankrin repeats of AKR1. A. Growth test. B. DIC light microscopy of cells of all 7 genotypes grown at 37ºC. At non-permissive temperature 37ºC, wild type (WT) yeast grew well but *akr1* did not. Expressing AtPAT14 in *akr1* (PAT14/*akr1*) largely restored the growth inhibition by 37ºC. This is particularly true with co-expression of PAT14 and AKR1C-S (ANK) where the Cys at its S-acyltransferase activity site DHHC was mutated to Serine so that the function of AKR1 only relies on its ankrin repeat region. Some rescue, although to a much lesser extent, was also found when expressing AKR1C-S (ANK), or co-expressing AtPAT14C^{157}S and AKR1C-S (ANK+PAT14C^{157}S) and this was due to the functional ankrin repeat domain of AKR1. However, expressing AtPAT14C^{157}S (PAT14C^{157}S/*akr1*) did not restore the growth inhibition of *akr1* at all. Five microlitres of 10-fold serial dilutions from 1 OD600 cells were spotted on solid medium supplemented with 2% galactose and grown at 37ºC for 3 days. Cells of WT and *akr1* were transformed with empty vectors pYES2 and pESC-Leu for positive and negative controls, respectively. Cells of mutant *akr1* were also transformed with AKR1C-S (ANK) and the empty vector pYES2, AtPAT14 and the empty vector pESC-Leu (PAT14), AKR1C-S and AtPAT14 (ANK+PAT14), AtPAT14C-S and the empty vector pESC-Leu (PAT14C^{157}S) and AKR1C-S and AtPAT14C^{157}S (ANK+PAT14C^{157}S) so that comparisons could be made on the same medium/plate.

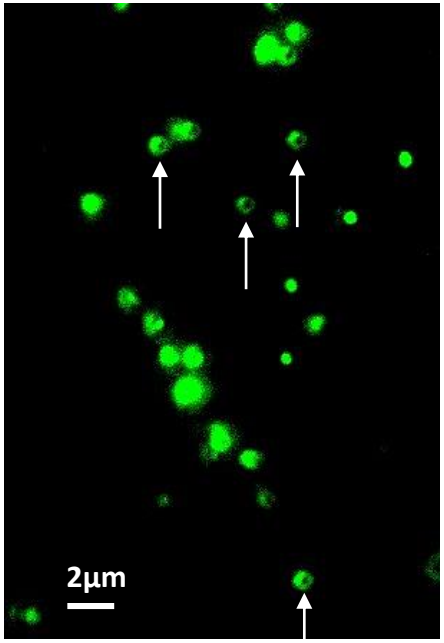

Supplemental Figure S7. AtPAT14 is predominantly localized in Golgi. The 'doughnut' shaped Golgi apparatus of PAT14-GFP (arrows) observed in the cotyledons of epidermal cells from 10-day-old seedlings of stably transformed Arabidopsis plants. A similar structure of Golgi bodies was reported with the *trans*-Golgi marker STtmd-GFP in tobacco leaf cells. Immunogold labelling localised STtmd-GFP to the Golgi bodies and this appeared to be predominately in the *trans*-half of the stacks (Boevink et al, 1998)

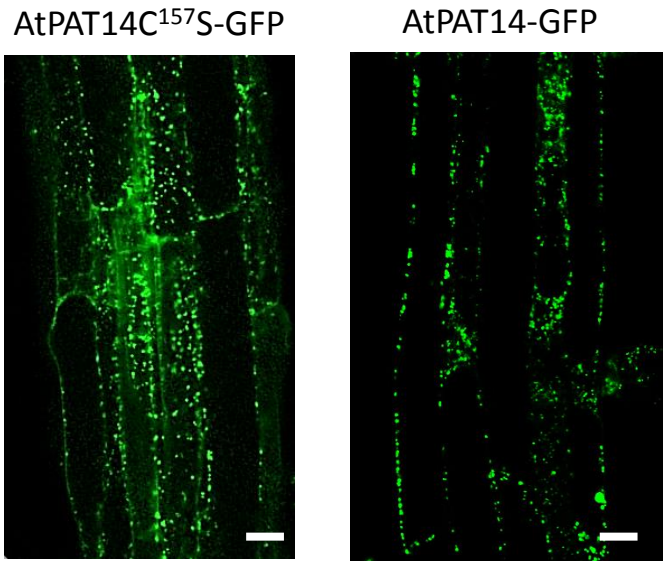

Supplemental Figure S8. Mutation in Cys157 of the DHHC motif has no effect on AtPAT14 localization. Confocal microscopy observation of the primary root of *atpat14-1* Arabidopsis seedlings transformed with the 35S:AtPAT14DHHC^{157}S-GFP and AtPAT14-GFP construct. A similar pattern between these lines was observed. Scale bar = 10 µm

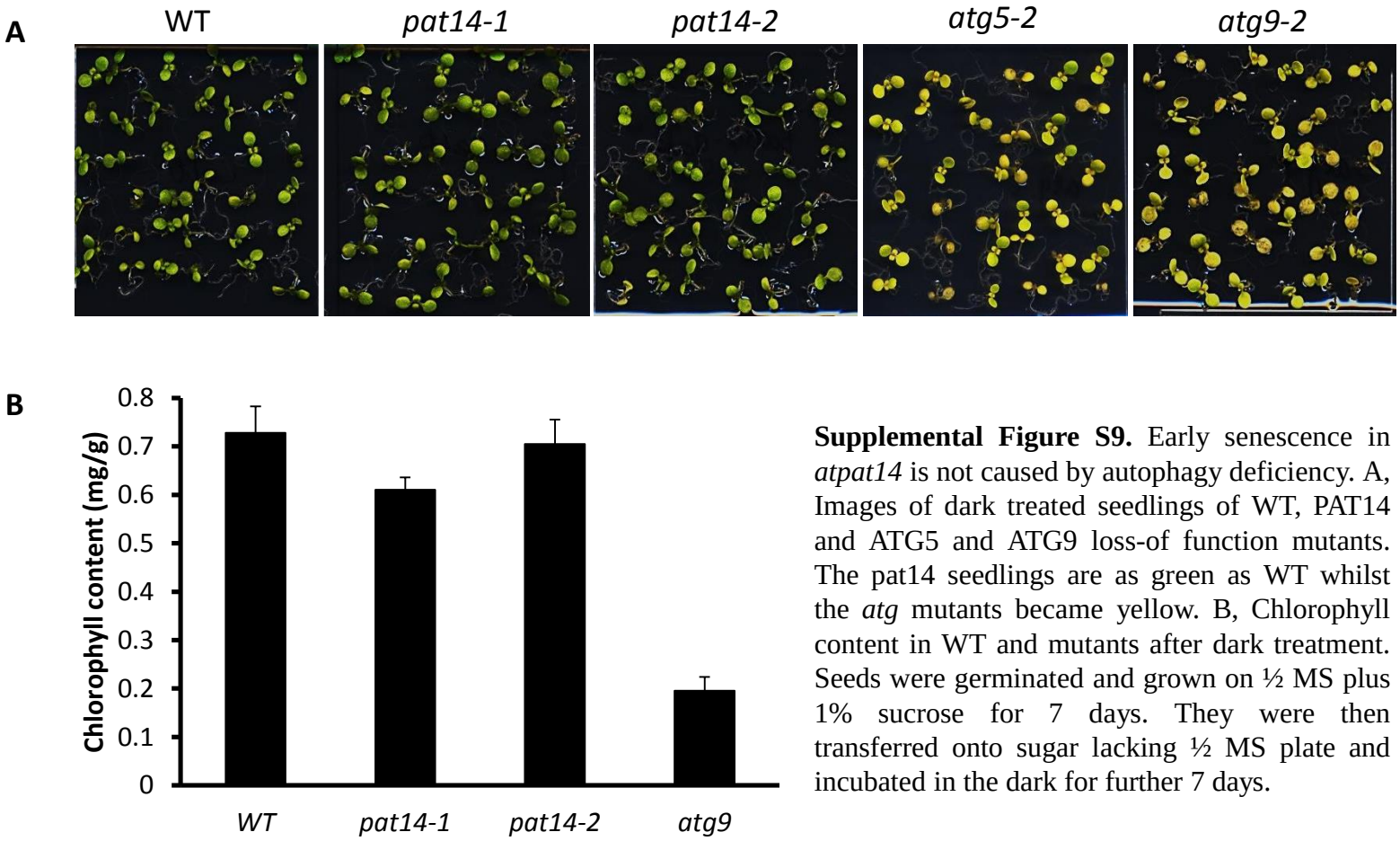

Supplemental Figure S9. Early senescence in *atpat14* is not caused by autophagy deficiency. A, Images of dark treated seedlings of WT, PAT14 and ATG5 and ATG9 loss-of function mutants. The pat14 seedlings are as green as WT whilst the *atg* mutants became yellow. B, Chlorophyll content in WT and mutants after dark treatment. Seeds were germinated and grown on ½ MS plus 1% sucrose for 7 days. They were then transferred onto sugar lacking ½ MS plate and incubated in the dark for further 7 days.

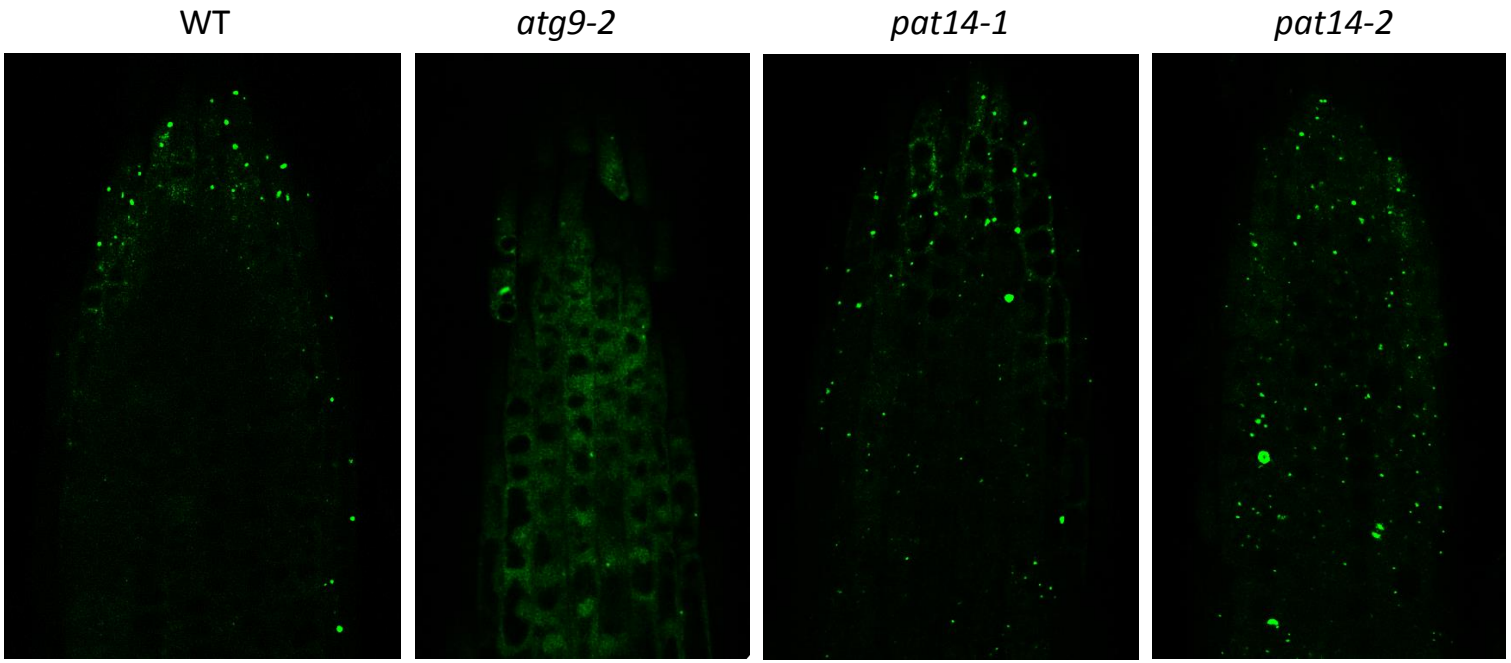

Supplemental Figure S10. The subcellular localization of ATG8-GFP is not changed in *pat14* mutant roots. UBQ10:ATG8-GFP were transformed into WT, *atg9-2* and *pat14* and the fluorescent signals in the roots of 7-day-old seedlings were observed using CLSM.

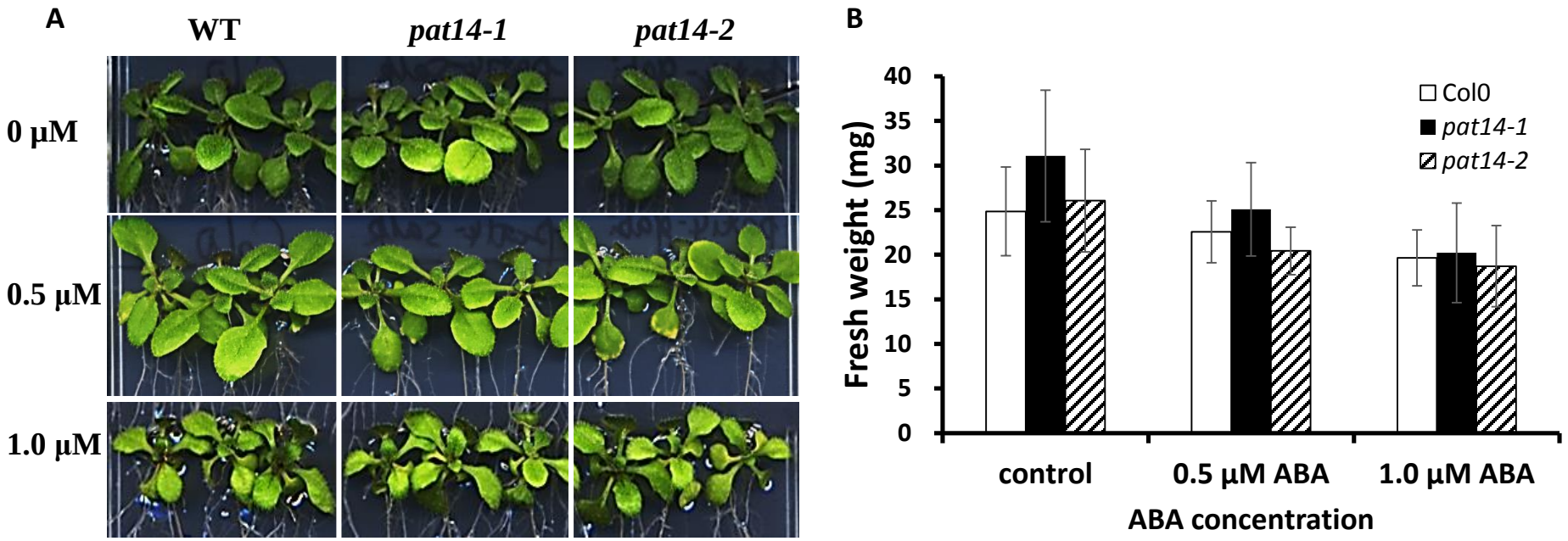

Supplemental Figure S11. PAT14 mutants are not sensitive to exogenous ABA treatment during early seedling growth. A, Images of seedlings. B, Fresh weight of seedlings. Seeds were geminated and grown on ½ MS plus 1% sucrose medium for 4-day. They were then transferred to the same fresh medium supplemented with 0 (control), 0.5 and 1.0 µM ABA and grown for further 15 days before being scanned and the weight of the shoot of each seedling was recorded.

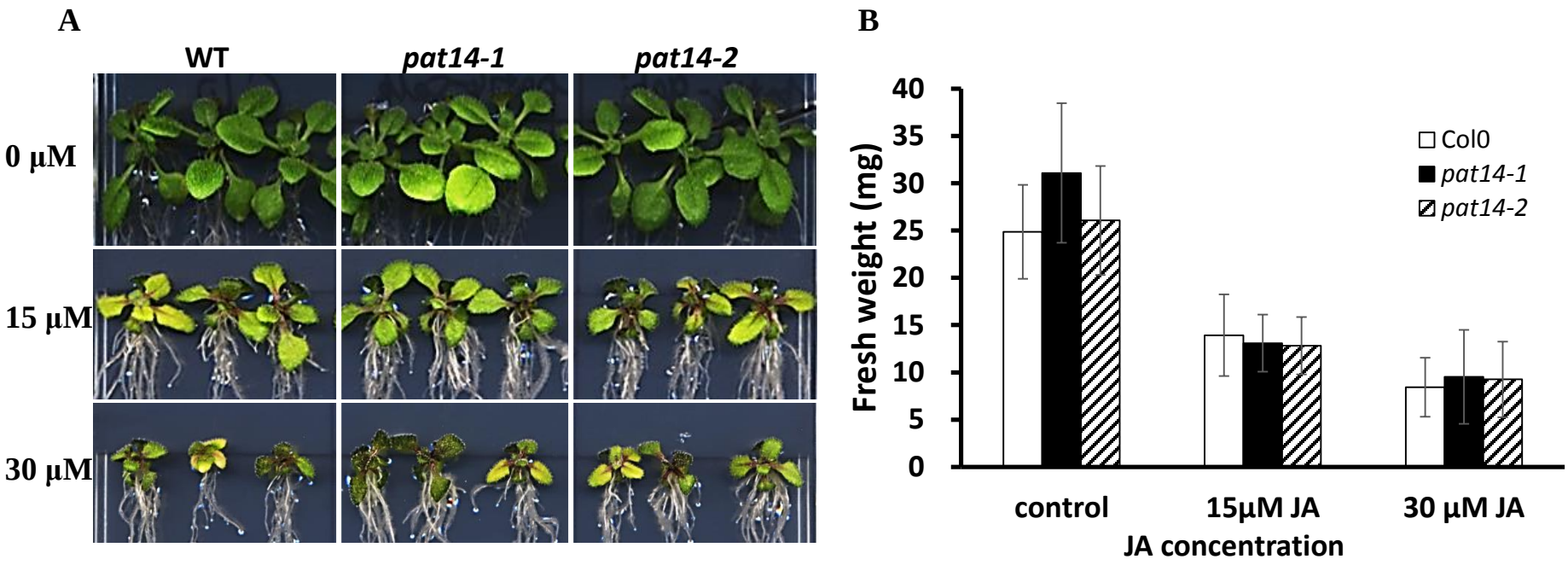

Supplemental Figure S12. *pat14* mutants are not sensitive to exogenous JA treatment during early seedling growth. A, Images of seedlings. B, Fresh weight of seedlings. Seeds were geminated and grown on ½ MS plus 1% sucrose medium for 4-day. They were then transferred to the same fresh medium supplemented with 0 (control), 15 and 30 µM ABA and grown for further 15 days before being scanned and the weight of the shoot of each seedling was recorded.

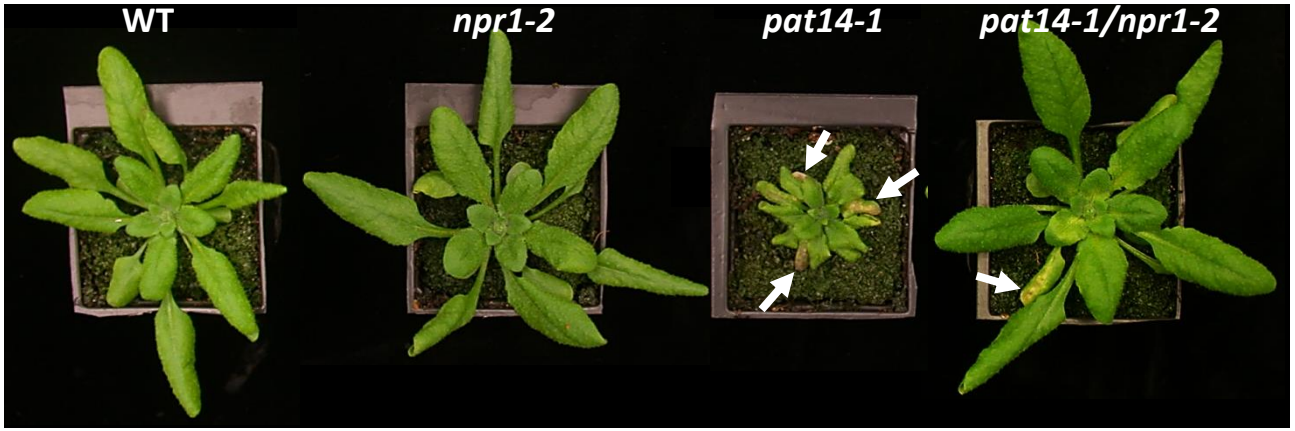

Supplemental Figure S13. The early senescence phenotype of pat14 is rescued by blocking SA signaling in the mutant. Pictures of 4-week old plants of WT, *pat14-1*, *npr1-2* and *pat14-1/npr1*-2 double mutant were taken. Arrows show the yellowing of *pat14-1* and *pat14-1/npr1-2* leaves.

Supplemental Table S1. Phenotypic analysis of WT, *pat14-1* and *pat14-2*

	WT	*pat14-1*	*pat14-2*
Leaf Area (mm^2)	179.2±11.1	57.9±15.2	116.8±8.4
Plant height (mm)	444.7±45.6	264.4±66.4	361.4±58.9
No. of branches	15.4±3.9	5.1±2.0	9.5±2.5
No. of siliques on main branch	48.7±7.1	27.4±6.7	36.3±7.9
No. of seeds per silique	60±2	47±6	56±7
Length of siliques (mm)	14.0±1.2	11.7±0.8	13.7±1.2
Cell number of petal	70±5.6	70±2.1	74±5.6
Cell size of petal (μm^2)	320.8±30.1	206.2±37.2	218.4±19.6

All the data was collected from 8-week old plants. The length of silique was measured for the 10^{th} silique counted from the base of the main branch. Cell number was counted from epidermal cells across the widest part of cleared petals of fully opened flowers.

Supplemental Table S2. Sequence of primers used for cloning and normal PCR

primer	sequence
attB1	5’-GGGGACAAGTTTGTACAAAAAAGCAGGCT-3’
attB2	5’-GGGGACCACTTTGTACAAGAAAGCTGGGT-3’
3g60800Beg	5’-CAAAAAAGCAGGCTccaccATGCATAGATCTGGTACAAC-3’
3g60800End	5’-CAAGAAAGCTGGGTcCTGGGAATCAAAGTCG-3’
PAT14DHHC-SFor	5’-GATGGATCACCATTCTGTTTGGGTTGTTAAC-3’
PAT14DHHC-SRev	5’-GTTAACAACCCAAACAGAATGGTGATCCATC-3’
GAPc For	5’-CACTTGAAGGGTGGTGCCAAG-3’
GAPc Rev	5’-CCTGTTGTCGCCAACGAAGTC-3’
F1	5’-GCTCCAAAAGAGGAAAACGA-3’
R1	5’-TCCACGCCATTGTTGTACC-3’
F2	5’-TCATGGGGTCTCTGCATCTT-3’
R2	5’-CCGAACTCTTGGGTTTGAAG-3’
F3	5’-TCTGTTTGTGGTCGGTGTGT-3’
R3	5’-TGAGCATCACTGGGAATCAA-3’
LBb1	5’-GCGTGGACCGCTTGCTGCAACT-3’
SALK026159LP	5’-TTCGACTATTCACCGTTCGAC-3’
SALK026159RP	5’-TCCAATTAGGAGGCACAACAC-3’
GABILBb1	5’-ATTTTGCCGATTTCGGAAC-3’
GABI_153A10LP	5’- CACACCGACCACCTATATTGG-3’
GABI_153A10RP	5’- CCAAAAGAGGAAAACGAATCC-3’
NPR1For	5’-TCTTCAAGAGCGCTTTAGCC-3’
NPR1Rev	5’-CGTCCAATAAGTGCCTCTGA-3’

Supplemental Table S3. Sequence of primers used for Real time PCR

primer	sequence
qAtEF-1αF	5’- TGAGCACGCTCTTCTTGCTTTCA -3’
qAtEF-1αF	5’- GGTGGTGGCATCCATCTTGTTACA -3’
qSAG12F	5’- TTACAGGTTATGAGGATG -3’
qSAG12R	5’- AGACGAATAGAATTGGAA -3’
qSAG101F	5’- GTCTCACCACTATGTTATGC -3’
qSAG101R	5’- ATTACAATCAACGAATCCTCAA -3’
qPR1F	5’- AGGTGTAACAATGGTGGAA -3’
qPR1R	5’- TTAGTATGGCTTCTCGTTCA -3’
qPAL1F	5’- AAGAGCAGCCTACGATAA -3’
qPAL1R	5’- CTATACAATGGATACGACCTAC -3’
qICS1F	5’- TTCTTCCGTGACCTTGAT -3’
qICS1R	5’- AACGCATACCACCATAGG -3’
qS3HF	5’- GCGACCATATAAGCAATA -3’
qS3HR	5’- AAGAAGGACAGTGATAAC -3’
qWES1F	5’- CTTGATGCCTGTGATGAG -3’
qWES1R	5’- TGGATTCGGACTTGATGA -3’
qEDS5F	5’- TTGGCGATACAATCCTAT -3’
qEDS5R	5’- AGAGAATCCATCATCATATAAG -3’
qPAD4F	5’- CCG ATG AAC CTC TAC CTA -3’
qPAD4R	5’- CCT AAC AAT TCC AAT TCC AAT -3’
qNPR1F	5’- CTATGGCGGTTGAATGTA -3’
qNPR1R	5’- TTGTCTTCTTGCTCTAGTATT -3’
qNHL25F	5’-GTTGCGGATTAGAGTTACC-3’
qNHL25R	5’-CGGATACACCACACCTAA-3’

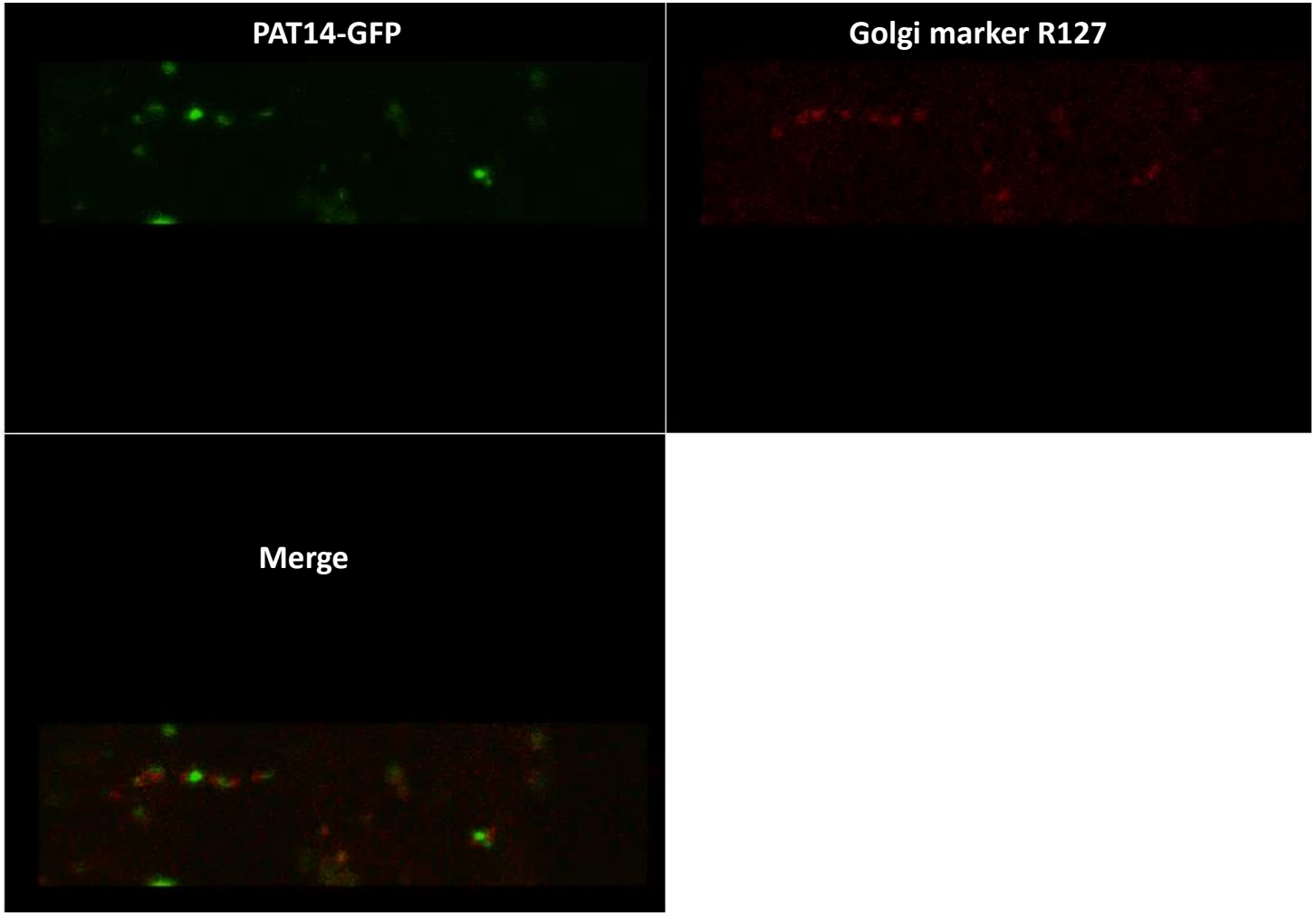

Supplementary Video S1. AtPAT14 co-localizes with the Golgi marker R127. The highly motile florescent foci labelled by AtPAT14-GFP is seen moving together with the mCherry labelled Golgi marker MEMB12 (At5g50440) in the merged picture.

3.3 Further results and discussion

3.3.1 SA induced senescence pathway is independent of SA-regulated biotic and abiotic defence responses

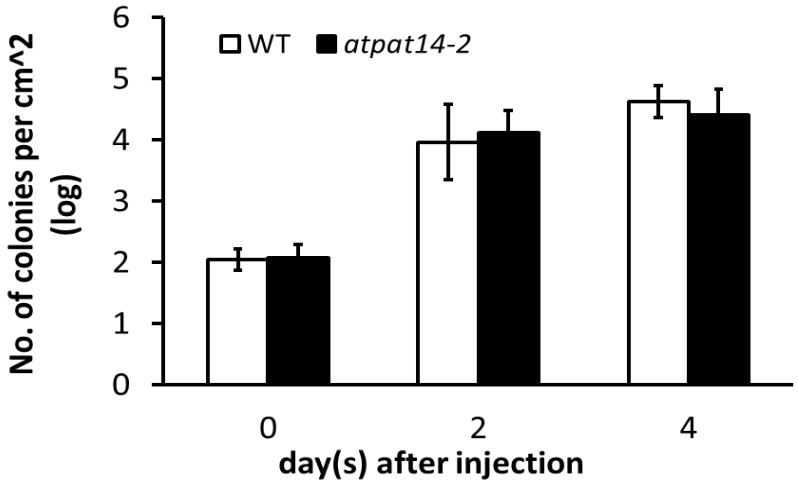

Figure 3-1. *atpat14-2* has similar biotic resistance against *Pseudomonas syringae pv. tomato* DC3000 as WT.
P. syringae pv. tomato DC3000 (10^6/ml) was injected into the rosette leaves of 4-week-old WT and *pat14-2* and the infected plants were incubated for 0, 2 and 4 days. Number of colonies were counted from at least 6 leaves for each time point. Values are means±SD of 6 replicates.

SA has been commonly known as a signal molecule in plant defence mechanism including pathogen infection and salt stress (Horvath et al., 2007). Because higher level of SA was accumulated in *atpat14* mutant plants we hypothesised that these mutant plants might be more resistant to biotic and abiotic stresses. This is because blockage in either the SA signalling mutant *npr1* or the SA synthesis mutant *ics1* plants result in enhanced disease sensitivity (Van Wees and Glazebrook, 2003; Wildermuth et al., 2001; Jayakannan et al., 2015). To verify this speculation, we tested the biotic resistance of *atpat14* by comparing the number of the bacterial pathogen *Pseudomonas syringae pv. tomato DC3000* (10^6/ml) in the infected leaves of both WT and *atpat14-2* mutant plants. As shown in Fig. 3-1 the number of colonies recovered from *atpat14-2* was compatible to

that of WT after 2 and 4 days inoculation, indicating that the mutant does not show more resistant to this pathogen than the WT.

Next, we tested to see if *atpat14* is more salt resistance. For this, 4-day old WT and *atpat14* mutant plants were transferred to the media supplemented with 50mM and 100mM NaCl. After 14 days, we observed these seedlings and found that WT and the mutant Arabidopsis plants showed similar sensitivity to salt stress because they exhibited similar phenotype under these conditons (Fig. 3-2). This is also consistent with the notion that SA induced senescence is specifically age-dependent but not related to dark or other external factors induced leaf senescence (Lim et al., 2007). Indeed, studies showed that the transcriptome change relied on SA pathway was very similar to the one mediated by age-dependant senescence (Morris et al., 2000; Lim et al., 2007). Consistent with this our results from studies of *atpat14* also demonstrated that the SA-dependent leaf senescence pathway is different from the SA-dependent biotic or abiotic stress pathways.

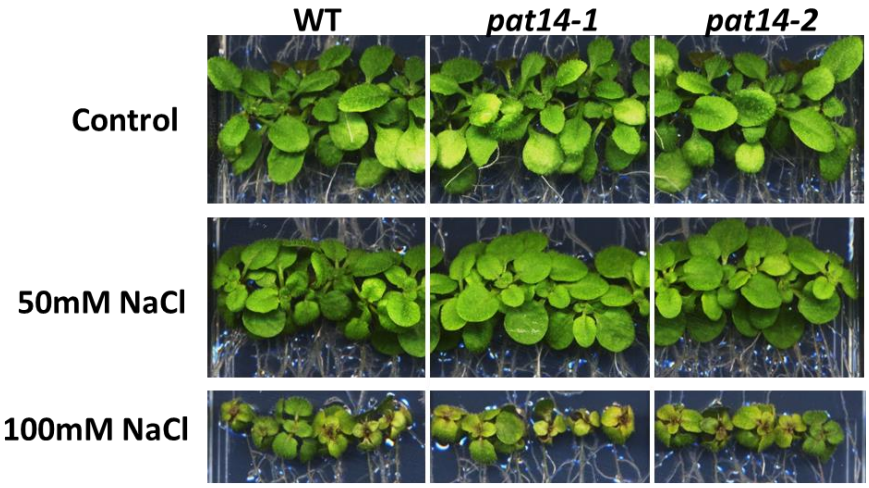

Figure 3-2. *atpat14* mutants show similar sensitivity to salt as WT.
4-day old seedlings were treated with 0 mM, 50 mM and 100 mM NaCl for 14 days.

3.3.2 Mode of action of AtPAT14 in SA induced leaf senescence

To validate the conclusion made above mutation causing defects in SA signalling was introduced in *atpat14* mutant by genetic crossing. Two genes, the *NDR1* (*Non race-*

specific disease resistance 1) and *NPR1* (*Non-expresser of PR genes 1*) are known to be important in the SA-mediated defence signalling pathway in plant (Ülker et al., 2007; Lu et al., 2013; Wu et al., 2012). While NDR1 functions upstream of SA, which can cause the accumulation of SA in response to reactive oxygen species (Shapiro and Zhang, 2001), NPR1, as a SA receptor can respond to the elevated SA levels and regulate the expression of other genes in the pathways when challenged with pathogen (Zhang and Shapiro, 2002; Wu et al., 2012). Study showed that the loss-of-function mutant of NPR1, *npr1-1*, which exhibits increased susceptibility to infections, also showed delayed senescence phenotype, indicating the converging roles of SA signalling in defence and senescence (Morris et al., 2002). In the double mutant of *atpat14-1/npr1-1* the early leaf senescence symptom of *atpat14-1* was largely rescued (Figs. 9 and S13). This demonstrates that the overproduction of SA due to the loss-of-function of PAT14 is overcome by the lack of SA signalling due to the SA receptor NPR1 is rendered non-functional in the double mutant. Therefore, the leaf senescence phenotype showed in *atpat14* mutant is indeed relied on SA pathway.

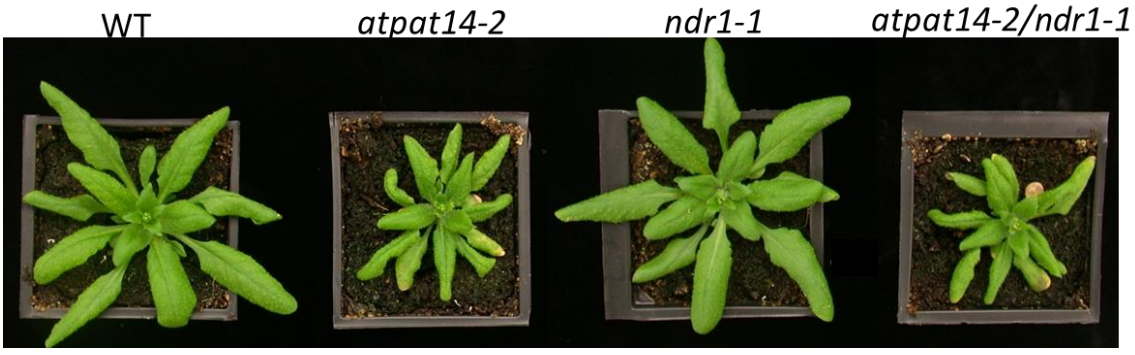

Figure 3-3. *atpat14/ndr1* double mutant shows similar phenotype as *atpat14*.
Images were taken from 4-week old plants of WT, *atpat14-2* and *ndr1-1* single and *atpat14-2/ndr1-1* double mutants.

The loss-of-function mutant *ndr1* cannot accumulate SA and is more sensitive to biotic stress than WT (Shapiro and Zhang, 2001). However, as to whether it also has delayed leaf senescence like other SA-deficient mutants is currently unknown. Therefore, we investigated this by comparing the phenotype of *ndr1* to the WT Col-0 under LD conditions. Surprisingly, we did not find any difference between them, i.e. *ndr1* did not show delayed senescence phenotype as expected (Fig. 3-3). Therefore, lack of SA production or signaling can cause plant more susceptible to biotic stress, but cannot cause early senescence. This suggested that NDR1 dependent SA signaling pathway plays important roles in defence but not leaf senescence.

To see if *ndr1* can rescue the early senescence phenotype of *atpat14* we crossed *atpat14-2* with *ndr1-1* to produce *atpat14-2/ndr1-1* double mutant. Interestingly the double mutant exhibited the same early senescence phenotype as the single *atpat14* mutant, therefore *ndr1-1* cannot rescue the early senescence phenotype of *atpat14-2* (Fig. 3-3). This result demonstrates that NDR1 and AtPAT14 may work independently, while NDR1 involves in the SA-dependent biotic stress AtPAT14 regulates the SA-dependent leaf senescence. This also explains why *atpat14* mutant did not show more resistant to biotic and salt stress compared to WT (Figs. 3-1 and 3-2).

Here, we propose a model to show how AtPAT14 is involved in leaf senescence mediated by the SA signalling pathway which is independent to the SA-dependent defence signalling pathways (Fig. 3-4). In this model SA is synthesised in two different compartments, resulting in the production of SA1 and SA2, and both are recognized by NPR1. The biosynthesis of SA1 is induced by pathogen and this is mediated by NDR1. SA1 is synthesised in the plastid mainly by ICS (Wildermuth et al., 2001; Kumar, 2014) and transported into cytoplasm through the reversible methyl SA form (MeSA) (Shulaev et al., 1997; Kumar, 2014). On the other hand, the senescence-associated SA2 is produced in the cytoplasm which is negatively regulated by yet to be characterised S-acylted proteins(s) mediated by the Golgi-localised AtPAT14. In this case, loss-of-function of AtPAT14 causes de-palmitoylation and subsequent cytosolic localization of the unknown

protein(s), resulting in SA2 biosynthesis. Both SA1 and SA2 can cause the de-association of the resting oligomeric NPR1 complex (Chi et al., 2013). The monomeric NPR1 migrates to the nucleus where it can trigger the transcription of the downstream genes to induce defense response or senescence.

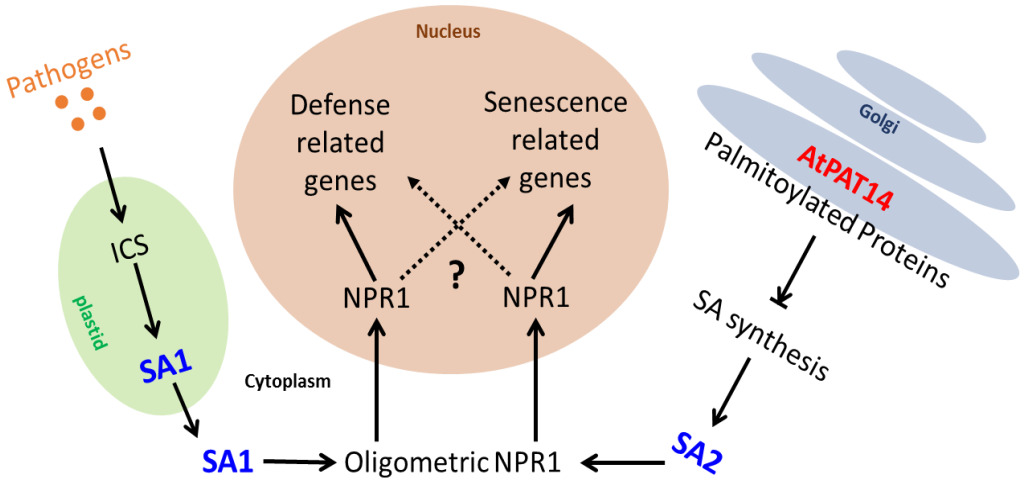

Figure 3-4. A proposed model to show the independent and converging roles of SA in defense pathway and leaf senescence pathway. Pathogens can induce NDR1 which in turn can enhances the activity ICS, leading to the accumulation of SA1 in plastid. SA1 is transported to cytoplasm through the reversible methyl SA form. During leaf senescence SA2 is synthesized through a different pathway which is regulated by AtPAT14, catalyzing the palmitoylation of some unknown protein(s). The accumulation of both SA1 and SA2 in cytoplasm can cause the disassociation of the resting oligomeric NPR1. The monomeric NPR1 migrates to the nucleus to induce the expression of defense or senescence related genes. SA, salicylic acids; ICS, isochorismate synthase; NPR1, Non-expresser of Pathogenesis-Related genes 1; NDR1, Non race-specific disease resistance 1. Solid line indicates pathways have been proved by previous studies or the current study; Dotted line indicates the possible pathways.

Future studies will be focused on the identification of the S-acylated protein(s) by AtPAT14 that are involved in the regulation of SA synthesis and signalling. This will provide further important clues regarding to the relationship between SA signalling and protein palmitoylation in plant leaf senescence.

Chapter 4 Protein S-Acyl Transferase 21, AtPAT21, Is Essential for Both Male and Female Fertility in Arabidopsis

4.1 Introduction

Sexual reproduction of spermatophytes involves in the generation of male and female sporophytes and gametophytes and the cross-talk between male and female gametophytes, resulting in fertilization and seed production (Dresselhaus and Franklin, 2013; Panoli et al., 2015). First, the pollen grains germinate on the stigma and produce long pollen tubes which navigate through papilla cells and the style and finally reach the embryo sac through micropyle (Dresselhaus and Franklin-Tong, 2013). Many proteins, such as cysteine-rich proteins (CRPs) (Silverstein et al., 2007), stigmatic protein Exo70A1 (Samuel et al., 2009), γ-aminobutyric acid (GABA) (Palanivelu et al., 2003), cation/proton exchangers (CHX) (Lu et al., 2011), Defensin-like polypeptide LUREs (Okuda et al., 2009) and Lost-In-Pollen tube guidance LIP1/LIP2 (Liu et al., 2013), are known to be involved in guiding the pollen tube to embryo sac. After the pollen tube enters the ovule, it releases its two sperm cells, one fertilizes the egg cell to produce the diploid embryo and the other fertilizes the central cell to produce the triploid endosperm. This double fertilization process is a unique characteristic of flowering plant, and is very important for plant reproduction (Dresselhaus and Franklin-Tong, 2013). A number of proteins are activated during the double fertilization process and these are the male gamete fusion factor HAP2/GCS1, egg cell-secreted EC1 proteins, central cell-expressed BAHD acyl-transferases, the male and female gametophytes expressed mitochondrial Ankyrin repeat protein ANK6 and others (Dresselhaus and Franklin-Tong, 2013; Mori et al., 2006; Sprunck et al., 2012; Leshem et al., 2010; Yu et al., 2010).

Meiosis is a unique type of cell division that happens in all eukaryotic organisms that reproduce sexually, including animals, plants and fungi, resulting in the production of the egg and sperm cells (Bernstein and Bernstein, 2010). In Arabidopsis, each diploid microsporocyte in the anther or megasporocyte in the ovule is first divided through

meiosis into a tetrad of microspores or four megaspores respectively (Yang et al., 2003). The microspores in the tetrad will further develop into pollen grains. Each mature pollen grain contain two sperm cells (male gametes) and one vegetative cell (Scott et al., 2004; Ma, 2005). In the ovule three of the four megaspores are degraded and the remaining functional megaspore will develop into a huge coenocyte through three rounds of karyokinesises to form the eight-nucleate embryo sac. The coenocytic embryo sac is divided into seven cells with four cell types, including three antipodal cells, two synergids, one diploid central cell and one egg cell (female gametes) (Yang et al., 2010; Panoli et al., 2015). Defects in any one of these processes may cause sterile gametes, leading to the failure in seed production. Many proteins are involved in the different phases of meiosis, and their loss-of-function mutants exhibit different levels of sterility (Mercier et al., 2015).

In this chapter, we will describe the identification and characterization of a novel PAT from Arabidopsis, AtPAT21. The biological function of AtPAT21 is investigated by the observation and characterization of a homozygous T-DNA knockout mutant line where the plants failed to produce any seeds, i.e., they are completely sterile. To understand the causes of the sterility of *atpat21-1* mutant, detailed studies were carried out and we found that both male and female sporophytes and gametophytes are defective that ultimately contribute to the failure in seed production. Therefore, AtPAT21 mediated protein palmitoylation plays essential roles in the reproduction of Arabidopsis.

4.2 Results

4.2.1 AtPAT21 shares the conserved sequence motifs with other known DHHC-CRD PATs

AtPAT21 (At2g33640), which has 1,698 base pairs of nucleotides and encodes a protein of 61 kDa, is one of largest PATs within the family of 24 PATs in Arabidopsis. Using the online software TMHMM v2.0 it is predicted that AtPAT21 has 4 trans-membrane domains (TMD) that locates between the 12-34th, 44-66th, 189-211st and 240-262nd amino acid positions, respectively, a short cytoplasmic N-terminal region and an

extended C-terminal domain (Fig. 4-1A, Batistic, 2012). The DHHC-CRD, which is the core S-acyl transferase activity functional domain, is predicted to be cytosolic and located between the second and the third TMDs. Sequence alignment with other known PATs shows that AtPAT21 shares high homology within the DHHC-CRD regions to other known DHHC-CRD PATs from Arabidopsis, yeast and mammals (Fig. 4-1B). Other conserved regions/motifs, such as DPG and TTxE (Mitchell et al., 2006), are also found in the AtPAT21 sequence (Fig. S1).

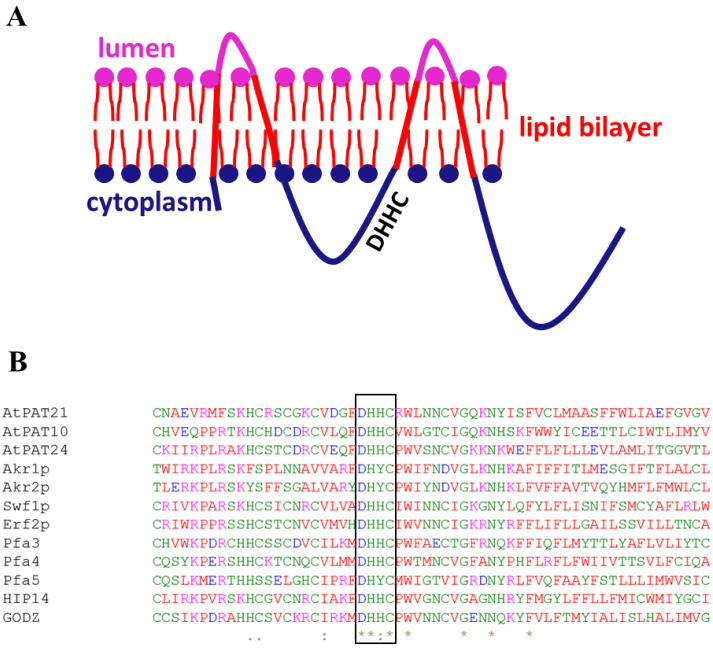

Figure 4-1. Secondary structure prediction and protein sequence alignment of AtPAT21 with other known DHHC-PATs.

A. Secondary structure prediction of AtPAT21 shows that it has 4 transmembrane domains, and DHHC-CRD as well as both the C- and N-termini are localised in the cytosol.

B. AtPAT21 shares sequence homology at the DHHC-CRD region with other known PATs from Arabidopsis, yeast and mammals. The DHHC motif is boxed. AtPAT21, ACCESSION NP_180922; AtPAT24 (TIP1), ACCESSION NP_197535; AtPAT10, ACCESSION NP_566950.1; Akr1, ACCESSION NP_010550; Akr2, ACCESSION NP_014677; Swf1, ACCESSION NP_010411; Erf2, ACCESSION Q06551; Pfa3, ACCESSION NP_014073; Pfa4, ACCESSION NP_014640; Pfa5, ACCESSION NP_010747; HIP14 (DHHC17), ACCESSION AAH50324; GODZ (DHHC3) ACCESSION NP_057682.

4.2.2 PAT21 is an S-acyl transferase

Yeast complementation in the yeast PAT Akr1 knockout mutant *akr1* has been used

previously to test the enzyme activity of 3 characterised plant PATs, AtPAT24 (TIP1) (Hemsley et al., 2005), AtPAT10 (Qi et al., 2013) and AtPAT14 (Li et al., 2015). To see if AtPAT21 also has S-Acyl transferase activity by this yeast complementation method we transformed pYES-AtPAT21 into *akr1* cells. The growth and cell phenotype of transgenic *akr1* were observed and compared at 25 ºC and the non-permissive temperature of 37ºC. As shown in Fig 6-2A, wild type (WT) yeast cells are normal round shape with a single nucleus at 37°C. However, majority of the *akr1* cells are elongated with multiple nuclei (arrows). Cells of *akr1* also grew poorly compared to WT (Fig. 4-2B). Although the transgenic *akr1* cells harbouring *AtPAT21* did not grow as well as WT they grew much better than the mutant *akr1*, and unlike the *akr1* these cells also became rounder with only one nucleus as found in WT (Fig. 4-2B). Therefore, AtPAT21 can partially rescue the growth defect of *akr1* at high temperature. In order to confirm the S-acyl transferase activity of PAT21 relies on its DHHC domain, we changed cysteine in the DHHC domain to serine and transformed the mutant GAL1-PAT21DHHC^{174}S into the yeast cells of *akr1*. It appeared that PAT21DHHC^{174}S cannot rescue the growth defects of *akr1* at all because the PAT21DHHC^{174}S transformed *akr1* cells remained elongated and grew as poorly as the *akr1* cells with multiple nuclei (arrows) (Fig. 4-2B).

One of the characteristics of all the known DHHC-CRD PATs is their ability to auto-acylate in vitro. To see if AtPAT21 also possesses this function we pulled down by the Acyl-RAC method the S-acyltated proteins from total cell lysates of transgenic akr1 cells that were expressing AtPAT21 and its point mutation variant AtPAT21DHHC174S. The presence of AtPAT21 and AtPAT21DHHC174S was detected by Western blotting with anti-V5 antibody. While AtPAT21 can be detected AtPAT21DHHC174S was not captured by the thiopropyl sepharose beads (Fig. 4-2C). Therefore, AtPAT21 is auto-acylated but AtPAT21DHHC174S is not.

These combined results demonstrate that PAT21 has PAT activity and its PAT activity is dependent on cysteine in the DHHC domain.

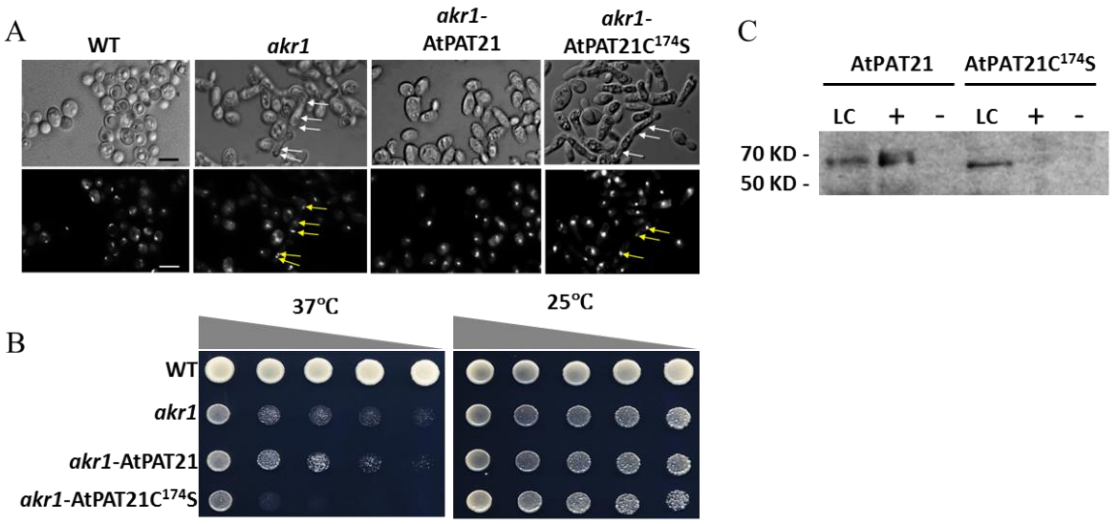

Figure 4-2. AtPAT21 is an S-acyltransferase by yeast complementation (A, B) and Acyl-RAC assay (C).

A. DIC light (upper panel) and UV microscopy of DAPI (1µg/ml) stained cells (lower panel) of all 4 genotypes grown at 37ºC. Arrows indicate multiple nuclei.

B. Growth test. At non-permissive temperature 37ºC (left), wild type (WT) yeast grew well but *akr1* did not. This growth defect was less obvious at 25ºC because all genotypes grew well (right). Expressing AtPAT21 in *akr1* partially restored the growth inhibition of *akr1* by 37ºC as more growth was observed, but AtPAT21C^{174}S-containing *akr1* cells did not grow much at all. Five microlitres of 1 OD_{600} cells followed by 10-fold serial dilutions were spotted on solid medium supplemented with 2% galactose and grown at 25ºC or 37ºC for 3 days. Scale bars = 10 µm. Cells were transformed with empty vector pYES2 (WT and *akr1*), or with AtPAT21 and AtPAT21C^{174}S (*akr1*-AtPAT21, *akr1*-PAT21C^{174}S).

C. AtPAT21 is auto-acylated. AtPAT21 and AtPAT21C^{174}S were detected by Western blotting with an anti-V5 antibody using the ECL method. The molecular weight of AtPAT21 and AtPAT21C^{174}S is ~70 kDa. A band corresponding to AtPAT21-V5 was detected in the + NH_2OH treated sample, indicating that it is bound to an acyl group via a labile thioester linkage confirming that it is auto-acylated. However, no signal was detected for AtPAT21C^{174}S indicating that it is not auto-acylated. LC: loading control, Lane +: NH_2OH treated and Lane -: non NH_2OH treated.

4.2.3 *AtPAT21* is expressed ubiquitously

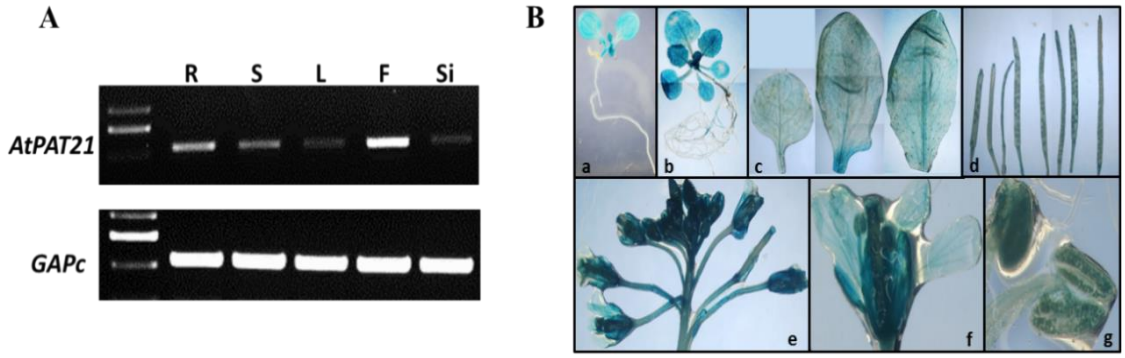

Figure 4-3. AtPAT21 expression pattern in Arabidopsis.

A. Transcript levels of AtPAT21 in different tissues. RT-PCR was carried out on total RNA isolated from different parts of WT plant in different developmental stages. R, roots of 2-week old seedlings grown on the 1/2 MS plate; S, stem of the first node of 35-day old soil-grown plants; L, the 5th and 6th rosette leaves of 4-week old soil-grown plants; F, fully-opened flowers; Si, 3-day-old siliques after pollination.

B. Histochemical localization of AtPAT21. AtPAT21promoter:GUS fusion construct was transformed to WT, and GUS-staining analysis was carried out in whole seedlings and different tissues of the mature transgenic plant. a, 1-week-old seedlings; b, 2-week-old seedlings; c, rosette leaves (left to right, young to old) from 5-week-old plant; d, siliques from 2-8 days after pollination from (left to right). Inflorescence (e), flower (f) and anthers (g) from 5-week-old plants.

Understanding the spatial and temporal expression patterns of a gene can provide important clues for its function. Therefore, we carried out RT-PCR to monitor the transcript levels of *AtPAT21* in roots, stems, leaves, flowers and siliques of mature WT Col-0 plants. It was found that *AtPAT21* is present in all of these tissues with the highest level in flowers (Fig. 4-3A). It is also noted that *AtPAT21* is expressed in much lower levels compared to other *AtPATs* (Batistic, 2012). To confirm this result, we transformed AtPAT21promoter: GUS fusion construct to WT Arabidopsis to check the histochemical localization of AtPAT21. Consistent with the RT-PCR, the GUS signal was found in all tissues with the strongest in flowers (Fig. 4-3B). Therefore, AtPAT21 is expressed constitutively with preference in reproductive tissues, indicating its importance in regulating general growth and development, especially in reproduction in Arabidopsis.

4.2.4 AtPAT21 is predominately localized at plasma membrane (PM)

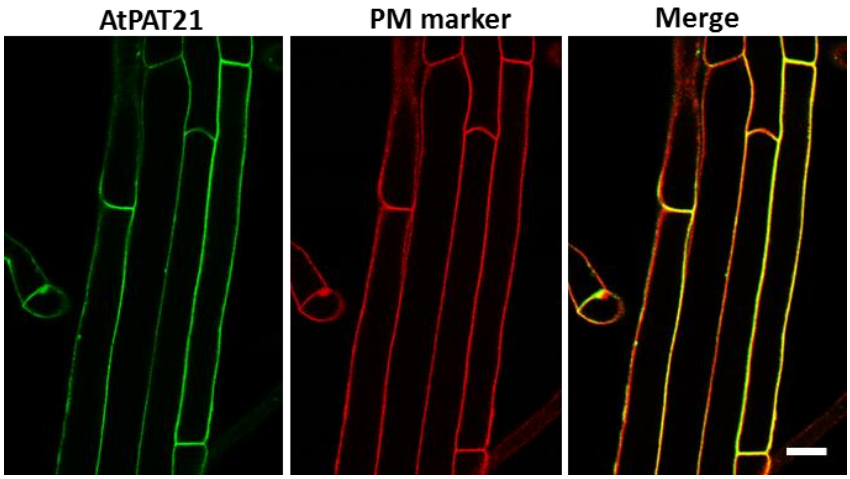

Figure 4-4. AtPAT21 is localised to the plasma membrane.
Confocal microscopy observation of 7-day-old primary root tissue of Arabidopsis seedlings derived from stably transformed plants harbouring the 35S:ATPAT21-GFP and the plasma membrane marker (specify the marker protein). Scale bar, 10 μm.

The subcellular localization of AtPAT21 was observed in primary roots of 7-day-old transgenic seedlings expressing AtPAT21-GFP fusion under the CaMV35S promoter. These lines complementing the growth defect of *atpat21-1* mutant. One of these transgenic lines was crossed with various mCherry tagged endomembrane marker Wavelines (Geldner et al, 2009). As shown in Fig. 4-4 that the GFP fluorescent signal (green) was largely co-localized with the mCherry PM marker (red) in line R138 (PIP1;4, Boursiac et al., 2005). This demonstrates that AtPAT21 is largely localizes on the plasma membrane. Same conclusion was made from studying transiently expressed AtPAT21 in tobacco leaves (Batistic, 2012).

4.2.5 Identification and characterization of AtPAT21 loss-of-function mutant

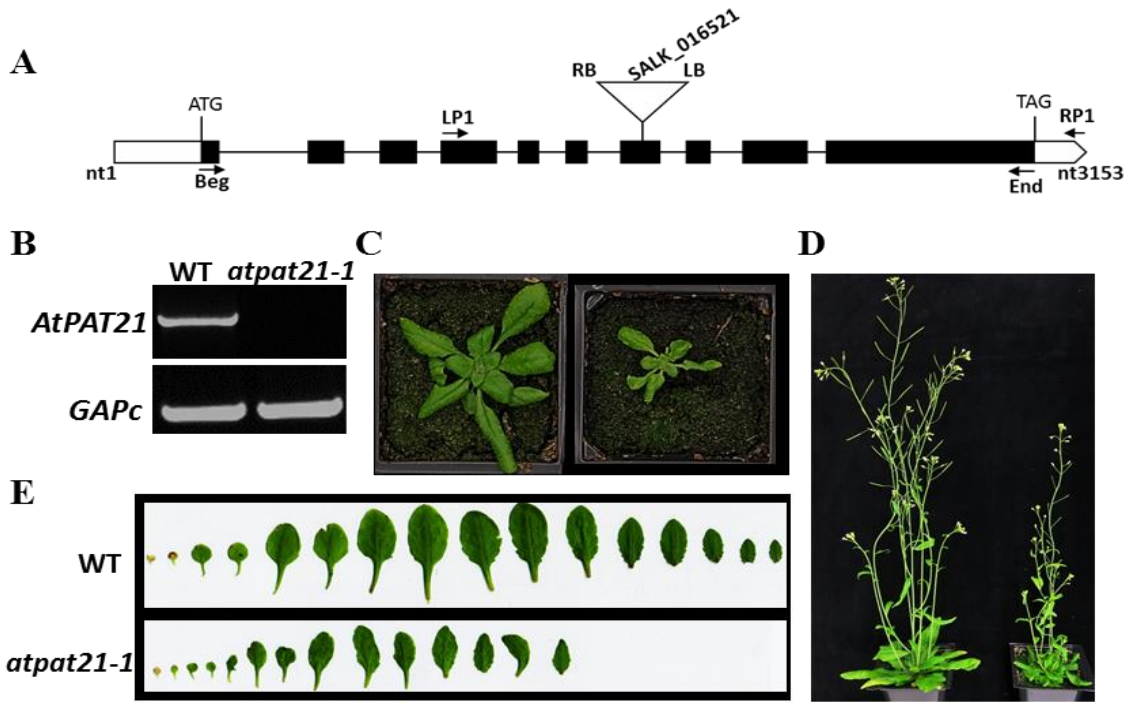

Figure 4-5. Isolation and characterization of AtPAT21 T-DNA insertion mutant.
A. Schematic presentation of the AtPAT21 gene (solid boxes represent exons, empty boxes untranslated regions and lines introns) and the positions of the T-DNA in *atpat21-1* mutant line SALK_016521. Arrows indicate the primers (Beg and End) used for RT-PCR and primers (LP1 and RP1) for genotyping PCR (Table S3). RB, right border; LB, left border.
B. Amplification of the full length of AtPAT21 transcript in wild-type and *atpat21-1* plants using primers Beg and End shown in A. The *GAPc* transcript was served as a control; C and D, 4- and 6-week-old WT Col-0 (left) and *atpat21-1* (right); E. Rosette leaves of 25-day old WT Col-0 (Top) and *atpat21-1* (bottom) plants.

In order to understand the biological roles of AtPAT21 play in growth and development of Arabidopsis, an AtPAT21 T-DNA knockout line, SALK_016521, was obtained from the Arabidopsis Biological Resource Center (ABRC). A number of homozygous T-DNA insertion plants were identified through PCR-based genotyping. Sequence analysis of the PCR products amplified by T-DNA left board primer LB and the gene-specific primer RP1 showed that the T-DNA was inserted at nt1748 in the 7th exon (Fig. 4-5A). RT-PCR was carried out using total RNA isolated from leaf tissue of both the WT and one of the homozygous T-DNA insertion plants (Fig. 4-5B). Corresponding DNA fragments of *AtPAT21* were successfully amplified from WT but not from the mutant thus

confirming this line is most likely a transcriptional null knockout mutant line, hence named as *atpat21-1*.

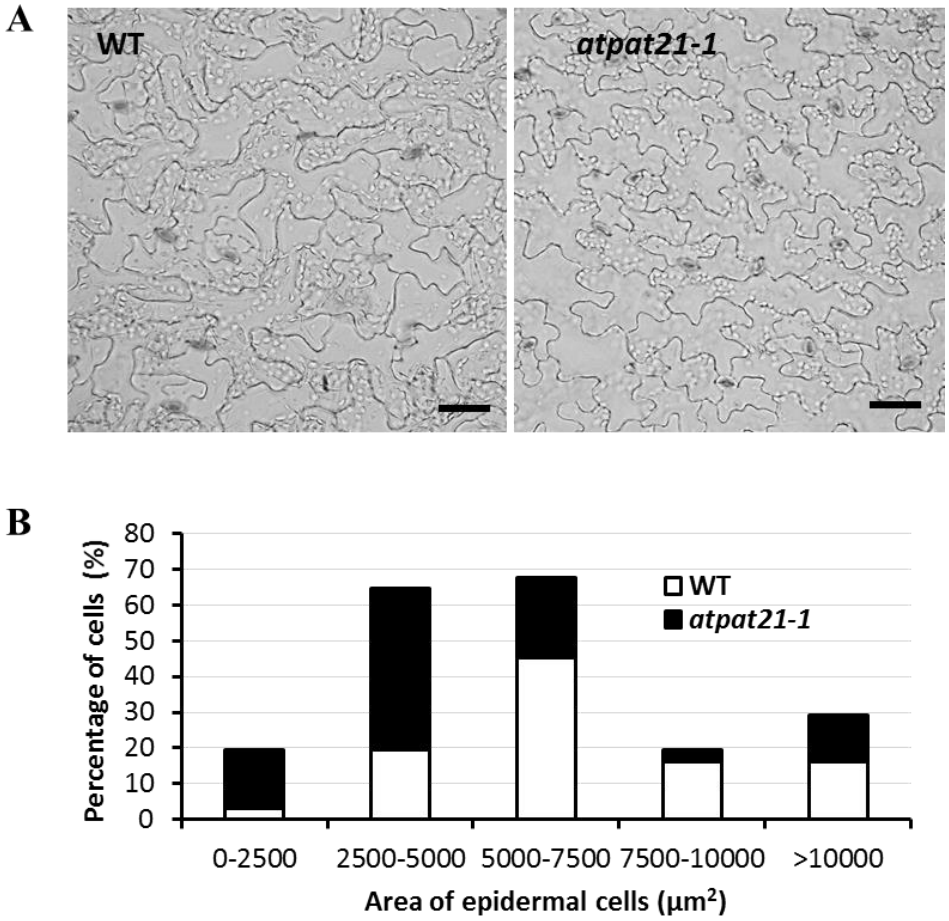

Figure 4-6. *atpat21-1* has smaller cells.

A. Epidermal cells. Bars, 50µm.

B. Percentage of cell number in each size range. Cells from epidermal peels of mature leaves

Detailed phenotypic analysis of *atpat21-1* was carried out. The mature *atpat21-1* plant appeared to be shorter, which was only 441.9 mm while the WT was 476.0mm in height (Table 4-1). The leaves were smaller than those of the WT and they were with uneven coloration (Fig. 4-5C-E). Generally, the epidermal cells of the mutant rosette leaves were much smaller compared to the WT (Fig. 4-6A). The areas of 45.2% of the epidermal cells in *atpat21-1* leaves were between 2,500-5,000µm^2. However, for WT, 45.2% of the leaf epidermal cells were between 5,000-7,500µm^2. Most importantly, the

mature siliques of *atpat21-1* which were only 3.0mm (Table 4-1) do not contain any seeds, but only shrivelled ovules (Fig. 4-8G). Therefore, *atpat21-1* was completely sterile. However, there were more siliques in the primary inflorescence stem of *atpat21-1* (63.3) than WT (55.8). Due to its sterility the mutant had prolonged growth period and extensive branching than WT (Table 4-1).

Table 4-1. Phenotypic analysis of WT and *atpat21-1*

	WT	***atpat21-1***
Plant height (mm) (n=10)	476.0±18.9	441.9±7.4*
Length of silique (mm) (n=30)	17.0±0.7	3.0±0*
No. of branches (n=10)	23.0±2.8	67.1±6.2*
No. of siliques in main branch (n=10)	55.8±1.9	63.3±3.3*
No. of ovules each silique (n=10)	57.5±3.2	38.0±3.5*

62-day-old plants were used. The 8th silique counting from the bottom of the primary inflorescence was used to monitor the length and numbers of ovules. * $p<0.01$ in Student's *t*-test. The sample sizes are indicated.

4.2.6 Defect of *atpat21-1* is caused by loss of enzyme activity of AtPAT21

To see if it was AtPAT21 loss-of-function that caused the phenotype observed in *atpat21-1*, we transformed the *atpat21-1* mutant plants with a construct containing the coding region of *AtPAT21* driven by the constitutive CaMV35S promoter. It appeared that the transgenic plants exhibited identical phenotype to WT plants, i.e., the defective phenotype of *atpat21-1* was completely rescued by *AtPAT21*. Interestingly, when we mutated the cysteine residue in the DHHC domain to serine (AtPAT21DHHS), the mutated variant could not rescue the *atpat21-1* phenotype and the transgenic plants look the same as the *atpat21-1* mutant (Fig. 4-7). Therefore, the results demonstrate that the defective phenotype of *atpat21-1* is caused by the loss of AtPAT21 functionality which lies in the DHHC domain.

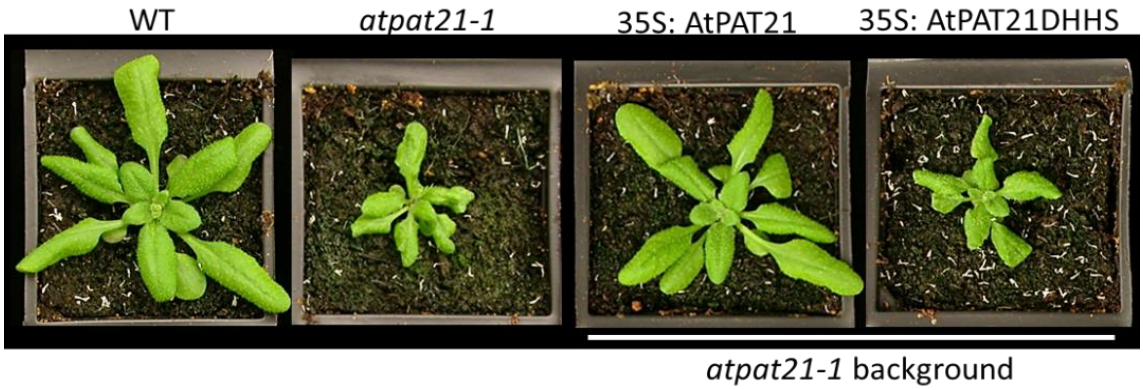

Figure 4-7. AtPAT21 can complement the phenotype of *atpat21-1* but AtPAT21DHHS can not. Images were taken from 4-week-old plants by a Nikon101 camera.

4.2.7 AtPAT21 loss-of-function causes both male sporophytic and gametophytic defects

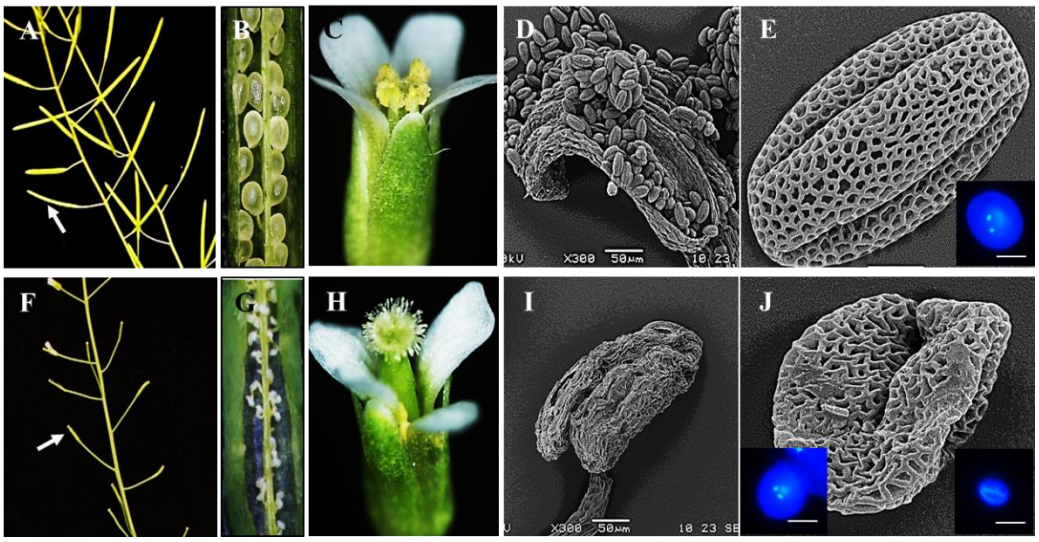

Figure 4-8. Defects in the reproduction tissues of *atpat21-1*. A-E, WT; F-J, *atpat21-1*.
A and F. fully elongated siliques (arrows).
B and G. ovules, 2 days after self-pollination; C and H, Fully opened flowers.
D and I. anthers observed by scanning electronic microscopy (SEM).
E and J. individual pollen grains observed by SEM and DAPI-stained pollen grains under UV (insets in the right bottom in E, and the left and right bottom in J. Bars, 20μm.

As mentioned earlier loss-of-function of AtPAT21 caused the mutant completely sterile. In order to find out the nature of sterility of *atpat21-1* mutant plants (Fig. 4-8A, B, F and G), we first observed the fully opened flowers from WT and *atpat21-1* (Fig. 4-

8C and H). It was noticed that unlike the WT stigma which was encircled by the anthers, the mutant stigma was higher up and away from the anthers. In addition, while the WT stigma and the anthers were covered by pollen grains that were released from its dehisced anthers (Fig. 4-8D), mutant anthers failed to dehisce and release pollen grains (Fig. 4-8I). Analysis of the pollen from *atpat21-1* anthers revealed greatly reduced size compared to WT pollen and with nuclei being generally absent (Fig. 4-8E and J). The small proportion of mutant pollen grains that did contain two sperm cell nuclei were also much smaller than the WT pollen grains (Fig. 4-8J left bottom).

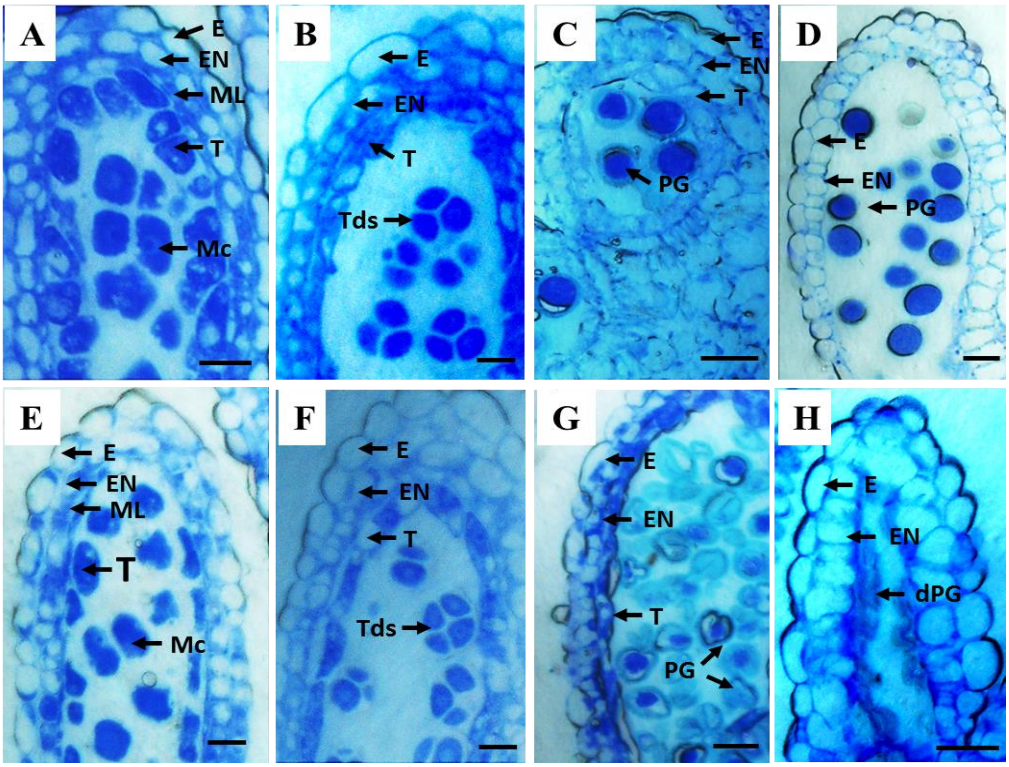

Figure 4-9. The *atpat21-1* mutant pollen grains start to degenerate after release from tetrad. Different developmental stages of WT and *atpat21-1* mutant anthers. A-D, WT; E-H, *atpat21-1*. A and E, Meiosis stage; B and F, Tetrad stage; C and G, pollen grains released from tetrad; D and H, well separated pollen grains. E, epidermis; EN, endothecium; ML, middle layer; T, tapetum; Mc, Meiocyte; Tds, tetrad; PG, pollen grain; dPG, degenerated pollen grain. Bars, 10μm.

To determine at what point pollen development is perturbed in *atpat21-1*, floral material covering all stages of anther development was embedded in plastic, sectioned and imaged with WT as control (Fig. 4-9). The mutant microsporocytes were able to complete meiosis however normal 'tetrads' were not formed, rather, asymmetrical

polyads containing 2-6 microspores made up the majority of meiotic products (Fig. 4-10 Top). Microspores were successfully released from polyads (Fig. 4-9G), however the sizes of released mutant pollen grains were not identical (Fig. 4-10 Bottom) and the majority degenerated soon thereafter (Fig. 4-9H). These may explain for the large proportion of the shrivelled pollen grains that we observed from *atpat21-1* mutant anthers (Fig. 4-8J).

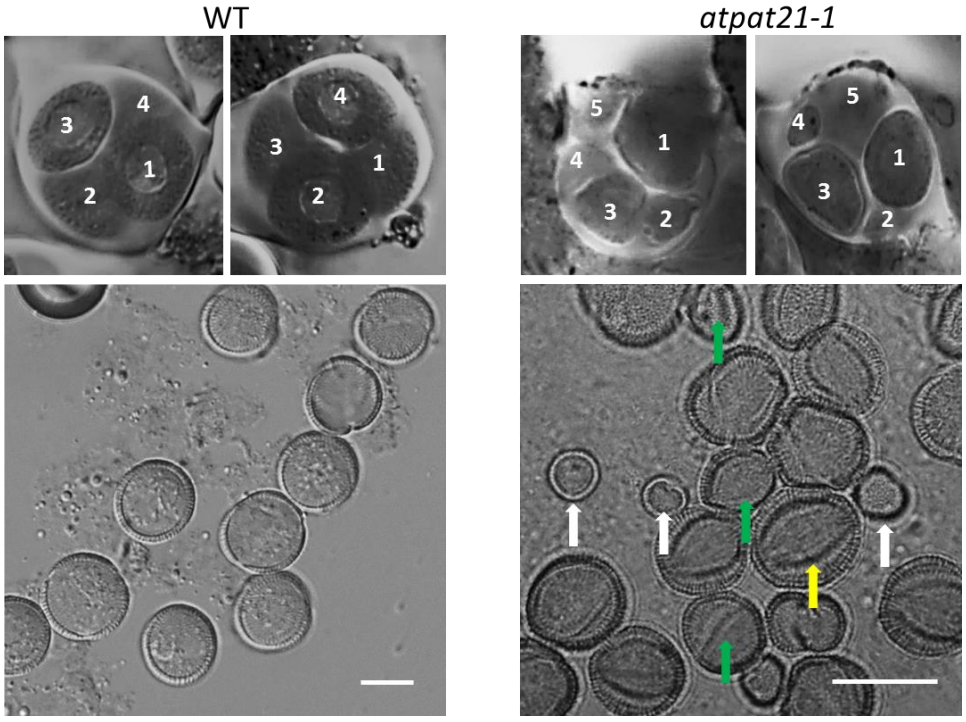

Figure 4-10. The *atpat21-1* mutant have asymmetrical polyads structure which will release variable sizes of pollen grains. Top, tetrads; bottom, pollen grains. Numbers mean individual microspores; White arrows indicate pollen grains with small size, green arrows indicate pollen grains with midium size, yellow arrow indicates pollen grain with large size. Bars, 25μm.

4.2.8 AtPAT21 loss-of-function causes female sporophytic and gametophytic defects

To verify whether *atpat21-1* is also defective in its female sporophytes and/or gametophytes we first observed the pistils in fully open flowers. We found that the mutant had shorter pistils with fewer ovules in them (38) compared to WT (58) (Table 4-1). The mutant ovules were also much smaller than WT (Fig. 4-11 top panel at 0 DAP). To see if these mutant ovules were functional we carried out artificial pollination. Because mutant anthers do not dehisce hence no pollen grains were naturally deposited on its stigma we

artificially pollinated its stigmas with WT pollen. The development of mutant and WT ovules at 1 day after pollination (DAP) were observed (Fig. 4-11 middle panel at 1 DAP) with unfertilized ovules as controls (Fig. 4-11 top panel at 0 DAP). At 1 DAP the WT ovules became enlarged where the globular embryo was clearly visible (arrow), however no such embryo in the mutant ovule was found (Fig. 4-11 middle panel). On maturity at 15 DAP, while the WT silique had a full set of ~55 seeds there were no seeds at all in the mutant, instead very small shriveled ovules in the places of seeds (Fig. 4-11 bottom panel). This implies that *atpat21-1* either did not support the WT pollen tube growth, or the pollen tube guidance was defective so that they did not find the ovules to deliver its sperms for double-fertilization.

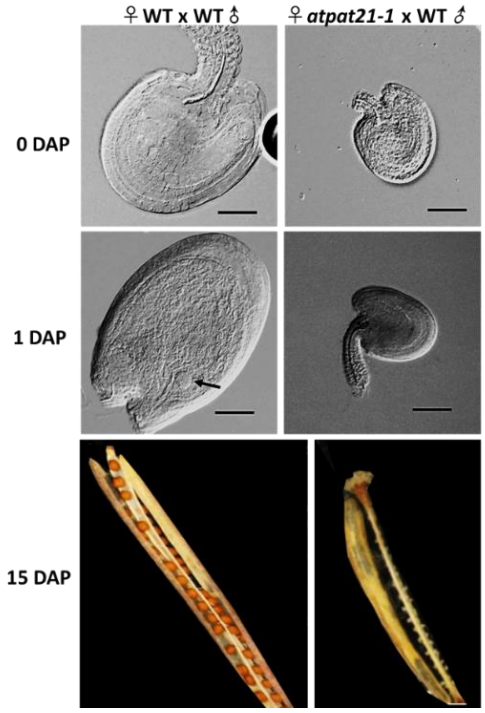

Figure 4-11. *atpat21-1* has female gametophytic defects.
WT and *atpat21-1* stigmas were hand-pollinated with plenty of WT pollen and their embryo development were observed. Ovules were cleared and the embryo development was observed at 0 and 1 day after pollination (DAP). Arrows indicate embryos in WTxWT ovules. Mature siliques at 15 DAP were also opened and the seed sets were observed. Bars, 20μm.

In order to find out if the WT pollen can germinate and pollen tube grow then be guided to the WT and *atpat21-1* ovules we observed the stigmas and the styles of WT and *atpat21-1* at 5- and 15 hours after pollination. At 5 hours, the pollen grains germinated and invaded the *atpat21-1* stigmas in a similar manner as they did to the WT as the pollen tubes were clearly seen on both the WT and mutant stigmas (Fig. 4-12A top panel). In the 15 hours pollinated pistils the pollen tubes could transmit through the style of *atpat21-1*

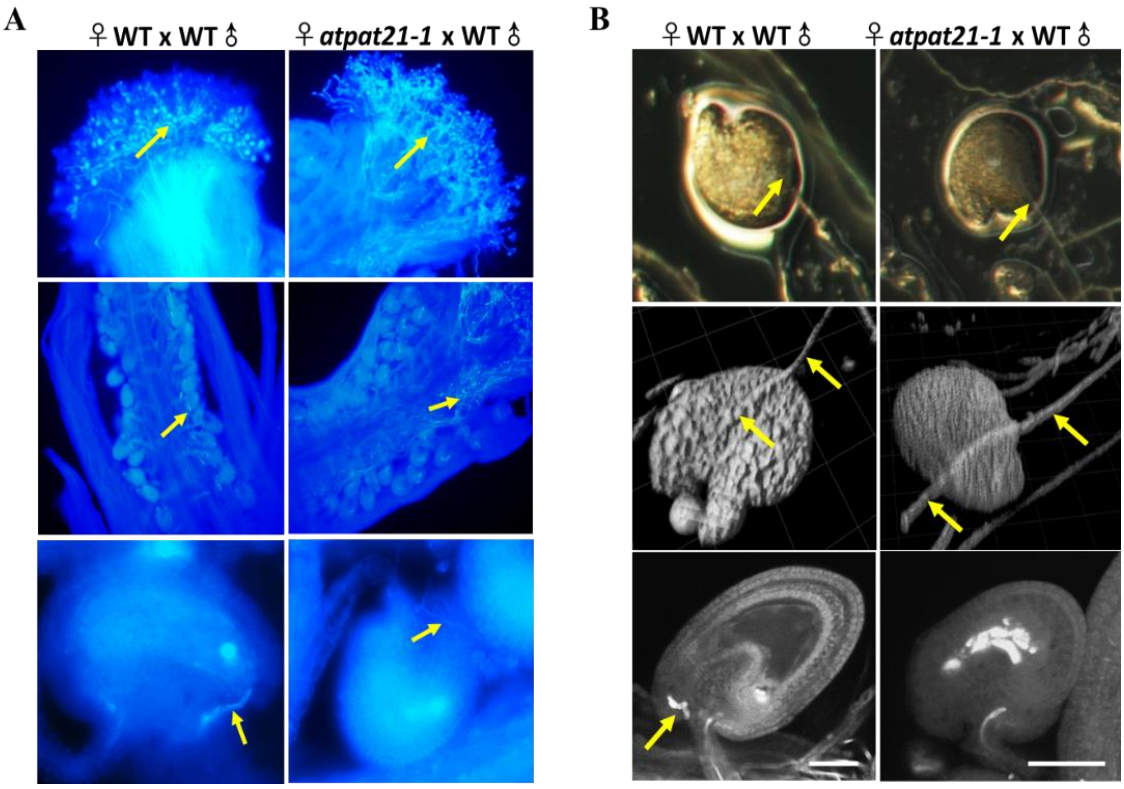

Figure 4-12. *atpat21-1* pistil failed to guide and attract the pollen tube into ovule.
A. Aniline blue stained WT pollen tubes *in vivo*. WT and *atpat21-1* stigmas were hand-pollinated with plenty of WT pollen. Pollen grains germination was observed 5 hours after pollination (top panel) and the pollen tube growth was observed at 15 hours after pollination (middle and bottom panels). The WT pollen grains can germinate and the pollen tubes can penetrate through the style but failed to find the micropyle of *atpat21-1* ovule (right), while they enter the WT ovule successfully (left). Arrows indicate pollen tubes.
B. Semi *in vivo* pollen tube growth assays. WT pollen grains were germinated on the stigmas of WT and *atpat21-1 in vivo*, and then pollen tube elongation and pollen tube/ovule interaction was carried out *in vitro* on the pollen tube growth media. WT pollen tube can enter the WT ovule (left) but not that of *atpat21-1* (right). Top panel pictures, dissecting microscopy; middle panel pictures, Confocal scanning microscopy. Ovules from *atpat21-1* (right bottom) do not have proper embryo sac as WT (left bottom). Arrows indicate pollen tubes. Bars, 50μm.

at a similar speed as WT as seen the pollen tubes reaching both the mutant and WT ovules (arrows in Fig. 4-12A middle panel). However, while we could clearly see that the pollen tube entering the WT ovule through micropyle (arrow) no pollen tubes were observed to enter the *atpat21-1* ovules (Fig. 4-12A bottom panel). Therefore, it seems that the mutant ovules failed to attract WT pollen tubes.

To confirm this, we further carried out semi-*in vivo* assays to observe the interaction between pollen tubes and ovules. For this we first hand-pollinated WT and *atpat21-1* stigmas with WT pollens. After 30 minutes the stigmas plus the shoulder of the styles were cut off and laid on the pollen tube growth media (Lu et al., 2011). About 10 ovules were removed carefully from pistils of fully open WT and mutant flowers and placed in half circle opposite to their corresponding stigma. After 15 hours, the pollen tubes had grown long enough to reach the ovules. While the WT pollen tube were clearly seen entering the WT ovules through the micropyle (arrow), it just passed the mutant ovules and continued to grow as if there were no ovules present (Fig. 4-12B top and middle panels). Therefore, it seems that there is no guided pollen tube growth from the mutant ovules to the WT pollen tubes, indicating there could be a defect in these mutant ovules. From WT ovule, we can see clear embryo sec, but it was not formed properly in the mutant ovule (Fig. 4-12B bottom panel).

The above combined results clearly demonstrated that *atpat21-1* has catastrophic female sporophytic and gametophytic defects, resulting in its sterility.

4.2.9 Both male and female gametophytic defects are partially independent of their sporophytic defects in *atpat21-1*

Table 4-2. Ratios of different genotypes observed in the F1 progeny of different crosses.

Crosses	Genotype	Expected ratio	Observed
♀Het x Het♂ (Selfed)	AtPAT21+/+: -/-	3:1	5.2:1 (178:34)
♀WT x Het♂	AtPAT21+/+: +/-	1:1	1.3:1 (84:65)
♀Het x WT♂	AtPAT21+/+: +/-	1:1	1.9:1 (95:50)

Genotype of the progeny from each crossing were identified individually by PCR, using the primers LB+RP1 and LP1+RP1 (Fig. 4-5A; Table S3).

Gametophytic defects can be either caused by sporophytic defects if the disrupted proteins exist in the diploid developmental stage in stamen or pistil, or independent of sporophytic defects if the disruption appears after meiosis (McCormick, 2004). For the sporophytic independent gametophytic defects this must be maintained in the heterozygotes (McCormick, 2004). To find out if the gametophytic defects are present in the heterozygous *atpat21-1*(+/-) mutant we genotyped seedlings germinated on agar plates from the progenies of heterozygotes which were naturally self-pollinated (♀Het x Het♂ (Selfed)), and reciprocal crossed between *atpat21-1*(+/-) heterozygotes and WT (♀WT x Het♂ or ♀Het x WT♂) (Table 4-2). In the progeny of selfed heterozygotes, the number of WT plants to homozygous *atpat21-1* mutant plants (AtPAT21+/+: -/-) was 5.2:1 from 212 seedlings genotyped. This was much higher than the expected 3:1, indicating that the gametophytic defect exists in either male or female gametes. When we let the heterozygote be the pollen donor to cross with WT (♀WT x Het♂), the ratio of WT to heterozygotes (AtPAT21+/+: +/-) from the F1 progeny was 1.3:1 which was higher than the expected 1:1 (Table 4-2). This means that not all the pollen grains produced in the heterozygous *atpat21-1*(+/-) were viable. There were about 23% of the pollen grains failed to fertilize the WT ovules that would subsequently develop into heterozygous seeds. Therefore, there were considerable number of male gametophytes in the heterozygous *atpat21-1*(+/-) were defective. On the other hand, in the F1 progeny of '♀Het x WT♂' cross, the number of WT plants recovered were almost twice as many as the heterozygous plants (AtPAT21+/+: +/- = 1.9:1 instead of 1:1) (Table 4-2). This indicates that there is also a female gametophytic defect(s), which is more severe than the male defects, in the heterozygous *atpat21-1*(+/-) plants. Consistent with these results, we found some un-fertilized ovules from these crosses (arrowheads in Fig. 4-13). However, different from what we observed in homozygous *atpat21-1* mutant, both *atpat21-1* male and female gametophytes were not completely sterile in the heterozygote since we did manage to recover a significant number of homozygous mutant plants. Therefore, the sterility of *atpat21-1* is not fully penetrate, and the fact that the number of heterozygous *atpat21-*

1(+/-) plants were much higher when pollen as donor than acceptor indicates that the female gametophyte (ovule) has more severe defects than the male gametophyte (pollen).

Figure 4-13. Opened siliques of different crosses.
Each cross was done by hand pollination, the corresponding silique was opened 5 days after pollination, with '♀WTxWT♂' as positive control. Un-fertilized ovules occupy around 40% of the total ovules in both crosses '♀AtPAT21Ht x AtPAT21Ht♂' and '♀AtPAT21Ht xWT♂'White arrow heads indicate un-fertilized ovules. Ht, heterozygote.

To confirm our conclusion, pollen grains from *atpat21-1*(+/-) were observed because the homozygous mutant anthers do not dehisce to produce pollen grains. While the majority of the heterozygous *atpat21-1*(+/-) pollen grains exhibit similar size and appearance as the WT, some much smaller pollen grains that were accounted for approximately 15% were also present (Fig. 4-14A, left). We also carried out *in vitro* pollen germination assays and found that while 87.3% of WT pollen grains germinated only 47.8% of pollens from heterozygote *atpat21-1*(+/-) did where none of the small pollen grains germinated (Fig. 4-14A right). Therefore, these abnormal small pollen grains may be the cause for the lower homozygous or heterozygous seedlings recovered in the progenies when heterozygote *atpat21-1*(+/-) was used as the pollen donor (Table 4-2). However, the ratio of the small pollens was less than 50%, which indicates that some mutant pollen grains that appeared to be similar phenotype as WT can function normally. This result explains why some heterozygous seedlings were recovered from the F1 progeny from the

♀WT x Het♂ cross (Table 4-2).

In summary, the gametophytic defects observed in the AtPAT21 loss-of-function mutant are partially related to sporophytic effects of the mutation.

We next phenotyped the female gametophytes in *atpat21-1*(+/-) plants. Stage 12c flowers derived from WT and heterozygous plants were emasculated and fixed 24 hours later permitting the female gametophyte to reach maturity (FG7, four-celled stage, Fig. 4-14B, -a). Of the 221 ovules examined from *atpat21-1*(+/-) plants, 55% contained a mature female gametophyte similar to that of WT (data not shown), suggesting that these ovules represent predominantly WT ovules. The remaining 45%, having an abnormal phenotype, likely correspond to those harbouring a mutant female gametophyte. The mutant female gametophytes at this stage displayed a range of abnormal phenotypes with some containing no discernible nuclei, being reduced in size and having an accumulation of small vacuoles (Fig. 4-14B, -b) or presence of a larger vacuole with mis-positioned nuclei (Fig. 4-14B-c). This result indicates that development of the mutant female gametophyte may be perturbed at an early stage. To determine at which stage the lesion occurs we analysed female gametophytes in pistils from heterozygous plants (n=67) at the FG1 to FG2 developmental stage. At FG1-2, 46% of ovules exhibited normal megaspore specification and the first nuclear division (Fig. 4-14B, -d and e), whilst 54% of ovules displayed several defects. These included gametophytes having an irregular nucleus with higher auto-fluorescence in the cytosol (Fig. 4-14B-f), abnormalities in the subsequent nuclear division where a central vacuole was formed but no nuclei were observed, indicating degeneration of nuclei (Fig. 4-14B-g), and a smaller megaspore with no apparent nucleus (Fig. 4-14B-h and i).

These combined results clearly demonstrate that *atpat21-1* female gametophytes have a defect that exerts its effects during megaspore specification, preventing progression into a functional 8-celled embryo sac.

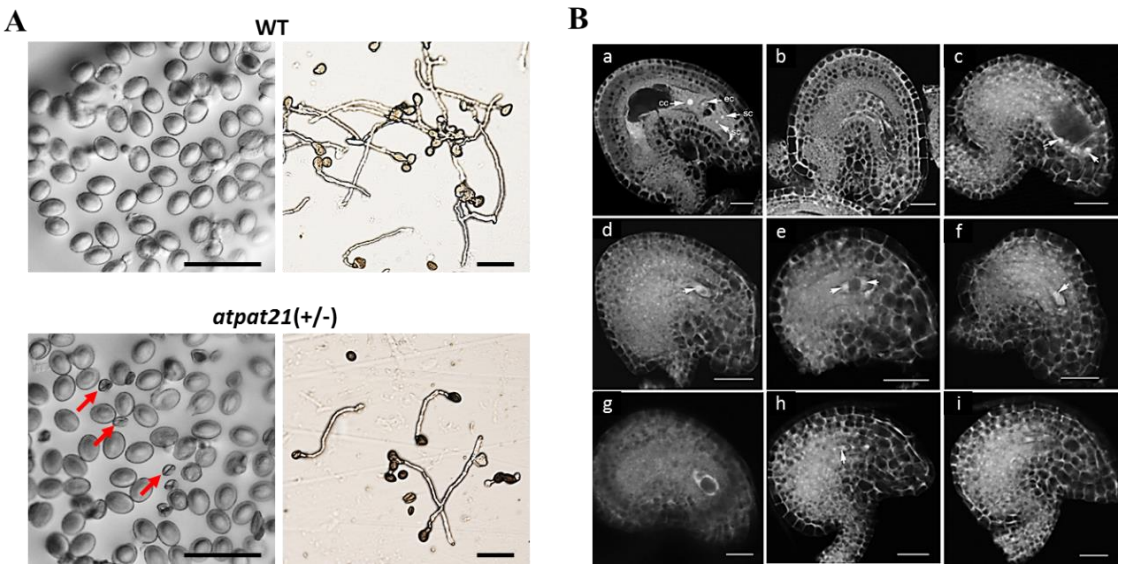

Figure 4-14. Male and female gametophytic defects in heterozygote *atpat21-1*(+/-).
A. Defects in male gametes of *atpat21-1*(+/-). Pollen (left) and *in vitro* pollen tube growth assay (right). Red arrows indicate smaller pollen grains that are probably derived from the mutant; Approximately 87.3% of WT pollen grains were germinated yet only about 47.8% of heterozygous grains germinated. Bars= 0.1mm.
B. Defects in female gametes. Observation of female gametophytes from WT and *atpat21-1*(+/-) using confocal laser scanning microscope (CLSM). a, normal gametophyte at FG7; b-c, abnormal gametophytes at FG7; d-e, normal megaspore specification from FG1 to FG2; f-i, gametophytes with different defects at FG1 to FG2 stage. Bars= 20μm.

4.3 Discussion

In this study we demonstrated that the knock-out mutant of a single gene, AtPAT21 leads to defects ranging from vegetative growth to reproductive development. This is perhaps not surprising as AtPAT21 is ubiquitously expressed with more transcripts present in the reproductive tissues (Fig. 4-3, Batistic, 2012). Mutant *atpat21-1* plants have shorter roots, coarse and smaller leaves and more branched inflorescences compared to the wild-type Col-0 Arabidopsis plants (Table 4-1), indicating that AtPAT21 is essential for normal vegetative and reproductive growth in Arabidopsis. Perhaps most strikingly, AtPAT21 loss-of-function causes both male and female sterility and the mutant plants do not produce seeds. We confirmed both *in vivo* and *in vitro* that AtPAT21 is an S-acyl transferase. Therefore, it may function through S-acylation of one or multiple target

proteins that are involved in a range of processes in Arabidopsis. We focused our study on the roles of AtPAT21 in reproduction, and this led to the discovery that the successful seed production in Arabidopsis relies on S-acylation of proteins that participate in the development and differentiation of both male and female reproductive tissues.

4.3.1 AtPAT21 is involved in anther dehiscence

Anthers of *atpat21-1* mutant plants fail to dehisce and as a result no pollen grains are released. Observation by scanning electron microscopy showed that the stomium of WT anthers was completely broken down at dehiscence, leading to the exposure and release of the anther contents, the pollen grains, whereas the stomium in *atpat21-1* anthers remained largely intact and their contents were not released (Fig. 4-8I). Pressure generated by swelling of a full set of pollen grains in the anther is required to split open the stomium. Indeed, anthers of the *lap5-1/ lap6-1* (LESS ADHESIVE POLLEN) double mutant failed to dehisce due to the shrivelled pollen grains (Dobritsa et al., 2010). This may also be the case for *atpat21-1* anthers as they contain largely degenerated pollen grains (Fig. 4-9H) which would exert much less pressure within the anther. However, anthers of the male sterile mutant *acos5* (Acyl-CoA Synthetase 5) are still able to dehisce despite the fact that they contain shrivelled and inviable pollen grains (de Azevedo Souza et al., 2009). This indicates that dehiscence of the Arabidopsis anther is more complex and does not depend on its contents alone. The fact that loss-of-function of AtPAT21 results in disruption in anther dehiscence demonstrates that protein palmitoylation may also involve in this important process.

4.3.2 Male and female sterility in the *AtPAT21* loss-of-function mutant may be caused by meiotic defects

Failure to produce pollen or the production of abnormal pollen can be caused by either meiotic defects or abnormalities in the cell layers surrounding the locules (Sanders et al., 1999). In the *atpat21-1* mutant all cell layers of the anthers were present and developed normally (Fig. 4-9). However, the production of tetrads was abnormal with

asymmetrical polyads containing 2-6 microspores being frequently observed (Fig. 4-9B). Thus, the defect caused by loss of *AtPAT21* could have affected the meiotic stage of pollen development leading to deviations from the typical number of 4 meiotic products found in tetrads of WT anthers (Fig. 4-10). On the other hand, the ovule development in *atpat21-1* also showed severe defects. At the FG7 developmental stage, *atpat21-1* ovules were found to be smaller, containing abnormal 'female gametophytes' with nuclei being absent or mis-positioned (Fig. 4-13B a-c). At earlier stages (FG1 to FG2), *atpat21-1* ovules were already displaying striking development defects with no functional megaspores being observed (Fig. 4-13B d-i). Therefore, the defects in female fertility observed in *atpat21-1* plants also seem to act at the meiotic stage of development.

Many genes have been reported to be involved in different stages of meiosis during both microsporogenesis and megasporogenesis, such as *XRI1* (X-ray-inducible 1) (Dean et al., 2009), *SPO11* (Sporulation 11) (Stacey et al., 2006), and *SDS* (Solo dancers) (Yoshitaka et al., 2002). Loss-of-function mutants of these genes have defects in both male and female fertility, mirroring what we observed in the *atpat21-1* mutant. While XRI1 is involved in meiotic DNA repair, the *spo11* mutant has severe defects in synapsis during the first meiotic division, whilst SDS regulates homolog synapsis and bivalent formation in prophase I. Thus it is tempting to speculate that AtPAT21 may function in one, or all of these processes.

Some unviable pollen grains and ovules were also produced in the heterozygous *atpat21*(+/-) plants (Fig. 4-13A), suggesting that both microsporogenesis and megasporogenesis requires both alleles of *AtPAT21* to be fully functional. This is also observed in other meiosis defective mutants including *rbr* (knockout of Retinoblastoma related), *mlh1* (MutL homologue 1) and *aesp* (Arabidopsis separase) (Chen et al., 2011; Dion et al., 2007; Liu and Makaroff, 2006). While loss of *RBR* during meiosis results in a reduction in the formation of crossovers and an associated failure in chromosome synapsis (Chen et al., 2011), the *mlh1* Arabidopsis mutant is defective in the DNA mismatch repair (MMR) system (Dion et al., 2007) and the separase AESP is essential for

embryo development and the release of cohesin during meiosis (Liu and Makaroff, 2006). Therefore, observation of chromosome behaviour in *atpat21-1* may provide information as to which stage(s) of meiosis is affected in the mutant.

4.3.3 Mechanism of AtPAT21 in meiosis

Our data clearly demonstrated that Arabidopsis PAT21 is involved in both male and female microsporogenesis and megasporogenesis, most likely through the regulation of meiosis. To date, over 80 genes have been implicated in the process of meiosis in plants, and with the majority of them being studied in some detail in Arabidopsis (reviewed by Mercier et al., 2015). In general, loss-of-function mutants of these genes have defects in both male and female fertilities because the gametes are the products of meiosis. However, there are exceptions where certain genes are involved in only male or female meiosis, not both. For example, on the female side AGO9 (Argonaute 9) prevents differentiation of multiple gametic cells (Olmedo-Monfil et al., 2010) and ARP6 (Actin-related protein 6) regulates female meiosis in prophase I (Qin et al., 2014). On the male side, MMD (Male meiocyte death), MPK (MAP kinase) and TES (Tetraspore) are involved in male meiotic cytokinesis (Mercier et al., 2015; Zeng et al., 2011; Spielman et al., 1997); PSS1 (Pollen semi-sterility 1) is specific to male meiosis (Zhou et al., 2011); CDKA1 (Cyclin dependent kinase A 1) controls proliferation of generative cells in male gametogenesis (Iwakawa et al., 2005); MS5 (Male sterile 5) and JASON controls cell division during Meiosis Ⅱ (Ross et al., 1999; De Storme and Geelem, 2011), KATA (Kinesin-like protein in Arabidopsis thaliana A) is required for spindle morphogenesis (Chen et al., 2002). As AtPAT21 likely functions through its PAT enzyme activity (Figs. 4-2 and 4-7), it is probable that AtPAT21 palmitoylates a protein or proteins that are involved in the meiotic process for the generation of both male and female gametes.

Due to the lack of consensus sequences for palmitoylation it is difficult to predict which proteins are palmitoylated. Therefore, we analysed the potential palmitoylation sites in the encoded proteins of genes known to be involved in male and female fertility using Clustering and Scoring Strategy software for the prediction of palmitoylation sites

(CSS-Palm 4.0) (Zhou et al., 2006; Ren et al., 2008). We restricted this analysis to those sequences where the respective knockout mutants have been shown to have similar defects in both male and female fertility to that of *atpat21-1* mutant.

As shown in Table 4-3 most of these proteins were predicted to have one or more palmitoylation sites. The higher the score is for a particular cysteine residue(s) within the predicted protein sequence the higher the possibility would be for this cysteine(s) to be palmitoylated (Ren et al., 2008). For instance, the cysteine residues at position 3 (C^3) and 6 (C^6) of HEI10 (Enhancer of cell invasion 10) were scored at 20 and 40, respectively; the ninth cysteine (C^9) of PRD1 (Putative recombination initiation defect 1) was 34 and the score of the 18th cysteine (C^{18}) of MRE11 was 26, indicating these proteins are most likely palmitoylated at the specific cysteine residues. Interestingly, the transcriptional null mutant of *HEI10* also has asymmetric tetrads or polyads containing more than four microsopres (Chelysheva et al., 2012). The loss-of-function mutant for *PRD1* has very short siliques that contain very few seeds (2.62 seeds/silique, table 1S) and this is caused by both male and female gametogenesis or/and sporogenesis defects (De Muyt et al., 2007). *mre11* mutant plants are dwarfed with shorter roots, and in addition no pollen grains produced (Bundock and Hooykaos, 2002). All of these defects have also been observed in *atpat21-1* anthers (Figs. 6-5, 6-8 and 6-10), suggesting that these proteins may be the palmitoylating targets of AtPAT21 in Arabidopsis. Therefore, loss-of-function of *AtPAT21* would lead to a failure in the palmitoylation of these proteins and loss of appropriate membrane localization resulting in the defects observed in these mutants.

Other protein sequences that have scores higher than 10 in the predicted palmitoylated cysteine sites include C^{402} in PHS1 (Poor homologous synapsis1), C^{46} in RAD50 (Radiation sensitive 50), C^{107} in MCM8 (Mini-chromosome maintainance 8), C^{568} in SDS (Solo dancers), C^{930} in MSH2 (MutS homologs 2), C^{788} in RBR (Retinoblastoma related), C^{262} in MLH1 (MutL-homologue 1), C^{610} in SCC3 (Sister chromatid cohesion 3), C^{1478} in AESP (Arabidopsis separase), C^{156} in OSD1 (Omission of second division 1), and C^{173} in SMG7 (suppressor with morphogenetic effects on

genitalia 7). It is not surprised that most of them localize at nucleus, but we also found

Table 4-3. Palmitoylation sites prediction of some meiosis related genes

Gene name	AGI No.	Position of S-acylated sites	Score*	Subcellular localization	References
MEI1	AT1G77320	C41, C42 and C97	9.129, 7.403 and 4.695	Intracellular, Nucleus	Mathilde et al., 2003
SWI1	AT5G51330	Not available		Nucleus	Mercier et al., 2001 and 2003
CDC45	AT3G25100	C524 and C526	3.965 and 4.940	DNA replication preinitiation complex	Stevens et al., 2004
XRI1	AT5G48720	C202	5.181	Nucleus	Dean et al., 2009
SPO11	AT1G63990	C107 and C128	5.270 and 4.242	Nucleus	Stacey et al., 2006
PRD1	AT1G01690	C9	33.549	Chloroplast	De Muyt et al., 2007
DFO	AT1G07060	C118	4.767	Mitochondrion	Zhang et al., 2012
PHS1	AT1G10710	C378, C379 and C402	8.786, 5.592 and 12.294	Cytoplasm, Nucleus	Ronceret et al., 2009
MRE11	AT5G54260	C18	26.065	Nucleus	Bundock and Hooykaos, 2002
RAD50	AT2G31970	C46, C697 and C698	11.807, 6.695 and 7.450	Cytoplasm, Nucleus	Bleuyard et al., 2004
RAD51	AT5G20850	Not available		Nucleoplasm, Nucleus	Li et al., 2004
XRCC3	AT5G57450	Not available		Cytoplasm	Bleuyard and White, 2004
GR1	AT3G52115	C267 and C339	3.738 and 4.389	Nucleus	Vanschou et al., 2007
MCM8	AT3G09660	C107, C183 and C464	10.977, 5.110 and 7.505	Nucleus	Crismani et al., 2013
DMC1	AT3G22880	Not available		Nucleus	Couteau et al., 1999
AHP2	AT1G13330	Not available		Nucleus	Schommer et al., 2003
MND1	AT4G29170	Not available		Nucleus	Kerzendorfer et al., 2006
SDS	AT1G14750	C568	11.205	Nucleus	Yoshitaka et al.,

					2002
BLAP75	AT5G63540	C154	4.270	Nucleus	Chelysheva et al., 2008
RFC1	AT5G22020	C687 and C688	7.058 and 5.747	ER	Liu et al., 2013
TOP3α	AT5G63920	C602 and C645	4.742 and 4.012	Nucleus	Hartung et al., 2008
MSH2	AT3G18524	C930	16.467	Nucleus, PM	Emmanuel et al., 2006
RBR	AT3G12280	C440, C504, C788 and C789	4.013, 4.296, 12.628 and 8.635	Cytosol, Nucleus	Chen et al., 2011
ZIP4	AT5G48390	Not available		Chloroplast, Chromosome, Nucleus	Chelysheva et al., 2007
MER3	AT3G27730	Not available		Nucleus	Wang et al., 2009
HEI10	AT1G53490	C3 and C6	19.682 and 40.154	Nucleus	Chelysheva et al., 2012
MLH1	AT4G09140	C262, C467 and C468	11.993, 7.401 and 4.244	Nucleus	Dion et al., 2007
ASY1	AT1G67370	Not available		Nucleoplasm, Nucleus	Caryl et al., 1999
SCC3	AT2G47980	C610 and C804	13.357 and 4.106	Chromosome, Nucleus	Chelysheva et al., 2005
CTF7	AT4G31400	Not available		Cytoplasm, Nucleus	Jauh et al., 2013
PANS1	AT3G14190	Not available		Nucleus	Juraniec et al., 2015
AESP	AT4G22970	C1182, C1226, C1477 and C1478	5.476, 7.266, 6.930 and 16.067	Cytoplasm, Nucleus	Liu and Makaroff, 2006
CYCA1	AT1G77390	C339	3.895	Cytoplasm, Nucleus	Wang et al., 2004; Jha et al., 2004
OSD1	AT3G57860	C156	14.297	Nucleus	Cromer et al., 2012
SMG7	AT5G19400	C173, C451 and C452	11.790, 5.094 and 6.761	Nucleus	Rieh et al., 2008

that some of them localized at other organelles, such as PRD1 and ZIP4 at chloroplast,

DFO at mitochondrion, RFC1 at ER and MSH2 at PM. PM localization of the putative target increase the chance to be S-acylated by AtPAT21 since they localize at the same place. Further experimentation will aim to determine whether these putative palmitoyalted proteins interact with and modified by AtPAT21 to shed new light on the roles played by palmitoylation in reproductive biology, especially during the meiotic process in Arabidopsis.

4.3.4 Summary and future work

We have clearly shown that Protein S-acyl transferase 21 is an S-acyltransferase and it is ubiquitously expressed with higher levels found in the reproductive tissues. It is a positive regulator in reproduction in Arabidopsis because disruption in AtPAT21 results in sterility. AtPAT21 acts by modulating both male and female microsporogenesis and megasporogenesis, most likely through the regulation of meiosis for the generation of pollen and ovules. Further study will be carried out to first observe the meiosis process in details in the *atpat21-1* mutant to find out in which step(s) the defects happen during meiosis. This will help to narrow down the number of possible target S-acylated proteins we proposed in Table 4-3. These proteins will be further characterised individually to see if they are indeed the substrate proteins for AtPAT21.

Chapter 5 AtPLP1 Is Involved in Triacylglycerol Catabolism During Early Seedling Establishment

5.1 Introduction

Seed germination and seedling establishment are two important processes for spermatophytes before they acquire efficient photosynthesis to achieve self-sufficiency for further growth. The process of seed germination is divided into three phases, the imbibition phase, the germination phase and the radicle emergence (Bewley and Black, 1994). Phytohormones play significant roles during seed germination, especially abscisic acid (ABA) and gibberellin (GA) (Koornneef et al., 2002). For example, extended seed dormancy in the imbibition stage was induced by over expression of the ABA positive regulators in tobacco (Frey et al., 1999), whereas the inhibitors of ABA synthesis can promote seed germination (Grappin et al., 2000). In Arabidopsis, chemically induction of 9-cis-epoxycarotenoid dioxygenase (NCED), the major enzyme that control ABA biosynthesis, can suppress seed germination (Martínez-Andújar et al., 2011). Some ABA related mutants such as *ABA insensitive 3* (*abi3*) and *enhanced response to ABA* (*era*) also have germination defective phenotype (Cutler et al., 1996; Mönke et al., 2012). All these studies demonstrate that ABA contributes to seed dormancy maintenance. Opposite to ABA, GA is an important phytohormone that promotes germination. This was demonstrated by the germination defect in GA-deficient mutants *ga1-3* and *ga2-1* (Koornneef and van der Veen, 1980). Paclobutrazol, an inhibitor of GA biosynthesis can also suppress seed germination (Jacobsen and Olszewski, 1993). Before radicle emergence, the expression levels of a set of GA-regulating genes increase, resulting in the simulation of higher level of endogenous active GA (Ogawa et al., 2003). Because the mRNAs of genes required for seed germination have already been transcribed and accumulated during seed maturation, the seed does not start novel gene transcription until it enters the seedling establishment stage, therefore, little energy is consumed (Rajjou et al., 2004). Different from germination, which consume little energy and only use extant mRNAs, seedling establishment need lots of energy and carbon skeletons, which are

usually released from catabolizing storage triacylglycerol (TAG) in oilseeds, to support many complex metabolic processes, such as cell division, radicle cells elongation, DNA synthesis, new mRNA transcription etc. (Bewley, 1997).

In Arabidopsis, up to 40% of the oil is present in its fresh seeds in the form of TAG. TAG is present in the cytosolic oil droplets that are enclosed by a phospholipid monolayer with some structural proteins embedded (Eastmond, 2006; Siloto et al., 2006). Complete oxidation of TAG can produce more than twice the energy than the hydrolysis of protein or carbohydrate (Quettier and Eastmond, 2009). TAG is hydrolysed via three enzymatic steps where it is firstly broken down to free fatty acids and the backbone glycerol by lipase, which happens at the oil/water interface (Quettier and Eastmond, 2009). Next, these free fatty acids or fatty acyl-CoAs are transported into the single-membrane-bound glyoxysomes and transformed to aceyl-CoA by β-oxidation. Finally, the aceyl-CoA is converted into two four-carbon dicarboxylic acids, succinate and oxaloacetate, by the glyoxylate cycle which happens also in the glyoxysomes (Eastmond and Graham, 2001). While oxaloacetate is combined with another aceyl-CoA to keep the glyoxylate cycle going, and succinate is used to generate sugars through gluconeogenesis in the mitochondria (Canvin and Beevers, 1961; Cornah et al., 2004; Theodoulou and Eastmond, 2012).

Many mutants that are defective in seedling establishment are caused by the disruption of one or more genes involved in storage oil catabolism (Graham, 2008), which are usually rescued by addition of external sugar, such as sucrose. For example, sugar dependent 1 (SDP1) which localizes at oil body membrane, is a TAG lipase, its knock out mutant showed seedling establishment defect which was rescued by supplementation of sugar in the media (Eastmond, 2006). Similar phenotype were found in the *Peroxisomal ABC Transporter1* (*PXA1*) loss-of-function mutant, which is involved in transporting free fatty acids or fatty acyl-CoAs that are released from TAG hydrolysis to peroxisomes (Zolman et al., 2001). Two peroxisomal long-chain acyl-CoA synthetases (LACS6/7), which convert free fatty acids to active fatty acyl-CoAs, are required for seedling

establishment (Fulda et al., 2004). The first step of β-oxidation is catalysed by the acyl-CoA oxidase (ACX) family and it has 6 ACXs in Arabidopsis (Pinfield-Wells et al., 2005). The double mutant *acx1acx2* failed to establish seedlings on the media without sugar (Pinfield-Wells et al., 2005). Multifunctional protein 2 (MFP2) and 3-ketoacyl-CoA thiolase 2 (KAT2), which catalyse the last second and the last steps of β-oxidation process, were also necessary for seedling establishment (Rylott et al., 2006; Germain et al., 2001). The isocitrate lyase (ICL) and malate synthase (MS), the key enzymes of glyoxylate cycle (Eastmond et al., 2000; Cornah et al., 2004) and phosphoenolpyruvate carboxykinase1 (PCK1), the catalytic enzyme to the first step of gluconeogenesis (Penfield et al., 2004) are also important in seedling establishment.

Protein S-acyl transferases (PATs) is a large family of enzymes that catalyse the palmitoylation reaction of many proteins that are involved in signalling and trafficking (Resh, 2006). AtPLP1 is a DHHC containing protein which is similar to a typical PAT, but different from AtPAT24 (Hemsley et al., 2005), AtPAT10 (Qi et al., 2013), AtPAT14 (Li et al., 2015) or AtPAT21, it cannot rescue the growth defect of yeast PAT mutant *akr1*. AtPLP1 loss-of-function mutant exhibits multiple defects, such as delayed germination, de-etiolation in the dark, failed seedling establishment, reduced vegetative growth, and abnormal shoot apical meristem. In this chapter, we will focus on the function of AtPLP1 in the catabolism of seed storage oil and seedling establishment.

5.2 Results

5.2.1 Expression pattern of AtPLP1

To understand how AtPLP1 functions in Arabidopsis, we monitored the transcript levels of AtPLP1 by RT-PCR from total RNA isolated from different tissues of WT plants. We found that AtPLP1 has universal expression in all organs with higher levels in young seedlings and rosette leaves (Fig. 4-1A). To further confirm this result, we observed the GUS distribution in transgenic Arabidopsis expressing AtPLP1promoter: GUS. Consistent with the RT-PCR result, GUS expression was found in much higher levels in

7-day-old seedlings and the rosette leaves, as well as in anthers (Fig. 4-1B). In 1-week and 2-week-old seedlings, AtPLP1 expressed especially high in leaf veins (Fig. 4-1B-a and b). And in flowers, it mainly expressed in anthers (Fig. 4-1B-d). These results are consistent with the expression pattern of AtPLP1 analysed by online Arabidopsis eFP Browser (http://bbc.botany.utoronto.ca/efp/cgi-bin/efpWeb.cgi).

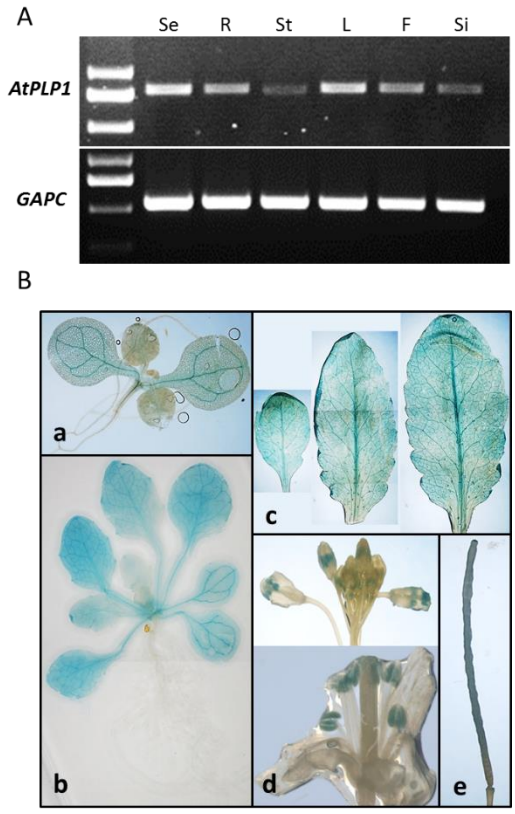

Figure 5-1. The expression level of *AtPLP1* in seedlings and different tissues of the mature plant of Arabidopsis.
A. RT-PCR was carried out on total RNA isolated form wild-type Col-0 whole seedlings and different parts of the mature plants. Se, 7-day old seedlings; R, roots of 2-week old seedlings grown on the 1/2 MS plate; St, stem of the first node of 35-day-old soil-grown plants; L, the 5th and 6th rosette leaves of 4-week-old soil-grown plants; F, fully-opened flowers; Si, 3-day-old siliques after pollination. B. Histochemical localization of AtPLP1. A construct containing AtPLP1promoter:GUS fusion was transformed to WT Arabidopsis plants. GUS-staining analysis was performed on whole seedlings and the different tissues of the mature transgenic plants. a, 1-week-old seedlings; b, 2-week-old seedlings; c, rosette leaves from 5-week-old plant, young (left) to old (right); d, inflorescence and flower from 5-week-old plants; e, silique, 5 days after pollination.

5.2.2 AtPLP1 is not a typical PAT as it cannot rescue the growth defect of yeast *pat* mutants

Previous studies showed that the knockout mutant of one of the 7 yeast PAT, Akr1, is sensitive to high temperature (37°C) and grows poorly under this restrictive temperature (Feng and Davis, 2000; Hemsley et al., 2005). The three functionally identified PATs in Arabidopsis can complement or partially complement the growth defects of *akr1*, including AtPAT24 (Hemsley et al., 2005), AtPAT10 (Qi et al., 2010) and AtPAT14 (Li et al., 2015). To see if AtPLP1 also has this ability, we first transformed

AtPLP1 into *akr1* to obtain the transgenic yeast cells harbouring *AtPLP1*. Growth assays show that at 37°C, *akr1* grows much poorer than wild type yeast strain BY4741 which were in line with previous studies. However, *akr1* yeast cells expressing AtPLP1 grew even poorer than the mutant *akr1* cells, i.e., AtPLP1 cannot rescue the growth defect of *akr1* (Fig. 5-2A).

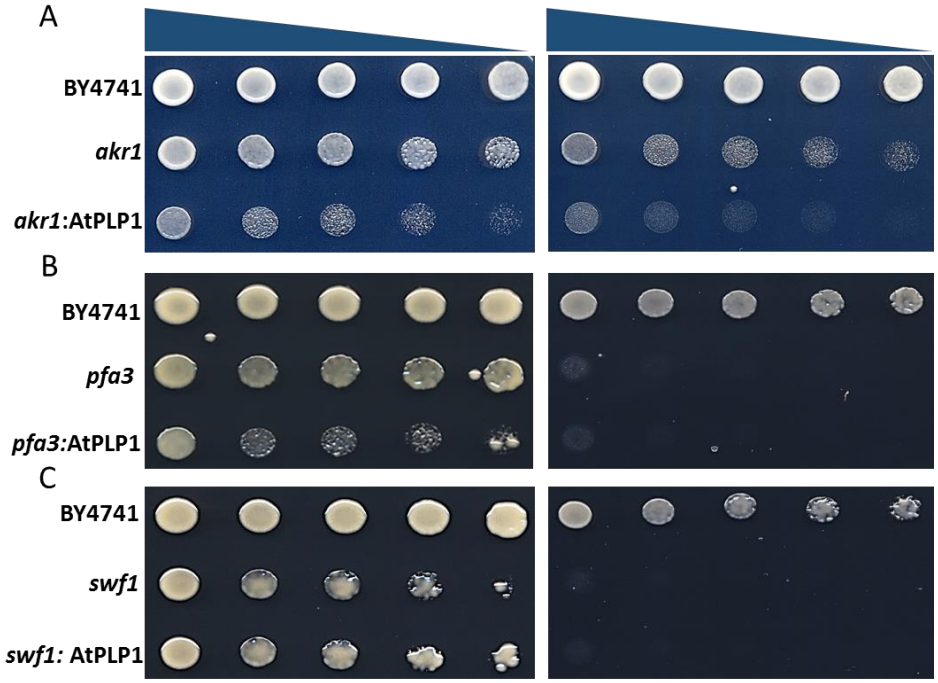

Figure 5-2. AtPLP1 cannot rescue the growth defects of yeast *PAT* k/o mutants *akr1, pfa3 or swf1*.

A. Complementation assay of *akr1*. At both 25℃ (left) and 37℃ (right), wild-type BY4741 (BY4741) yeast grew well but *akr1* did not. However, the AtPLP1 transformed *akr1* (*akr1*:AtPLP1) grew even worse than the mutant *akr1*, therefore, AtPLP1 cannot restore the growth defect of *akr1*.

B and C. Yeast *PAT k/o* mutants *pfa3* (B) and *swf1* (C) cannot grow on the media when 0.85M NaCl was present (right) although they could grow well without NaCl (left). However, neither of the transgenic *pfa3* and *swf1* yeast cell lines harbouring *AtPLP1* (*pfa3*:AtPLP1 in B and *swf1*: AtPLP1 in C) can rescue the salt sensitivity of the mutant.

For all the samples, 8 µl of 1:1, 1:5, 1:10, 1:20 and 1:40 diluted 1 OD_{600} cells were spotted on the media plate and grown for 3 days.

We were puzzled with this result, therefore, carried out further yeast complementation studies using 2 other yeast PATs mutants, *pfa3* and *swf1* to see if

AtPLP1 can rescue their growth defects on the media supplemented with 0.85M NaCl (Montoro et al., 2011). As shown in Fig. 5-2B and C on the control media without NaCl WT (BY4741) yeast grow well at all dilutions. Significant amount of growth was also observed with *pfa3* and swf1 yeast cells although not as well as the WT. Similarly, in the mutants harbouring AtPLP1 (*pfa3*:AtPLP1 and *swf1*:AtPLP1) also showed respectable growth. When 0.85M NaCl was added into the media, as expected, the WT cells still grew well, but neither *pfa3* nor *swf1* showed much growth. However, to our surprise, no growth was found in the AtPLP1 transformed *pfa3* and *swf1* cells (*pfa3*:AtPLP1 and *swf1*:AtPLP1) (Fig. 5-2B and C), i.e., the growth defects of the mutants on NaCl were not rescued by the presence of AtPLP1.

Therefore, the results demonstrate that AtPLP1 could not complement the activities of the yeast PATs Akr1, Pfa3 and Swf1.

5.2.3 Identification of AtPLP1 loss-of-function mutant

In order to understand the biological roles that AtPLP1 plays in the growth and development of Arabidopsis, an *AtPLP1* T-DNA insertion line was obtained from the Arabidopsis Biological Resource Center (ABRC). RT-PCR using cDNA synthesized from RNA isolated from leaves of WT and this T-DNA insertion line as templates was carried out to determine the knockout status of this line (*GAPC* was used as an internal control). The result showed that no full length transcript of *AtPLP1* was detected while the corresponding PCR product was amplified from the WT (Fig. 5-3A). This data confirms this is most likely a transcript null mutant for *AtPLP1*, hereafter named *atplp1-1*.

Next, we performed detailed phenotypic analysis of this line. As shown in Fig. 5-3B and C the rosette leaves of *atplp1-1* were smaller, more rounded and crinkled compared to WT. The growth of *atplp1-1* mutant plant during early developmental stages was very slow with smaller and rounder leaves and the plant struggled to establish (Fig. 5-3B). However, after bolting the *atplp1-1* mutant plant showed little difference compared to WT. Although the fully grown plant of *atplp1-1* was slightly shorter than WT, it had similar number of branches to the WT (Table 5-1). The flower size of *atplp1-1* was

identical to that of WT. Germination of the pollen grains of the mutant didn't show any defects (Fig. 5-4). However, the mutant seeds were about 20% larger than WT seeds (Fig. 5-5).

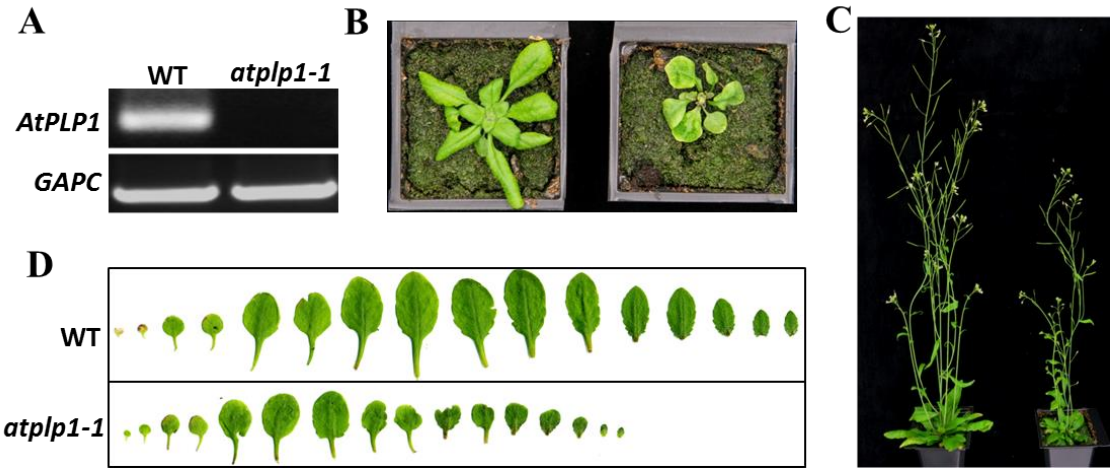

Figure 5-3. Characterization of *Arabidopsis thaliana* T-DNA insertion mutant line for *AtPLP1*.

A. RT-PCR analysis showed that the *atplp1-1* mutant is devoid of AtPLP1 transcript. WT, wild type.

B and C. 4-week (B) and 6-week (C) old WT (left) and *atplp1-1* plants (right).

D. Rosette leaves of WT (top) and *atplp1-1* plants (bottom). Leaves were taken from 26-day-old plants.

Table 5-1. Phenotypic analysis of WT and *atplp1-1*

	WT (n=9)	***atplp1-1* (n=10)**
Plant height (mm)	476.0±18.9	420.9±10.1*
Length of silique (mm)	17.0±0.7	16.3±1.1
No. of branches	23.0±2.8	20.1±3.2
No. of siliques in main branch	55.8±1.9	45.4±3.8*

62-day old plants were measured. *p<0.01 in Student's *t*-test.

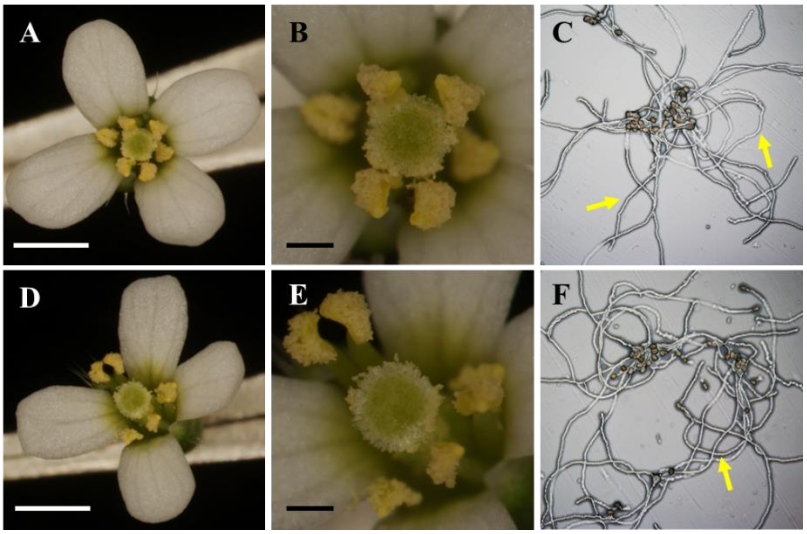

Figure 5-4. Fully opened flowers and *in vitro* pollen grain germination assays of WT and *atplp1-1*. A-C, WT; D-F, *atplp1-1*.
A, B, D and E. Fully opened flowers were observed under dissecting microscope with different magnifications. Scale bars in A and D, 1mm; Scale bars in B and E, 0.25mm.
C and F. Pollen grains were germinated *in vitro* on the pollen germination media for overnight and then observed under light microscope. Yellow arrows, pollen tubes.

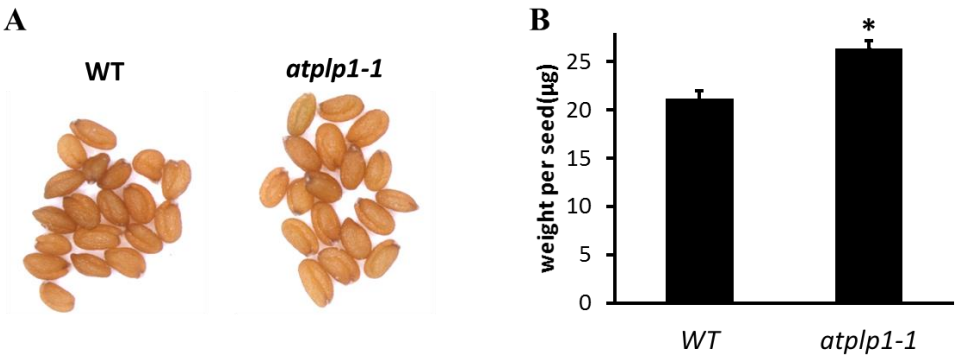

Figure 5-5. The seeds of *atplp1-1* are bigger and heavier than WT.
A. The morphology of mature seeds from WT (left) and *atplp1-1* plants (right).
B. Dry weight per seed of WT and *atplp1-1*. The experiment was repeated five times using approximately 100 seeds in each replicate. * $p<0.05$ in Student's *t*-test.

5.2.4 Post-germination growth of the *atplp1-1* mutant is sugar dependent

While carrying out seed germination on ½ MS media we noticed that *atplp1-1* was slower in germination, and most importantly most of the seedlings failed to develop further to produce true leaves. Therefore, we investigated this further. As shown in Fig. 5-6 seed germination and seedling establishment of WT Arabidopsis do not require sucrose in the media. However, the seedlings of *atplp1-1* mutant failed to establish because the cotyledon expansion and primary root elongation on media lacking sucrose were arrested (Fig. 5-6B right). This was not due to failure in germination of *atplp1-1* seeds because 92% of the mutant seeds germinated after 72 hours compared to 98% of WT seeds germinated on the media without sucrose although *atplp1-1* seeds were slower to germinate (Fig. 5-6A). Therefore, the majority of mutant seeds can germinate without sugar if longer period of incubation time was given. When 1% sucrose was added to the ½ MS media the mutant seedlings could develop and grow in a comparable rate as the WT seedlings (Fig. 5-6B left). Therefore, the AtPLP1 loss-of-function mutant is sugar dependent during early seedling establishment.

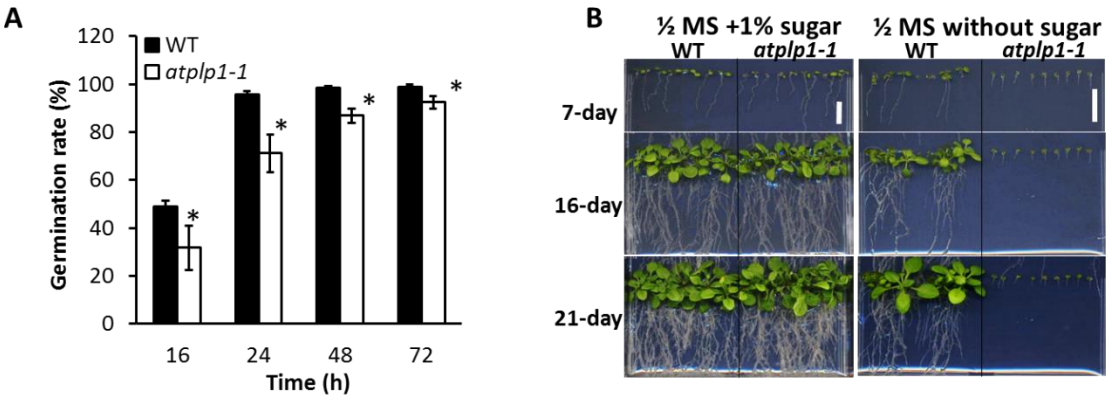

Figure 5-6. *atplp1-1* seed germination is slower than WT, and early seedling growth is sugar dependent.

A. Germination rate of WT and *atplp1-1* after 16h, 24h, 48h and 72h on ½ MS media without 1% sucrose. * $p<0.05$ in Student's *t*-test.

B. *atplp1-1* is sugar dependent during early seedling growth. Seedlings were vertically cultured on 1/2MS media for 7 (top), 16 (middle) and 21 (bottom) days with (left) or without (right) 1% sucrose. Bars, 1cm.

5.2.5 Defect in *atplp1-1* is rescued by both the WT *AtPLP1* and the point mutant *AtPLP1DHHS*

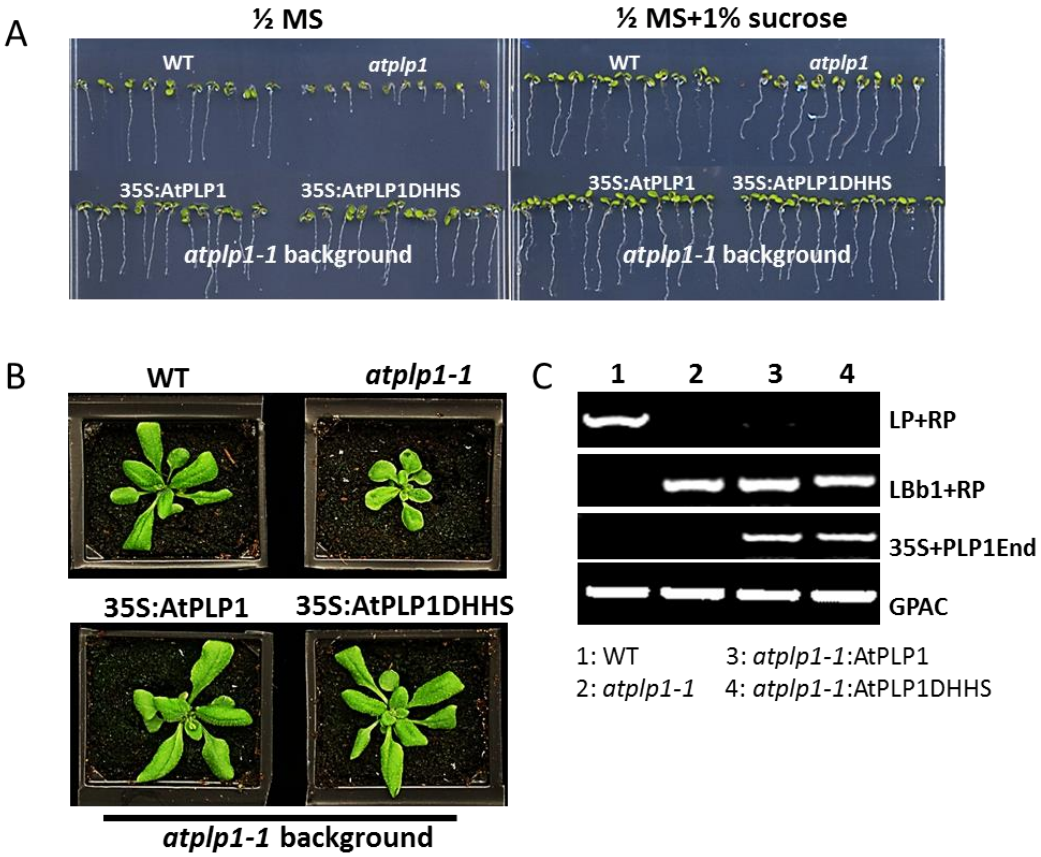

Figure 5-7. Both AtPLP1 and AtPLP1DHHS can rescue the growth defect of *atplp1-1*.

A. Sugar dependence of *atplp1-1* can be rescued by either AtPLP1 or the point-mutant AtPLP1DHHS. *atplp1-1* mutant was transformed by transgenic agrobacteria harbouring the *35S:AtPLP1* (*atplp1-1*:AtPLP1) or *35S:AtPLP1DHHS* (*atplp1-1*:AtPLP1DHHS). Arabidopsis of WT, *atplp1-1*, transgenic *atplp1-1*:AtPLP1 or *atplp1-1*:AtPLP1DHHS were grown on ½ MS without (left) or with (right) 1% sucrose for 5 days.

B. Both *AtPLP1* and *AtPLP1DHHS* can rescue the growth defects of *atplp1-1* in soil-grown plants. 7-day-old WT, *atplp1-1*, *atplp1-1*:AtPLP1 and *atplp1-1*:AtPLP1DHHS were transferred to soil and grown for 3 weeks.

C. PCR products amplified with different pairs of primers to confirm the genotypes of the plants photographed in B. Genomic DNA of WT, *atplp1-1*, *atplp1-1*:AtPLP1 and *atplp1-1*:PLP1DHHS were used as templates. House-keeping gene *GAPC* was used as an internal control.

To determine the growth defects of *atplp1-1* is caused by *AtPLP1* loss of function,

we transformed 35S:AtPLP1 construct to *atplp1-1* mutant. The results showed that AtPLP1 can completely rescue the growth defects of *atplp1-1* mutant, demonstrating that the growth defect of the mutant is caused by AtPLP1 being rendered non-functional in the mutant (Fig. 5-7). However, surprisingly, when we mutated the cysteine residue to serine in the DHHC domain and transferred it to the *atplp1-1* mutant plants the transgenics harbouring the *AtPLP1DHHS* can also rescue the growth defects of *atplp1-1* because these plants look identical to the WT plants (Fig. 5-7). The *atplp1-1* background of both *AtPLP1* and *AtPLP1DHHS* transgenic lines were confirmed by two PCR reactions with gene specific primer pairs of LP and RP, and left border primer located at T-DNA LBb1 and RP, respectively, using WT and *atplp1-1* as positive and negative controls (Fig. 5-7C top two panels). PCR result with 35S and AtPLP1End primers showed these plants contained the transgenes (Fig. 5-7C the third panel). Therefore, our results demonstrate that the function of AtPLP1 does not rely on the Cys in the DHHC motif of AtPLP1. Therefore, AtPLP1 is not a typical PAT and its enzyme activity domain does not rely on the cysteine in the DHHC motif.

5.2.6 *atplp1-1* has defect in lipid breakdown during early seedling development

In Arabidopsis, seed germination relies on the very limited reserved sugar in the seed. However, post-germination growth is support by the breakdown of oil reserves accumulated and stored in seeds (Cornah et al., 2004). Because seedlings of *atplp1-1* failed to develop properly after germination, we suspected the lipid breakdown pathway during post germination growth could be defective. Therefore, we measured the fatty acid C20:1, which is frequently used as a reliable marker to show the levels of triacylglycerol (Thazar-Poulot et al., 2015), in dark-grown *atplp1-1* seedlings at the post-germination stage. A direct comparison was made between WT, *atplp1-1* and the Sugar Dependent Protein1 loss-of-function mutant *sdp1* that has similar phenotype to *atplp1-1* in post-germination growth due to defect in lipid breakdown (Eastmond, 2006). First, we compared the C20:1 levels in seeds of these three lines, however no significant difference was found between them (Fig. 4-9), indicating they accumulated TAG normally. However,

in 5-day-old dark-grown seedlings the C20:1 content of WT dramatically decreased to only 9.7% of that in seed whilst C20:1 in *sdp1* seedlings was 96.8%, confirming the previous observation that most of the TAG in *sdp1* seedlings remain un-digested (Eastmond, 2006). Interestingly, C20:1 in *atplp1-1* seedlings was 24.9%, which was significantly higher than WT but lower than *sdp1* (Fig. 4-9). This demonstrates that *atplp1-1* mutant has defect in post-germination lipid breakdown, but it is not as severe as *sdp1*.

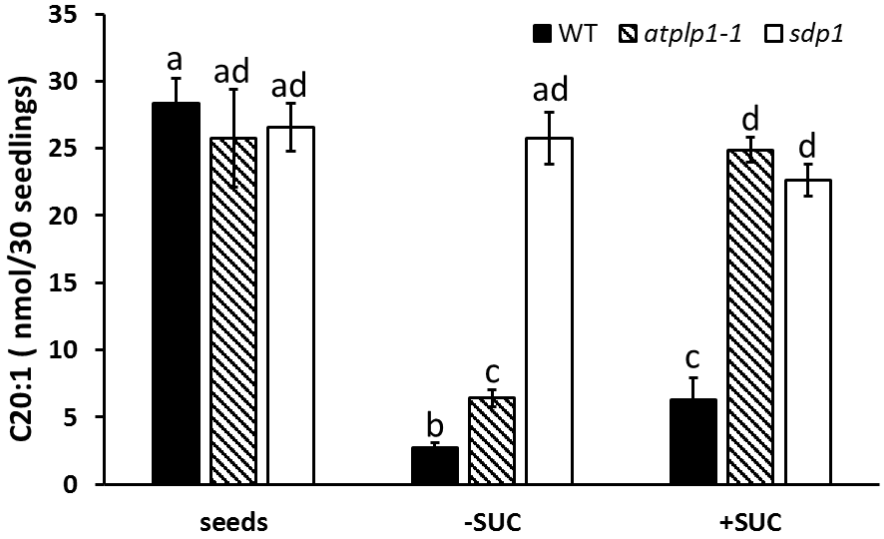

Figure 5-8. *atplp1-1* has defect in lipid breakdown during post-germination growth. Total fatty acids were extracted from seeds or 5-day old etiolated seedlings of WT, *atplp1-1* and *sdp1* that were grown on ½ MS without (-SUC) or with 1% sucrose (+SUC). Content of C20:1, as the marker of TAG, was analysed by GC-MS. The values are the means±SE of measurements from four separate batches of 30 seeds or seedlings. Different letters above the columns indicate statistically different values analyzed by one-way ANOVA and Tukey's HSD test, $p<0.05$.

Next, we analysed the C20:1 contents in 5-day-old etiolated seedlings grown on 1/2 MS media supplemented with 1% sucrose. Less lipid was broken down for all three lines compared seedlings grown on sugar free 1/2 MS media (Fig. 4-9). C20:1 level in WT seedlings increased from 9.7% to 22.2% of the level in seed, whilst 85.1% and 96.7% of C20:1 remained in seedlings of *sdp1* and *atplp1-1,* respectively. This result indicate that post-germination growth of *atplp1-1* consumed very little storage lipid when sucrose was

supplied as external energy source.

The combined data clearly demonstrated that AtPLP1 plays important roles during early seedling establishment and this is mediated by the regulation in lipid breakdown.

To further validate the above conclusion we observed the lipid droplets in hypocotyls of 5-day old etiolated seedlings using Nile red. Consistent with the quantitative data above while there hardly any oil droplets were observed in WT hypocotyls the oil droplets were densely packed in *atplp1-1* seedling. The mutant appeared to have even more oil droplets when grown in 1% sucrose containing media which was in line with the higher C20:1 content detected in these seedlings compared to when they were grown on sucrose free media (Figs. 5-8 and 5-9).

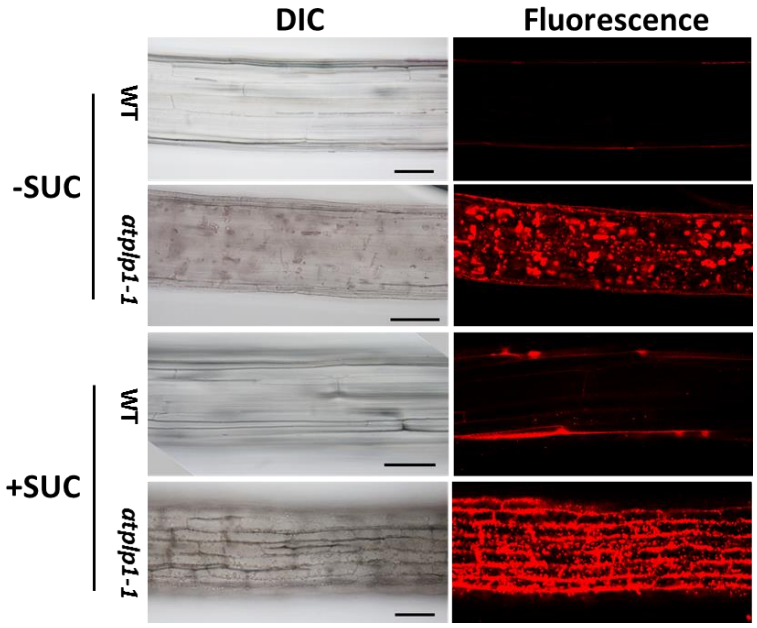

Figure 5-9. *atplp1-1* seedlings had more oil droplets in their hypocotyls.
5-day-old etiolated seedlings were stained with 10μg/ml Nile Red for 5 minutes, and the stained hypocotyls were observed by confocal scanning microscopy under normal DIC (differential interference contrast) model (left) or excited by 583nm laser (right). –SUC, ½ MS media without external supplemented sucrose; +SUC, ½ MS media with external supplemented 1% sucrose. Bars, 0.1mm.

5.2.7 Transcripts of key genes regulating lipid breakdown were down-regulated

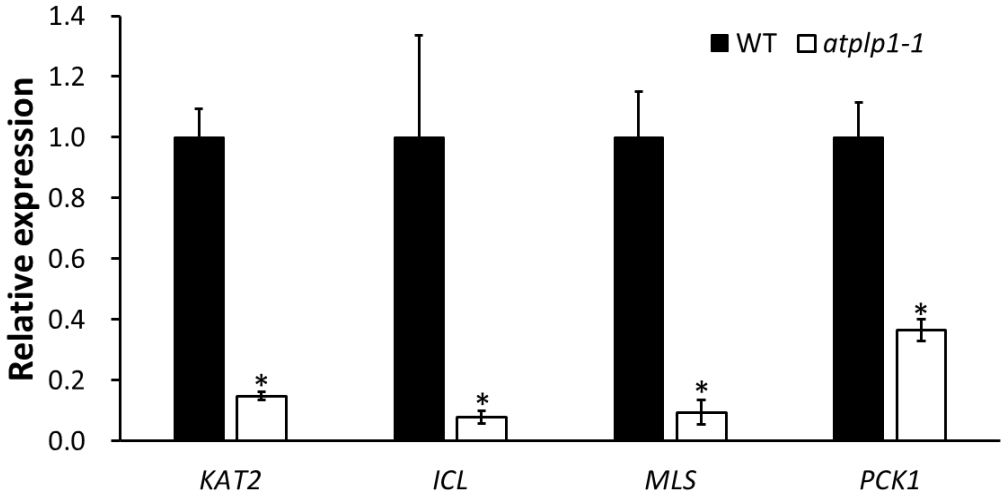

Figure 5-10. Transcript levels of the key genes in lipid breakdown pathway were down-regulated during early seedling establishment.
Total RNA was extracted from 10 seedlings of WT or *atplp1-1* that were grown on 1/2MS+1% Suc for 10 days in the dark. The relative expression level of each gene in the mutant was calculated where the transcript level of WT was regarded as 1. The experiments were repeated three times. * $p<0.05$ in Student's *t*-test. *KAT2, 3-ketoacyl-CoA thiolase 2; ICL, isocitrate lyase; MLS, malate synthase; PCK1, phosphoenolpyruvate carboxykinase1*.

The above data clearly demonstrated that AtPLP1 is involved in lipid breakdown during seedling growth. In order to see which step(s) is defective in *atplp1-1* we monitored the transcript levels of some key genes involved in the different steps of lipid breakdown pathway by real time PCR using cDNAs that were synthesized from total RNAs extracted from 10-day-old dark-grown WT and *atplp1-1* seedlings. The genes tested included those encoding for 3-ketoacyl-CoA thiolase 2 (KAT2) which catalyses the last step of β-oxidation, Isocitrate lyase (ICL) and malate synthase (MLS) which are key enzymes in glyoxylate cycle, phosphoenolpyruvate carboxykinase1 (PCK1) that catalyses the first step of gluconeogenesis. The null mutants of all these genes have severe defect in lipid breakdown, leading to failed seedling establishment (Eastmond et al., 2000; Germainet al., 2001; Cornah et al., 2004; Penfield et al., 2004). As shown in Fig. 5-10 the expression levels of all these 4 genes in *atplp1-1* were much lower than in those in WT. The expression level of *KAT2* in *atplp1-1* was only 14.9% of that in WT. The transcripts

of *ICL* and *MLS* in the mutant were even lower, accounted for only 7.8% and 9.5% of those in WT respectively. At 36.6% the reduction in the transcript level of *PCK1* was not as severe as the other 3 genes but it was still less than half of that in WT. Therefore, it seems that the key genes for lipid breakdown in young seedlings of *atplp1-1* were much less active than those in WT. This could lead much less lipid breakdown as described earlier (Figs. 5-8 and 5-9). The results further confirmed the regulating role ATPLP1 plays during lipid breakdown in the early seedling establishment stage of Arabidopsis.

5.2.8 AtPLP1 affects lipid breakdown through β-oxidation process

As shown in Fig. 5-10 KAT2, the key enzyme involved in β-oxidation was down regulated in the mutant. Therefore, we carried out further experimentation to compare the efficiency of β-oxidation between the WT and *atplp1-1* seedlings. 2, 4-Dichlorophenoxyacetic acid (2, 4-D) is a common herbicide which can arrest root elongation in the light and hypocotyl elongation in the dark (Estelle and Somerville, 1987). 4-(2, 4-dichlorophenoxy) butyric acid (2, 4-DB) is the precursor of 2, 4-D and it can be converted to 2, 4-D through β-oxidation. Hence this process has been used previously in other mutants that are defective in β-oxidation (Richmond and Bleecker, 1999; Eastmond et al., 2000). As expected the roots of both WT and *atplp1-1* seedlings were arrested when 0.5 μM of 2, 4-D was added in the ½ MS+1% sucrose media (Fig. 5-11A). However, when 0.5 μM of 2, 4-DB was present the roots of WT seedlings cannot elongate at all because it can be converted to 2, 4-D by β-oxidation, whilst the roots of *atplp1-1* seedlings still can elongate although they were shorter compared to those grown on the control media without 2, 4-DB (Fig. 5-11B). Similar results were achieved when the hypocotyl length was measured from the dark grown seedlings. Although the length of mutant hypocotyl was even shorter on the control media or with 1μM 2, 4-D, On the media with 2 μM 2, 4-DB supplemented, the hypocotyls of *atplp1-1* seedlings bacame longer than those of WT (Figs. 5-11C and D). The combined data demonstrated that *atplp1-1* seedlings produced less herbicide 2, 4-D from 2, 4-DB and this is most likely due to the fact that β-oxidation was less efficiency in the mutant than in the WT.

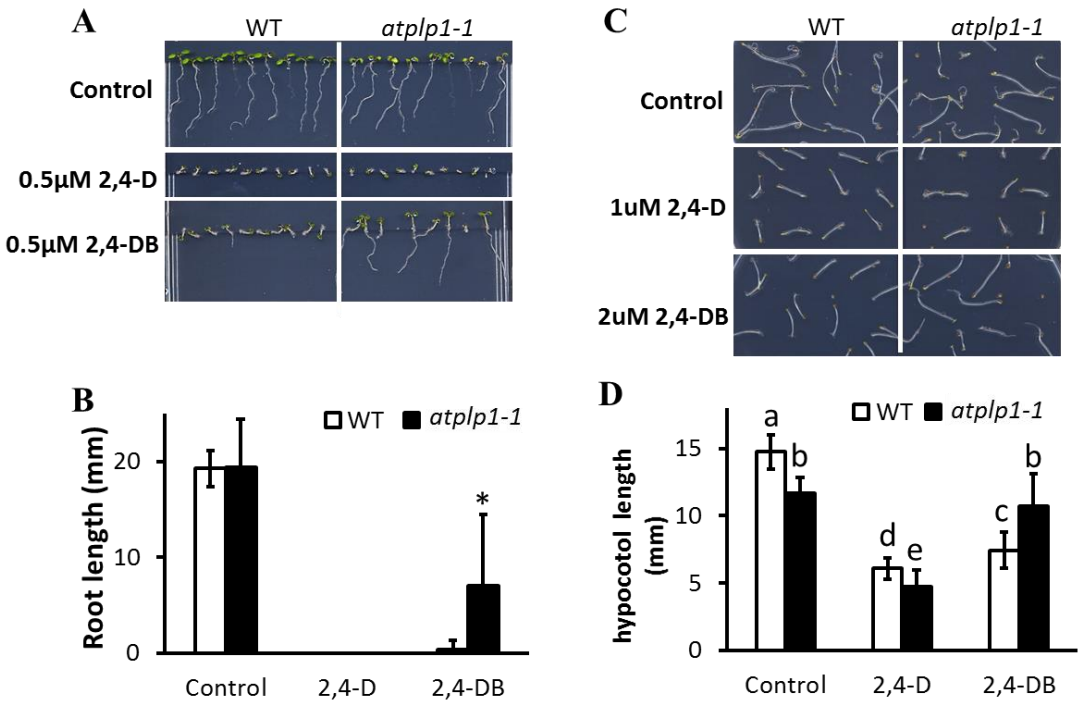

Figure 5-11. *atplp1-1* mutant has defect in β-oxidation process.

A. Effect of 2, 4-D and 2, 4-DB on root length. Both WT and *atp1p1-1* seedlings were grown on agar plates containing 1/2MS+1% sucrose (control), 1/2MS+1% sucrose with 0.5 μM 2, 4-DB or 2, 4-D as indicated. The seedlings were grown under LD (16h light: 8h dark) conditions for 7 days.

B. Root length. Root length of 20 seedlings were measured from each line showed in A. * $p<0.01$ in Student's *t*-test.

C. Effect of 2, 4-D and 2, 4-DB on hypocotyl length. Both WT and *atplp1-1* seedlings were grown on 1/2MS (control), 1/2MS with 1μM 2, 4-D or 2, 4-DB in the dark for 4 days.

D. Hypocotyl length. The hypocotyl lengths were measured from at least 30 seedlings of each line showed in C. Different letters show statistically different analyzed by one-way ANOVA and Tukey's HSD test, $p<0.05$.

5.3 Discussion

5.3.1 Cys in the DHHC domain is not essential for the functionality of AtPLP1

AtPLP1 shares the most conserved domains of typical PATs, such as the enzymatic activity domain DHHC, the conserved domains DPG and TTxE (Gonzalez Montoro et al., 2009; Batistic, 2012). We therefore initially treated AtPLP1 as one of the PATs and carried out yeast and Arabidopsis complementation assays to validate its PAT activity and

functional domain. The *akr1* mutant of yeast PAT Akr1 is unable to grow at the restrictive high temperature of 37ºC. This phenotype is commonly used as a means to test the PAT activity of a newly characterised DHHC-PAT in a yeast complementation assay (Pryciak and Hartwell, 1996). Indeed, 4 yeast PATs (Akr1, Pfa3, Pfa4 and Pfa5), 17 human PATs (DHHC1, 2, 3, 5–9, 10, 12, 14–18, 20 and 21) and 3 Arabidopsis PATs (AtPAT10, 14 and 24) have been confirmed to have PAT activity because of their abilities to complement the growth defect of *akr1* (Ohno et al., 2012; Hemsley et al., 2005; Qi et al., 2013; Li et al., 2015). However, when we transformed AtPLP1 into *akr1* the growth defect of *akr1* was not restored at all (Fig. 5-2A). Since AtPLP1 did not have the ankrin repeat (AR) domains at its N-terminus as Akr1, we reasoned that complementation in other yeast k/o mutants of PATs that do not have the AR may be better strains to use in the complementation assay for AtPLP1. Studies showed that the k/o mutants of *Pfa3* and *Swf1*, the 2 yeast PATs that do not possess the AR at their N-terminii, cannot grow on salt containing media which is relied on their DHHC domain (Gonzalez Montoro et al., 2011). Therefore, we carried out experiments to see if AtPLP1 can rescue the salt sensitivity of *pfa3* and *swf1*. However, again, we did not see rescue of their salt sensitivity by AtPLP1 (Fig. 5-2B and C). We were puzzled and thought the reason for the failure could be due to the fact that being a plant specific PAT AtPLP1 may not function well in yeast although 3 other Arabidopsis PATs did function as PATs and able to rescue the growth defects of *akr1* in yeast before (Hemsley et al., 2005; Qi et al., 2013; Li et al., 2015).

We next carried out complementation studies in Arabidopsis and discovered that both the WT and the point-mutated AtPLP1 where the cysteine in DHHC was changed to serine (DHHS) can fully complement the growth defect of *atplp1-1* (Fig. 5-7). This is a surprise finding as the same mutation in AtPAT10, 14 and 24 did not rescue the phenotype of their respective knockout mutants in Arabidopsis, confirming Cys in the DHHC is essential for their enzyme activity (Hemsley et al., 2005; Li et al., 2015; Qi et al., 2013). Therefore, the combined results from yeast and plant complementation studies demonstrated that DHHC (or the cysteine in the DHHC) is not essential for the functionality of AtPLP1.

Similar results were reported for the yeast PATs Swf1 and Pfa4 where the mutants DHHR-Swf1 and DHHR- or DHHA-Pfa4 can still rescue the defects of *swf1* and *pfa4* (González Montoro1 et al., 2015). Therefore, it seems that the cysteine residue in the DHHC motif might not be the key functional residue in some PATs and AtPLP1 falls into this category of PATs. As suggested these PATs may use a different domain(s) to carry out their PAT activity, such as the PaCCT (Palmitoyltransferase Conserved C-Terminus) motif in Pfa3 and Swf1 (Gonzalez et al., 2009) and the N-terminal ankyrin repeats in Akr1 (Hemsley and Grierson, 2011). In the future, it will be very interesting to find out where the functional domain(s) reside in AtPLP1 and this will enrich our knowledge to understand how PATs function in plants.

5.3.2 Sucrose rescues seedling establishment but inhibits lipid breakdown in *atplp1-1*

Arabidopsis, like all other oilseed crops, relies on the breakdown of its seed storage TAG to supply carbon skeletons and energy to fuel post-germination seedling growth but not for seed germination (Eastmond, 2006; Eastmond, 2007). Seed germination can be supported by the small amount of soluble carbohydrates present in seeds instead of the major lipid stores, which may explain why *atplp1-1* did not have obvious germination defects although it germinated a little slower than WT seeds (Fig. 5-6A). Similar to other mutants defective in lipid breakdown pathway, seedlings of *atplp1-1* cannot develop beyond cotyledon stage on media lacking sugar and sucrose can rescue this defect (Eastmond, 2006; Zolman et al., 2001; Rylott et al., 2006).

TAG is mainly stored in lipid droplets in Arabidopsis, and this can be visualized after staining with Nile red. An obvious difference was found in the number of lipid droplets present in hypocotyl of seedlings of WT and *atplp1-1* where virtually none in the WT while the mutant was packed with them. With the presence of 1% sucrose this phenotype of the mutant was further enhanced (Fig. 5-9), demonstrating that *atplp1-1* cannot break down the storage lipid during post-germination growth, especially when external carbon source was added. As eicosinoic acid (C20:1) was specially found in TAG (Lemieux et

al., 1990), it is regarded as a reliable marker to detect TAG level in Arabidopsis (Eastmond, 2007; Thazar-Poulot et al., 2015). Therefore, we analysed the contents of this fatty acid instead of the TAG in *atplp1-1* seeds and seedlings grown on ½ MS with and without sugar, with WT as a positive control (Fig. 5-8). The data from the media without sugar showed *atplp1-1* had significant defects in hydrolyzing TAG compared to WT. However, for the *atplp1-1* seedlings grown on the media with sugar, C20:1 content became much higher than the ones grown on ½ MS, which means AtPLP1 would prefer using external sugar as carbon and energy source for development rather than hydrolyzing the internal TAG. The WT seeds also used less internal lipid reserve when they were grown on the media with external sugar (Fig. 5-8). This is consistent with the result from Nile Red staining (Fig. 5-9). Similar result was also reported that sugar, including glucose, sucrose and trechalose, can regulate lipid breakdown by modifying the expression of related genes (Smeekens et al., 2010; Borek and Nuc, 2011). Sugar deficiency can increase the lipase activity and also decrease the number of oleosome (Borek and Nuc, 2011). The activities of key enzymes in glyoxylate cycle, such as ACO (cytosolic aconitase) and ICL were down-regulated under sugar-depleted conditions (Borek and Nuc, 2011). Similarly, the enhanced lipid beakdown defect in *atplp1-1* seedlings could be due to the down revaluation of one or more of these genes. Further research will need to confirm this assumption.

From these results we can conclude that AtPLP1 plays positive roles in post-germination growth of Arabidopsis through the involvement of breakdown of the seed storage lipid.

5.3.3 The lipid breakdown defects of *atplp1-1* is different from either *sdp1* or *icl*

For TAG in oilseed fully accessible to support early seedling growth it will need to be firstly hydrolyzed by lipases to free fatty acids and glycerol. This is followed by β-oxidation, glyoxylate cycle and gluconeogenesis to generate sugar to support seedling growth and development before they become fully self-sufficient by photosynthesis. If any of these processes fail the seed storage lipid will not breakdown properly, leading to

defect in seedling growth and establishment (Theodoulou and Eastmond, 2012). SDP1 encodes a triacylglycerol lipase, which initiates lipid reserves breakdown by removing the fatty acids from the glycerol backbone (Eastmond, 2006). The loss-of-function mutant *sdp1* has complete blockage in lipid breakdown and this results in the failure in seedling establishment whilst its germination is unaffected (Eastmond, 2006). In our TAG analysis experiment we used *sdp1* as the negative control and found that when the seedlings grown on sugar free media *sdp1* retained higher percentage of lipid storage than *atplp1-1* as revealed by its higher content of C20:1 (Fig. 5-8). This indicates that when external carbon source is void *sdp1* failed to generate energy from its TAG to support growth whilst *atplp1-1* can still do so although to a small extent. This may explain why there is still a small proportion of *atplp1-1* (<10%) managed to develop into mature seedlings without external carbon source (data not shown). However, for majority of the *atplp1-1* seedlings this small amount of hydrolyzed lipid reserves is not enough to support their further growth, therefore failed to develop into full mature seedlings. This suggests that AtPLP1 functions differently from SDP1, therefore, it may not be involved in the SDP1 mediated lipid breakdown pathway.

Further, we have also observed that the external carbon source can block lipid breakdown in *atplp1-1* during early seedling growth. On the contrary the lipid breakdown efficiency was enhanced by the addition of external sugar in the *icl* mutant which is defective in the glyoxylate cycle (Eastmond et al., 2000). Therefore, it is unlikely that the lipid breakdown defect in the loss-of-function mutant of AtPLP1 is caused by its involvement in the glyoxylate cycle, the last step of lipid breakdown that is mediated by ICL.

5.3.4 Multiple functions of β-oxidation in plant development

Our results demonstrated that AtPLP1 loss-of-function can cause defect in β-oxidation (Fig. 5-11). β-oxidation, as the major pathway for degradation of both straight- and branched-chain fatty acids, plays an important role in the breakdown of reserved TAG (Dulermo and Nicaud, 2011). Our data clearly demonstrated that β-oxidation defect

results in sugar-dependent for seedling establishment in *atplp1-1*. Therefore, AtPLP1 plays important roles in β-oxidation during lipid breakdown.

Beyond its role in the breakdown of storage lipids, β-oxidation in plants has been shown to be active in the biosynthesis of fatty acid-based plant signalling molecules, such as jasmonic acid (JA), indole-3-acetic acid (IAA) and salicylic acid (SA) that are involved in growth, development and stress responses in plants (Li et al., 2005; Baker et al., 2006; Nyathi and Baker, 2006; Goepfert and Poirier, 2007; Zolman et al., 2008). Consistent with this many mutants that have β-oxidation defect also exhibit altered growth and development patterns apart from the usual reduction of lipid breakdown (Goepfert and Poirier, 2007). For example, AIM1 (abnormal influorescence meristem1) is a multifunctional enzyme that catalyses the second step of β-oxidation during lipid catabolism, and its loss-of-function mutant showed severe defects in both vegetative and reproductive growth (Richmond and Bleecker, 1999). PXA1 (or PED3) supplies substrates for β-oxidation, and its loss-of-function mutant not only shows severe defects in seedling establishment but also strong phenotype in vegetative growth and seed size (Hayashi et al., 2002; Mendiondo et al., 2014). Acyl-coenzyme A oxidases (ACX) which catalyse the first step of β-oxidation are also essential for JA production in peroxisomes, and the wound-induced JA accumulation was abolished in the double mutant *acx1acx5*. Growth and developmental defects in the double mutant were demonstrated as it is more sensitive to chewing insects and has reduced male reproductive function (Schilmiller et al., 2007). Some loss-of-function mutants of β-oxidation genes can also cause sterility in Arabidopsis, such as the double mutant of short- and medium- chain acyl-CoA oxidase ACX4 and ACX3 have aborted embryos during early development (Rylott et al., 2003). As a homologue of AIM1, MLF2 (multifunctional protein 2) also plays important roles in catabolism of fatty acids and their double mutant *aim1/mlf2* are embryo lethal (Rylott et al., 2006). Interestingly, none of the above mentioned mutants resemble the JA or IAA related mutants, indicating β-oxidation is also involved in other processes duting plant growth and development except for pathways related phyhormones (Goepfert and Poirier, 2007).

Similarly, *atplp1-1* also shows multiple defects throughout its growth and development in addition to the early seedling stage (Figs. 5-3C and D, 5-7A). The fact that sucrose could not rescue the growth defect of larger seedlings that were grown on sugar containing agar plates or mature plants grown in soil where sugar is synthesized by photosynthesis demonstrates abnormality in the biosynthesis and signalling by phytoharmones, such as IAA could be the cause (Woodward and Barted, 2005). IAA can be converted from indole-3-butyric acid (IBA) by β-oxidation. As *atplp1-1* is defective in β-oxidation the amount of IAA synthesised via this route may be reduced, resulting in the accumulation of IBA. Study shows that IBA can induce the formation of lateral roots (Zolman et al., 2008). Consistent with this, AtPLP1 loss-of-function mutant had more lateral roots than WT (Fig. 4-11B). This suggests that AtPLP1 may regulate auxin mediated growth and development via β-oxidation.

5.3.5 The mechanism of the involvement of AtPLP1 in lipid catabolism during early seedling growth

AtPLP1 is involved in the seed storage lipid breakdown process during early seedling establishment by regulating β-oxidation. The question is how this is carried out on a molecular level, i.e., what are the protein targets of AtPLP1 in this process? As a PAT it functions by S-acylating one or multiple proteins for their correct localization to membrane system or to prevent their degradation by ubiquitination (Valdez-Taubas and Pelham, 2005). In order to identify the potential palmitoylated proteins modified by AtPLP1 we looked through the dataset of over 500 putative S-acylated proteins recently identified from Arabidopsis through the biotin switch - isobaric tagging for relative and absolute quantification (iTRAQ)-based method (Hemsley et al., 2013). We found that some key enzymes involved in β-oxidation of fatty acids such as KAT2, ACX1 and ACX3 are included in the dataset. However, KAT2 and ACX1 contain thioester bonds which are not involved in S-acylation. Based on the limitation of the specific method the study used, KAT2 and ACX1 cannot be confirmed to be S-acylated although they appeared in the dataset (Hemsley et al., 2013). Therefore, the only protein left is ACX3 and it could be

the most likely target protein of ATPLP1. In this model (Fig. 5-12) ACX3 is a medium-chain acyl-CoA oxidase, which is cytoplasmic protein localized in peroxisome (Eastmond et al., 2000). After it is S-acylated by peroxisomal membrane localized AtPLP1, ACX3 can target to the same membrane to be functional. However, in the AtPLP1 loss-of-function mutant the lipid molecule attached to ACX3 by the action of AtPLP1 is lost, causing the mis-localization hence dysfunction of ACX3 mediated lipid breakdown. This is supported by the fact that the *acx3* mutant showed similar resistance to 2, 4-DB as *atplp1-1* (Rylott et al., 2003). Further experimentation by observing ACX3 subcellular localizations in both WT and *atplp1-1* will validate this assumption.

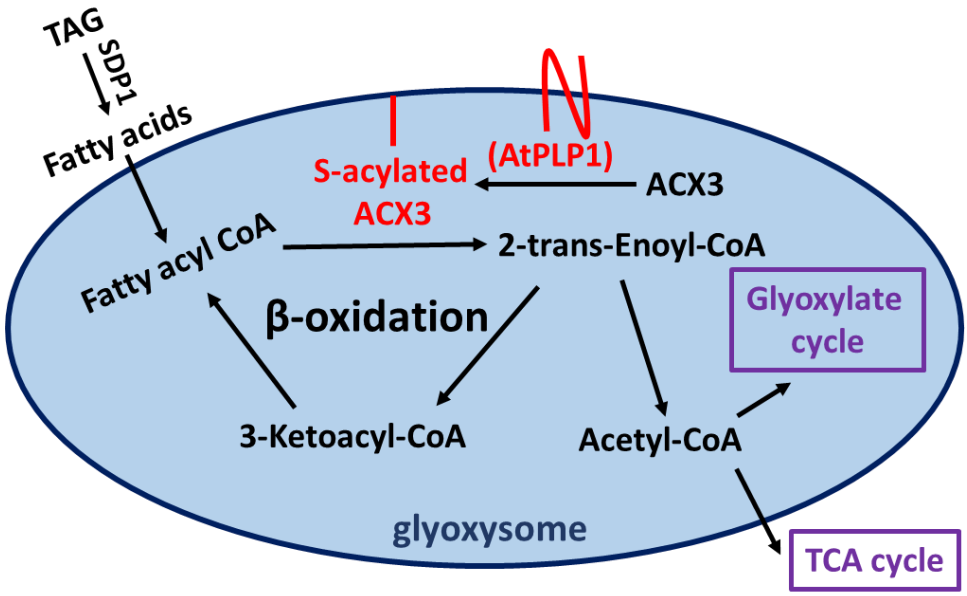

Figure 5-12. A proposed model for the involvement of AtPLP1 in fatty acid β-oxidation through S-acylating acyl-CoA oxidase 3 (ACX3). In Arabidopsis, fatty acids are first released from the seed storage lipid triacylglycerides (TAG) by lipases, such as SDP1. These FAs are transferred into peroxisome where they are converted to fatty acyl CoA to enter the β-oxidation pathway. Cytoplasmic protein ACX3 is S-acylated by the peroxisome membrane localized AtPLP1. Through this modification the S-acylated ACX3 localizes to the peroxisome membrane to carry out its function catalyse the first step of β-oxidation to convert fatty acyl-CoA to 2-trans-enoyl-CoA. This is followed by further rounds of reaction and one Acetyl-CoA is produced from each cycle of β-oxidation. Acety-CoA then enters the glyoxylate cycle or tricarboxylic acid (TCA) cycle to produce sugar and ATP to support early seedling growth before photosynthesis functions properly.

5.3.6 Summary and future work

In this study we characterized a plant S-acyltransferase from Arabidopsis, AtPLP1. We found that *AtPLP1* has a broad expression pattern during each stage of growth and development in Arabidopsis. It has the conserved DHHC domain of a typical PAT, however, unlike other PATs characterized so far its PAT activity does not rely on the Cys residue in this domain. The biological function was studied from a T-DNA insertion line of *AtPLP1*, *atplp1-1*. We found that the mutant has impaired function in hydrolyzing the storage lipid in the seed due to the defective β-oxidation. This leads to the failed seedling establishment of *atplp1-1* without external sugar being present. From the proteins that catalyze β-oxidation during fatty acids breakdown, ACX3 is predicted to be S-acylated. Therefore, we propose that AtPLP1 functions through S-acylating ACX3, and perhaps other proteins for their proper targeting to the peroxisome membrane. It is noteworthy, however, AtPLP1 was shown to be localized at the ER when it was transiently expressed in *Nicotiana benthamiana* leaves Batistic (2012). How the peroxisome membrane localized ACX3 is modified by the ER localized AtPLP1 is currently unknown. Therefore, the future work will be focused on:

1) PAT activity of AtPLP1 and its functional domain will be carried out – Its auto-acylation activity will be further confirmed by *in vitro* Acyl-RAC (resin-assisted capture) method; Point mutation of each cysteine in other domains will be done to verify the functional motif of AtPLP1;

2) Subcellular localization of AtPLP1 through stable transformation in Arabidopsis;

3) The relationship between AtPLP1 as the PAT for ACX3 will be characterized;

4) Other S-acylated proteins of AtPLP1 will also be identified;

5) Finally, the pathways of AtPLP1 mediated lipid breakdown during early seedling establishment will be elucidated.

Chapter 6 AtPLP1 Plays Important Roles in De-etiolation in the Dark, Responses to Cytokinin, ABA and Sugar

6.1 Introduction

Etiolation, also referred as skotomorphogenesis, happens in angiosperms when grown in the dark their seedlings develop long hypocotyls and tightly closed cotyledons to form the apical hook. Etiolated seedlings are yellowish in colour as chlorophyll synthesis and chloroplast development depend on light (Burgess, 1985). Etiolation is required in a natural situation when the seedling is growing through the soil or in the shade from competing plants and attempting to reach the light as fast as possible (Shinkle, 2016). The apical hook protects the shoot apical meristem from damage while pushing through the soil. De-etiolation, or photomorphogenesis, on the other hand, is the process where seedlings grown in the light develop short hypocotyls and open cotyledons exposing the epicotyl (Neff et al., 2000).

De-etiolation is triggered by light where the cotyledons open and become green, forming the first photosynthetic organs of the young plant. Until this stage, the seedling lives off the energy reserves stored in the seed. The opening of the cotyledons exposes the shoot apical meristem consisting of the first true leaves of the young plant, signaling the beginning of self-sufficiency by photosynthesis in plant life. Plants sense light through photoreceptors and different photoreceptors can sense different wave length light signals, such as cryptochromes (CRYs) for blue light, UVR8 for UV light and phyA to phyE phytochromes for red/far-red light (Rizzini et al., 2011). Cryptochromes and phytochromes function through the inhibition of the expression of a key repressor of light induced photomorphogenesis, constitutively photomorphogenic 1 (COP1), which is a ubiquitin E3 ligase (Yi and Deng, 2005). The *cop1* mutant showed strong de-etiolation phenotype when grown in the dark (Deng et al., 1991). COP1 induces the degradation of transcription factors long hypocotyl 5 (HY5) and long hypocotyl 5 homolog (HYH), which are necessary for photomorphogenesis. And it can also stabilize the

skotomorphogenesis-promoting transcription factors, such as phytochrome interacting factor 3 (PIF3) (Alabadí et al., 2008). The mutant *hy5* has defects in responding to light with different wavelengths (Ballesteros et al., 2001; Koornneef et al., 1980), while mutation in PIF3 causes hypersensitivity to light-induced de-etiolation (Kim et al., 2003). De-etiolation can also occur when the levels of endogenous phytohormones become imbalanced during seedling growth in the dark which is manifested as inhibition of hypocotyl elongation, opening of the apical hook of cotyledons, expansion of true leaves and development of chloroplasts (Szekeres et al., 1996; Symons and Reid, 2003).

Recent studies show that instead of working independently, light and phytohormones often cooperatively regulate plant growth and development. For example, a report shows that cytokinin (CK) can up-regulate the expression of some light-related genes (Flores and Tobin 1986). The de-etiolation phenotype of *amp1* (*altered meristem program 1*) mutant is caused by increased endogenous CKs (Chin-Atkins et al., 1996). The interaction between Arabidopsis response regulator 4 (ARR4) and photoreceptor phytochrome B (PhyB) is the most significant element to link the CKs and light signal pathways because ARR4, which is induced by CKs, can stabilize the active form of PhyB (Sweere et al., 2001). CKs can also mimic blue-light-dependent activities to increase the stability of HY5 (Vandenbussche et al., 2007). During seed germination, phytochrome-interacting transcription factor 3-like 5 (PIL5, also known as PIF1) directly interacts with cytokinin-related genes, such as CRF1, CRF2, CRF3 and AHP5, to affect CK signaling in imbibed seeds, even though the significance of this interaction is still unknown (Oh et al., 2009).

Cytokinins were first found in tobacco more than 50 years ago (Miller et al., 1955). They are known to play important roles in stimulating cell division, promoting cell expansion, delaying leaf senescence and releasing apical dominance in shoots and roots (Hwang et al., 2012). The biological functions of CKs are influenced by their conformation and side chain (Zdarska et al., 2015). The naturally active CKs include isoprenoid and aromatic CKs, in which isoprenoid CKs, including N-isopentenyladenine (iP), *trans*-zeatin (*t*Z), *cis*-zeatin (*c*Z) and dihydrozeatin (DZ), occur more frequently in

plants. They exist as free bases, nucleosides-, glycosides- and nucleotides-conjugated forms. Their distributions in plant vary based on plant species, tissue types and developmental stages (Sakakibara, 2006). The major forms of CKs in Arabidopsis are tZ and iP, while cZ is most frequently found in maize and rice (Izumi et al., 1988; Veach et al., 2003).

Another phytohormone that plays important role in etiolation is Gibberellin (GA). GAs comprise a large group of tetracyclic diterpenoid carboxylic acids that are widely found in plants, fungi and bacteria (Hedden and Thomas, 2012; Lor and Olszewski, 2015). GA was first identified in the pathogenic fungus *Gibberella fujikuroi* as its liquid culture can induce stem elongation of rice plants (Kurosawa, 1926; Yabuta and Sumiki, 1938). Since then, over 130 types of GAs have been identified within which only a few have biological activity, such as GA_1, GA_3, GA_4 and GA_7 (Yamaguchi, 2008; Davière and Achard, 2013). GA_4 is the main active GA in Arabidopsis (Eriksson et al., 2006). It is now well recognized that GAs play essential roles in seed germination, stem elongation, leaf expansion, trichome development, pollen maturation and flower induction (Achard and Genschik, 2009; Davière and Achard, 2013).

GAs can repress photomorphogenesis and plants deficient in GA synthesis or signaling show a partially de-etiolated phenotype in darkness (Alabadí et al., 2004). This is because the crosstalk exists between GA and COP1-mediated pathways, with HY5 and PIF3 as the nodes of the interaction (Alabadí et al., 2008). GAs can down-regulate photomorphogenesis-promoting transcription factor HY5 and up-regulate skotomorphogenesis-promoting factor PIF3 to induce etiolation in the dark (Alabadí et al., 2008). Cryptochromes decrease the levels of active GAs through down-regulating the expressions of GA synthases GA20ox and GA3ox and up-regulating the expression of GA2ox that catalyzes the conversion of active GAs to its inactive forms, resulting in the suppression of hypocotyl elongation (Zhao et al., 2007). Phytochromes can also regulate GA responsiveness through the interaction between PIF4 and DELLA proteins which function as repressor of GA responses (de Lucas et al., 2008). PIF4, which plays a central

role in mediating cell elongation, is negatively regulated by the light photoreceptor PhyB and DELLA proteins. DELLAs inhibit PIF4 transcriptional activity, and this process can be blocked by GAs through destabilizing DELLAs (de Lucas et al., 2008). A recent study showed that COP1 could repress photosynthesis in the dark partially by reducing the abundance of DELLA proteins (Li et al., 2015).

ABA, another important plant hormone which plays antagonistic roles to GA during seed germination, is also essential in the adaptive responses of plants to environmental stress (Finch-Savage and Leubner-Metzger, 2006; Xu et al., 2014). The fact that a de-etiolated tobacco mutant, *pew1*, has higher level of abiotic acid (ABA) than WT demonstrates that there is a strong interaction between light and ABA (Kraepiel et al., 1994). Indeed, a recent study showed that HY5 is required for the expression of ABI5 (ABA insensitive 5) and ABI5-targeted genes, providing further evidence for this argument (Chen et al., 2008). B-box (BBX) family proteins act as important transcriptional regulators in positively regulating photomorphogenesis, and studies showed that BBX21 was involved in ABA signaling (Khanna et al., 2009; Xu et al., 2014).

Other phytohormones that show effects on de-etiolation in the dark are brassinosteroids (BRs) which act as negative regulators for de-etiolation in the dark (Symons et al., 2002). Phytochrome mediated de-etiolation is synchronous to the reduction of indole-3-acetic acid (IAA) (Chory et al., 1996), and the apical hook formation in the dark is ethylene-dependent (Swarup et al., 2002), indicating the involvement of auxin and ethylene in de-etiolation.

Sugars are essential to plant growth and metabolism not only as energy source and structure components, but also as signal molecules (Rook et al., 2006). It was reported that sugar signaling had complex cross-talk with different phytohormone signaling pathways (Gibson, 2004). This is because some initially identified sugar-response mutants are found later to be also involved in ABA biosynthesis and/or signaling, and vice versa. For example, GIN6 (glucose-insensitive 6), SIS5 (sugar-insensitive 5), SUN6 (sucrose-uncoupled 6) and ISI3 (impaired sucrose induction 3) are allelic to ABI4 (ABA-

insensitive 4); GIN2, SIS4 and ISI4 are allelic to ABA2; and GIN5 is an allele of ABA3 (Rook et al., 2006). In Arabidopsis, sucrose-induced hypocotyl elongation is GA dependent, but not dependent on GA-induced degradation of DELLAs (Zhang et al., 2010). The function of HXK1 (hexokinase1), the first identified glucose sensor in plant (Moore et al., 2003), relies on the presence of BRs to function (Zhang et al., 2015).

Therefore, it is clear that different phytohormones often function in concert to regulate certain aspects of the plant life cycle. For instance, ethylene regulate some plant growth and development processes through DELLA proteins which is directly regulated by GA (Achard et al., 2003; Saibo et al., 2003); crosstalk between GA and BR occurs in Arabidopsis hypocotyl elongation process (Alabadí et al., 2004); the balance between CK and auxin controls the shoot differentiation and root initiation (Catterou et al., 2002); CK can partially evoke ethylene response (Sun et al., 2003); a GA response inhibitor SPY (SPINDLY) positively regulate CK signaling (Greenboim-Wainberg et al., 2005). Phytohormones also regulate the expression of genes in the sugar-response pathways (Gibson, 2004).

In this study, we will describe the strong de-etiolation phenotype found in the dark grown seedlings of AtPLP1 loss-of-function mutant *atplp1-1*. The effect of 6-benzylaminopurine (6-BA), a synthetic active cytokinin, and GA_3, on de-etiolation of *atplp1-1* was also investigated. Our results showed that 6-BA can partially evoke de-etiolation in WT seedlings which is similar to that found in dark grown *atplp1-1* seedlings. The de-etiolation phenotype of *atplp1-1* can be partially rescued by exogenous application of GA_3. In addition, we found that seed germination of *atplp1-1* were supersensitive to ABA, and sucrose inhibited *atplp1-1* growth at the very early seedling stage before the expansion of their cotyledons. All these results indicate that the homeostasis of phytohormones in *atplp1-1* is disrupted, leading to the alterated phenotype observed in this mutant.

6.2 Results

6.2.1 AtPLP1 loss-of-function results in de-etiolation phenotype in the dark

When grown in the dark wild-type Arabidopsis seedlings were etiolated with long hypocotyl and yellow closed cotyledons, and most importantly the seedlings still remain small after 11 days (Figs. 5-1A, left). However, under the same conditions the *atplp1-1* seedlings grew much bigger with much shorter hypocotyls, large open cotyledons, true leaves (red arrows). The root system of *atplp1-1* seedlings were well defined with much longer primary and lateral roots while the WT seedlings only developed short primary roots with no lateral roots observed (Fig. 6-1A, right). Therefore, AtPLP1 is involved in photomorphogenesis of Arabidopsis.

6.2.2 De-etiolation phenotype of *atplp1-1* in the dark can be partially mimicked by CK

Because defects in biosynthesis and/or signaling of phytohormones such as CK and GA can cause de-etiolation (Chin-Atkins et al., 1996; de Lucas et al., 2008) we treated the seedlings with these two phytohormones and observed their effects on dark-grown seedlings of both WT and the *atplp1-1* mutant.

For CK treatment, WT and *atplp1-1* seeds were germinated and grown on ½ MS media without or with 1, 5 and 10 μM 6-Benzylaminopurine (6-BA), which is a synthetic cytokinin commonly used in CK response assays in plants (Koshimizu and Iwamura, 1986; Kusnetsov et al., 1998). As shown in Fig. 6-1B, when 1 μM 6-BA was added to the media the WT seedlings became partially de-etiolated with much shorter hypocotyls, fully opened cotyledons and visible true leaves although they were still yellow due to lack of chlorophyll. The de-etiolation phenotype of WT was enhanced by the higher concentration of 6-BA present in the media. Compared to non-treated seedlings the hypocotyl length of WT seedlings were reduced to 68.2%, 65.0% and 62.5% when grown on the media containing 1, 5 and 10 μM 6-BA. This is 32%, 35% and 37.5% reduction in hypocotyl lengths of WT seedlings compared to those grown on 6-BA minus media.

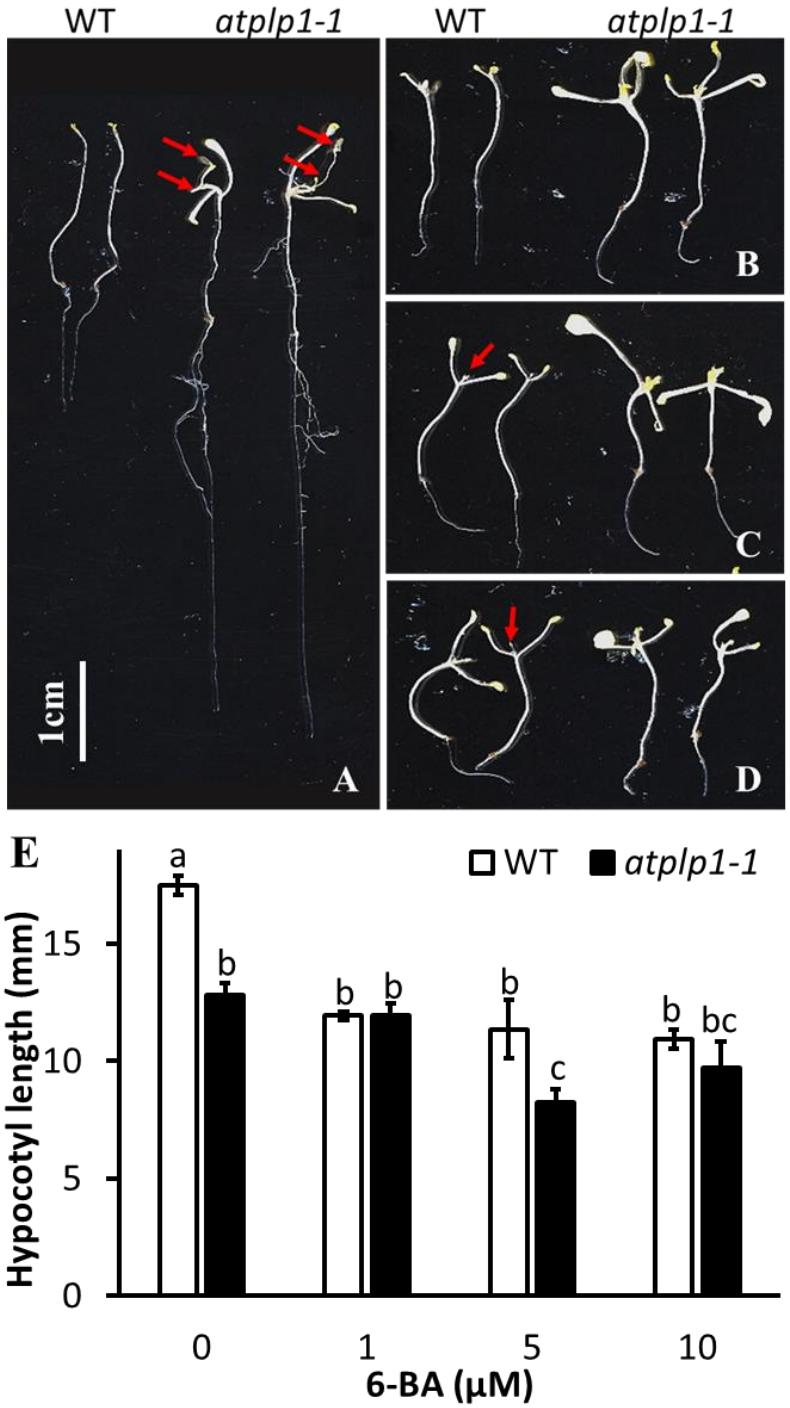

Figure 6-1. AtPLP1 loss-of-function results in de-etiolation phenotype in the dark and cytokinin can induce de-etiolation in WT seedlings in the dark.

A. Seedlings grown without 6-BA.

B–D. Seedlings grown in media containing 1 (B), 5 (C) and 10 (D) μM 6-BA. Dark grown seedlings of WT and *atplp1-1* for 11 days were scanned.

E. The length of hypocotyl from 7 WT and *atplp1-1* seedlings showed in A-D were measured. Different letters show statistically different analyzed by one-way ANOVA and Tukey's HSD test, $p<0.05$.

These 6-BA treated seedlings were also much bigger than un-treated ones. For *atplp1-1*, 6-BA can also inhibit hypocotyl elongation, however, to a less extent because the mutant hypocotyl length was only 6.6%, 35.6% and 24.3% reduction when 1, 5 and 10 μM present, respectively (Fig. 6-1B). This implies that *atplp1-1* is not as sensitive to 6-BA as WT in its effect in de-etiolation in the dark. Therefore, CKs can largely induce de-etiolation phenotype in WT, which is similar to what was found in dark-grown *atplp1-1* seedlings. These combined results strongly suggest that the de-etiolation phenotype observed in dark grown seedlings of *atplp1-1* could be caused by over production of CKs.

To validate the above findings we next observed much younger seedlings of WT and *atplp1-1* when they were only 4-day old. As shown in Fig. 6-2A and B while the mutant *atplp1-1* seedlings has already showed de-etiolated phenotype with short hypocotyl and opened cotyledons, the WT cotyledons were still closed and the hypocotyl was 1.2-fold longer than the *atplp1-1*. On the media with 1μM 6-BA, the length of WT hypocotyl was reduced to 51.0% of those grown on media without 6-BA, i.e., nearly 50% reduction in hypocotyl length caused by 6-BA. Similarly, the hypocotyl elongation was also inhibited by 6-BA in *atplp1-1* mutant seedlings as its length was 75.4% of the control grown on 6-BA free media, i.e. a 24.6% reduction when 1μM 6-BA was present. Interestingly, the WT cotyledons remained closed while the mutant cotyledons were open. Similar results were found from the seedlings grown on the media with 10 μM 6-BA, the WT and mutant hypocotyl became 40.2% and 57.4% in length of the ones grown on the control media respectively (Fig. 6-2B). Again, the cotyledons of WT seedlings were still closed while those of the mutant were fully opened (Fig. 6-2A). This result demonstrated that in the early seedling stage exogenous CK can induce de-etiolation of WT and partially mimick the mutant phenotype by inhibiting hypocotyl elongation. This further confirms the notion that AtPLP1 is involved in CK biosynthesis or perception.

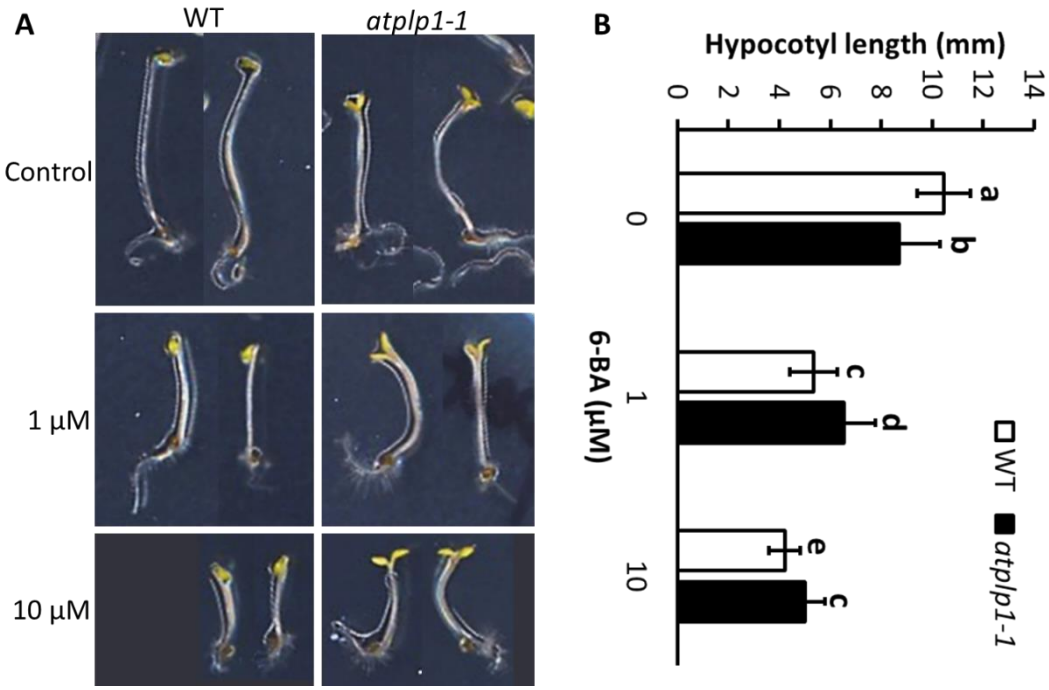

Figure 6-2. Cytokinin can induce shorter hypocotyl in the dark in the early growth stage of WT seedlings.

A. Seedlings grown in the media without 6-BA (Control) and with 1 and 10 μM 6-BA. WT and *atplp1-1* seedlings were grown in the dark for 4 days.

B. Hypocotyl length of WT and *atplp1-1* showed in A. About 30 seedlings were measured. Different letters above the columns indicate statistically different values analyzed by one-way ANOVA and Tukey's HSD test.

6.2.3 *atplp1-1* seedlings produces more CKs than WT

To further confirm our hypothesis that *atplp1-1* has defects in CK biosynthesis or signaling pathways, we next quantified the different types of CKs in 11-day-old dark grown seedlings of both WT and *atplp1-1* mutant. As shown in Fig. 6-3, the total amount of CKs in *ataplp1-1* was about 100 pmol/g of fresh tissues and this was twice more than the CKs in WT (50 pmol/g of fresh tissues). The level of tZ, one of the major forms of CKs in Arabidopsis, was found 2.2-fold higher in the *atplp1-1* mutant than that in WT. The mutant seedlings also contained much more DHZ (4-fold) than WT. However, iP, the second major CK in Arabidopsis and cZ did not show any difference between WT and the mutant. Therefore, the different levels of tZ in WT and the mutant contribute to the

significant differences in total CKs between them. In another word, *atplp1-1* has defects in tZ biosynthesis or signaling pathways, which resulted in the observed partial de-etiolation phenotype in the dark-grown seedlings of *atplp1-1*.

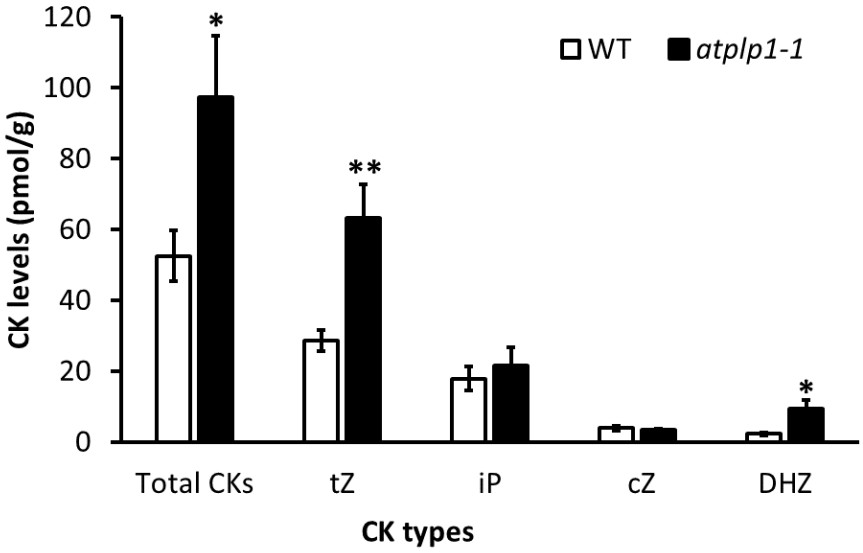

Figure 6-3. Levels of different types of CKs in WT and *atplp1-1*.
11-day- old dark grown seedlings were used to measure the content of different types of CKs in both WT and *atplp1-1*. Three samples were used for each measurement. *0.01<p<0.05 and **p<0.01 in Student's *t*-test.

6.2.4 Cytokinin receptors AHK3 and CRE1 are down-regulated in *atplp1-1*

Because there were more CKs in *atplp1-1* mutant than WT (Fig. 6-3) we wonder if the mutant also has enhanced CK perception. Since transcript levels of CK receptors can be induced by exogenous cytokinins (Ueguchi et al., 2001; Rashotte et al., 2003; Nishimura et al., 2004), we monitored the expression levels of the two CK receptors, AHK3 and CRE1. However, to our surprise we found that the transcript levels of both *AHK3* and *CRE1* in 9-day-old dark grown seedlings were much lower in *atplp1-1* than that in the WT, which were only 7.3% and 2.1% of their expressions levels compared to WT (Fig. 6-4). Therefore, it is very unlikely that the de-etiolation phenotype in these dark-grown *atplp1-1* seedlings were caused by the over-expression of these two receptors. This implies de-etiolation caused by over-produced CKs in *atplp1-1* is regulated by other CK

receptors.

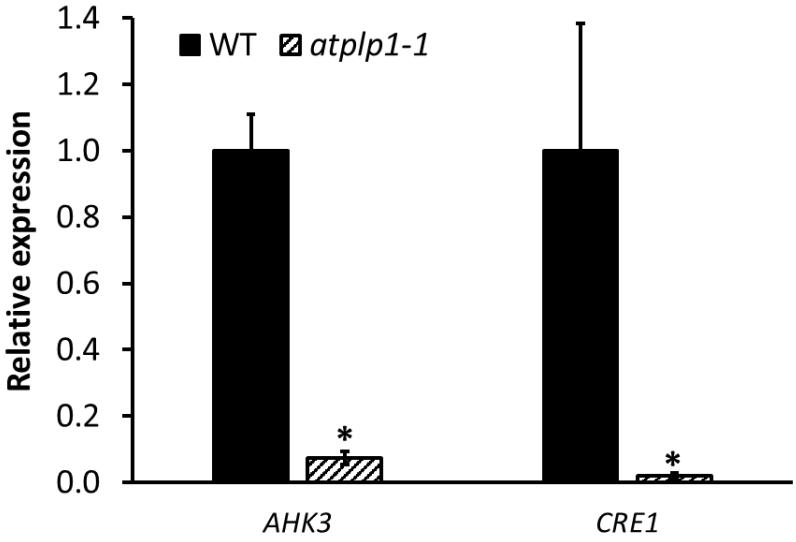

Figure 6-4. Transcript levels of *AHK3* and *CRE1*.
9-day-old dark grown WT and *atplp1-1* seedlings were collected for RNA extraction and reverse transcription followed by real-time PCR. Expression level of the gene in the WT seedlings was regarded as 1 and their relative expression levels in *atplp1-1* were calculated. The experiments were repeated three times. Each bar represents the mean ± SE (n = 3). *p<0.01 in Student's *t*-test.

6.2.5 Exogenous GA can partially rescue the de-etiolation phenotype of *atplp1-1*

GAs can repress photomorphogenesis and plants deficient in GA synthesis or signaling show a partially de-etiolated phenotype in the dark (Alabadí et al., 2004; Vriezen et al., 2004; Alabadí et al., 2008). GA insensitive mutant *gai* which has defect in GA signaling pathway, showed partially de-etiolated phenotype in the dark, exhibited as short hypocotyl and partial opening of its apical hooks (Cowling and Harberd, 1999). To see if *atplp1-1* mutant has defect in GA signaling we treated *atplp1-1* seedlings with different concentrations of GA_3 (an active synthetic GA) in the dark, with WT and *gai* as positive and negative controls. The results show that on the media without GA, WT hypocotyl was 11.7 mm long on average, while that of *gai* and *atplp1-1* were only 7.2 mm and 4.3 mm, respectively. When 1μM GA_3 was added to the media, the hypocotyl length of WT was similar to untreated ones. However, the lengths of *gai* and *atplp1-1*

were increased to 8.1 mm and 5.2 mm, respectively. This result demonstrated that GA can increase the hypocotyl lengths of *gai* and *atplp1-1*, indicating the de-etiolation phenotype of both mutants was partially rescued by 1μM GA_3. However, when we treated seedlings with 10 μM GA3 we found that compared to the seedlings grown on the media without GA_3, the WT hypocotyl length decreased from 11.7 mm to 10.6 mm, but those of *gai* and *atplp1-1* remained the same as their untreated counterparts (Fig. 6-5). Therefore, higher concentration of GA_3, such as 10μM, inhibits WT hypocotyl growth and could not rescue the de-etiolation phenotype of *gai* or *atplp1-1*. These combined results suggest that the de-etiolation phenotype of *atplp1-1* in the dark could be due to defect in GA biosynthesis and/or GA signaling.

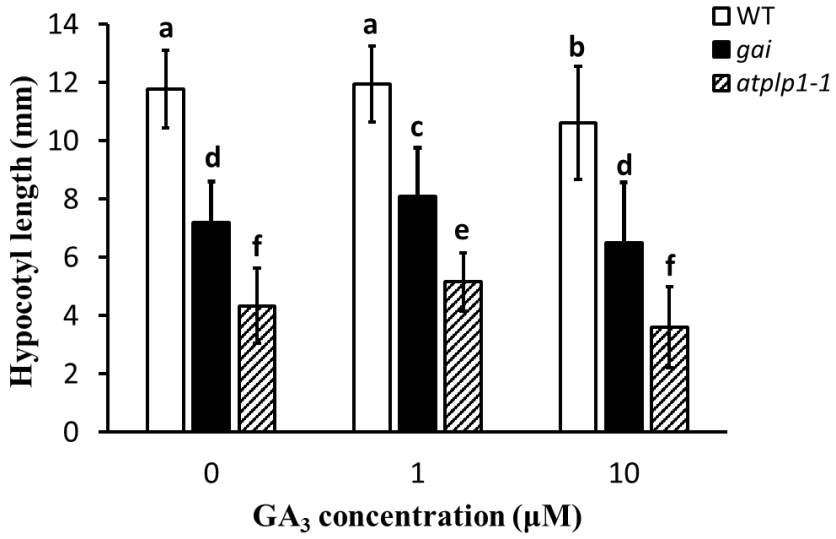

Figure 6-5. GA_3 can partially rescue the de-etiolation phenotype of *atplp1-1* in the dark. 4-day old WT, *gai-1* and *atplp1-1* seedlings were grown in the dark on ½ MS+1% sucrose with 0, 1 and 10 μM GA_3. At least 30 seedlings were measured for each sample. Different letters above the columns indicate statistically different values analyzed by one-way ANOVA and Tukey's HSD test.

6.2.6 Key genes involved in GA metabolic pathway were down-regulated in *atplp1-1*

Next, we monitored the transcript levels of some key genes for GA biosynthesis and signaling pathway. Gibberellin 2-oxidase (GA2ox) catalyzes the conversion of the

bioactive GAs to inactive forms to maintain the homeostasis of the internal levels of GAs in plants (Otani et al., 2013). Gibberellin 20-oxidase (GA20ox) and gibberellin 3-oxidase (GA3ox) catalyze the last steps in biosynthesis of bioactive GAs (Hu et al., 2008). We monitored the transcript levels of GA2ox1, GA20ox1 and GA3ox1 by real-time quantitative PCR (RT-qPCR) using first strand cDNA prepared from total RNA isolated from 9-day-old dark grown seedlings. As shown in Fig. 6-6, all these three genes had significantly less amount of transcripts in *atplp1-1* than in WT, especially GA2ox1 and GA20ox1, WT has 12.8- and 21.7-fold higher than the mutant. Although more GA3ox1 transcripts were found but it was still 1.5-fold higher in WT than in the mutant. Therefore, this result demonstrated that the GA metabolic pathway is defective in *atplp1-1* mutant and AtPLP1 plays positive roles in GA-regulated etiolation.

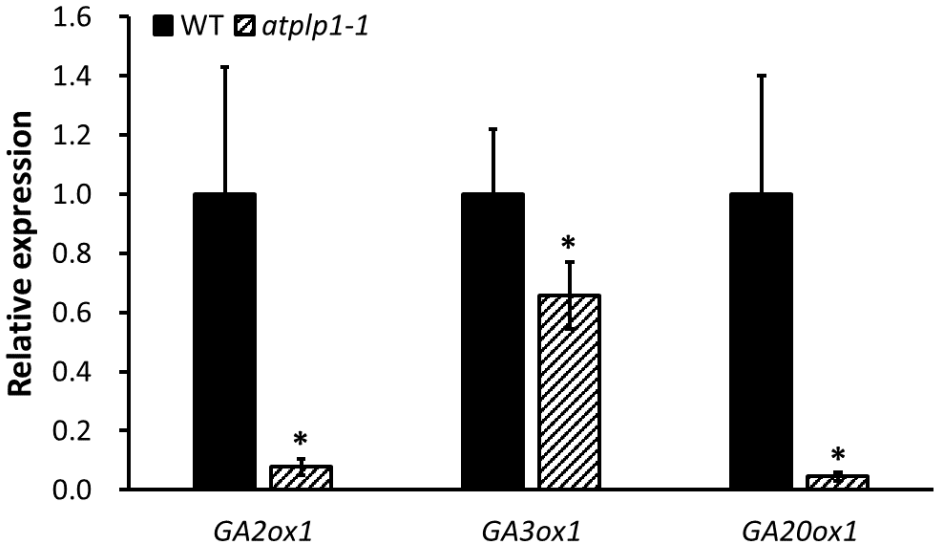

Figure 6-6. Transcript levels of GA biosynthetic genes are down-regulated in dark-grown *atplp1-1* seedlings. 9-day-old dark grown WT and *atplp1-1* seedlings were collected for total RNA extraction and reverse transcription followed by real-time PCR. Expression level of each gene in the WT seedlings was regarded as 1 and their relative expression levels in *atplp1-1* were calculated. The experiments were repeated three times. Each bar represents the mean ± SE (n = 3). *p<0.01 in Student's *t*-test.

6.2.7 Sucrose inhibits the growth of *atplp1-1* during the very early post-germination growth

Although the lipid reserves in the seed is usually enough to support seed germination and cotyledon expansion during early seedling growth in Arabidopsis, sugar, such as sucrose in low concentration (typically 1%) is routinely added to the rich growth media when grown on agar plate. In most cases the addition of 1% sucrose can help the establishment of seedlings and no observable negative effect have been reported in WT Arabidopsis. Consistent with this the WT seedlings grew slightly better on the medium with than without 1% sucrose in the light (Fig. 6-7A and B), or grew equally well with or without 1% sucrose in the dark (Fig. 6-7C and D) during the first 5 days. However, 1% sucrose severely inhibited the root growth of *atplp1-1* seedlings and the length of the primary root was reduced from 5.5 mm when they grew on sugar free media to 4.4 mm on media supplemented with 1% sucrose (Fig. 6-7A and B). In addition, the *atplp1-1* cotyledons were brown while those of the WT were green (Fig. 6-7A). Similar inhibitory effect of 1% sucrose was found when *atplp1-1* seedlings was grown in the dark. After 5 days grown in the dark, while the WT hypocotyls of seedlings grown on both ½ MS and ½ MS+1% sucrose were comparable the hypocotyls of *atplp1-1* seedlings grown on 1% sucrose containing media were only 41.4% of those from sucrose-free media (Fig. 6-7C and D). These results clearly demonstrated that early seedling growth of *atplp1-1* is strongly inhibited by sucrose.

6.2.8 Sucrose can reduce the sensitivity of *atplp1-1* to ABA during early seedling growth

As a stress hormone ABA can inhibit seed germination and early seedling growth in Arabidopsis. Indeed, ABA had a profound negative effect on both germination and early seedling growth and this is particularly true in *atplp1-1* mutant. As shown in Fig. 6-8A on the media without ABA all the seeds of WT and *atplp1-1* were germinated and developed into seedlings with fully opened green cotyledons and primary roots after they were grown for 4 days. However, when *atplp1-1* seeds were germinated on 1μM ABA

containing media none of them germinated while 100% of the WT seeds did (Fig. 6-8C). Interestingly, if 1% sucrose was added to the media, both WT and *atplp1-1* seedlings developed faster than those on the media without sucrose. On the 4th day, the WT seedlings were much bigger with larger developed cotyledons on sucrose containing media compared to those on the media without sucrose. Perhaps most noticeably was the effect of sucrose on the mutant *atplp1-1* where germination rate was increased from 0% on the medium without sucrose to 96.3% with 1% sucrose (Fig. 6-8C). Therefore, the inhibition effect of ABA on germination and early seedling growth was rescued by the addition of 1% sucrose, and this is particularly true with *atplp1-1* mutant.

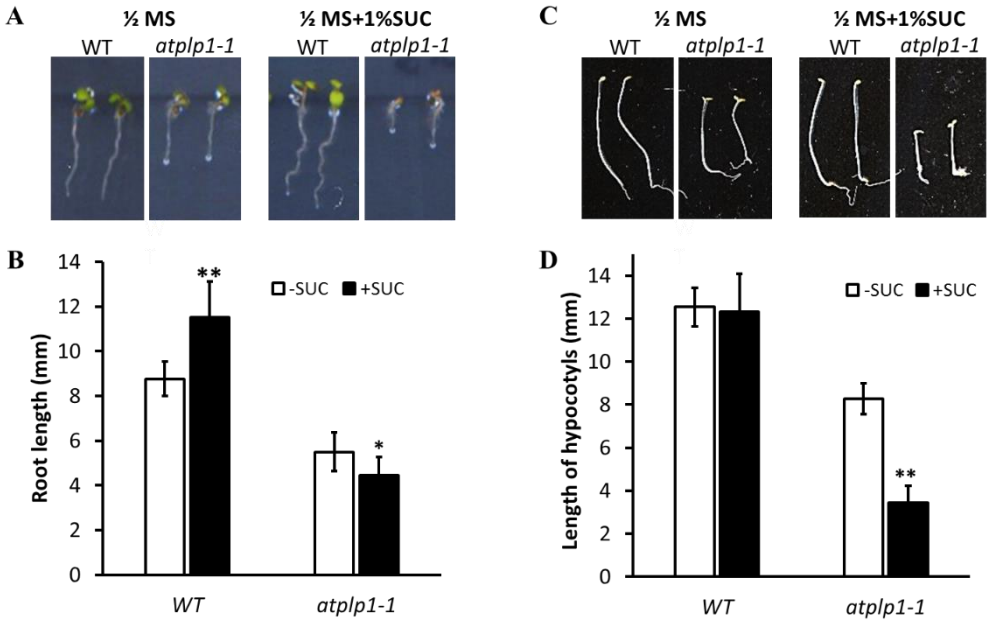

Figure 6-7. Sucrose restrains *atplp1-1* growth in the very early post-germinative stage.
A. 4-day-old WT and *atplp1-1* seedlings grown in LD (light) on media without (1/2 MS), or with 1% sucrose (1/2 MS+1% SUC).
B. Root length of 4-day old light grown seedlings. At least 20 seedlings were measured for each sample.
C. 5-day-old dark grown seedlings.
D. Hypocotyl length of 5-day old dark grown seedlings. 50 seedlings were measured for each sample. * $0.01<p<0.05$ and ** $p<0.01$ in Student's *t*-test.

Next, we tested to see if sucrose also has similar effect in the dark on germination and post-germination growth. As shown in Fig. 6-9A and B on the control media alone plates (minus ABA, minus sucrose), both WT and *atplp1-1* germinated and developed hypocotyls at 4-days. The hypocotyl length of *atplp1-1* seedlings was much shorter at 9.8

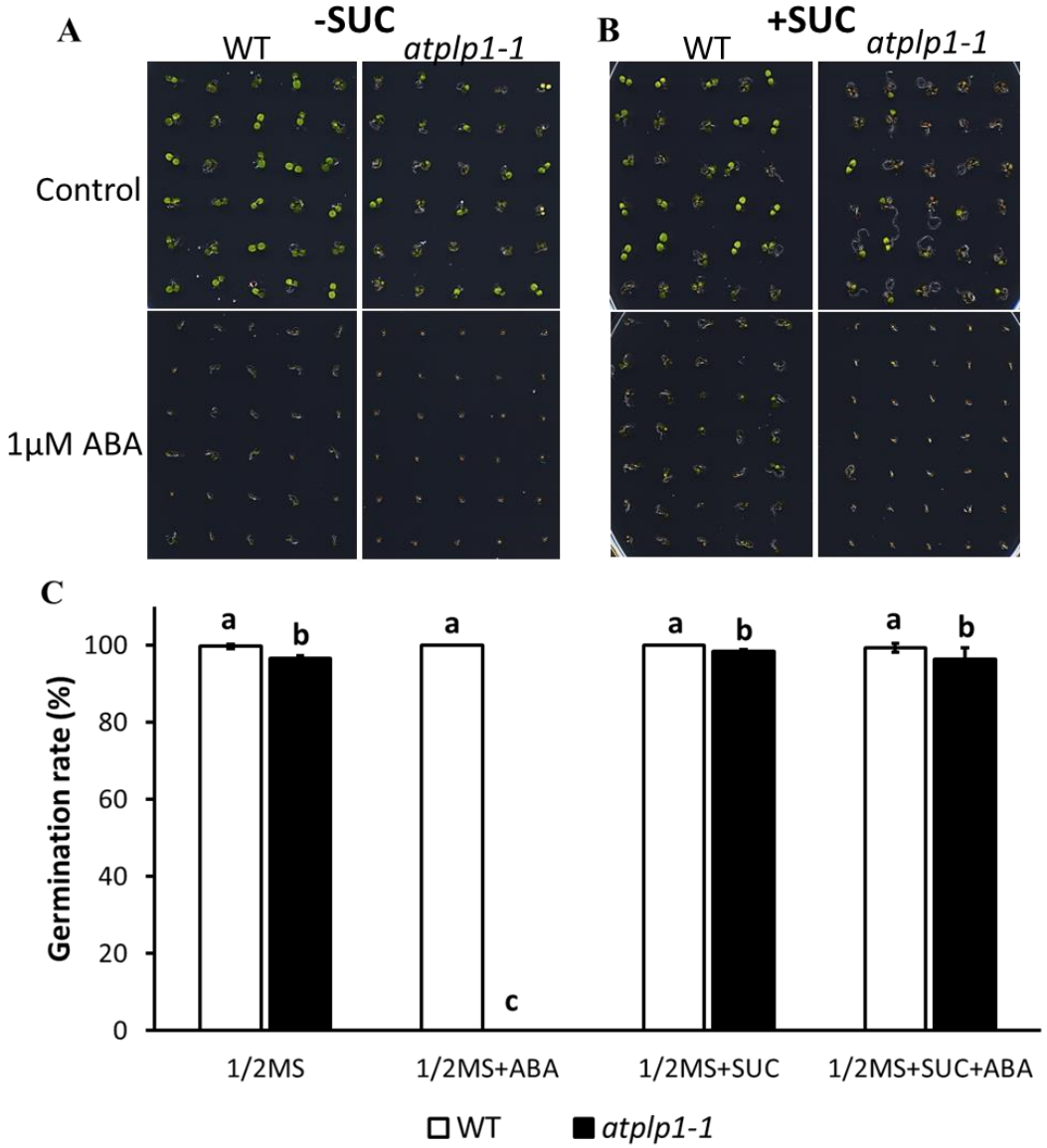

Figure 6-8. *atplp1-1* is more sensitive to ABA during germination in the light and sucrose can remit the sensitivities of both WT and *atplp1-1*.

A and B. 4-day old seedlings (seeds) were germinated and grown under LD (16h light/8h dark) on agar plates with 1μM ABA containing 1/2MS media without (A) or with (B) 1% sucrose. The seedlings grown on the media without ABA were used as controls.

C. Germination rate of 4-day WT and *atplp1-1* grown under different growth conditions described in A and B. At least 100 seeds were counted for each calculation, and 3 repeats were done for each line. Different letters above the columns indicate statistically different values analyzed by one-way ANOVA and Tukey's HSD test.

mm than that of the WT (12.5 mm). When 1 μM ABA was added to the media, all the WT seeds had germinated on the 4th day where most of them developed hypocotyls (6.1mm

on average) although it was only half of the untreated ones (Fig. 6-9A and B). However, none of the *atplp1-1* seeds germinated under the same conditions, therefore, no growth of hypocotyl was observed (Fig. 6-9A). To see if sucrose could cancel out the inhibitory effect of ABA as observed the light grown seedlings (Fig. 6-8) we added 1% sucrose to the 1μM ABA containing ½ MS media. To our surprise although all the WT seeds were germinated on the 4th day the average radicle length was only around 1.8 mm, which was significantly shorter than the ones grown on the media with 1 μM ABA alone (Fig. 6-9A and B). Therefore, it seems that in the dark sucrose acts as an inhibitor, rather than a stimulator in the light, to inhibit the elongation of hypocotyls of WT seedlings. Even more interestingly that for *atplp1-1*, the seed germination rate was increased to 50% and the radicle was clearly visible when 1% sucrose was added to the ABA containing media (Fig. 6-9A).

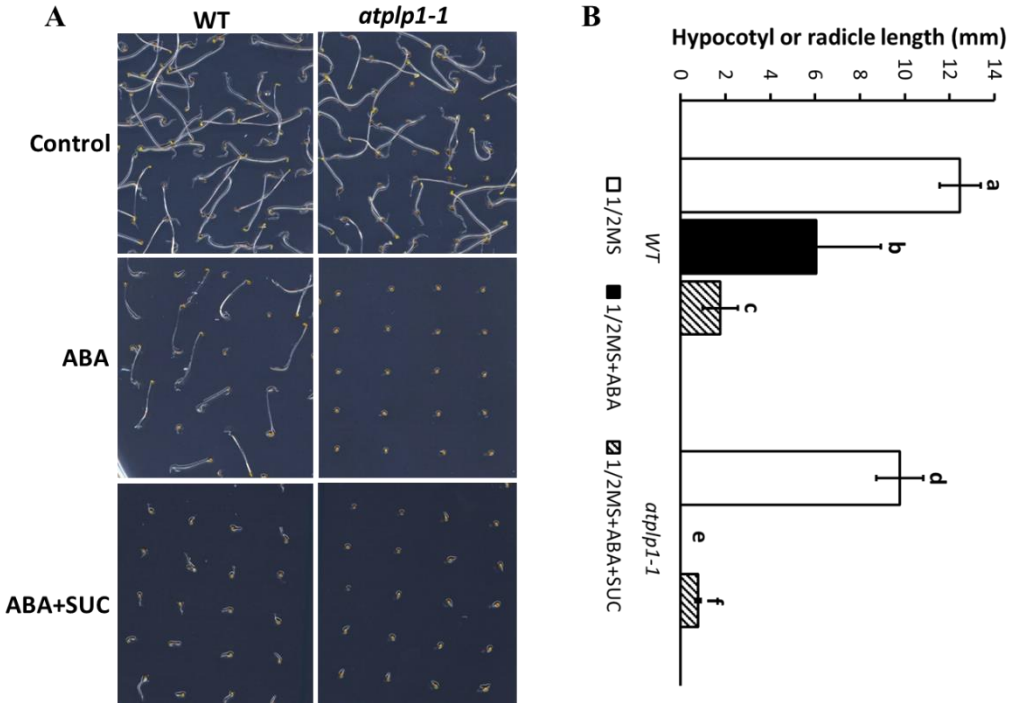

Figure 6-9. Effect of sucrose on ABA sensitivity during germination and post-germination growth in the dark.

A. Germination and post-germination growth after 4 days in the dark on 1 μM ABA containing ½ MS media without or with the addition of 1% sucrose.

B. Hypocotyl or radicle length of 5-day-old WT and *atplp1-1* seedlings grown on different media shown in A. 20 seedlings were measured for each sample. Different letters above the columns indicate statistically different values analyzed by one-way ANOVA and Tukey's HSD test.

Therefore, the combined data demonstrated that ABA has much stronger inhibitory effect on both seed germination and post-germination growth on the mutant *atplp1-1* than to WT in both light and dark. However, while sugar (1% sucrose) can repress the germination inhibition of ABA to both light grown WT and *atplp1-1*, in the dark it can relieve the sensitivity of *atplp1-1* to ABA to some extent, but exacerbate this sensitivity for WT, i.e., ABA and sugar have additive inhibitory effect to germination and post-germination growth in WT, but sugar can cancel out this effect in *atplp1-1*. Therefore, AtPLP1 loss-of-function results in defects in ABA and sugar signaling during seed germination and post-germination growth.

6.2.9 AtPLP1 is involved in the maintenance of shoot apical meristem (SAM)

Under long day condition the *atplp1-1* exhibited different phenotype from WT. The 7-day-old plate-grown mutant seedlings had diamond-shaped and curled cotyledons while the WT cotyledons were round and flat (Fig. 6-10A and D). In the soil-grown plants the shoot tip of *atplp1-1* struggled to develop into new leaves. We therefore observed the SAM of 3-week-old WT and *atplp1-1* soil-grown plants by scanning electronic microscopy (SEM). It was found that the central zone (CZ) of WT SAM was exposed with symmetrical leaf primordial around it (Fig. 6-10B), however the CZ of *atplp1-1* SAM was covered by the peripheral leaf primordial which was much smaller than that of the WT. The primordia of *atplp1-1* mutant was asymmetrically arranged (Fig. 6-10E). These abnormal SAMs may cause the rough and twisted rosette leaves and closed shoot tips observed in *atplp1-1* (Fig. 6-10C and F).

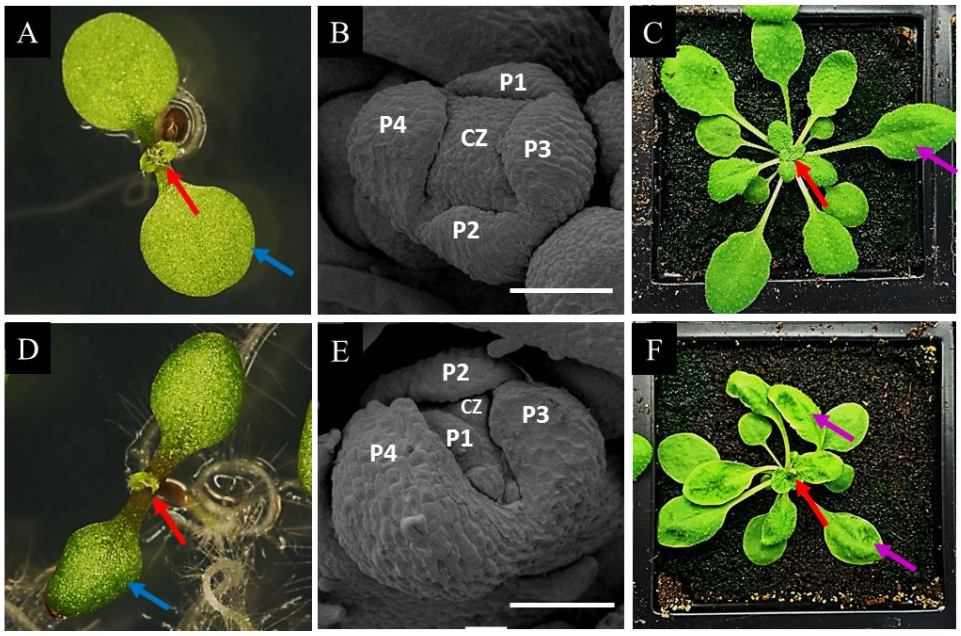

Figure 6-10. *atplp1-1* has abnormal shoot apical meristem (SAM). A-C, WT; D-F, *atplp1-1*.
A and D. 7-day old seedlings (red arrows indicate SAMs and blue arrows cotyledons).
B and E. Scanning electronic microscopy (SEM) of SAM from 3-week-old soil-grown WT (B) and *atplp1-1* (E) plants. CZ, central zone, P1, P2, P3 and P4 indicate leaf primordial. Bars, 50μm.
C and F. 4-week-old soil-grown WT and *atplp1-1* plants. Red arrows indicate SAMs and purple arrows trues leaves.

6.2.10 *atplp1-1* has longer root hairs and more lateral roots

Cytokinin plays important roles in root development and studies show that mutants that are defective in cytokinin signaling and synthesis also showed abnormal root phenotypes (King et al., 1995; Chin-Atkins et al., 1996; Laxmi et al., 2006). Based on it has more CKs in the dark grown mutant seedlings, it is possible that the light-grown mutant seedlings also have defects in its CKs biosynthesis or signaling pathways. Consistent with this hypothesis, we found that root hairs of 5-day-old *atplp1-1* mutant seedlings grew longer than those of WT (Fig. 6-11A). Root hairs around 6mm to root apical were measured the length, WT root hairs were only 0.098mm compared to 0.460mm for *atplp1-1* (Fig. 6-11B). The mutant also obviously had developed more root hairs than the WT from the 5-day old seeddlings (Fig. 6-11A). The average number of lateral roots of 8-day-old *atplp1-1* seedlings was 4.6 compared to only 1.6 in WT

seedlings (Fig. 6-11B and C). Therefore AtPLP1 regulates the growth and development of root hair and lateral roots, which is might dependent on cytokinin signaling pathways.

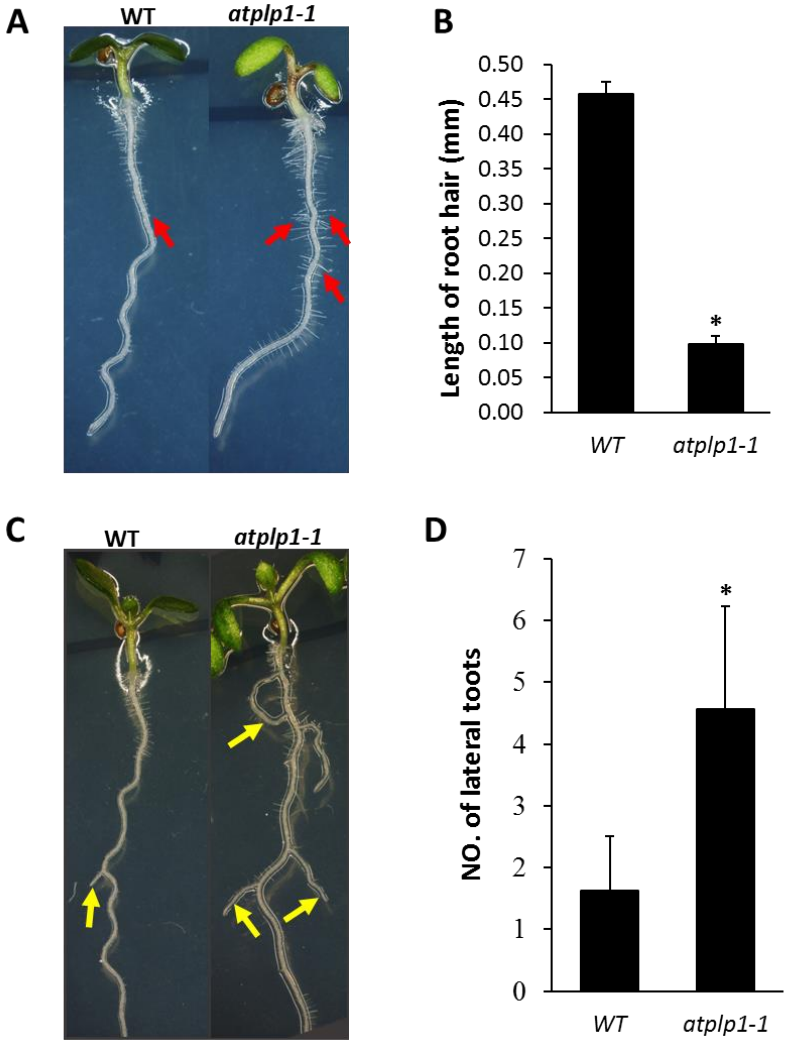

Figure 6-11. *atplp1-1* has more root hairs and lateral roots.

A. 5-day-old WT and *atplp1-1* seedlings. More and longer root hairs were found in the mutant than WT. Red arrows indicate root hairs.

B. Root hair length. Root hairs of WT and atplp1-1 from the area about 6mm to the root apical were measured. 6 root hairs from each seedling were measured and 5 seedlings were randomly picked from WT and *atplp1-1* for measurements. * $p<0.01$ indicates statically significant different in Student's *t*-test (n=30).

B and C. 8-day old seedlings of WT and *atplp1-1* mutant. Significantly more lateral roots (yellow arrows) were found in mutant plants than WT. * $p<0.05$ indicates statically significant different in Student's *t*-test (n=20).

6.2.11 AtPLP1 loss-of-function mutant were more resistant to salt

AHK3 and CRE1 are negative regulators for ABA and osmotic stress and both *ahk3* and *cre1* mutants were more sensitive to ABA treatment and tolerant to salt stress (Tran et al., 2007). Because the transcript levels of both *AHK3* and *CRE1* were down-regulated in *atplp1-1* mutant and *atplp1-1* was more sensitive to ABA than WT, we wonder if it is also more resistant to salt stress. For this we first grew *atplp1-1* seedlings on ½ MS+1% sucrose media for 7 days old WT before transferring them to the same media but containing 125mM NaCl. After another 7 days, we found that *atplp1-1* had much longer primary roots which was 42.5 mm long on average compared to 32.6 mm of WT roots (Fig. 6-12A and B). On the control plates containing ½ MS+1% sucrose media the root lengths of both WT and *atplp1-1* seedlings were comparable after 14 days (Fig. 6-12A). These results indicate that *atplp1-1* mutant is more resistant to salt stress than WT.

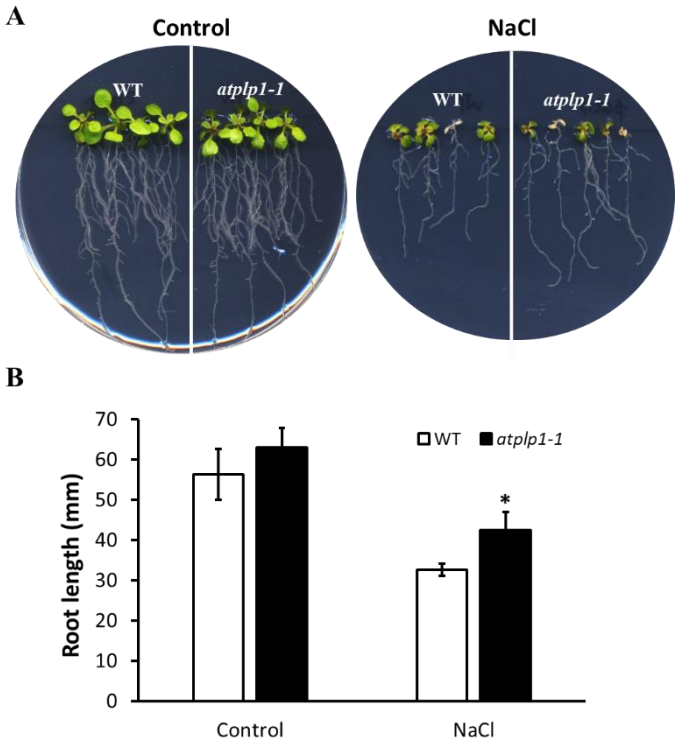

Figure 6-12. *atplp1-1* seedlings had longer primary roots under salt stress.
A. Left: control seedlings that were grown on 1/2MS + 1%SUC medium continuously for 2 weeks. Right: salt treated seedlings. 1-week-old WT and *atplp1-1* seedlings grown on 1/2MS + 1%SUC were transferred to 1/2MS + 1%SUC + 125mM NaCl medium for further 2 weeks. B. Root length of WT and *atplp1-1* grown in different conditions described in A. 10 seedlings were measured for each sample. *p<0.01 in Student's *t*-test.

6.3 Discussion

6.3.1 AtPLP1 is involved in Arabidopsis etiolation in the dark

In nature, etiolation happens as a normal process in angiosperm seedlings as the seeds are buried and germinated below the soil surface. By extending their hypocotyls the seedlings can push themselves out of the soil so that they can reach sunlight for photosynthesis (Lochmanova et al., 2008). The apical hook with closed cotyledons can protect them from damage under ground. Therefore, etiolation is an important first step towards to self-sufficiency by photosynthesis during the life cycle of a plant. Indeed, the WT Arabidopsis seedlings were etiolated with long hypocotyls, yellow closed cotyledons and short roots when grown in the dark (Fig. 6-1A). However, the seedlings of *atplp1-1* had much shorter hypocotyls, open cotyledons and developed true leaves as if they grew in the light although they remain yellow due to lack of chlorophyll (Fig. 6-1A). Therefore, *atplp1-1* shows obvious de-etiolation phenotype in the dark, indicating that AtPLP1 plays positive role in etiolation in the dark during early seedling growth for Arabidopsis.

6.3.2 AtPLP1 loss-of-function causes defects in phytohormone signaling in Arabidopsis

Previous studies have shown that etiolation is a result of inhibition of de-etiolation, or photomorphegenesis (Lochmanova et al., 2008; Kami et al., 2010). The direct trigger to induce photomorphogenesis is light (De Wit et al., 2016), such as the loss-of-function of *DET1*, which is one of the most important genes in light-induced photomorphogenesis signaling pathway, shows a de-etiolation phenotype in the dark (Chory et al., 1994). However, studies show that light is not the only trigger for de-etiolation and other factors such as phytohormones can also cause de-etiolation in the dark (Symons and Reid, 2003). It was reported that exogenously applied CKs can result in de-etiolated WT seedlings in the dark (Chory et al., 1994). This is supported by another study where it showed that the CK over-producing mutant *hoc* also showed de-etiolation phenotype in the dark (Catterou et al., 2002). Because *atplp1-1* seedlings are de-etiolated in the dark it is possible that the

CKs level is higher in these mutant seedlings than the WT. Therefore, we measured and compared the CK levels and found that the total CK content in the mutant is twice as high as in the WT seedlings, confirming our assumption that the de-etiolation phenotype observed in *atplp1-1* mutant seedlings in the dark is due to the over-production of CKs in these seedlings (Fig. 6-1 and 6-3). However, the transcript levels of two CK receptors, *AHK3* and *CRE1 (AHK4)* were down-regulated in the *atplp1-1* mutant (Fig. 6-4), suggesting that these over-produced CKs in the mutant seedlings were very unlikely perceived by these two receptors. Other CK receptor, such as AHK2, may be involved in this process. It was reported that combination of AHK3 and AHK2 regulate de-etiolation (Riefler et al., 2006). Therefore, we suggest that AtPLP1 positively regulate expression of *AHK3* and *AHK4*, but not *AHK2*, and the over-produced CKs mediate de-etiolation mainly relying on AHK2 in *atplp1-1*.

Etiolation is also regulated by GA signaling pathway where GAs play positive roles in keeping the plant etiolated in the dark (Alabadí et al., 2008). Consistent with this the GA insensitive mutant *gai1* seedlings exhibited partially de-etiolated phenotype with shorter hypocotyls when grown in the dark compared to the WT and application of GA_3 in the media can rescue this phenotype (Fig. 6-5). Similarly, GA_3 could also partially rescue the de-etiolation phenotype of *atplp1-1* in the dark-grown seedlings, however to a lesser extent as their hypocotyl lengths were still much shorter than the GA_3 treated WT and *gai1* seedlings (Fig. 6-5). Therefore, AtPLP1 plays positive roles in GA-regulated etiolation of seedlings in the dark.

Defects in GA-related pathways in *atplp1-1* was also evident during seed germination where no seeds were germinated when the *atplp1-1* seeds were treated with 1 μM of ABA while 100% germination was found in WT (Fig. 6-8 and 6-9). Indeed, studies show that GAs and ABA work antagonistically to regulate seed germination in plant, during which GAs promote germination while ABA acts as a germination repressor to inhibit germination (Finkelstein et al., 2008; Dave et al., 2016). Previous study has also shown that germination of GA-deficient mutant (*gib-1*) tomato seeds is more sensitive to

exogenous ABA (Ni and Bradford, 1993). The fact that germination of *atplp1-1* seeds was more sensitive to ABA than WT (Fig. 6-8 and 6-9), again suggests that *atplp1-1* may have defects in GA biosynthesis and or signaling pathways.

Loss-of-function of AtPLP1 also resulted in abnormal SAM development in light grown seedlings and mature plants (Fig. 6-10), more root hairs and lateral roots (Fig. 6-11) and more resistant to salt stress (Fig. 6-12). All of these phenotypes, again, could be due to defects of *atplp1-1* in phytohormone-related pathways. It is commonly accepted that the antagonistic interactions between CKs and auxin control the development of SAM (Shani et al., 2006). We found that *atplp1-1* mutant plants have smaller meristems and this might be because of the less active CK receptors AHK3 and CRE1, however their transcript levels in the light-grown seedlings need to be further confirmed. Smaller meristem of *atplp1-1* plant could lead to the asymmetrical primordia distribution observed (Fig. 6-10E). This is supported by a computer modelling of phyllotaxis where it is demonstrated that the size of central zone affects the phyllotactic patterns (Jönsson et al., 2006; Shani et al., 2006). More root hairs observed in *atplp1-1* could also be another indication of CK overproduction or signaling as CKs can stimulate root hairs formation (Fig. 6-11A) (Tien et al., 1979).

The response to salt stress in plants is regulated by many phytohormones signaling pathways, including ABA-, auxin-, CKs-, GA-, BRs-, jasmonates (JA)- and SA-related pathways (Javid et al., 2011). Salt stress increases the endogenous ABA levels in Brassica (He and Cramer, 1996), *Phaseolus volgaris* (Cabot et al., 2009), *Zea mays* (Cramer and Quarrie, 2002) and rice (Kang et al., 2002). CKs enhance the resistance to salt stress in plant by interacting with other phytohormones, such as ABA and auxin (Barciszewski et al., 2000; Iqbal et al., 2006). When plants were exposed to abiotic stress, GAs accumulated quickly (Lehmann et al., 1995) and exogenous GA_3 improved wheat and rice growth under saline conditions (Parasher and Varma, 1988; Prakash and Prathapasenan, 1990). Loss-of-function of AtPLP1 results in enhanced salt resistance (Fig. 6-12). This implies that AtPLP1 may play in one, or several of these phytohormone-

related pathways during salt stress. Further studies will provide insights to this.

6.3.3 Crosstalk between phytohormones and sugar

The successful establishment of *atplp1-1* seedlings are dependent on exogenous sucrose (Fig. 5-6B). However, during the early stage of growth in the first 4 days after germination *atplp1-1* was hypersensitive to sucrose, i.e., sucrose has inhibitory effect on seedling growth (Fig. 6-7). Sucrose not only acts as important carbon and energy sources, but also as signaling molecule that regulates various developmental processes (Ruan, 2014; Shin et al., 2015). This is achieved by complicated crosstalks between sugar and phytohormones (Lastdrager et al., 2014). For example, a CK resistant mutant *cnr1* that is de-etiolated in the dark, the germination of which is also more sensitive to sucrose and glucose (Laxmi et al., 2006). The loss-of-function mutant of the CK receptor AHK3 exhibits higher sugar sensitivity when grown on the media with higher sucrose concentration (275mM) (Franco-Zorrilla et al., 2005). The glucose receptor hexokinase 1 (HXK1) loss-of-function mutant *gin2* shows both decreased sugar sensitivity and increased CKs sensitivity in light, which demonstrated the antagonistic interaction between glucose and CK signaling (Moore et al., 2003). In the dark grown Arabidopsis seedlings, sugar promotes hypocotyl elongation and this is dependent on BRs (Zhang and He, 2015). Sugar also induces auxin transport and signal transduction in hypocotyls of the dark grown seedlings of Arabidopsis (Stokes et al., 2013). Sugar increases the concentrations of IAA precursors in various synthesis pathways, such as IAM (indole-3-acetamide), IAOX (indole-3-acetaldoxime) and IAN (indole-3-acetonitrile) pathways (Sairanen et al., 2012). In the case of GAs, sucrose negatively regulate GAs signaling by stabilizing DELLA protein, the repressor of GA biosynthesis (Li et al., 2014; Ljung et al., 2015). Sugar also plays important roles in ABA-related pathways where ABA insensitive 4 (ABI4) is a key linker and its expression is induced by higher concentration, such as 7%, of glucose (Arroyo et al., 2003). Therefore, the reason for *atplp1-1* mutant is hypersensitive to sucrose in the early seedling development stage could be due to: 1) lower enzyme activities of the two CK receptors AHK3 and CRE1 as their transcript

levels were down-regulated in the dark-grown seedlings of *atplp1-1* (Fig. 6-4), leading to lower CK signaling, hence more sensitivity of these seedlings to exogenous sugar; 2) sucrose induces the production of ABA or signaling and ABA has inhibitory effect on seedling growth of *atplp1-1*; 3) Sucrose decreases the already lower activity of GAs by stabilizing DELLAs in *atplp1-1* seedlings. Lower GAs result in enhanced sensitivity to sucrose in *atplp1-1* seedlings in the dark. However, this cannot explain why the sensitivity also exists in light-grown seedlings we observed (Fig. 6-7A). Therefore, AtPLP1 is the master regulator in the crosstalks between sugar and phytoharmones during early seedling growth and development.

6.3.4 Working model of the functionality of AtPLP1 in Arabidopsis

AtPLP1 loss-of-function mutant has growth and development defects throughout the life cycle of Arabidopsis, including photomorphogenesis (de-etiolation), sensitivity to ABA and sugar, root architecture and response to salt stress during seedling stage and shoot apical meristem maintenance. Therefore, AtPLP1 plays central roles in the regulation of these processes. To draw a clearer picture of how AtPLP1 functions in Arabidopsis we propose the following working model which is illustrated in Fig. 6-13. Under light, de-etiolation happens because light inhibits COP1 activity through receptors such as PhyB and the transcription factors such as HY5 and HYH positively regulate de-etiolation (the yellow area). In the absence of light, COP1, an E3 ubiquitin ligase, induces the degradation of HY5 and HYH and stabilizes transcription factors PIFs which promote the etiolation process (Alabadí et al., 2008). In the meanwhile, GA_4 can promote etiolation through negatively regulating DELLA proteins where that negatively regulate PIFs transcription factors (Kamiya and García-Martínez, 1999). Because the transcript levels of GA_4 biosynthesis genes, such as *GA20ox* and *GA3ox*, were down-regulated in the dark-grown seedlings of the knock-out mutant plants of AtPLP1 (Fig. 6-6). We suggest that AtPLP1 promotes etiolation in the dark by positively regulating the biosynthesis of GA_4 (the active form of GAs in Arabidopsis). And we also found the total content of CKs was increased in *atplp1-1* mutant with down-regulated *AHK3* and *AHK4* transcript levels

(Figs. 5-3 and 5-4). It is possible that AtPLP1 also positively regulates CK receptors AHK3/4, and to compensate the lower activities of AHK3/4 the mutant plant has to produce more CKs to balance the downstream signaling pathways (Riefler at al., 2006). These over-produced CKs were transduced by other receptor, such as AHK2. Through its interaction to ARR4 and PhyB de-etiolation of *atplp1-1* seedlings in the dark is maintained (Sweere et al., 2001). CKs can also mediate the growth of SAM and root architecture (Tien et al., 1979; Shani et al., 2006). The diagram also shows the antagonistic relationship between ABA and GAs in seed germination via ABI4. Crosstalk between sugar and phytohormones is shown as sugar positively regulating ABI4 and DELLAs. Crosstalk between GA and CK signaling might also exist in this study. The key enzyme in the glyoxylate cycle, ICL, was induced by GAs (Eastmond and Jones, 2005) and this can explain the lower *ICL* expression level in *atplp1-1* (Fig. 4-11).

The fact that none of the single mutant as mentioned in these pathways shown in Fig. 6-13 shares the same phenotype with *atplp1-1* suggests that AtPLP1 is involved in multiple pathways through the modification of multiple substrate proteins to promote etiolation in the dark. Therefore, this study provides important clues to link protein S-acylation and photomorphogenesis in terms of light, phytohormones and sugar signaling pathways.

6.3.5 Summary and future perspectives

In this chapter, we demonstrate that AtPLP1 regulate etiolation in the dark through both GA and CK signaling pathways. Apart from etiolation, AtPLP1 is also involve in seed germination, SAM formation, root architecture and salt stress response. So far, we have proved that AtPLP1 loss-of-function caused disorders of phytohormones and sugar signaling pathways. However, more work need to be done to find out the exact molecular mechanism of AtPLP1 in these processes. These include:

1) To measure CK and GA levels, and monitor the transcription levels of the key genes in CK and GA signaling pathways in the light-grown *atplp1-1* seedlings. This will

help to find out the reasons that cause all the abnormal growth phynotypes of *atplp1-1*;

2) To explore the relationship between defects in β-oxidation and phytohormone signaling pathways in *atplp1-1*. As we found that there are defects in both β-oxidation and phytohormone signaling in *atplp1-1*, we need to find out whether one defect leads to another or they affact plant growth independently;

3) To isolate the S-acylated substrate proteins (or the direct interacted proteins) of AtPLP1 to elucidate the molecular mechanism that AtPLP1 functions.

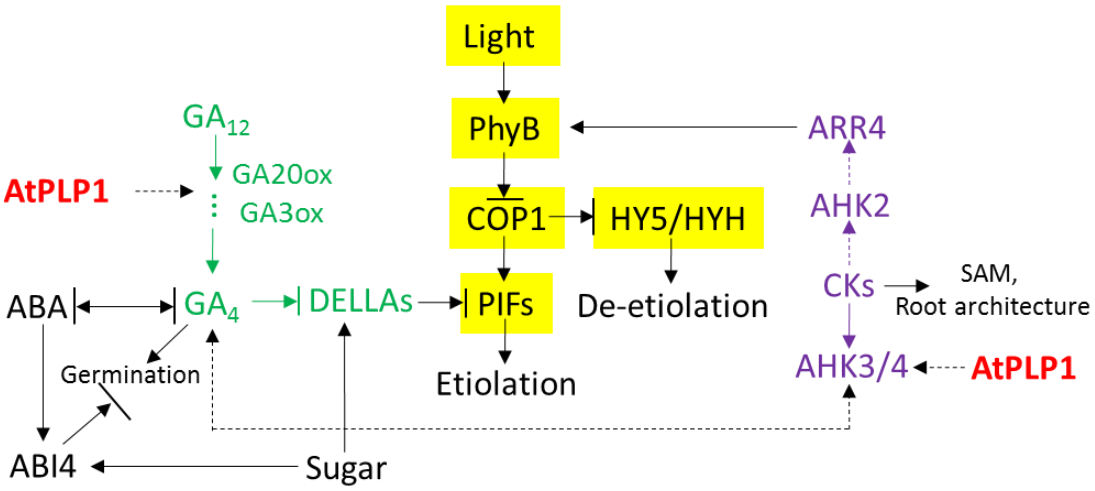

Figure 6-13. The proposed mode of action of AtPLP1 in Arabidopsis. De-etiolation of *atplp1-1* is regulated by multiple pathways. In the light (yellow area), PhyB is activated by light signal which can repress COP1 regulated photomorphogenesis. In the green area, it shows that AtPLP1 positively regulate GA_4 biosynthesis and GA_4 promotes etiolation through inhibition of its repressor DELLA proteins. DELLAs negatively regulates PIFs in the dark. In the purple area, it shows that AtPLP1 positively regulate AHK3/4 and its loss-of-function leads over-production of CKs. These CKs are recognized and transduced by AHK2 in the dark, which promotes de-etiolation through ARR4 which activates PhyB. PhyB can release the inhibition of COP1 to HY5/HYH by repressing COP1, resulting in etiolation in the dark. It is also indicated the interaction between GA4 and ABA to regulate seed germination and CKs regulate SAM formation and root architecture. Sugar is also involved in the signaling network by regulating ABI4 and DELLAs. Green area, GA biosynthesis and signaling pathway; Yellow area, light signaling pathway; Purple area, CKs signaling pathway. → Positive regulation; ⊣ Negative regulation; ⊣→⊣ Antagonisitic interaction. Solid lines mean confirmed regulations; Dotted lines mean hypothetical regulations through this study.

Chapter 7 General Discussion and Future Work

There are at least 24 DHHC-PAT proteins in Arabidopsis (Hemsley et al, 2005; Batistic, 2012). Previous studies demonstrated that they play important roles in growth, development, reproduction and stress throughout the plant life cycle (Hemsley et al., 2005; Qi et al., 2013; Zhou et al., 2013). For example, AtPAT24 (TIP1), the first plant PAT identified in 2005, is found to be involved in cell division and polar growth. Its loss-of-function results in smaller stature, short and branched root hairs and reduced seed production (Hemsley et al., 2005). Loss-of-function mutant plants of AtPAT10 are semi-dwarf with very poor seed set and sensitivity to salt stress (Qi et al., 2013; Zhou et al., 2013). To dissect the functions of PATs in Arabidopsis we screened the mutant collections and found knockout lines for 18 of the remaining 22 AtPATs. However, only 3 of them, AtPAT14, AtPLP1 and AtPAT21 showed growth defects while others did not show observable changes in their appearances. Disruption by T-DNA insertion in *AtPAT14* causes early leaf senescence phenotype due to over-production of salicylic acid (SA). Loss-of-function mutant plant of *AtPLP1* fails to grow without external sugar supplementation during early seedling stage because of its defect in seed storage lipid breakdown. In addition, *atplp1-1* seedlings are de-etiolated in the dark and the mature plant has a defective shoot apical meristem. AtPAT21, on the other hand, plays central role in male and female gametogenesis and seed production. These combined results clearly demonstrate that protein S-acyltransferases-mediated lipid modification of proteins plays essential and diverse roles during all stages of growth and development of Arabidopsis. It highlights the importance in understanding the mechanism of this lipid modification in plant in order to guide crop breeding programmes in the future.

7.1 S-acylation in seed germination and seedling establishment

Germination vigor of seed is dependent on the quality of the embryo developed in the mother plant, including messenger RNAs (mRNAs) which decide successful germination, proteostasis and DNA integrity which contribute to germination phenotype

(Rajjou et al., 2012). For example, I4G1 and I4G2 are two important plant-specific eukaryotic translation initiation factors that function in the embryo. As such, the *i4g1/i4g2* double mutant of Arabidopsis has reduced germination rates, slow growth rates and reduced seed viability (Lellis et al., 2010). Genome damage leads to a loss of seed vigor and viability (Cheah and Osborne, 1978), and proteostasis plays pivotal roles in cell metabolism and hormone signaling (Fait et al., 2006), which control the germination.

The most important phytohormones regulating seed germination are ABA and GA, and the ratio of which controls seed metabolic transition from dormancy to germination (Yamaguchi, 2008; Nambara et al., 2010). Other phytohormones include CKs, BRs, ethylene and IAA (Miransari and Smith, 2013). Environmental chemicals such as nitric oxide (NO) and reactive oxygen species (ROS) play positive roles in triggering seed germination (Bethke et al., 2016; Liu et al., 2010). It was reported that *atpat10* mutants can only produce very few abnormal looking seeds in very few siliques while majority of the siliques do not contain any seeds at all. In addition, these abnormal looking seeds germinate poorly as only about 20% of them can germinate and develop into seedlings due to defects in embryo development (Qi et al., 2013). Seeds of the knock-out mutant of AtPLP1 also showed defects in germination since they were much slower to germinate than WT although a similar germination rate between them was found after prolonged incubation at 72 hours (Fig. 5-7). The mutant *atplp1-1* seeds were bigger than WT, indicating defects in seed development although we could not find any difference in the phenotype of the embryos between WT and the mutant (Fig. 5-6). Both *atpat10* and *atplp1-1* are hypersensitive to ABA during seed germination (Qi et al, 2013; Figs. 6-8 and 6-9). This could result in the inhibition of translation initiation in their embryos which decide successful germination as shown in the *i4g1/i4g2* double mutant (Lellis et al., 2010). Loss-of-function mutant of *DA1*, an important ABA signaling gene, has increased seed size but deceased sensitivity to ABA (Li et al., 2008). Triple mutant of cytokinin receptors *ahk2/ahk3/ahk4* also has increased seed size but the seed germination speed is faster than WT (Riefler et al., 2005). Therefore, both AtPAT10 and AtPLP1 mediated protein palmitoylation are involved in seed germination most likely through the

regulation of ABA, perhaps also other phytohormones and pathways.

Different from seed germination where no energy is needed, seedling establishment is fueled by the breakdown of seed reserves such as starch, lipids and proteins (Graham, 2008). Lipid, mainly in the form of triacylglycerol (TAG) is the main seed storage reserve of many crops such as oilseed rape and others in the Brassicacea family, peanut and sunflower seeds. As a member of the Brassicacea Arabidopsis seed contains about 40% TAG per dry seed weight (Baker et al., 2006; Graham, 2008). TAG is synthesized in the ER through the *Kennedy pathway* and these TAG molecules coalesce to form the lipid (oil) droplets. During seed germination and early seedling growth TAG lipases are able to hydrolyze the insoluble TAGs to release the free fatty acids from its glycerol backbone. The fatty acids are then transported to the peroxisomes where the β-oxidation takes place (Li-Beisson et al., 2013), resulting in the production of acetyl-CoA. This is followed by either the TCA (tricarboxylic acid) cycle or glyoxylate cycle to produce succinate and malate. These four-carbon compounds will be further converted to the final product sucrose through gluconeogenesis that will be used to support seedling growth. Defects in a single one of these steps can result in blockage of sucrose synthesis then cause abnormal seedling establishment (Graham, 2008).

Some key enzymes that are involved in fatty acid breakdown were predicted to be S-acylated proteins. They are the long-chain acyl-CoA synthetases (LACS6 and LACS9) that are involved in the conversion of free fatty acids to active fatty acyl-CoAs; acyl-CoA oxidases (ACX3) which is the first step of β-oxidation to add a trans double bond between α and β carbons; and phosphoenolpyruvate carboxykinase1 (PCK1) that catalyzes the first step of gluconeogenesis (Hemsley et al., 2013). Our studies on AtPLP1 loss-of-function mutant showed that the mutant relies on sugar for seedling growth due to the disruption in β-oxidation of seed lipid breakdown process (Fig. 6-11). Interestingly, disruption of the functions of acyl-CoA oxidases (ACXs) also cause similar sugar dependency during the seedling stage (Pinfield-Wells et al., 2005). Therefore, AtPLP1 could be the S-acyltransferase for one, or more of these proteins. Disruption by T-DNA insertion in

AtPLP1 renders it to be dysfunctional, subsequently causing the mis-targeting of these substrate proteins, hence the phenotype observed in the k/o mutant. In addition, it was reported that GA induces TAG breakdown and enhance the conversion of this storage reserve to sugar (Eastmond and Jones, 2005). The mutant *atplp1-1* seedlings contain much less transcripts of GA synthesis genes (Fig. 6-6). This can result in less GA produced, therefore, it is also possible that defects in GA biosynthesis or signaling pathway cause abnormal lipid breakdown in *atplp1-1*.

The typical phenotype of Arabidopsis seedling grown in the dark is its long hypocotyl, short root and yellow closed apical hook of cotyledons, and this is the so-called etiolation, or skotomorphogenesis. The long hypocotyl is a mechanism that increases the probability of the seedling reaching the light, and the formation of the apical hook protects the fragile shoot apical meristem when it breaks through the soil during germination (Josse and Halliday, 2008). It is noted that the seedlings of many sugar dependent mutants are etiolated in the dark when sugar is supplemented (Theodoulou and Eastmond, 2012). However, *atplp1-1* seedlings were de-etiolated in the dark when exogenous sugar was added to the media (Fig. 6-1A), indicating that AtPLP1 plays positive roles in promoting etiolation in the dark. To understand the mechanism of how AtPLP1 is involved in etiolation we measured the levels of CKs and monitored the transcript levels of genes for CK and GA signaling and biosynthesis in dark grown seedlings of both WT and *atplp1-1* mutant. Interestingly, we found that the mutant contains twice as much total CKs as the WT (Fig. 6-3). This over-produced CKs were very unlikely transduced by AHK3 and 4 (CRE1) as their transcript levels were down-regulated in the mutant (Fig. 6-4). On the other hand, the GA levels were likely to be lower in the mutant than in the WT because the transcript levels of *GA2ox1, GA3ox1* and *GA20ox1* were greatly down-regulated in the mutant (Fig. 6-6). Interestingly, gibberellin 3-oxidase 3 (GA3ox3) was predicted to be S-acylated (Hemsley et al., 2013). As to whether AtPLP1 is the PAT for GA3ox3 is yet to be determined.

Many mutants defective in phytohormone biosynthesis and/or signaling have been

identified to have de-etiolation phenotype in the dark. For example, the seedlings of *amp1* (altered meristem program 1) which has higher CKs levels (Chin-Atkins et al., 1995), *gai1* (GA insensitive) which has lower GA level (Alabadi et al., 2008), and *det2* (de-etiolation 2) which affects BRs biosynthesis (Li et al., 1999; Symons et al., 2002) exhibit de-etiolation phenotype when grown in the dark. Therefore, it is likely that AtPLP1-mediated protein S-acylation plays important roles in etiolation in the dark by the regulation of the biosynthesis and signaling of CKs, GAs, and/or perhaps other phytohormones (Fig. 6-13).

7.2 S-acylation in growth and development

One common feature of the loss-of-function mutation in AtPATs characterized so far is the reduced stature of the mature plants. For example, *atpat10* is only ¼ of the height of the WT (Qi et al., 2013), followed by *atpat21-1* (Fig. 4-5), *atpat24* (*tip1*) (Hemsley et al., 2005), *atpat14* (Li et al., 2015), and *atplp1-1* (Fig. 5-4). Indeed, both cell number and cell size are reduced in *atpat10* (Qi et al., 2013), *atpat14* (Li et al, 2016), *atpat21-1* (Fig. 4-6) and *atpat24* (Hemsley et al., 2005). This suggests that AtPATs-mediated protein S-acylation plays very important roles in cell division and/or cell expansion during growth and development of Arabidopsis. Rate of cell expansion determines how big and fast the plant grows (McCann et al., 2001). In plants, cell expansion is driven by vacuolar turgor pressure but restricted by the strong and unflexible cell wall (Bringmann et al., 2012). During cell expansion, the existing cells must loosen their structure to integrate the newly synthesized wall polymers and other materials (McCann et al., 2001). Cellulose forms the main scaffolding structure of cell wall and it is very important to plant growth (McCann et al., 2001; McFarlane et al., 2014). It has been reported that the mutant lacking the cellulose biosynthesis gene *AtCesA7* showed reduction in growth rate and stature (Turner and Somerville, 1997). Interestingly, many enzymes related to cellulose biosynthesis are recently predicted and then confirmed to be S-acylated in Arabidopsis, such as CESA1, CESA3, CESA4, CESA7 and CESA8 (Hemsley et al., 2013; Kumar et al., 2016). It is noteworthy that CESA1, CESA3 and CESA6 are present in the primary cell wall,

controlling cell expansion and cell elongation (McCann et al., 2001; Bringmann et al., 2012). Future research to match these cellulose synthases to their individual modifying PAT(s) will shed light as to how cellulose biosynthesis has been regulated.

Defects in the phyllotaxy with a much smaller shoot apical meristem and asymmetrically arranged leaf primordial around it was observed in *atplp1-1* mutant (Fig. 6-10 B and E). The SAM is made up of a population of pluripotent stem cells that are formed during embryogenesis. These stem cells rapidly proliferate and turn into differentiating leaf, flower primordial and all other shoot structures. Therefore, defect found at the SAM of *atplp1-1* mutant plant maybe the cause for slow and uneven cell proliferation of the leaf primordial, leading to much smaller and distorted leaves at the early stages of leaf development (Fig. 5-4C and E). However, once the transition to flowering occurred the flowering/branching habit and seed production were the difference between the mutant and WT became less obvious. This indicates that the inflorescence meristem is less affected than the vegetative SAM by the mutation in AtPLP1. As a protein S-acyltransferase AtPLP1 would exert its role by palmitoylating a substrate protein(s). A study identified two S-acylated protein phosphatase type 2C (PP2C) proteins, POL and PLL1, that are essential for the maintenance of shoot stem cells (Gagne and Clark, 2010). Loss-of-function mutants of POL and PLL1 lead to the loss of stem cells and termination of the shoot and floral meristems. Therefore, AtPLP1 could play its role in the SAM via POL and PLL1. However, while AtPLP1 is localized at ER (Batistic, 2012), POL and PLL1 are localized at the PM. Future studies will clarify the relationship between AtPLP1 and POL/PLL1 as well as other S-acylated substrate proteins so that its roles in growth and development of Arabidopsis will be elucidated.

Leaf Senescence is the final step of leaf development, which is controlled by multiple developmental and environmental signals (Morris et al., 2000). During this process, the nutrient in leaves is translocated to newly formed tissues or reproductive organs to support seed production, therefore it is a very important process for the normal growth and development of plant. Senescence is an age-dependent developmental process,

but it is also regulated by environmental factors such as temperature, nutrient, drought and pathogen (Woo et al., 2001). Leaf senescence is also regulated by phtohormones in both molecular and physiological levels, such as ABA (Zeevaart and Creelman, 1988), ethylene (Abeles et al., 1988), JA (Creelman et al., 1992) and SA (Morris et al., 2000). S-acylation is proved to be involved in leaf senescence as shown in *atpat13, atpat14* and double mutant *atpat13/atpat14* where precocious leaf senescence was found (Lai et al., 2015; Li et al., 2015). Further analysis in *atpat14* showed that the mutant accumulated more SA than WT (Li et al., 2015). The early senescence phenotype of *atpat14* was rescued by introducing the mutation in NPR1, the SA receptor (Li et al, 2015). Therefore, it seems that AtPAT14 mediated leaf senescence is via the regulation of the biosynthesis and signaling of the SA pathways. Future studies will aim to identify the S-acylated proteins that AtPAT13 and AtPAT14 modify and this will provide the molecular mechanism how these 2 AtPATs regulate leaf senescence.

7.3 S-acylation in reproduction

S-acylation is not only involved in vegetative growth, but also the reproduction process in Arabidopsis. While transcriptional null mutants of *AtPAT24* have defective male transmission (Schiefelbein et al., 1993; Ryan et al., 1998) and those of *AtPAT10* have greatly reduced fertility due to both male and female defects (Qi et al., 2013; Zhou et al., 2013), the loss-of-function mutant of *AtPAT21* is completely sterile (Fig. 4-8G). Detailed studies revealed that *atpat21-1* mutant has defects in both male and female sporogenesis and gametogenesis. This is most likely due to the impaired meiosis and mitosis during the production of microspores and embryo sac, leading to abnormal pollen and ovules (Figs. 4-9 and 4-14B). So far, more than 80 proteins have been found to be involved in the meiosis process. We first surveyed these proteins to see which ones are predicted to be S-acylated. For these putative S-acylated proteins we then compared the phenotype of their k/o mutants in fertility. We found that the loss-of-function of 24 of them have similar phenotype as *atpat21-1* in both male and female defects (Table 4-3). Future studies will be focused on the characterization of the relationship between AtPAT21 and these proteins,

which will help us to understand how AtPAT21 is involved in meiosis for the generation of microspores and embryo sac.

It is noteworthy that a recent study confirmed that the pollen tube tip specific Lost In Pollen tube guidance 1 (LIP1) and 2 (LIP2) were involved in pollen tube guidance and the double mutant is male sterile (Liu et al., 2013). Although the sterility in *atpat21-1* is not caused by failure in pollen tube guidance the fact that *atpat21-1* is the only sterile AtPAT mutant, and it is localized in PM, the same compartment as LIP1 and LIP2, implying that it could be the PAT that targets LIP1/2 to the membrane by palmitoylation.

7.4 S-acylation in abiotic and biotic stress response

Based on our studies of AtPATs reported here, targeted studies of individually S-acylated proteins and large scale proteomic isolation of S-acylated proteins in Arabidopsis, it is clear that S-acylation of proteins not only participates in growth, development and reproduction, but also in abiotic or biotic stress signaling pathways that enable plant to survive its unfavorable environment. For example, it was found that *atpat10* is hypersensitive to salt, such as LiCl, $CaCl_2$ and NaCl, and particularly $CaCl_2$ (Zhou et al., 2013; Qi et al., unpublished). The calcium sensors, CBL2, CBL3 and CBL6, which play important roles in abiotic stress response via regulating transporting proteins involved in uptake and translocation of K^+ and Na^+ (Batistic and Kudla, 2009; Luan, 2009), were found mis-localized in *atpat10* tonoplast (Zhou et al., 2013). This is interesting because the main membrane compartment AtPAT10 localizes is also tonoplast (Qi et al, 2013), demonstrating the positive roles that AtPAT10 plays in salt stress via targeting these calcium sensors to the correct membranes. Opposite function in salt stress response was found in AtPLP1 loss-of-function mutant where the mutant seedlings were more resistant to NaCl in the media and grew much longer roots (Fig. 6-13). Therefore, AtPLP1 plays a negative role in salt resistance.

S-acylation of proteins also plays important roles in biotic stress signaling pathways. This is because some important proteins related to plant immune responses upon invasion

by pathogens are S-acylated, including RPM1 interacting protein 4 (RIN4) which regulates plant immune responses to pathogen-associated molecular patterns and type III effectors (Hemsley et al., 2013; Sun et al., 2014), and flagellin sensitive 2 (FLS2) which is involved in MAP kinase signalling relay involved in innate immunity (Hemsley et al., 2013; Boyle et al., 2016). Biotic response of plant is mediated by salicylic acid which is one of the key phytohormones involved in both abiotic (Kunihiro et al., 2011; Drzewiecka et al., 2012; Liu et al., 2012) and biotic (Vlot et al., 2008; Dempsey et al., 2011) stress adaptation. It has been shown that SA plays a central role as a signaling molecule involved in both local defense reactions and in the induction of systemic resistance (Durner and Klessig, 1999; Herrera-Vásquez et al., 2015). Indeed, reduced synthesis of SA in transgenic plants due to disruption of SA pathways results in vulnerability toward fungal (*Phytophtora parasitica, Cercospora nicotianae*), bacterial (*Pseudomonas syringae*), and viral (*tobacco mosaic virus*) pathogens (Delaney et al., 1994). Because the early senescence in *atpat14* is coincided with the much higher level of SA being accumulated in the mutant leaves than WT we wondered if this might improve its biotic resistance. However, to our surprise, *atpat14-2* did not behave differently compared to WT to the pathogen *Pseudomonas syringae pv.* tomato DC3000 (Fig. 3-1).

Therefore, PATs mediated S-acylation of proteins in Arabidopsis is essential in abiotic and biotic adaptation. However, the mechanism is complex and requires further investigation in the future.

7.5 Mode of action of PATs in Arabidopsis

Hemsley and co-workers identified about 600 S-acylated proteins from cultured cells of Arabidopsis (Hemsley et al., 2013). This number is largely under-represented due to the limitation of the method and plant materials (tissue culture) used and the actual number could be more than 3,000 (see also in introduction). However, there are only 24 DHHC containing PATs proteins were found in its genome (Batistic, 2012). Therefore, it is clear that each PAT have more than one substrate and the average number would be about 125 for Arabidopsis. Similar case also happens in poplar since only 39 putative

PATs were found yet more than 400 putative S-acylated proteins were isolated (Yuan et al., 2013; Srivastava et al., 2016). This is probably why disruption of one PAT leads to abnormality from seed germination, seedling growth, reproduction to stress response. For example, knockout mutants of AtPAT24 have defects in both root architecture and male transmission (Ryan et al., 1998; Hemsley et al., 2005); AtPAT10 loss-of-function not only causes dwarf phenotype, but also affect plant fertility (Qi et al., 2013) and salt sensitivity (Zhou et al, 2013); *atpat14* mutants have smaller stature and show early leaf senescence (Li et al., 2015); *atplp1-1* mutant has defects in lipid breakdown (Fig. 5-8), skotomorphogenesis (Fig. 6-1), shoot apical meristem development (Fig. 6-10), root architecture (Fig. 6-11) and it also produces bigger seeds than WT (Fig. 4-6); and *atpat21-1* mature plant is shorter with smaller and uneven rosette leaves and completely sterile (Figs. 6-8 and 6-11).

However, we also found that not all knock-out mutants of AtPATs exhibit altered phenotype compared to WT. In fact, only 6 of the 24 PATs k/o mutants have impaired phenotype in growth, development, reproduction and salt stress (Hemsley et al., 2005; Qi et al., 2013; Lai et al., 2015; Li et al., 2015; Fig. 4-4; Fig. 6-1; Fig. 4-5). Individual k/o mutant of the other 18 AtPATs does not show observable phenotypic alterations (data not shown). It is hard to believe that more than 3000 S-acylated proteins are palmitoylated by the 6 AtPATs that have phenotypic defects. Therefore, redundancy between AtPATs could be a common feature for palmitoylation in plants, i.e., a large number of the identified S-acylated proteins in Arabidopsis are palmitoylated by more than one corresponding PATs. These PATs work redundantly to modify the same S-acylated substrate protein, or a subset of the S-acylated proteins. For example, each of the subunits of cellulose synthase complex (CSC) in Arabidopsis have multiple S-acylation sites and the average is 8, suggesting that the S-acylation of different cysteines in the same CSC might be catalyzed by different AtPATs (Kumar et al., 2016).

Therefore, PATs and their substrate S-acylated proteins are not a simple one-to-one relationship, and this makes the research on the mechanism of S-acylation difficult.

Further, there are no conserved domains or common features found in the S-acylated proteins. Although CSS-PALM can predict if a protein is palmitoylated or not this still needs to be confirmed experimentally (Zhou et al., 2006). Through large scale proteomics based studies in yeast and human systems substrate priorities or specificities for some PATs were noted (Roth et al., 2006; Ohno et al., 2012). However, very little is known about plant PATs-substrates interaction. Therefore, this is the big challenge in the plant S-acylation research field which slows down the characterization of the molecular mechanism of S-acylation in plant.

7.6 Perspectives and future work

Study on human PATs have shown that they are involved in cancer and many diseases, which make them ideal targets for drug development (Ivaldi et al., 2012; Chavda et al., 2014; Hornemann, 2015; Yeste-velasco et al., 2015). Although research in S-acylation in plant is still in its infancy information gathered on S-acylation in the model plant Arabidopsis so far clearly demonstrates that it is essential throughout the life cycle from seed germination to seed production. This can be utilized as a guide for crop breeding in the future. For example, AtPAT10 controls cell size and number and its knockout mutant showed a severe dwarfed phenotype (Qi et al., 2013). Homologous PATs in trees such as apple or pear can be identified and knocked out by CRISPR-Cas9 to create dwarf rootstocks for grafting. AtPAT14 is involved in leaf senescence and its mutant is early flowering (Li et al., 2015), therefore, this can be used as a target for gene modification to breed early or late mature crops. Loss-of-function of AtPAT21 results in male and female sterility and this can be utilized in generating male- or female-sterile lines for hybrid in crops. AtPLP1 loss-of-function mutant produces bigger seeds, and this can be applied to grain crops and nuts in the improvement of seed size and yield. AtPAT10 is also involved in salt response pathway which can be used to produce transgenic crops that are resistant to salt stress. However, there still many un-answered questions remain as to how these PATs exert their roles in the range of activities they are participating in. For example, what is the downstream substrate(s) for these AtPATs? How

are the PATs regulated? What are the functions of the remaining 18 AtPATs in Arabidopsis?

PATs, as a big gene family which are involved in a variety of processes during growth and development in Arabidopsis. Further studies will need to be carried out to broaden our knowledge in this field.

1) First of all, the target S-acylated proteins for each AtPAT will be identified/verified to dissect the mechanisms of their involvement in growth and development. With the 6 AtPATs characterised so far, only AtPAT10 was found to modify CBL2, CBL3 and CBL6 through *in vitro* experiment (Zhou et al., 2013). Therefore, the identification of the substrate proteins for other PATs will be required in the future.

2) *In vivo* and *in vitro* confirmation of PAT activity of all the other 19 AtPATs. Although all 24 AtPATs have the DHHC-CRD motif that does not guarantee them having PAT activity, or their functional domain lies on the DHHC domain. This is what we found with AtPLP1 where its functionality does not rely on Cys in the DHHC domain. Therefore, further verification of other AtPATs by *in vivo* and *in intro* studies will be needed to support this conclusion.

3) As only 6 out of the 24 AtPATs knockout mutants have abnormal phenotype and others look identical to the WT we wonder what the functions of these 18 putative AtPATs? Therefore, double, triple, quadrangle mutants will be generated by crossing single *atpat* homozygous mutant plants in order to characterise the biological functions of the remaining AtPATs.

4) Redundancy of AtPATs. As mentioned above, the single mutants of many AtPATs did not show any abnormal phenotypes compare to WT, which means they have redundant functions in regulating plant growth and development. By observing the phenotype of double, triple or quadruple mutants in different combinations redundancy between these AtPATs can be identified.

5) Many S-acylated proteins that are involved in different pathways, or a subset of

proteins that function in the same pathway can be modified by a single AtPAT, such as AtPAT10 is the PAT for the palmitoylation of at least 3 CBLs. Using similar approaches this aspect of other AtPATs will be addressed.

6) Finally, the ‘palmitoylation map’ between AtPATs and their specific S-acylated substrate proteins will be constructed.

Reference

Abeles FB, Dunn LJ, Morgens P, Callahan A, Dinterman RE, Schmidt J (1988) Induction of 33-kD and 60-kD peroxidases during ethylene-induced senescence of cucumber cotyledons. Plant Physiology **87:** 609-615

Abrami L, Kunz B, Iacovache I, Van der Goot FG (2008) Palmitoylation and ubiquitination regulate exit of the Wnt signaling protein LRP6 from the endoplasmic reticulum. Proceedings of the National Academy of Sciences **105:** 5384-5389

Abrami L, Leppla SH, van der Goot FG (2006) Receptor palmitoylation and ubiquitination regulate anthrax toxin endocytosis. The Journal of Cell Biology **172:** 309-320

Achard P, Genschik P (2009) Releasing the brakes of plant growth: how GAs shutdown DELLA proteins. Journal of Experimental Botany **60:** 1085-1092

Achard P, Vriezen WH, Van Der Straeten D, Harberd NP (2003) Ethylene regulates Arabidopsis development via the modulation of DELLA protein growth repressor function. The Plant Cell **15:** 2816-2825

Adams M, Harrington B, He Y, Davies C, Wallace S, Chetty N, Crandon A, Oliveira N, Shannon C, Coward J (2015) EGF inhibits constitutive internalization and palmitoylation-dependent degradation of membrane-spanning procancer CDCP1 promoting its availability on the cell surface. Oncogene **34:** 1375-1383

Adjobo-Hermans MJ, Goedhart J, Gadella TW (2006) Plant G protein heterotrimers require dual lipidation motifs of Gα and Gγ and do not dissociate upon activation. Journal of Cell Science **119:** 5087-5097

Akimzhanov AM, Boehning D (2015) Rapid and transient palmitoylation of the tyrosine kinase Lck mediates Fas signaling. Proceedings of the National Academy of Sciences **112:** 11876-11880

Al Abdallah Q, Fortwendel JR (2015) Exploration of Aspergillus fumigatus Ras pathways for novel antifungal drug targets. Frontiers in Microbiology **6**

Alabadi D, Gallego-Bartolomé J, Orlando L, García-Cárcel L, Rubio V, Martínez C, Frigerio M, Iglesias-Pedraz JM, Espinosa A, Deng XW (2008) Gibberellins modulate light signaling pathways to prevent Arabidopsis seedling de-etiolation in darkness. The Plant Journal **53:** 324-335

Alabadí D, Gil J, Blázquez MA, García-Martínez JL (2004) Gibberellins repress photomorphogenesis in darkness. Plant Physiology **134:** 1050-1057

Antinone SE, Ghadge GD, Lam TT, Wang L, Roos RP, Green WN (2013) Palmitoylation of superoxide dismutase 1 (SOD1) is increased for familial amyotrophic lateral sclerosis-linked SOD1 mutants. Journal of Biological Chemistry **288:** 21606-21617

Arroyo A, Bossi F, Finkelstein RR, León P (2003) Three genes that affect sugar sensing (*ABSCISIC ACID INSENSITIVE 4*, *ABSCISIC ACID INSENSITIVE 5*, and *CONSTITUTIVE TRIPLE RESPONSE 1*) are differentially regulated by glucose in Arabidopsis. Plant Physiology **133:** 231-242

Avila-Ospina L, Moison M, Yoshimoto K, Masclaux-Daubresse C (2014) Autophagy, plant senescence, and nutrient recycling. Journal of Experimental Botany**:** eru039

Azumi Y, Liu D, Zhao D, Li W, Wang G, Hu Y, Ma H (2002) Homolog interaction during meiotic prophase I in Arabidopsis requires the *SOLO DANCERS* gene encoding a novel cyclin-like protein. The EMBO Journal **21:** 3081-3095

Babu P, Deschenes RJ, Robinson LC (2004) Akr1p-dependent palmitoylation of Yck2p yeast casein kinase 1 is necessary and sufficient for plasma membrane targeting. Journal of Biological Chemistry **279:** 27138-27147

Baekkeskov S, Kanaani J (2009) Palmitoylation cycles and regulation of protein function (Review). Molecular Membrane Biology **26:** 42-54

Baker A, Graham IA, Holdsworth M, Smith SM, Theodoulou FL (2006) Chewing the fat: β-oxidation in signalling and development. Trends in Plant Science **11:** 124-132

Baker TL, Zheng H, Walker J, Coloff JL, Buss JE (2003) Distinct rates of palmitate turnover on membrane-bound cellular and oncogenic H-ras. Journal of Biological Chemistry **278:** 19292-19300

Ballesteros MaL, Bolle C, Lois LM, Moore JM, Vielle-Calzada J-P, Grossniklaus U, Chua N-H (2001) LAF1, a MYB transcription activator for phytochrome A signaling. Genes & Development **15:** 2613-2625

Bannan BA, Van Etten J, Kohler JA, Tsoi Y, Hansen NM, Sigmon S, Fowler E, Buff H, Williams TS, Ault JG (2008) The Drosophila protein palmitoylome: characterizing palmitoyl-thioesterases and DHHC palmitoyl-transferases. Fly **2:** 198-214

Barciszewski J, Siboska G, Clark BF, Rattan SI (2000) Cytokinin formation by oxidative metabolism. Journal of Plant Physiology **157:** 587-588

Bartels DJ, Mitchell DA, Dong X, Deschenes RJ (1999) Erf2, a novel gene product that affects the localization and palmitoylation of Ras2 in *Saccharomyces cerevisiae*. Molecular and Cellular Biology **19:** 6775-6787

Batistič O (2012) Genomics and Localization of the Arabidopsis DHHC-Cysteine-Rich Domain S-Acyltransferase Protein Family. Plant Physiology **160:** 1597-1612

Batistič O, Kudla J (2009) Plant calcineurin B-like proteins and their interacting protein kinases. Biochimica et Biophysica Acta (BBA)-Molecular Cell Research **1793:** 985-992

Batistič O, Rehers M, Akerman A, Schlücking K, Steinhorst L, Yalovsky S, Kudla J (2012) S-acylation-dependent association of the calcium sensor CBL2 with the vacuolar membrane is essential for proper abscisic acid responses. Cell Research **22:** 1155-1168

Batistič O, Sorek N, Schültke S, Yalovsky S, Kudla J (2008) Dual fatty acyl modification determines the localization and plasma membrane targeting of CBL/CIPK Ca2+ signaling complexes in Arabidopsis. The Plant Cell **20:** 1346-1362

Baumgart F, Corral-Escariz M, Pérez-Gil J, Rodríguez-Crespo I (2010) Palmitoylation of R-Ras by human DHHC19, a palmitoyl transferase with a CaaX box. Biochimica et Biophysica Acta (BBA)-Biomembranes **1798:** 592-604

Beck JR, Rodriguez-Fernandez IA, De Leon JC, Huynh M-H, Carruthers VB, Morrissette NS, Bradley PJ (2010) A novel family of Toxoplasma IMC proteins displays a hierarchical organization and functions in coordinating parasite division. PLoS Pathogern **6:** e1001094

Benjannet S, Elagoz A, Wickham L, Mamarbachi M, Munzer JS, Basak A, Lazure C, Cromlish JA, Sisodia S, Checler F (2001) Post-translational processing of β-secretase (β-Amyloid-converting Enzyme) and its ectodomain shedding the pro- and transmembrane/cytosolic domains affect its cellular activity and amyloid-β production. Journal of Biological Chemistry **276:** 10879-10887

Bethke PC, Libourel IG, Jones RL (2006) Nitric oxide reduces seed dormancy in Arabidopsis. Journal of Experimental Botany **57:** 517-526

Bewley JD (1997) Seed germination and dormancy. The Plant Cell **9:** 1055

Bewley JD, Black M (1994) Seeds. Springer

Bijlmakers MJ (2009) Protein acylation and localization in T cell signaling (Review). Molecular Membrane Biology **26:** 93-103

Bijlmakers MJ, Marsh M (2003) The on–off story of protein palmitoylation. Trends in Cell Biology **13:** 32-42

Bishop RE (2005) The lipid A palmitoyltransferase PagP: molecular mechanisms and role in bacterial pathogenesis. Molecular Microbiology **57:** 900-912

Bishop RE, Kim SH, El Zoeiby A (2005) Role of lipid A palmitoylation in bacterial pathogenesis. Journal of Endotoxin Research **11:** 174-180

Blaskovic S, Blanc M, Goot FG (2013) What does S-palmitoylation do to membrane proteins? FEBS Journal **280:** 2766-2774

Bleecker AB, Patterson SE (1997) Last exit: senescence, abscission, and meristem arrest in Arabidopsis. The Plant Cell **9:** 1169

Borek S, Nuc K (2011) Sucrose controls storage lipid breakdown on gene expression level in germinating yellow lupine (*Lupinus luteus L.*) seeds. Journal of Plant Physiology **168:** 1795-1803

Boursiac Y, Chen S, Luu DT, Sorieul M, van den Dries N, Maurel C (2005) Early effects of salinity on water transport in Arabidopsis roots. Molecular and Cellular Features of Aquaporin Expression. Plant Physiology **139:** 790-805

Boyle PC, Schwizer S, Hind SR, Kraus CM, Diaz ST, He B, Martin GB (2016) Detecting N-myristoylation and S-acylation of host and pathogen proteins in plants using click chemistry. Plant Methods **12:** 38

Breeze E, Harrison E, McHattie S, Hughes L, Hickman R, Hill C, Kiddle S, Kim Y-s, Penfold CA, Jenkins D (2011) High-resolution temporal profiling of transcripts during Arabidopsis leaf senescence reveals a distinct chronology of processes and regulation. The Plant Cell **23:** 873-894

Brett K, Kordyukova LV, Serebryakova MV, Mintaev RR, Alexeevski AV, Veit M (2014) Site-specific S-acylation of influenza virus Hemagglutinin -the location of the acylation site relative to the membrane border is the decisive factor for attachment of stearate. Journal of Biological Chemistry **289**: 34978-34989

Brigidi GS, Santyr B, Shimell J, Jovellar B, Bamji SX (2015) Activity-regulated trafficking of the palmitoyl-acyl transferase DHHC5. Nature Communications **6**

Brigidi GS, Sun Y, Beccano-Kelly D, Pitman K, Mobasser M, Borgland SL, Milnerwood AJ, Bamji SX (2014) Palmitoylation of [delta]-catenin by DHHC5 mediates activity-induced synapse plasticity. Nature Neuroscience **17:** 522-532

Bringmann M, Li E, Sampathkumar A, Kocabek T, Hauser M-T, Persson S (2012) POM-POM2/cellulose synthase interacting1 is essential for the functional association of cellulose synthase and microtubules in Arabidopsis. The Plant Cell **24:** 163-177

Buglino JA, Resh MD (2012) Palmitoylation of Hedgehog proteins. Vitamins and Hormones **88:** 229

Bundock P, Hooykaas P (2002) Severe developmental defects, hypersensitivity to DNA-damaging agents, and lengthened telomeres in Arabidopsis MRE11 mutants. The Plant Cell **14:** 2451-2462

Bürger M, Zimmermann TJ, Kondoh Y, Stege P, Watanabe N, Osada H, Waldmann H, Vetter IR (2012) Crystal structure of the predicted phospholipase LYPLAL1 reveals unexpected functional plasticity despite close relationship to acyl protein thioesterases. Journal of Lipid Research **53:** 43-50

Burgess J (1985) Introduction to plant cell development. CUP Archive

Butland SL, Sanders SS, Schmidt ME, Riechers S-P, Lin DT, Martin DD, Vaid K, Graham RK, Singaraja RR, Wanker EE (2014) The palmitoyl acyltransferase HIP14 shares a high proportion of interactors with huntingtin: implications for a role in the pathogenesis of Huntington's disease. Human Molecular Genetics **23:** 4142-4160

Cabot C, Sibole JV, Barceló J, Poschenrieder C (2009) Sodium-calcium interactions with growth, water, and photosynthetic parameters in salt-treated beans. Journal of Plant Nutrition and Soil Science/Zeitschrift für Pflanzenernährung und Bodenkunde **172:** 637

Canvin DT, Beevers H (1961) Sucrose synthesis from acetate in the germinating castor bean: kinetics and pathway. Journal of Biological Chemistry **236:** 988-995

Casey PJ (1995) Protein lipidation in cell signaling. Science **268:** 221-225

Casey PJ, Seabra MC (1996) Protein prenyltransferases. Journal of Biological Chemistry **271:** 5289-5292

Catterou M, Dubois F, Smets R, Vaniet S, Kichey T, Van Onckelen H, Sangwan-Norreel BS, Sangwan RS (2002) hoc: an Arabidopsis mutant overproducing cytokinins and expressing high in vitro organogenic capacity. The Plant Journal **30:** 273-287

Cavalier-Smith T (1993) Kingdom protozoa and its 18 phyla. Microbiological Reviews **57:** 953-994

Chakrabandhu K, Hérincs Z, Huault S, Dost B, Peng L, Conchonaud F, Marguet D, He HT, Hueber AO (2007) Palmitoylation is required for efficient Fas cell death signaling. The EMBO Journal **26:** 209-220

Charollais J, Van Der Goot FG (2009) Palmitoylation of membrane proteins (Review). Molecular Membrane Biology **26:** 55-66

Charych EI, Jiang LX, Lo F, Sullivan K, Brandon NJ (2010) Interplay of palmitoylation and phosphorylation in the trafficking and localization of

phosphodiesterase 10A: implications for the treatment of schizophrenia. The Journal of Neuroscience **30:** 9027-9037

Chavda B, Arnott JA, Planey SL (2014) Targeting protein palmitoylation: selective inhibitors and implications in disease. Expert Opinion on Drug Discovery **9:** 1005-1019

Cheah K, Osborne DJ (1978) DNA lesions occur with loss of viability in embryos of ageing rye seed. Nature **272:** 593-599

Chelysheva L, Vezon D, Chambon A, Gendrot G, Pereira L, Lemhemdi A, Vrielynck N, Le Guin S, Novatchkova M, Grelon M (2012) The Arabidopsis HEI10 is a new ZMM protein related to Zip3. PLoS Genetics **8:** e1002799

Chen C, Marcus A, Li W, Hu Y, Calzada JPV, Grossniklaus U, Cyr RJ, Ma H (2002) The Arabidopsis ATK1 gene is required for spindle morphogenesis in male meiosis. Development **129:** 2401-2409

Chen H, Zhang J, Neff MM, Hong S-W, Zhang H, Deng X-W, Xiong L (2008) Integration of light and abscisic acid signaling during seed germination and early seedling development. Proceedings of the National Academy of Sciences **105:** 4495-4500

Chen YH, Li HJ, Shi DQ, Yuan L, Liu J, Sreenivasan R, Baskar R, Grossniklaus U, Yang WC (2007) The central cell plays a critical role in pollen tube guidance in Arabidopsis. The Plant Cell **19:** 3563-3577

Chen Z, Higgins JD, Hui JTL, Li J, Franklin FCH, Berger F (2011) Retinoblastoma protein is essential for early meiotic events in Arabidopsis. The EMBO Journal **30:** 744-755

Chen ZH, Lam HC, Jin Y, Kim HP, Cao J, Lee SJ, Ifedigbo E, Parameswaran H, Ryter SW, Choi AM (2010) Autophagy protein microtubule-associated protein 1 light chain-3B (LC3B) activates extrinsic apoptosis during cigarette smoke-induced emphysema. Proceedings of the National Academy of Sciences **107:** 18880-18885

Chi YH, Paeng SK, Kim MJ, Hwang G, Melencion SMB, Oh H, Lee SY (2014) Redox-dependent functional switching of plant proteins accompanying with their structural changes. Thiol-based Redox Homeostasis and Signalling**:** 84

Chin-Atkins AN, Craig S, Hocart CH, Dennis ES, Chaudhury AM (1996) Increased endogenous cytokinin in the Arabidopsis amp1 mutant corresponds with de-etiolation responses. Planta **198:** 549-556

Chory J, Chatterjee M, Cook R, Elich T, Fankhauser C, Li J, Nagpal P, Neff M, Pepper A, Poole D (1996) From seed germination to flowering, light controls plant development via the pigment phytochrome. Proceedings of the National Academy of Sciences **93:** 12066-12071

Cocca SM (2014) Phylogenetic analysis, modeling and experimental studies of the *Saccharomyces cerevisiae* palmitoylated protein kinase gene, *ENV7*. California State University, Long Beach

Cohen E (1993) Chitin synthesis and degradation as targets for pesticide action. Archives of Insect Biochemistry and Physiology **22:** 245-261

Coleman DT, Soung YH, Surh YJ, Cardelli JA, Chung J (2015) Curcumin prevents

palmitoylation of integrin β4 in breast cancer cells. Plos one **10**: e0125399

Cornah JE, Germain V, Ward JL, Beale MH, Smith SM (2004) Lipid utilization, gluconeogenesis, and seedling growth in Arabidopsis mutants lacking the glyoxylate cycle enzyme malate synthase. Journal of Biological Chemistry **279:** 42916-42923

Couve A, Protopopov V, Gerst JE (1995) Yeast synaptobrevin homologs are modified posttranslationally by the addition of palmitate. Proceedings of the National Academy of Sciences **92:** 5987-5991

Cowling RJ, Harberd NP (1999) Gibberellins control Arabidopsis hypocotyl growth via regulation of cellular elongation. Journal of Experimental Botany **50:** 1351-1357

Cramer GR, Quarrie SA (2002) Abscisic acid is correlated with the leaf growth inhibition of four genotypes of maize differing in their response to salinity. Functional Plant Biology **29:** 111-115

Creelman RA, Tierney ML, Mullet JE (1992) Jasmonic acid/methyl jasmonate accumulate in wounded soybean hypocotyls and modulate wound gene expression. Proceedings of the National Academy of Sciences **89:** 4938-4941

Curtis MD, Grossniklaus U (2003) A gateway cloning vector set for high-throughput functional analysis of genes in planta. Plant Physiology **133:** 462-469

Cutler S, Ghassemian M, Bonetta D, Cooney S, McCourt P (1996) A protein farnesyl transferase involved in abscisic acid signal transduction in Arabidopsis. Science **273:** 1239

Dave A, Hernández ML, He Z, Andriotis VM, Vaistij FE, Larson TR, Graham IA (2011) 12-Oxo-phytodienoic acid accumulation during seed development represses seed germination in Arabidopsis. The Plant Cell **23:** 583-599

Dave A, Vaistij FE, Gilday AD, Penfield SD, Graham IA (2016) Regulation of *Arabidopsis thaliana* seed dormancy and germination by 12-oxo-phytodienoic acid. Journal of Experimental Botany **67:** 2277-2284

Davière JM, Achard P (2013) Gibberellin signaling in plants. Development **140:** 1147-1151

de Azevedo Souza C, Kim SS, Koch S, Kienow L, Schneider K, McKim SM, Haughn GW, Kombrink E, Douglas CJ (2009) A novel fatty acyl-CoA synthetase is required for pollen development and sporopollenin biosynthesis in Arabidopsis. The Plant Cell **21:** 507-525

de Lucas M, Davière J-M, Rodríguez-Falcón M, Pontin M, Iglesias-Pedraz JM, Lorrain S, Fankhauser C, Blázquez MA, Titarenko E, Prat S (2008) A molecular framework for light and gibberellin control of cell elongation. Nature **451:** 480-484

De Muyt A, Vezon D, Gendrot G, Gallois JL, Stevens R, Grelon M (2007) AtPRD1 is required for meiotic double strand break formation in *Arabidopsis thaliana*. The EMBO Journal **26:** 4126-4137

De Storme N, Geelen D (2011) The Arabidopsis mutant jason produces unreduced first division restitution male gametes through a parallel/fused spindle mechanism in meiosis II. Plant Physiology **155:** 1403-1415

De Wit M, Galvão VC, Fankhauser C (2016) Light-mediated hormonal regulation of

plant growth and development. Annual Review of Plant Biology **67:** 513-537

Dean PJ, Siwiec T, Waterworth WM, Schlögelhofer P, Armstrong SJ, West CE (2009) A novel ATM-dependent X-ray-inducible gene is essential for both plant meiosis and gametogenesis. The Plant Journal **58:** 791-802

Delaney TP, Uknes S, Vernooij B, Friedrich L (1994) A central role of salicylic acid in plant disease resistance. Science **266:** 1247

Dempsey DMA, Vlot AC, Wildermuth MC, Klessig DF (2011) Salicylic acid biosynthesis and metabolism. The Arabidopsis Book**:** e0156

Deng XW, Caspar T, Quail PH (1991) *COP1*: a regulatory locus involved in light-controlled development and gene expression in Arabidopsis. Genes & Development **5:** 1172-1182

Deschenes R, Resh M, Broach J (1990) Acylation and prenylation of proteins. Current Opinion in Cell Biology **2:** 1108-1113

Dietrich LE, Gurezka R, Veit M, Ungermann C (2004) The SNARE Ykt6 mediates protein palmitoylation during an early stage of homotypic vacuole fusion. The EMBO Journal **23:** 45-53

Dietrich LE, Ungermann C (2004) On the mechanism of protein palmitoylation. EMBO Reports **5:** 1053-1057

Dion É, Li L, Jean M, Belzile F (2007) An Arabidopsis MLH1 mutant exhibits reproductive defects and reveals a dual role for this gene in mitotic recombination. The Plant Journal **51:** 431-440

Dobritsa AA, Lei Z, Nishikawa S-i, Urbanczyk-Wochniak E, Huhman DV, Preuss D, Sumner LW (2010) LAP5 and LAP6 encode anther-specific proteins with similarity to chalcone synthase essential for pollen exine development in *Arabidopsis thaliana*. Plant Physiology**:** pp. 110.157446

Dresselhaus T, Franklin-Tong N (2013) Male–Female crosstalk during pollen germination, tube growth and guidance, and double fertilization. Molecular Plant **6:** 1018-1036

Drzewiecka K, Mleczek M, Gąsecka M, Magdziak Z, Goliński P (2012) Changes in *Salix viminalis L. cv.* 'Cannabina' morphology and physiology in response to nickel ions–Hydroponic investigations. Journal of Hazardous Materials **217:** 429-438

Dulermo T, Nicaud JM (2011) Involvement of the G3P shuttle and β-oxidation pathway in the control of TAG synthesis and lipid accumulation in *Yarrowia lipolytica*. Metabolic Engineering 13: 482-491

Durner J, Klessig DF (1999) Nitric oxide as a signal in plants. Current Opinion in Plant Biology **2:** 369-374

Earley KW, Haag JR, Pontes O, Opper K, Juehne T, Song K, Pikaard CS (2006) Gateway-compatible vectors for plant functional genomics and proteomics. The Plant Journal **45:** 616-629

Eastmond PJ (2006) SUGAR-DEPENDENT1 encodes a patatin domain triacylglycerol lipase that initiates storage oil breakdown in germinating Arabidopsis seeds. The Plant Cell **18:** 665-675

Eastmond PJ (2007) MONODEHYROASCORBATE REDUCTASE4 is required for

seed storage oil hydrolysis and postgerminative growth in Arabidopsis. The Plant Cell **19:** 1376-1387

Eastmond PJ, Germain V, Lange PR, Bryce JH, Smith SM, Graham IA (2000) Postgerminative growth and lipid catabolism in oilseeds lacking the glyoxylate cycle. Proceedings of the National Academy of Sciences **97:** 5669-5674

Eastmond PJ, Graham IA (2001) Re-examining the role of the glyoxylate cycle in oilseeds. Trends in Plant Science **6:** 72-78

Eastmond PJ, Jones RL (2005) Hormonal regulation of gluconeogenesis in cereal aleurone is strongly cultivar-dependent and gibberellin action involves SLENDER1 but not GAMYB. The Plant Journal **44:** 483-493

Edmonds MJ, Morgan A (2014) A systematic analysis of protein palmitoylation in *Caenorhabditis elegans*. BMC Genomics **15:** 841

El-Husseini AED, Schnell E, Dakoji S, Sweeney N, Zhou Q, Prange O, Gauthier-Campbell C, Aguilera-Moreno A, Nicoll RA, Bredt DS (2002) Synaptic strength regulated by palmitate cycling on PSD-95. Cell **108:** 849-863

Eriksson S, Böhlenius H, Moritz T, Nilsson O (2006) GA4 is the active gibberellin in the regulation of *LEAFY* transcription and Arabidopsis floral initiation. The Plant Cell **18:** 2172-2181

Estelle MA, Somerville C (1987) Auxin-resistant mutants of *Arabidopsis thaliana* with an altered morphology. Molecular and General Genetics MGG **206:** 200-206

Fait A, Angelovici R, Less H, Ohad I, Urbanczyk-Wochniak E, Fernie AR, Galili G (2006) Arabidopsis seed development and germination is associated with temporally distinct metabolic switches. Plant Physiology **142:** 839-854

Fang C, Deng L, Keller CA, Fukata M, Fukata Y, Chen G, Lüscher B (2006) GODZ-mediated palmitoylation of GABAA receptors is required for normal assembly and function of GABAergic inhibitory synapses. The Journal of Neuroscience **26:** 12758-12768

Feller UK, Soong TST, Hageman RH (1977) Leaf proteolytic activities and senescence during grain development of field-grown corn (*Zea mays L.*). Plant Physiology **59:** 290-294

Feng Y, Davis NG (2000) Akr1p and the type I casein kinases act prior to the ubiquitination step of yeast endocytosis: Akr1p is required for kinase localization to the plasma membrane. Molecular and Cellular Biology **20:** 5350-5359

Fernández-Hernando C, Fukata M, Bernatchez PN, Fukata Y, Lin MI, Bredt DS, Sessa WC (2006) Identification of Golgi-localized acyl transferases that palmitoylate and regulate endothelial nitric oxide synthase. The Journal of Cell Biology **174:** 369-377

Finch-Savage WE, Leubner-Metzger G (2006) Seed dormancy and the control of germination. New Phytologist **171:** 501-523

Finkelstein R, Reeves W, Ariizumi T, Steber C (2008) Molecular aspects of seed dormancy. Plant Biology **59:** 387

Flannery AR, Czibener C, Andrews NW (2010) Palmitoylation-dependent association with CD63 targets the Ca^{2+} sensor synaptotagmin VII to lysosomes. The Journal of Cell Biology **191:** 599-613

Flores S, Tobin EM (1986) Benzyladenine modulation of the expression of two genes for nuclear-encoded chloroplast proteins in *Lemna gibba*: apparent post-transcriptional regulation. Planta **168:** 340-349

Forcat S, Bennett MH, Mansfield JW, Grant MR (2008) A rapid and robust method for simultaneously measuring changes in the phytohormones ABA, JA and SA in plants following biotic and abiotic stress. Plant Methods **4:** 1

Forrester MT, Hess DT, Thompson JW, Hultman R, Moseley MA, Stamler JS, Casey PJ (2011) Site-specific analysis of protein S-acylation by resin-assisted capture. Journal of Lipid Research **52:** 393-398

Fox CS, Liu Y, White CC, Feitosa M, Smith AV, Heard-Costa N, Lohman K, Johnson AD, Foster MC, Greenawalt DM (2012) Genome-wide association for abdominal subcutaneous and visceral adipose reveals a novel locus for visceral fat in women. PLoS Genetics **8:** e1002695

Franco-Zorrilla JM, Martín AC, Leyva A, Paz-Ares J (2005) Interaction between phosphate-starvation, sugar, and cytokinin signaling in Arabidopsis and the roles of cytokinin receptors CRE1/AHK4 and AHK3. Plant Physiology **138:** 847-857

Fredericks GJ, Hoffmann PR (2015) Selenoprotein K and protein palmitoylation. Antioxidants and Redox Signaling **23**: 854-862

Frénal K, Kemp LE, Soldati-Favre D (2014) Emerging roles for protein S-palmitoylation in Toxoplasma biology. International Journal for Parasitology **44:** 121-131

Frénal K, Polonais V, Marq J-B, Stratmann R, Limenitakis J, Soldati-Favre D (2010) Functional dissection of the apicomplexan glideosome molecular architecture. Cell host & Microbe **8:** 343-357

Frénal K, Tay CL, Mueller C, Bushell ES, Jia Y, Graindorge A, Billker O, Rayner JC, Soldati-Favre D (2013) Global analysis of apicomplexan protein S-acyl transferases reveals an enzyme essential for invasion. Traffic **14:** 895-911

Frey A, Audran C, Marin E, Sotta B, Marion-Poll A (1999) Engineering seed dormancy by the modification of zeaxanthin epoxidase gene expression. Plant Molecular Biology **39:** 1267-1274

Fröhlich M, Dejanovic B, Kashkar H, Schwarz G, Nussberger S (2014) S-palmitoylation represents a novel mechanism regulating the mitochondrial targeting of BAX and initiation of apoptosis. Cell Death & Disease **5:** e1057

Fukasawa M, Varlamov O, Eng WS, Söllner TH, Rothman JE (2004) Localization and activity of the SNARE Ykt6 determined by its regulatory domain and palmitoylation. Proceedings of the National Academy of Sciences of the United States of America **101:** 4815-4820

Fukata M, Fukata Y, Adesnik H, Nicoll RA, Bredt DS (2004) Identification of PSD-95 palmitoylating enzymes. Neuron **44:** 987-996

Fukata Y, Dimitrov A, Boncompain G, Vielemeyer O, Perez F, Fukata M (2013) Local palmitoylation cycles define activity-regulated postsynaptic subdomains. The Journal of Cell Biology **202:** 145-161

Fukata Y, Fukata M (2010) Protein palmitoylation in neuronal development and synaptic plasticity. Nature Reviews Neuroscience **11:** 161-175

Fukata Y, Iwanaga T, Fukata M (2006) Systematic screening for palmitoyl transferase activity of the DHHC protein family in mammalian cells. Methods **40:** 177-182

Fulda M, Schnurr J, Abbadi A, Heinz E (2004) Peroxisomal acyl-CoA synthetase activity is essential for seedling development in *Arabidopsis thaliana*. The Plant Cell **16:** 394-405

Furne C, Corset V, Hérincs Z, Cahuzac N, Hueber A-O, Mehlen P (2006) The dependence receptor DCC requires lipid raft localization for cell death signaling. Proceedings of the National Academy of Sciences of the United States of America **103:** 4128-4133

Gagne JM, Clark SE (2010) The Arabidopsis stem cell factor POLTERGEIST is membrane localized and phospholipid stimulated. The Plant Cell **22:** 729-743

Galli LM, Barnes TL, Secrest SS, Kadowaki T, Burrus LW (2007) Porcupine-mediated lipid-modification regulates the activity and distribution of Wnt proteins in the chick neural tube. Development **134:** 3339-3348

Ganesan L, Levental I (2015) Pharmacological inhibition of protein lipidation. The Journal of Membrane Biology **248:** 929-941

Gargantini PR, Gonzalez-Rizzo S, Chinchilla D, Raices M, Giammaria V, Ulloa RM, Frugier F, Crespi MD (2006) A CDPK isoform participates in the regulation of nodule number in *Medicago truncatula*. The Plant Journal **48:** 843-856

Gaughran JP, Lai MH, Kirsch DR, Silverman SJ (1994) Nikkomycin Z is a specific inhibitor of *Saccharomyces cerevisiae* chitin synthase isozyme Chs3 in vitro and in vivo. Journal of Bacteriology **176:** 5857-5860

Geldner N, Dénervaud-Tendon V, Hyman DL, Mayer U, Stierhof YD, Chory J (2009) Rapid, combinatorial analysis of membrane compartments in intact plants with a multicolor marker set. The Plant Journal **59:** 169-178

Germain V, Rylott EL, Larson TR, Sherson SM, Bechtold N, Carde JP, Bryce JH, Graham IA, Smith SM (2001) Requirement for 3-ketoacyl-CoA thiolase-2 in peroxisome development, fatty acid β-oxidation and breakdown of triacylglycerol in lipid bodies of Arabidopsis seedlings. The Plant Journal **28:** 1-12

Gibson SI (2004) Sugar and phytohormone response pathways: navigating a signalling network. Journal of Experimental Botany **55:** 253-264

Gleason EJ, Lindsey WC, Kroft TL, Singson AW, L'Hernault SW (2006) SPE-10 encodes a DHHC–CRD zinc-finger membrane protein required for endoplasmic reticulum/Golgi membrane morphogenesis during *Caenorhabditis elegans* spermatogenesis. Genetics **172:** 145-158

Goepfert S, Poirier Y (2007) β-Oxidation in fatty acid degradation and beyond. Current Opinion in Plant Biology **10:** 245-251

Gonzalez MA, Quiroga R, Maccioni H, Valdez TJ (2009) A novel motif at the C-terminus of palmitoyltransferases is essential for Swf1 and Pfa3 function in vivo. Biochemical Journal **419:** 301-308

Gorleku OA, Barns AM, Prescott GR, Greaves J, Chamberlain LH (2011) Endoplasmic reticulum localization of DHHC palmitoyltransferases mediated by lysine-based sorting signals. Journal of Biological Chemistry **286:** 39573-39584

Gottlieb CD, Zhang S, Linder ME (2015) The cysteine-rich domain of the DHHC3

palmitoyltransferase is palmitoylated and contains tightly bound Zinc. Journal of Biological Chemistry **290:** 29259-29269

Graham IA (2008) Seed storage oil mobilization. Annual Review of Plant Biology **59:** 115-142

Grappin P, Bouinot D, Sotta B, Miginiac E, Jullien M (2000) Control of seed dormancy in *Nicotiana plumbaginifolia*: post-imbibition abscisic acid synthesis imposes dormancy maintenance. Planta **210:** 279-285

Grassie MA, McCallum J, Guzzi F, Magee A, Milligan G, Parenti M (1994) The palmitoylation status of the G-protein Go1 α regulates its activity of interaction with the plasma membrane. Biochemical Journal **302:** 913-920

Greaves J, Chamberlain LH (2007) Palmitoylation-dependent protein sorting. The Journal of Cell Biology **176:** 249-254

Greaves J, Chamberlain LH (2010) S-acylation by the DHHC protein family. Biochemical Society Transactions **38:** 522-524

Greaves J, Chamberlain LH (2011) DHHC palmitoyl transferases: substrate interactions and (patho) physiology. Trends in Biochemical Sciences **36:** 245-253

Greaves J, Gorleku OA, Salaun C, Chamberlain LH (2010) Palmitoylation of the SNAP25 protein family specificity and regulation by DHHC palmitoyl transferases. Journal of Biological Chemistry **285:** 24629-24638

Greaves J, Prescott GR, Fukata Y, Fukata M, Salaun C, Chamberlain LH (2009) The hydrophobic cysteine-rich domain of SNAP25 couples with downstream residues to mediate membrane interactions and recognition by DHHC palmitoyl transferases. Molecular Biology of the Cell **20:** 1845-1854

Greaves J, Salaun C, Fukata Y, Fukata M, Chamberlain LH (2008) Palmitoylation and membrane interactions of the neuroprotective chaperone cysteine-string protein. Journal of Biological Chemistry **283:** 25014-25026

Greenboim-Wainberg Y, Maymon I, Borochov R, Alvarez J, Olszewski N, Ori N, Eshed Y, Weiss D (2005) Cross talk between gibberellin and cytokinin: the Arabidopsis GA response inhibitor SPINDLY plays a positive role in cytokinin signaling. The Plant Cell **17:** 92-102

Guardiola-Serrano F, Rossin A, Cahuzac N, Lückerath K, Melzer I, Mailfert S, Marguet D, Zörnig M, Hueber A (2010) Palmitoylation of human FasL modulates its cell death-inducing function. Cell Death & Disease **1:** e88

Guiboileau A, Sormani R, Meyer C, Masclaux-Daubresse C (2010) Senescence and death of plant organs: nutrient recycling and developmental regulation. Comptes Rendus Biologies **333:** 382-391

Guo Y, Gan S (2006) AtNAP, a NAC family transcription factor, has an important role in leaf senescence. The Plant Journal **46:** 601-612

Hanaoka H, Noda T, Shirano Y, Kato T, Hayashi H, Shibata D, Tabata S, Ohsumi Y (2002) Leaf senescence and starvation-induced chlorosis are accelerated by the disruption of an Arabidopsis autophagy gene. Plant Physiology **129:** 1181-1193

Harada T, Matsuzaki O, Hayashi H, Sugano S, Matsuda A, Nishida E (2003) AKRL1 and AKRL2 activate the JNK pathway. Genes to Cells **8:** 493-500

Harashima T, Heitman J (2005) Gα subunit Gpa2 recruits kelch repeat subunits that

inhibit receptor-G protein coupling during cAMP-induced dimorphic transitions in *Saccharomyces cerevisiae*. Molecular Biology of the Cell **16:** 4557-4571

Hayashi M, Nito K, Takei-Hoshi R, Yagi M, Kondo M, Suenaga A, Yamaya T, Nishimura M (2002) Ped3p is a peroxisomal ATP-binding cassette transporter that might supply substrates for fatty acid β-oxidation. Plant and Cell Physiology **43:** 1-11

Hayashi T, Rumbaugh G, Huganir RL (2005) Differential regulation of AMPA receptor subunit trafficking by palmitoylation of two distinct sites. Neuron **47:** 709-723

He T, Cramer GR (1996) Abscisic acid concentrations are correlated with leaf area reductions in two salt-stressed rapid-cycling Brassica species. Plant and Soil **179:** 25-33

Heakal Y, Woll MP, Fox T, Seaton K, Levenson R, Kester M (2011) Neurotensin receptor-1 inducible palmitoylation is required for efficient receptor-mediated mitogenic-signaling within structured membrane microdomains. Cancer Biology & Therapy **12:** 427-435

Hedden P, Thomas SG (2012) Gibberellin biosynthesis and its regulation. Biochemical Journal **444:** 11-25

Hemler ME (2014) Tetraspanin proteins promote multiple cancer stages. Nature Reviews Cancer **14:** 49-60

Hemsley PA (2009) Protein S-acylation in plants (Review). Molecular Membrane Biology **26:** 114-125

Hemsley PA (2015) The importance of lipid modified proteins in plants. New Phytologist **205:** 476-489

Hemsley PA, Grierson CS (2011) The ankyrin repeats and DHHC S-acyl transferase domain of AKR1 act independently to regulate switching from vegetative to mating states in yeast. PloS One **6:** e28799

Hemsley PA, Kemp AC, Grierson CS (2005) The TIP GROWTH DEFECTIVE1 S-acyl transferase regulates plant cell growth in Arabidopsis. The Plant Cell **17:** 2554-2563

Hemsley PA, Taylor L, Grierson CS (2008) Assaying protein palmitoylation in plants. Plant Methods **4:** 1

Hemsley PA, Weimar T, Lilley KS, Dupree P, Grierson CS (2013) A proteomic approach identifies many novel palmitoylated proteins in Arabidopsis. New Phytologist **197:** 805-814

Herrera-Vásquez A, Salinas P, Holuigue L (2015) Salicylic acid and reactive oxygen species interplay in the transcriptional control of defense genes expression. Frontiers in Plant Science **6:** 171

Hirschman JE, Jenness DD (1999) Dual lipid modification of the yeast Gγ subunit Ste18p determines membrane localization of Gβγ. Molecular and Cellular Biology **19:** 7705-7711

Hodson N, Invergo B, Rayner JC, Choudhary JS (2015) Palmitoylation and palmitoyl-transferases in *Plasmodium parasites*. Biochemical Society Transactions **43:** 240-245

Hornemann T (2015) Palmitoylation and depalmitoylation defects. Journal of Inherited

Metabolic Disease **38:** 179-186

Horváth E, Pál M, Szalai G, Páldi E, Janda T (2007) Exogenous 4-hydroxybenzoic acid and salicylic acid modulate the effect of short-term drought and freezing stress on wheat plants. Biologia Plantarum **51:** 480-487

Hou H, Subramanian K, LaGrassa TJ, Markgraf D, Dietrich LE, Urban J, Decker N, Ungermann C (2005) The DHHC protein Pfa3 affects vacuole-associated palmitoylation of the fusion factor Vac8. Proceedings of the National Academy of Sciences of the United States of America **102:** 17366-17371

Hu J, Mitchum MG, Barnaby N, Ayele BT, Ogawa M, Nam E, Lai WC, Hanada A, Alonso JM, Ecker JR (2008) Potential sites of bioactive gibberellin production during reproductive growth in Arabidopsis. The Plant Cell **20:** 320-336

Hu LL, Wan SB, Niu S, Shi XH, Li HP, Cai YD, Chou KC (2011) Prediction and analysis of protein palmitoylation sites. Biochimie **93:** 489-496

Huang K, Kang MH, Askew C, Kang R, Sanders SS, Wan J, Davis NG, Hayden MR (2010) Palmitoylation and function of glial glutamate transporter-1 is reduced in the YAC128 mouse model of Huntington disease. Neurobiology of Disease **40:** 207-215

Huang K, Sanders S, Singaraja R, Orban P, Cijsouw T, Arstikaitis P, Yanai A, Hayden MR, El-Husseini A (2009) Neuronal palmitoyl acyl transferases exhibit distinct substrate specificity. The FASEB Journal **23:** 2605-2615

Huang K, Yanai A, Kang R, Arstikaitis P, Singaraja RR, Metzler M, Mullard A, Haigh B, Gauthier-Campbell C, Gutekunst CA (2004) Huntingtin-interacting protein HIP14 is a palmitoyl transferase involved in palmitoylation and trafficking of multiple neuronal proteins. Neuron **44:** 977-986

Hundt M, Harada Y, De Giorgio L, Tanimura N, Zhang W, Altman A (2009) Palmitoylation-dependent plasma membrane transport but lipid raft-independent signaling by linker for activation of T cells. The Journal of Immunology **183:** 1685-1694

Hurst CH, Hemsley PA (2015) Current perspective on protein S-acylation in plants: more than just a fatty anchor? Journal of Experimental Botany**:** erv053

Hwang I, Sheen J, Müller B (2012) Cytokinin signaling networks. Annual Review of Plant Biology **63:** 353-380

Iqbal M, Ashraf M, Jamil A (2006) Seed enhancement with cytokinins: changes in growth and grain yield in salt stressed wheat plants. Plant Growth Regulation **50:** 29-39

Ivaldi C, Martin BR, Kieffer-Jaquinod S, Chapel A, Levade T, Garin J, Journet A (2012) Proteomic analysis of S-acylated proteins in human B cells reveals palmitoylation of the immune regulators CD20 and CD23. PLoS One **7:** e37187

Ivanov SS, Roy C (2013) Host lipidation: a mechanism for spatial regulation of *Legionella* effectors. Molecular Mechanisms in Legionella Pathogenesis. Springer, pp 135-154

Iwakawa H, Shinmyo A, Sekine M (2006) Arabidopsis *CDKA; 1*, a *cdc2* homologue, controls proliferation of generative cells in male gametogenesis. The Plant Journal **45:** 819-831

Izumi K, Nakagawa S, Kobayashi M, Oshio H, Sakurai A, Takahashi N (1988) Levels of IAA, cytokinins, ABA and ethylene in rice plants as affected by a gibberellin biosynthesis inhibitor, Uniconazole-P. Plant and Cell Physiology **29:** 97-104

Jacobsen SE, Olszewski NE (1993) Mutations at the SPINDLY locus of Arabidopsis alter gibberellin signal transduction. The Plant Cell **5:** 887-896

Javid MG, Sorooshzadeh A, Moradi F, Sanavy SAMM, Allahdadi I (2011) The role of phytohormones in alleviating salt stress in crop plants. Australian Journal of Crop Science **5:** 726

Jayakannan M, Bose J, Babourina O, Shabala S, Massart A, Poschenrieder C, Rengel Z (2015) The NPR1-dependent salicylic acid signalling pathway is pivotal for enhanced salt and oxidative stress tolerance in Arabidopsis. Journal of Experimental Botany **66:** 1865-1875

Jefferson RA (1987) Assaying chimeric genes in plants: the GUS gene fusion system. Plant Molecular Biology Reporter **5:** 387-405

Jennings BC, Nadolski MJ, Ling Y, Baker MB, Harrison ML, Deschenes RJ, Linder ME (2009) 2-Bromopalmitate and 2-(2-hydroxy-5-nitro-benzylidene)-benzo [b] thiophen-3-one inhibit DHHC-mediated palmitoylation *in vitro*. Journal of Lipid Research **50:** 233-242

Jones TL, Degtyarev MY, Backlund PS (1997) The stoichiometry of Gαs palmitoylation in its basal and activated states. Biochemistry **36:** 7185-7191

Jönsson H, Heisler MG, Shapiro BE, Meyerowitz EM, Mjolsness E (2006) An auxin-driven polarized transport model for phyllotaxis. Proceedings of the National Academy of Sciences **103:** 1633-1638

Josse E-M, Halliday KJ (2008) Skotomorphogenesis: the dark side of light signalling. Current Biology **18:** R1144-R1146

Kami C, Lorrain S, Hornitschek P, Fankhauser C (2010) Chapter two-light-regulated plant growth and development. Current Topics in Developmental Biology **91:** 29-66

Kamiya Y, García-Martínez JL (1999) Regulation of gibberellin biosynthesis by light. Current Opinion in Plant Biology **2:** 398-403

Kang J-y, Choi H-i, Im M-y, Kim SY (2002) Arabidopsis basic leucine zipper proteins that mediate stress-responsive abscisic acid signaling. The Plant Cell **14:** 343-357

Kang R, Wan J, Arstikaitis P, Takahashi H, Huang K, Bailey AO, Thompson JX, Roth AF, Drisdel RC, Mastro R (2008) Neural palmitoyl-proteomics reveals dynamic synaptic palmitoylation. Nature **456:** 904-909

Kato Y, Murakami S, Yamamoto Y, Chatani H, Kondo Y, Nakano T, Yokota A, Sato F (2004) The DNA-binding protease, CND41, and the degradation of ribulose-1, 5-bisphosphate carboxylase/oxygenase in senescent leaves of tobacco. Planta **220:** 97-104

Katsiarimpa A, Kalinowska K, Anzenberger F, Weis C, Ostertag M, Tsutsumi C, Schwechheimer C, Brunner F, Hückelhoven R, Isono E (2013) The deubiquitinating enzyme AMSH1 and the ESCRT-III subunit VPS2. 1 are required for autophagic degradation in Arabidopsis. The Plant Cell **25:** 2236-2252

Keith DJ, Sanderson JL, Gibson ES, Woolfrey KM, Robertson HR, Olszewski K,

Kang R, El-Husseini A, Dell'Acqua ML (2012) Palmitoylation of A-kinase anchoring protein 79/150 regulates dendritic endosomal targeting and synaptic plasticity mechanisms. The Journal of Neuroscience **32:** 7119-7136

Keller CA, Yuan X, Panzanelli P, Martin ML, Alldred M, Sassoè-Pognetto M, Lüscher B (2004) The γ2 subunit of GABAA receptors is a substrate for palmitoylation by GODZ. The Journal of Neuroscience **24:** 5881-5891

Khanna R, Kronmiller B, Maszle DR, Coupland G, Holm M, Mizuno T, Wu SH (2009) The Arabidopsis B-box zinc finger family. The Plant Cell **21:** 3416-3420

Kho YO, Baer J (1968) Observing pollen tubes by means of fluorescence. Euphytica **17:** 298-302

Kihara A, Kurotsu F, Sano T, Iwaki S, Igarashi Y (2005) Long-chain base kinase Lcb4 Is anchored to the membrane through its palmitoylation by Akr1. Molecular and Cellular Biology **25:** 9189-9197

Kim J, Yi H, Choi G, Shin B, Song PS, Choi G (2003) Functional characterization of phytochrome interacting factor 3 in phytochrome-mediated light signal transduction. The Plant Cell **15:** 2399-2407

Kim MG, da Cunha L, McFall AJ, Belkhadir Y, DebRoy S, Dangl JL, Mackey D (2005) Two Pseudomonas syringae type III effectors inhibit RIN4-regulated basal defense in Arabidopsis. Cell **121:** 749-759

King JJ, Stimart DP, Fisher RH, Bleecker AB (1995) A mutation altering auxin homeostasis and plant morphology in Arabidopsis. The Plant Cell **7:** 2023-2037

Kleuss C, Krause E (2003) Gαs is palmitoylated at the N-terminal glycine. The EMBO Journal **22:** 826-832

Koornneef M, Bentsink L, Hilhorst H (2002) Seed dormancy and germination. Current Opinion in Plant Biology **5:** 33-36

Koornneef M, Van der Veen J (1980) Induction and analysis of gibberellin sensitive mutants in *Arabidopsis thaliana* (L.) Heynh. Theoretical and Applied Genetics **58:** 257-263

Koshimizu K, Iwamura H (1986) Cytokinins. Chemistry of Plant Hormones**:** 153-199

Kraepiel Y, Rousselin P, Sotta B, Kerhoas L, Einhorn J, Caboche M, Miginiac E (1994) Analysis of phytochrome-and ABA-deficient mutants suggests that ABA degradation is controlled by light in *Nicotiana plumbaginifolia*. The Plant Journal **6:** 665-672

Kumar D (2014) Salicylic acid signaling in disease resistance. Plant Science **228:** 127-134

Kumar M, Wightman R, Atanassov I, Gupta A, Hurst CH, Hemsley PA, Turner S (2016) S-Acylation of the cellulose synthase complex is essential for its plasma membrane localization. Science **353:** 166-169

Kumari B, Kumar R, Kumar M (2014) PalmPred: an SVM based palmitoylation prediction method using sequence profile information. PloS One **9:** e89246

Kunihiro S, Hiramatsu T, Kawano T (2011) Involvement of salicylic acid signal transduction in aluminum-responsive oxidative burst in *Arabidopsis thaliana* cell suspension culture. Plant Signaling & Behavior **6:** 611-616

Kurayoshi M, Yamamoto H, Izumi S, Kikuchi A (2007) Post-translational

palmitoylation and glycosylation of Wnt-5a are necessary for its signalling. Biochemical Journal **402:** 515-523

Kurosawa E (1926) Experimental studies on the nature of the substance secreted by the" bakanae" fungus. Transactions, Natural History Society of Formosa **16:** 213-227

Kusnetsov V, Herrmann R, Kulaeva O, Oelmüller R (1998) Cytokinin stimulates and abscisic acid inhibits greening of etiolated Lupinus luteus cotyledons by affecting the expression of the light-sensitive protochlorophyllide oxidoreductase. Molecular and General Genetics **259:** 21-28

Lai J, Yu B, Cao Z, Chen Y, Wu Q, Huang J, Yang C (2015) Two homologous protein S-acyltransferases, PAT13 and PAT14, cooperatively regulate leaf senescence in Arabidopsis. Journal of Experimental Botany **66:** 6345-6353

Lakkaraju AK, Abrami L, Lemmin T, Blaskovic S, Kunz B, Kihara A, Dal Peraro M, van der Goot FG (2012) Palmitoylated calnexin is a key component of the ribosome–translocon complex. The EMBO Journal **31:** 1823-1835

Lam KK, Davey M, Sun B, Roth AF, Davis NG, Conibear E (2006) Palmitoylation by the DHHC protein Pfa4 regulates the ER exit of Chs3. The Journal of Cell Biology **174:** 19-25

Lane SR, Liu Y (1997) Characterization of the palmitoylation domain of SNAP-25. Journal of Neurochemistry **69:** 1864-1869

Lastdrager J, Hanson J, Smeekens S (2014) Sugar signals and the control of plant growth and development. Journal of Experimental Botany **65:** 799-807

Lavy M, Bracha-Drori K, Sternberg H, Yalovsky S (2002) A cell-specific, prenylation-independent mechanism regulates targeting of type II RACs. The Plant Cell **14:** 2431-2450

Lawrence DS, Zilfou JT, Smith CD (1999) Structure-activity studies of cerulenin analogues as protein palmitoylation inhibitors. Journal of Medicinal Chemistry **42:** 4932-4941

Laxmi A, Paul LK, Raychaudhuri A, Peters JL, Khurana JP (2006) Arabidopsis cytokinin-resistant mutant, *cnr1*, displays altered auxin responses and sugar sensitivity. Plant Molecular Biology **62:** 409-425

Leclercq J, Ranty B, Sanchez-Ballesta M-T, Li Z, Jones B, Jauneau A, Pech J-C, Latché A, Ranjeva R, Bouzayen M (2005) Molecular and biochemical characterization of LeCRK1, a ripening-associated tomato CDPK-related kinase. Journal of Experimental Botany **56:** 25-35

Lellis AD, Allen ML, Aertker AW, Tran JK, Hillis DM, Harbin CR, Caldwell C, Gallie DR, Browning KS (2010) Deletion of the eIFiso4G subunit of the Arabidopsis eIFiso4F translation initiation complex impairs health and viability. Plant Molecular Biology **74:** 249-263

Lemieux B, Miquel M, Somerville C (1990) Mutants of Arabidopsis with alterations in seed lipid fatty acid composition. Theoretical and Applied Genetics **80:** 234-240

Lemonidis K, Sanchez-Perez MC, Chamberlain LH (2015) Identification of a novel sequence motif recognized by the ankyrin repeat domain of zDHHC17/13 S-acyltransferases. Journal of Biological Chemistry **290:** 21939-21950

Leshem Y, Johnson C, Wuest SE, Song X, Ngo QA, Grossniklaus U, Sundaresan V

(2012) Molecular characterization of the glauce mutant: a central cell–specific function is required for double fertilization in Arabidopsis. The Plant Cell **24:** 3264-3277

Levental I, Lingwood D, Grzybek M, Coskun Ü, Simons K (2010) Palmitoylation regulates raft affinity for the majority of integral raft proteins. Proceedings of the National Academy of Sciences **107:** 22050-22054

Li C, Schilmiller AL, Liu G, Lee GI, Jayanty S, Sageman C, Vrebalov J, Giovannoni JJ, Yagi K, Kobayashi Y (2005) Role of β-oxidation in jasmonate biosynthesis and systemic wound signaling in tomato. The Plant Cell **17:** 971-986

Li F, Vierstra RD (2014) Arabidopsis ATG11, a scaffold that links the ATG1-ATG13 kinase complex to general autophagy and selective mitophagy. Autophagy **10:** 1466-1467

Li K, Gao Z, He H, Terzaghi W, Fan L-M, Deng XW, Chen H (2015) Arabidopsis DET1 represses photomorphogenesis in part by negatively regulating DELLA protein abundance in darkness. Molecular Plant **8:** 622-630

Li P, Zhou H, Shi X, Yu B, Zhou Y, Chen S, Wang Y, Peng Y, Meyer RC, Smeekens SC (2014) The ABI4-induced Arabidopsis ANAC060 transcription factor attenuates ABA signaling and renders seedlings sugar insensitive when present in the nucleus. PLoS Genet **10:** e1004213

Li Y, Martin BR, Cravatt BF, Hofmann SL (2012) DHHC5 protein palmitoylates flotillin-2 and is rapidly degraded on induction of neuronal differentiation in cultured cells. Journal of Biological Chemistry **287:** 523-530

Li Y, Scott RJ, Doughty J, Grant M, Qi B (2015) Protein S-acyltransferase 14: a specific role for palmitoylation in leaf senescence in Arabidopsis. Plant Physiology: pp. 00448.02015

Li Y, Zheng L, Corke F, Smith C, Bevan MW (2008) Control of final seed and organ size by the DA1 gene family in *Arabidopsis thaliana*. Genes & Development **22:** 1331-1336

Li-Beisson Y, Shorrosh B, Beisson F, Andersson MX, Arondel V, Bates PD, Baud S, Bird D, DeBono A, Durrett TP (2013) Acyl-lipid metabolism. The Arabidopsis Book **11:** e0161

Lim PO, Kim HJ, Nam HG (2007) Leaf senescence. Annual Review of Plant Biology **58:** 115-136

Lim PO, Woo HR, Nam HG (2003) Molecular genetics of leaf senescence in Arabidopsis. Trends in Plant Science **8:** 272-278

Linder ME, Deschenes RJ (2007) Palmitoylation: policing protein stability and traffic. Nature reviews Molecular Cell Biology **8:** 74-84

Liu J, Zhong S, Guo X, Hao L, Wei X, Huang Q, Hou Y, Shi J, Wang C, Gu H, Qu LJ (2013) Membrane-bound RLCKs LIP1 and LIP2 are essential male factors controlling male-female attraction in Arabidopsis. Current Biology **23:** 993-998

Liu Y, Fisher DA, Storm DR (1993) Analysis of the palmitoylation and membrane targeting domain of neuromodulin (GAP-43) by site-specific mutagenesis. Biochemistry **32:** 10714-10719

Liu Y, Ye N, Liu R, Chen M, Zhang J (2010) H_2O_2 mediates the regulation of ABA

catabolism and GA biosynthesis in Arabidopsis seed dormancy and germination. Journal of Experimental Botany**:** erq125

Liu Z, Makaroff CA (2006) Arabidopsis separase AESP is essential for embryo development and the release of cohesin during meiosis. The Plant Cell **18:** 1213-1225

Ljung K, Nemhauser JL, Perata P (2015) New mechanistic links between sugar and hormone signalling networks. Current Opinion in Plant Biology **25:** 130-137

Lobo S, Greentree WK, Linder ME, Deschenes RJ (2002) Identification of a Ras palmitoyltransferase in *Saccharomyces cerevisiae*. Journal of Biological Chemistry **277:** 41268-41273

Lochmanová G, Zdráhal Z, Konečná H, Koukalová Š, Malbeck J, Souček P, Válková M, Kiran NS, Brzobohatý B (2008) Cytokinin-induced photomorphogenesis in dark-grown Arabidopsis: a proteomic analysis. Journal of Experimental Botany **59:** 3705-3719

Loisel TP, Adam L, Hebert TE, Bouvier M (1996) Agonist stimulation increases the turnover rate of β2AR-bound palmitate and promotes receptor depalmitoylation. Biochemistry **35:** 15923-15932

López-Barragán MJ, Lemieux J, Quiñones M, Williamson KC, Molina-Cruz A, Cui K, Barillas-Mury C, Zhao K, Su XZ (2011) Directional gene expression and antisense transcripts in sexual and asexual stages of *Plasmodium falciparum*. BMC Genomics **12:** 1

Lor VS, Olszewski NE (2015) GA signalling and cross-talk with other signalling pathways. Essays in Biochemistry **58:** 49-60

Lu D, Sun HQ, Wang H, Barylko B, Fukata Y, Fukata M, Albanesi JP, Yin HL (2012) Phosphatidylinositol 4-kinase IIα is palmitoylated by Golgi-localized palmitoyltransferases in cholesterol-dependent manner. Journal of Biological Chemistry **287:** 21856-21865

Lu H, Zhang C, Albrecht U, Shimizu R, Bowman K (2013) Overexpression of a citrus NDR1 ortholog increases disease resistance in Arabidopsis. Frontiers in Plant Science **4:** 157

Lu Y, Chanroj S, Zulkifli L, Johnson MA, Uozumi N, Cheung A, Sze H (2011) Pollen tubes lacking a pair of K^+ transporters fail to target ovules in Arabidopsis. The Plant Cell **23:** 81-93

Luan S (2009) The CBL–CIPK network in plant calcium signaling. Trends in Plant Science **14:** 37-42

Ma H (2005) Molecular genetic analyses of microsporogenesis and microgametogenesis in flowering plants. Annual Review of Plant Biology **56:** 393-434

Maciaszczyk-Dziubinska E, Migocka M, Wawrzycka D, Markowska K, Wysocki R (2014) Multiple cysteine residues are necessary for sorting and transport activity of the arsenite permease Acr3p from *Saccharomyces cerevisiae*. Biochimica et Biophysica Acta (BBA)-Biomembranes **1838:** 747-755

Maeda A, Okano K, Park PSH, Lem J, Crouch RK, Maeda T, Palczewski K (2010) Palmitoylation stabilizes unliganded rod opsin. Proceedings of the National Academy of Sciences **107:** 8428-8433

Magnani E, Bartling L, Hake S (2006) From Gateway to MultiSite Gateway in one recombination event. BMC Molecular Biology **7**: 1

Maisse C, Rossin A, Cahuzac N, Paradisi A, Klein C, Haillot M-L, Hérincs Z, Mehlen P, Hueber A-O (2008) Lipid raft localization and palmitoylation: identification of two requirements for cell death induction by the tumor suppressors UNC5H. Experimental Cell Research **314:** 2544-2552

Marin EP, Derakhshan B, Lam TT, Davalos A, Sessa WC (2012) Endothelial cell palmitoylproteomic identifies novel lipid-modified targets and potential substrates for protein acyl transferases. Circulation Research **110:** 1336-1344

Martin BR, Cravatt BF (2009) Large-scale profiling of protein palmitoylation in mammalian cells. Nature Methods **6:** 135-138

Martin BR, Wang C, Adibekian A, Tully SE, Cravatt BF (2012) Global profiling of dynamic protein palmitoylation. Nature Methods **9:** 84-89

Martínez-Andújar C, Ordiz MI, Huang Z, Nonogaki M, Beachy RN, Nonogaki H (2011) Induction of 9-cis-epoxycarotenoid dioxygenase in *Arabidopsis thaliana* seeds enhances seed dormancy. Proceedings of the National Academy of Sciences **108:** 17225-17229

Mattoo AK, Edelman M (1987) Intramembrane translocation and posttranslational palmitoylation of the chloroplast 32-kDa herbicide-binding protein. Proceedings of the National Academy of Sciences **84:** 1497-1501

McCann MC, Roberts K, Carpita NC (2001) Plant cell growth and elongation. eLS

McCormick PJ, Dumaresq-Doiron K, Pluviose AS, Pichette V, Tosato G, Lefrancois S (2008) Palmitoylation controls recycling in lysosomal sorting and trafficking. Traffic **9:** 1984-1997

McCormick S (2004) Control of male gametophyte development. The Plant Cell **16:** S142-S153

McFarlane HE, Döring A, Persson S (2014) The cell biology of cellulose synthesis. Annual Review of Plant Biology **65:** 69-94

Mendiondo GM, Medhurst A, van Roermund CW, Zhang X, Devonshire J, Scholefield D, Fernández J, Axcell B, Ramsay L, Waterham HR (2014) Barley has two peroxisomal ABC transporters with multiple functions in β-oxidation. Journal of Experimental Botany **65:** 4833-4847

Mercier R, Mézard C, Jenczewski E, Macaisne N, Grelon M (2015) The molecular biology of meiosis in plants. Annual Review of Plant Biology **66:** 297-327

Merino MC, Zamponi N, Vranych CV, Touz MC, Ropolo AS (2014) Identification of *Giardia lamblia* DHHC proteins and the role of protein S-palmitoylation in the encystation process. PLoS Neglected Tropical Diseases **8(7)**: e2997.

Merrick BA, Dhungana S, Williams JG, Aloor JJ, Peddada S, Tomer KB, Fessler MB (2011) Proteomic profiling of S-acylated macrophage proteins identifies a role for palmitoylation in mitochondrial targeting of phospholipid scramblase 3. Molecular & Cellular Proteomics **10:** M110. 006007

Mill P, Lee AW, Fukata Y, Tsutsumi R, Fukata M, Keighren M, Porter RM, McKie L, Smyth I, Jackson IJ (2009) Palmitoylation regulates epidermal homeostasis and hair follicle differentiation. PLos Genetics **5(11)**: e1000748

Miller CO, Skoog F, Von Saltza MH, Strong F (1955) Kinetin, a cell division factor from deoxyribonucleic acid. Journal of the American Chemical Society **77:** 1392-1392

Miransari M, Riahi H, Eftekhar F, Minaie A, Smith D (2013) Improving soybean (*Glycine max L.*) N2 fixation under stress. Journal of Plant Growth Regulation **32:** 909-921

Miransari M, Smith D (2014) Plant hormones and seed germination. Environmental and Experimental Botany **99:** 110-121

Mitchell DA, Farh L, Marshall TK, Deschenes RJ (1994) A polybasic domain allows nonprenylated Ras proteins to function in *Saccharomyces cerevisiae*. Journal of Biological Chemistry **269:** 21540-21546

Mitchell DA, Vasudevan A, Linder ME, Deschenes RJ (2006) Thematic review series: lipid posttranslational modifications. Protein palmitoylation by a family of DHHC protein S-acyltransferases. Journal of Lipid Research **47:** 1118-1127

Miura GI, Buglino J, Alvarado D, Lemmon MA, Resh MD, Treisman JE (2006) Palmitoylation of the EGFR ligand Spitz by Rasp increases Spitz activity by restricting its diffusion. Developmental Cell **10:** 167-176

Mockler T, Yang H, Yu X, Parikh D, Cheng YC, Dolan S, Lin C (2003) Regulation of photoperiodic flowering by Arabidopsis photoreceptors. Proceedings of the National Academy of Sciences **100:** 2140-2145

Mönke G, Seifert M, Keilwagen J, Mohr M, Grosse I, Hähnel U, Junker A, Weisshaar B, Conrad U, Bäumlein H (2012) Toward the identification and regulation of the *Arabidopsis thaliana* ABI3 regulon. Nucleic Acids Research **40:** 8240-8254

Montoro AG, Ramirez SC, Quiroga R, Taubas JV (2011) Specificity of transmembrane protein palmitoylation in yeast. PLoS One **6:** e16969

Moore B, Zhou L, Rolland F, Hall Q, Cheng WH, Liu YX, Hwang I, Jones T, Sheen J (2003) Role of the Arabidopsis glucose sensor HXK1 in nutrient, light, and hormonal signaling. Science **300:** 332-336

Mori T, Kuroiwa H, Higashiyama T, Kuroiwa T (2006) GENERATIVE CELL SPECIFIC 1 is essential for angiosperm fertilization. Nature Cell Biology **8:** 64-71

Morris K, Mackerness SAH, Page T, John CF, Murphy AM, Carr JP, Buchanan-Wollaston V (2000) Salicylic acid has a role in regulating gene expression during leaf senescence. The Plant Journal **23:** 677-685

Motoki K, Kume H, Oda A, Tamaoka A, Hosaka A, Kametani F, Araki W (2012) Neuronal β-amyloid generation is independent of lipid raft association of β-secretase BACE1: analysis with a palmitoylation-deficient mutant. Brain and Behavior **2:** 270-282

Mukai J, Dhilla A, Drew LJ, Stark KL, Cao L, MacDermott AB, Karayiorgou M, Gogos JA (2008) Palmitoylation-dependent neurodevelopmental deficits in a mouse model of 22q11 microdeletion. Nature Neuroscience **11:** 1302-1310

Mukai J, Liu H, Burt RA, Swor DE, Lai WS, Karayiorgou M, Gogos JA (2004) Evidence that the gene encoding ZDHHC8 contributes to the risk of schizophrenia.

Nature Genetics **36:** 725-731

Mumby SM, Kleuss C, Gilman AG (1994) Receptor regulation of G-protein palmitoylation. Proceedings of the National Academy of Sciences **91:** 2800-2804

Nambara E, Okamoto M, Tatematsu K, Yano R, Seo M, Kamiya Y (2010) Abscisic acid and the control of seed dormancy and germination. Seed Science Research **20:** 55-67

Neff MM, Fankhauser C, Chory J (2000) Light: an indicator of time and place. Genes & Development **14:** 257-271

Ni BR, Bradford KJ (1993) Germination and dormancy of abscisic acid-and gibberellin-deficient mutant tomato (*Lycopersicon esculentum*) seeds (sensitivity of germination to abscisic acid, gibberellin, and water potential). Plant Physiology **101:** 607-617

Nichols CB, Ost KS, Grogan DP, Pianalto K, Hasan S, Alspaugh JA (2015) Impact of protein palmitoylation on the virulence potential of *Cryptococcus neoformans*. Eukaryotic Cell **14:** 626-635

Nishimura C, Ohashi Y, Sato S, Kato T, Tabata S, Ueguchi C (2004) Histidine kinase homologs that act as cytokinin receptors possess overlapping functions in the regulation of shoot and root growth in Arabidopsis. The Plant Cell 16: 1365-1377

Noguchi T, Fujioka S, Takatsuto S, Sakurai A, Yoshida S, Li J, Chory J (1999) Arabidopsis *det2* is defective in the conversion of (24R)-24-methylcholest-4-en-3-one to (24R)-24-methyl-5α-cholestan-3-one in brassinosteroid biosynthesis. Plant Physiology **120:** 833-840

Noodén LD (2012) Senescence and aging in plants. Elsevier

Novák O, Hauserová E, Amakorová P, Doležal K, Strnad M (2008) Cytokinin profiling in plant tissues using ultra-performance liquid chromatography–electrospray tandem mass spectrometry. Phytochemistry **69:** 2214-2224

Nyathi Y, Baker A (2006) Plant peroxisomes as a source of signalling molecules. Biochimica et Biophysica Acta (BBA)-Molecular Cell Research **1763:** 1478-1495

Oddi S, Dainese E, Sandiford S, Fezza F, Lanuti M, Chiurchiù V, Totaro A, Catanzaro G, Barcaroli D, De Laurenzi V (2012) Effects of palmitoylation of Cys415 in helix 8 of the CB1 cannabinoid receptor on membrane localization and signalling. British Journal of Pharmacology **165:** 2635-2651

Ogawa M, Hanada A, Yamauchi Y, Kuwahara A, Kamiya Y, Yamaguchi S (2003) Gibberellin biosynthesis and response during Arabidopsis seed germination. The Plant Cell **15:** 1591-1604

Oh E, Kang H, Yamaguchi S, Park J, Lee D, Kamiya Y, Choi G (2009) Genome-wide analysis of genes targeted by PHYTOCHROME INTERACTING FACTOR 3-LIKE5 during seed germination in Arabidopsis. The Plant Cell **21:** 403-419

Oh Y, Jeon Y, Hong G, Kim I, Woo H, Jung Y (2012) Regulation in the targeting of TRAIL receptor 1 to cell surface via GODZ for TRAIL sensitivity in tumor cells. Cell Death & Differentiation **19:** 1196-1207

Ohno Y, Kashio A, Ogata R, Ishitomi A, Yamazaki Y, Kihara A (2012) Analysis of substrate specificity of human DHHC protein acyltransferases using a yeast expression system. Molecular Biology of the Cell **23:** 4543-4551

Ohno Y, Kihara A, Sano T, Igarashi Y (2006) Intracellular localization and tissue-specific distribution of human and yeast DHHC cysteine-rich domain-containing proteins. Biochimica et Biophysica Acta (BBA)-Molecular and Cell Biology of Lipids **1761:** 474-483

Ohyama T, Verstreken P, Ly CV, Rosenmund T, Rajan A, Tien A-C, Haueter C, Schulze KL, Bellen HJ (2007) Huntingtin-interacting protein 14, a palmitoyl transferase required for exocytosis and targeting of CSP to synaptic vesicles. The Journal of Cell Biology **179:** 1481-1496

Okuda S, Tsutsui H, Shiina K, Sprunck S, Takeuchi H, Yui R, Kasahara RD, Hamamura Y, Mizukami A, Susaki D (2009) Defensin-like polypeptide LUREs are pollen tube attractants secreted from synergid cells. Nature **458:** 357-361

Olmedo-Monfil V, Durán-Figueroa N, Arteaga-Vázquez M, Demesa-Arévalo E, Autran D, Grimanelli D, Slotkin RK, Martienssen RA, Vielle-Calzada J-P (2010) Control of female gamete formation by a small RNA pathway in Arabidopsis. Nature **464:** 628-632

Otani M, Meguro S, Gondaira H, Hayashi M, Saito M, Han DS, Inthima P, Supaibulwatana K, Mori S, Jikumaru Y (2013) Overexpression of the gibberellin 2-oxidase gene from Torenia fournieri induces dwarf phenotypes in the liliaceous monocotyledon *Tricyrtis sp.* Journal of Plant Physiology **170:** 1416-1423

Palanivelu R, Brass L, Edlund AF, Preuss D (2003) Pollen tube growth and guidance is regulated by POP2, an Arabidopsis gene that controls GABA levels. Cell **114:** 47-59

Palanivelu R, Preuss D (2006) Distinct short-range ovule signals attract or repel *Arabidopsis thaliana* pollen tubes *in vitro*. BMC Plant Biology **6:** 1

Panoli A, Martin MV, Alandete-Saez M, Simon M, Neff C, Swarup R, Bellido A, Yuan L, Pagnussat GC, Sundaresan V (2015) Auxin import and local auxin biosynthesis are required for mitotic divisions, cell expansion and cell specification during female gametophyte development in *Arabidopsis thaliana*. PLoS One **10:** e0126164

Parasher A, Varma S (1988) Effect of pre-sowing seed soaking in gibberellic-acid on growth of wheat (triticum-aestivum l) under different saline conditions. Indian Journal Of Experimental Biology **26:** 473-475

Park S, Patterson EE, Cobb J, Audhya A, Gartenberg MR, Fox CA (2011) Palmitoylation controls the dynamics of budding-yeast heterochromatin via the telomere-binding protein Rif1. Proceedings of the National Academy of Sciences **108:** 14572-14577

Patterson SI, Skene J (1995) Inhibition of dynamic protein palmitoylation in intact cells with tunicamycin. Methods in Enzymology **250:** 284

Penfield S, Rylott EL, Gilday AD, Graham S, Larson TR, Graham IA (2004) Reserve mobilization in the Arabidopsis endosperm fuels hypocotyl elongation in the dark, is independent of abscisic acid, and requires PHOSPHOENOLPYRUVATE CARBOXYKINASE1. The Plant Cell **16:** 2705-2718

Percherancier Y, Planchenault T, Valenzuela-Fernandez A, Virelizier J-L, Arenzana-

Seisdedos F, Bachelerie F (2001) Palmitoylation-dependent control of degradation, life span, and membrane expression of the CCR5 receptor. Journal of Biological Chemistry **276:** 31936-31944

Pinfield-Wells H, Rylott EL, Gilday AD, Graham S, Job K, Larson TR, Graham IA (2005) Sucrose rescues seedling establishment but not germination of Arabidopsis mutants disrupted in peroxisomal fatty acid catabolism. The Plant Journal **43:** 861-872

Ponimaskin E, Behn H, Adarichev V, Voyno-Yasenetskaya TA, Offermanns S, Schmidt MF (2000) Acylation of Gα13 is important for its interaction with thrombin receptor, transforming activity and actin stress fiber formation. FEBS Letters **478:** 173-177

Ponimaskin E, Dityateva G, Ruonala MO, Fukata M, Fukata Y, Kobe F, Wouters FS, Delling M, Bredt DS, Schachner M (2008) Fibroblast growth factor-regulated palmitoylation of the neural cell adhesion molecule determines neuronal morphogenesis. The Journal of Neuroscience **28:** 8897-8907

Ponimaskin E, Harteneck C, Schultz G, Schmidt MF (1998) A cysteine-11 to serine mutant of Gα12 impairs activation through the thrombin receptor. FEBS Letters **429:** 370-374

Porra R, Thompson W, Kriedemann P (1989) Determination of accurate extinction coefficients and simultaneous equations for assaying chlorophylls a and b extracted with four different solvents: verification of the concentration of chlorophyll standards by atomic absorption spectroscopy. Biochimica et Biophysica Acta (BBA)-Bioenergetics **975:** 384-394

Prakash L, Prathapasenan G (1990) NaCl-and gibberellic acid-induced changes in the content of auxin and the activities of cellulase and pectin lyase during leaf growth in rice (*Oryza sativa*). Annals of Botany **65:** 251-257

Pryciak PM, Hartwell LH (1996) AKR1 encodes a candidate effector of the G beta gamma complex in the Saccharomyces cerevisiae pheromone response pathway and contributes to control of both cell shape and signal transduction. Molecular and Cellular Biology **16:** 2614-2626

Qi B, Doughty J, Hooley R (2013) A Golgi and tonoplast localized S-acyl transferase is involved in cell expansion, cell division, vascular patterning and fertility in Arabidopsis. New Phytologist **200:** 444-456

Qin Y, Zhao L, Skaggs MI, Andreuzza S, Tsukamoto T, Panoli A, Wallace KN, Smith S, Siddiqi I, Yang Z (2014) ACTIN-RELATED PROTEIN6 regulates female meiosis by modulating meiotic gene expression in Arabidopsis. The Plant Cell **26:** 1612-1628

Quettier A-L, Eastmond PJ (2009) Storage oil hydrolysis during early seedling growth. Plant Physiology and Biochemistry **47:** 485-490

Raíces M, Ulloa RM, MacIntosh GC, Crespi M, Téllez-Iñón MT (2003) StCDPK1 is expressed in potato stolon tips and is induced by high sucrose concentration. Journal of Experimental Botany **54:** 2589-2591

Rajjou L, Duval M, Gallardo K, Catusse J, Bally J, Job C, Job D (2012) Seed germination and vigor. Annual Review of Plant Biology **63:** 507-533

Rajjou L, Gallardo K, Debeaujon I, Vandekerckhove J, Job C, Job D (2004) The effect of α-amanitin on the Arabidopsis seed proteome highlights the distinct roles of stored and neosynthesized mRNAs during germination. Plant Physiology **134:** 1598-1613

Rashotte AM, Carson SD, To JP, Kieber JJ (2003) Expression profiling of cytokinin action in Arabidopsis. Plant Physiology **132**: 1998-2011

Raymond FL, Tarpey PS, Edkins S, Tofts C, O'Meara S, Teague J, Butler A, Stevens C, Barthorpe S, Buck G (2007) Mutations in *ZDHHC9*, which encodes a palmitoyltransferase of NRAS and HRAS, cause X-linked mental retardation associated with a marfanoid habitus. The American Journal of Human Genetics **80:** 982-987

Ren J, Wen L, Gao X, Jin C, Xue Y, Yao X (2008) CSS-Palm 2.0: an updated software for palmitoylation sites prediction. Protein Engineering Design and Selection **21:** 639-644

Resh MD (2006) Palmitoylation of ligands, receptors, and intracellular signaling molecules. Science Signaling **2006:** re14-re14

Richmond AE, Lang A (1957) Effect of kinetin on protein content and survival of detached Xanthium leaves. Science **125:** 650-651

Richmond TA, Bleecker AB (1999) A defect in β-oxidation causes abnormal inflorescence development in Arabidopsis. The Plant Cell **11:** 1911-1923

Riefler M, Novak O, Strnad M, Schmülling T (2006) Arabidopsis cytokinin receptor mutants reveal functions in shoot growth, leaf senescence, seed size, germination, root development, and cytokinin metabolism. The Plant Cell **18:** 40-54

Rizzini L, Favory J-J, Cloix C, Faggionato D, O'Hara A, Kaiserli E, Baumeister R, Schäfer E, Nagy F, Jenkins GI (2011) Perception of UV-B by the Arabidopsis UVR8 protein. Science **332:** 103-106

Roberts IN, Caputo C, Criado MV, Funk C (2012) Senescence-associated proteases in plants. Physiologia Plantarum **145:** 130-139

Robinson LJ, Busconi L, Michel T (1995) Agonist-modulated palmitoylation of endothelial nitric oxide synthase. Journal of Biological Chemistry **270:** 995-998

Rocks O, Gerauer M, Vartak N, Koch S, Huang Z-P, Pechlivanis M, Kuhlmann J, Brunsveld L, Chandra A, Ellinger B (2010) The palmitoylation machinery is a spatially organizing system for peripheral membrane proteins. Cell **141:** 458-471

Rocks O, Peyker A, Kahms M, Verveer PJ, Koerner C, Lumbierres M, Kuhlmann J, Waldmann H, Wittinghofer A, Bastiaens PI (2005) An acylation cycle regulates localization and activity of palmitoylated Ras isoforms. Science **307:** 1746-1752

Rodriguez-Enriquez M, Mehdi S, Dickinson H, Grant-Downton R (2013) A novel method for efficient in vitro germination and tube growth of *Arabidopsis thaliana* pollen. New Phytologist **197:** 668-679

Rogers HJ (2013) From models to ornamentals: how is flower senescence regulated? Plant Molecular Biology **82:** 563-574

Rogers HJ (2015) Senescence-associated programmed cell death. Plant Programmed Cell Death. Springer, pp 203-233

Rook F, Hadingham SA, Li Y, Bevan MW (2006) Sugar and ABA response pathways and the control of gene expression. Plant, Cell & Environment **29:** 426-434

Rossin A, Derouet M, Abdel-Sater F, Hueber A (2009) Palmitoylation of the TRAIL receptor DR4 confers an efficient TRAIL-induced cell death signalling. Biochemical Journal **419:** 185-192

Roth AF, Feng Y, Chen L, Davis NG (2002) The yeast DHHC cysteine-rich domain protein Akr1p is a palmitoyl transferase. The Journal of Cell Biology **159:** 23-28

Roth AF, Papanayotou I, Davis NG (2011) The yeast kinase Yck2 has a tripartite palmitoylation signal. Molecular Biology of the Cell **22:** 2702-2715

Roth AF, Wan J, Bailey AO, Sun B, Kuchar JA, Green WN, Phinney BS, Yates JR, Davis NG (2006) Global analysis of protein palmitoylation in yeast. Cell **125:** 1003-1013

Ruan Y-L (2014) Sucrose metabolism: gateway to diverse carbon use and sugar signaling. Annual Review of Plant Biology **65:** 33-67

Running MP (2014) The role of lipid post-translational modification in plant developmental processes. Regulation of Cell Fate Determination in Plants**:** 76

Ryan E, Grierson CS, Cavell A, Steer M, Dolan L (1998) TIP1 is required for both tip growth and non-tip growth in Arabidopsis. New Phytologist **138:** 49-58

Rylott EL, Eastmond PJ, Gilday AD, Slocombe SP, Larson TR, Baker A, Graham IA (2006) The *Arabidopsis thaliana* multifunctional protein gene (MFP2) of peroxisomal β-oxidation is essential for seedling establishment. The Plant Journal **45:** 930-941

Rylott EL, Rogers CA, Gilday AD, Edgell T, Larson TR, Graham IA (2003) Arabidopsis mutants in short-and medium-chain acyl-CoA oxidase activities accumulate acyl-CoAs and reveal that fatty acid β-oxidation is essential for embryo development. Journal of Biological Chemistry **278:** 21370-21377

Saibo NJ, Vriezen WH, Beemster GT, Van Der Straeten D (2003) Growth and stomata development of Arabidopsis hypocotyls are controlled by gibberellins and modulated by ethylene and auxins. The Plant Journal **33:** 989-1000

Sairanen I, Novák O, Pěnčík A, Ikeda Y, Jones B, Sandberg G, Ljung K (2012) Soluble carbohydrates regulate auxin biosynthesis via PIF proteins in Arabidopsis. The Plant Cell **24:** 4907-4916

Sakakibara H (2006) Cytokinins: activity, biosynthesis, and translocation. Annual Review of Plant Biology. **57:** 431-449

Saleem AN, Chen YH, Baek HJ, Hsiao YW, Huang HW, Kao HJ, Liu KM, Shen LF, Song IW, Tu CPD (2010) Mice with alopecia, osteoporosis, and systemic amyloidosis due to mutation in *ZDHHC13*, a gene coding for palmitoyl acyltransferase. PLoS Genetics **6:** e1000985

Samuel MA, Chong YT, Haasen KE, Aldea-Brydges MG, Stone SL, Goring DR (2009) Cellular pathways regulating responses to compatible and self-incompatible pollen in Brassica and Arabidopsis stigmas intersect at Exo70A1, a putative component of the exocyst complex. The Plant Cell **21:** 2655-2671

Sanders PM, Bui AQ, Weterings K, McIntire K, Hsu YC, Lee PY, Truong MT, Beals T, Goldberg R (1999) Anther developmental defects in *Arabidopsis thaliana*

male-sterile mutants. Sexual Plant Reproduction **11:** 297-322

Schiefelbein J, Galway M, Masucci J, Ford S (1993) Pollen tube and root-hair tip growth is disrupted in a mutant of *Arabidopsis thaliana*. Plant Physiology **103:** 979-985

Schilmiller AL, Koo AJ, Howe GA (2007) Functional diversification of acyl-coenzyme A oxidases in jasmonic acid biosynthesis and action. Plant Physiology **143:** 812-824

Schippers JH, Jing HC, Hille J, Dijkwel PP (2007) Developmental and hormonal control of leaf senescence. Senescence Processes in Plants**:** 145-170

Schmick M, Kraemer A, Bastiaens PI (2015) Ras moves to stay in place. Trends in Cell Biology **25:** 190-197

Schmidt MF, Schlesinger MJ (1979) Fatty acid binding to vesicular stomatitis virus glycoprotein: a new type of post-translational modification of the viral glycoprotein. Cell **17:** 813-819

Scott RJ, Spielman M, Dickinson HG (2004) Stamen structure and function. The Plant Cell **16:** S46-S60

Shani E, Yanai O, Ori N (2006) The role of hormones in shoot apical meristem function. Current Opinion in Plant Biology **9:** 484-489

Shapiro AD, Zhang C (2001) The role of NDR1 in avirulence gene-directed signaling and control of programmed cell death in Arabidopsis. Plant Physiology **127:** 1089-1101

Sharma C, Rabinovitz I, Hemler ME (2012) Palmitoylation by DHHC3 is critical for the function, expression, and stability of integrin α6β4. Cellular and Molecular Life Sciences **69:** 2233-2244

Shchedrina VA, Everley RA, Zhang Y, Gygi SP, Hatfield DL, Gladyshev VN (2011) Selenoprotein K binds multiprotein complexes and is involved in the regulation of endoplasmic reticulum homeostasis. Journal of Biological Chemistry **286:** 42937-42948

Shi SP, Sun XY, Qiu JD, Suo SB, Chen X, Huang SY, Liang RP (2013) The prediction of palmitoylation site locations using a multiple feature extraction method. Journal of Molecular Graphics and Modelling **40:** 125-130

Shin DH, Kim TL, Cho MH, Lee SW, Bhoo SH (2015) Characterization of Arabidopsis mutants insensitive to high sugar concentrations. Journal of the Korean Society for Applied Biological Chemistry **58:** 741-744

Shinkle JR (1986) Photobiology of phytochrome-mediated growth responses in sections of stem tissue from etiolated oats and corn. Plant Physiology **81:** 533-537

Shmueli A, Segal M, Sapir T, Tsutsumi R, Noritake J, Bar A, Sapoznik S, Fukata Y, Orr I, Fukata M (2010) Ndel1 palmitoylation: a new mean to regulate cytoplasmic dynein activity. The EMBO Journal **29:** 107-119

Shulaev V, Silverman P, Raskin I (1997) Airborne signalling by methyl salicylate in plant pathogen resistance. Nature **385**:718-721

Siloto RM, Findlay K, Lopez-Villalobos A, Yeung EC, Nykiforuk CL, Moloney MM (2006) The accumulation of oleosins determines the size of seed oilbodies in Arabidopsis. The Plant Cell **18:** 1961-1974

Silverstein KA, Moskal WA, Wu HC, Underwood BA, Graham MA, Town CD, VandenBosch KA (2007) Small cysteine-rich peptides resembling antimicrobial peptides have been under-predicted in plants. The Plant Journal **51:** 262-280

Silvius JR, l'Heureux F (1994) Fluorometric evaluation of the affinities of isoprenylated peptides for lipid bilayers. Biochemistry **33:** 3014-3022

Singaraja RR, Kang MH, Vaid K, Sanders SS, Vilas GL, Arstikaitis P, Coutinho J, Drisdel RC, El-Husseini AED, Green WN (2009) Palmitoylation of ATP-binding cassette transporter A1 is essential for its trafficking and function. Circulation Research **105:** 138-147

Smeekens S, Hellmann HA (2014) Sugar sensing and signaling in plants. Frontiers in Plant Science **5**

Smeekens S, Ma J, Hanson J, Rolland F (2010) Sugar signals and molecular networks controlling plant growth. Current Opinion in Plant Biology **13:** 273-278

Smotrys JE, Linder ME (2004) Palmitoylation of intracellular signaling proteins: regulation and function. Annual Review of Biochemistry **73:** 559-587

Smotrys JE, Schoenfish MJ, Stutz MA, Linder ME (2005) The vacuolar DHHC-CRD protein Pfa3p is a protein acyltransferase for Vac8p. The Journal of Cell Biology **170:** 1091-1099

Song IW, Li WR, Chen LY, Shen LF, Liu KM, Yen JJ, Chen YJ, Chen YJ, Kraus VB, Wu JY (2014) Palmitoyl acyltransferase, ZDHHC13, facilitates bone mass acquisition by regulating postnatal epiphyseal development and endochondral ossification: a mouse model. PLoS One **9:** e92194

Song J, Dohlman HG (1996) Partial constitutive activation of pheromone responses by a palmitoylation-site mutant of a G protein α subunit in yeast. Biochemistry **35:** 14806-14817

Song J, Hirschman J, Gunn K, Dohlman HG (1996) Regulation of membrane and subunit interactions by N-myristoylation of a G protein α subunit in yeast. Journal of Biological Chemistry **271:** 20273-20283

Sorek N, Poraty L, Sternberg H, Bar E, Lewinsohn E, Yalovsky S (2007) Activation status-coupled transient S acylation determines membrane partitioning of a plant Rho-related GTPase. Molecular and Cellular Biology **27:** 2144-2154

Soung YH, Chung J (2011) Curcumin inhibition of the functional interaction between integrin α6β4 and the epidermal growth factor receptor. Molecular Cancer Therapeutics **10:** 883-891

Spielman M, Preuss D, Li FL, Browne WE, Scott RJ, Dickinson HG (1997) TETRASPORE is required for male meiotic cytokinesis in *Arabidopsis thaliana*. Development **124:** 2645-2657

Sprunck S, Rademacher S, Vogler F, Gheyselinck J, Grossniklaus U, Dresselhaus T (2012) Egg cell–secreted EC1 triggers sperm cell activation during double fertilization. Science **338:** 1093-1097

Srivastava V, Weber JR, Malm E, Fouke BW, Bulone V (2016) Proteomic analysis of a poplar cell suspension culture suggests a major role of protein S-acylation in diverse cellular processes. Frontiers in Plant Science **7**

Stacey NJ, Kuromori T, Azumi Y, Roberts G, Breuer C, Wada T, Maxwell A, Roberts

K, Sugimoto-Shirasu K (2006) Arabidopsis SPO11-2 functions with SPO11-1 in meiotic recombination. The Plant Journal **48:** 206-216

Stokes ME, Chattopadhyay A, Wilkins O, Nambara E, Campbell MM (2013) Interplay between sucrose and folate modulates auxin signaling in Arabidopsis. Plant Physiology **162:** 1552-1565

Sun J, Niu QW, Tarkowski P, Zheng B, Tarkowska D, Sandberg G, Chua NH, Zuo J (2003) The Arabidopsis *AtIPT8/PGA22* gene encodes an isopentenyl transferase that is involved in de novo cytokinin biosynthesis. Plant Physiology **131:** 167-176

Swarthout JT, Lobo S, Farh L, Croke MR, Greentree WK, Deschenes RJ, Linder ME (2005) DHHC9 and GCP16 constitute a human protein fatty acyltransferase with specificity for H-and N-Ras. Journal of Biological Chemistry **280:** 31141-31148

Swarup R, Parry G, Graham N, Allen T, Bennett M (2002) Auxin cross-talk: integration of signalling pathways to control plant development. Auxin Molecular Biology. Springer, pp 411-426

Sweere U, Eichenberg K, Lohrmann J, Mira-Rodado V, Bäurle I, Kudla J, Nagy F, Schäfer E, Harter K (2001) Interaction of the response regulator ARR4 with phytochrome B in modulating red light signaling. Science **294:** 1108-1111

Symons GM, Reid JB (2003) Hormone levels and response during de-etiolation in pea. Planta **216:** 422-431

Symons GM, Schultz L, Kerckhoffs LHJ, Davies NW, Gregory D, Reid JB (2002) Uncoupling brassinosteroid levels and de-etiolation in pea. Physiologia Plantarum **115:** 311-319

Szekeres M, Németh K, Koncz-Kálmán Z, Mathur J, Kauschmann A, Altmann T, Rédei GP, Nagy F, Schell J, Koncz C (1996) Brassinosteroids rescue the deficiency of CYP90, a cytochrome P450, controlling cell elongation and de-etiolation in Arabidopsis. Cell **85:** 171-182

Takemoto-Kimura S, Ageta-Ishihara N, Nonaka M, Adachi-Morishima A, Mano T, Okamura M, Fujii H, Fuse T, Hoshino M, Suzuki S (2007) Regulation of dendritogenesis via a lipid-raft-associated Ca^{2+}/calmodulin-dependent protein kinase CLICK-III/CaMKIγ. Neuron **54:** 755-770

Termini CM, Cotter ML, Marjon KD, Buranda T, Lidke KA, Gillette JM (2014) The membrane scaffold CD82 regulates cell adhesion by altering α4 integrin stability and molecular density. Molecular Biology of the Cell **25:** 1560-1573

Thaa B, Levental I, Herrmann A, Veit M (2011) Intrinsic membrane association of the cytoplasmic tail of influenza virus M2 protein and lateral membrane sorting regulated by cholesterol binding and palmitoylation. Biochemical Journal **437:** 389-397

Thazar-Poulot N, Miquel M, Fobis-Loisy I, Gaude T (2015) Peroxisome extensions deliver the Arabidopsis SDP1 lipase to oil bodies. Proceedings of the National Academy of Sciences **112:** 4158-4163

Theodoulou FL, Eastmond PJ (2012) Seed storage oil catabolism: a story of give and take. Current Opinion in Plant Biology **15:** 322-328

Tian L, McClafferty H, Jeffries O, Shipston MJ (2010) Multiple palmitoyltransferases

are required for palmitoylation-dependent regulation of large conductance calcium-and voltage-activated potassium channels. Journal of Biological Chemistry **285:** 23954-23962

Tien T, Gaskins M, Hubbell D (1979) Plant growth substances produced by *Azospirillum brasilense* and their effect on the growth of pearl millet (P*ennisetum americanum L.*). Applied and Environmental Microbiology **37:** 1016-1024

Tomatis VM, Trenchi A, Gomez GA, Daniotti JL (2010) Acyl-protein thioesterase 2 catalizes the deacylation of peripheral membrane-associated GAP-43. PLoS One **5:** e15045

Topinka JR, Bredt DS (1998) N-terminal palmitoylation of PSD-95 regulates association with cell membranes and interaction with K^+ channel K v 1.4. Neuron **20:** 125-134

Toyoda T, Sugimoto H, Yamashita S (1999) Sequence, expression in *Escherichia coli*, and characterization of lysophospholipase II. Biochimica et Biophysica Acta (BBA)-Molecular and Cell Biology of Lipids **1437:** 182-193

Tran LSP, Urao T, Qin F, Maruyama K, Kakimoto T, Shinozaki K, Yamaguchi-Shinozaki K (2007) Functional analysis of AHK1/ATHK1 and cytokinin receptor histidine kinases in response to abscisic acid, drought, and salt stress in Arabidopsis. Proceedings of the National Academy of Sciences **104:** 20623-20628

Tsutsumi R, Fukata Y, Noritake J, Iwanaga T, Perez F, Fukata M (2009) Identification of G protein α subunit-palmitoylating enzyme. Molecular and Cellular Biology **29:** 435-447

Turner SR, Somerville CR (1997) Collapsed xylem phenotype of Arabidopsis identifies mutants deficient in cellulose deposition in the secondary cell wall. The Plant Cell **9:** 689-701

Ueda T, Yamaguchi M, Uchimiya H, Nakano A (2001) Ara6, a plant-unique novel type Rab GTPase, functions in the endocytic pathway of *Arabidopsis thaliana*. The EMBO Journal **20:** 4730-4741

Ueguchi C, Sato S, Kato T, Tabata S (2001) The *AHK4* gene involved in the cytokinin-signaling pathway as a direct receptor molecule in *Arabidopsis thaliana*. Plant and Cell Physiology **42**: 751-755

Ülker B, Shahid Mukhtar M, Somssich I (2007) The WRKY70 transcription factor of Arabidopsis influences both the plant senescence and defense signaling pathways. Planta **226:** 125-137

Valdez-Taubas J, Pelham H (2005) Swf1-dependent palmitoylation of the SNARE Tlg1 prevents its ubiquitination and degradation. The EMBO Journal **24:** 2524-2532

Van Wees S, Glazebrook J (2003) Loss of non-host resistance of Arabidopsis NahG to *Pseudomonas syringae pv. phaseolicola* is due to degradation products of salicylic acid. The Plant Journal **33:** 733-742

Vandenbussche F, Habricot Y, Condiff AS, Maldiney R, Straeten DVD, Ahmad M (2007) HY5 is a point of convergence between cryptochrome and cytokinin signalling pathways in *Arabidopsis thaliana*. The Plant Journal **49:** 428-441

Veach YK, Martin RC, Mok DW, Malbeck J, Vankova R, Mok MC (2003) O-

glucosylation of cis-zeatin in maize. Characterization of genes, enzymes, and endogenous cytokinins. Plant Physiology **131:** 1374-1380

Vesa J, Hellsten E, Verkruyse LA, Camp LA, Rapola J, Santavuori P, Hofmann SL, Peltonen L (1995) Mutations in the palmitoyl protein thioesterase gene causing infantile neuronal ceroid lipofuscinosis. Nature **376**:584

Vetrivel KS, Meckler X, Chen Y, Nguyen PD, Seidah NG, Vassar R, Wong PC, Fukata M, Kounnas MZ, Thinakaran G (2009) Alzheimer disease Aβ production in the absence of S-palmitoylation-dependent targeting of BACE1 to lipid rafts. Journal of Biological Chemistry **284:** 3793-3803

Vlot AC, Liu PP, Cameron RK, Park SW, Yang Y, Kumar D, Zhou F, Padukkavidana T, Gustafsson C, Pichersky E (2008) Identification of likely orthologs of tobacco salicylic acid-binding protein 2 and their role in systemic acquired resistance in *Arabidopsis thaliana*. The Plant Journal **56:** 445-456

Vriezen WH, Achard P, Harberd NP, Van Der Straeten D (2004) Ethylene-mediated enhancement of apical hook formation in etiolated *Arabidopsis thaliana* seedlings is gibberellin dependent. The Plant Journal **37:** 505-516

Wagner R, Aigner H, Pružinská A, Jänkänpää HJ, Jansson S, Funk C (2011) Fitness analyses of *Arabidopsis thaliana* mutants depleted of FtsH metalloproteases and characterization of three FtsH6 deletion mutants exposed to high light stress, senescence and chilling. New Phytologist **191:** 449-458

Wagner R, Herwig A, Azzouz N, Klenk HD (2005) Acylation-mediated membrane anchoring of avian influenza virus hemagglutinin is essential for fusion pore formation and virus infectivity. Journal of Virology 79: 6449-6458

Wan J, Roth AF, Bailey AO, Davis NG (2007) Palmitoylated proteins: purification and identification. Nature Protocols **2**: 1573-1584

Wang X, Sutton VR, Peraza-Llanes JO, Yu Z, Rosetta R, Kou Y-C, Eble TN, Patel A, Thaller C, Fang P (2007) Mutations in X-linked PORCN, a putative regulator of Wnt signaling, cause focal dermal hypoplasia. Nature Genetics **39:** 836-838

Webb Y, Hermida-Matsumoto L, Resh MD (2000) Inhibition of protein palmitoylation, raft localization, and T cell signaling by 2-bromopalmitate and polyunsaturated fatty acids. Journal of Biological Chemistry **275:** 261-270

Wedegaertner PB, Chu D, Wilson P, Levis MJ, Bourne H (1993) Palmitoylation is required for signaling functions and membrane attachment of Gq alpha and Gs alpha. Journal of Biological Chemistry **268:** 25001-25008

Wetzel J, Herrmann S, Swapna LS, Prusty D, John Peter AT, Kono M, Saini S, Nellimarla S, Wong TW, Wilcke L, Ramsay O, Cabrera A, Biller L, Heincke D, Mossman K, Spielmann T, Ungermann C, Parkinson J, Gilberger TW (2015) The role of palmitoylation for protein recruitment to the inner membrane complex of the malaria parasite. The Journal of Biologival Chemistry **290:** 1712-1728

Wildermuth MC, Dewdney J, Wu G, Ausubel FM (2001) Isochorismate synthase is required to synthesize salicylic acid for plant defence. Nature **414:** 562-565

Wolven A, Okamura H, Rosenblatt Y, Resh M (1997) Palmitoylation of p59fyn is reversible and sufficient for plasma membrane association. Molecular Biology of

the Cell **8:** 1159-1173

Woo HR, Chung KM, Park JH, Oh SA, Ahn T, Hong SH, Jang SK, Nam HG (2001) ORE9, an F-box protein that regulates leaf senescence in Arabidopsis. The Plant Cell **13:** 1779-1790

Woodward AW, Bartel B (2005) Auxin: regulation, action, and interaction. Annals of Botany **95:** 707-735

Wu Y, Zhang D, Chu JY, Boyle P, Wang Y, Brindle ID, De Luca V, Després C (2012) The Arabidopsis NPR1 protein is a receptor for the plant defense hormone salicylic acid. Cell reports **1:** 639-647

Xie Y, Wolff DW, Wei T, Wang B, Deng C, Kirui JK, Jiang H, Qin J, Abel PW, Tu Y (2009) Breast cancer migration and invasion depend on proteasome degradation of regulator of G-protein signaling 4. Cancer Research **69:** 5743-5751

Xu D, Li J, Gangappa SN, Hettiarachchi C, Lin F, Andersson MX, Jiang Y, Deng XW, Holm M (2014) Convergence of light and ABA signaling on the ABI5 promoter. PLoS Genetics **10:** e1004197

Xue Y, Ren J, Cao J, Liu Z (2011) Computational prediction of post-translational modification sites in proteins. INTECH Open Access Publisher

Yabuta T, Sumiki Y (1938) The crystallization of gibberellins A and B. Journal of the Agricultural Chemical Society of Japan **14:** 1526

Yamaguchi S (2008) Gibberellin metabolism and its regulation. Annual Review of Plant Biology **59:** 225-251

Yang CY, Spielman M, Coles J, Li Y, Ghelani S, Bourdon V, Brown R, Lemmon B, Scott RJ, Dickinson H (2003) *TETRASPORE* encodes a kinesin required for male meiotic cytokinesis in Arabidopsis. The Plant Journal **34:** 229-240

Yang G, Cynader MS (2011) Palmitoyl acyltransferase zD17 mediates neuronal responses in acute ischemic brain injury by regulating JNK activation in a signaling module. The Journal of Neuroscience **31:** 11980-11991

Yang W, Di Vizio D, Kirchner M, Steen H, Freeman MR (2010) Proteome scale characterization of human S-acylated proteins in lipid raft-enriched and non-raft membranes. Molecular & Cellular Proteomics **9:** 54-70

Yang W-C, Shi D-Q, Chen Y-H (2010) Female gametophyte development in flowering plants. Annual Review of Plant Biology **61:** 89-108

Yeste-Velasco M, Linder ME, Lu Y-J (2015) Protein S-palmitoylation and cancer. Biochimica et Biophysica Acta (BBA)-Reviews on Cancer **1856:** 107-120

Yi C, Deng XW (2005) COP1–from plant photomorphogenesis to mammalian tumorigenesis. Trends in Cell Biology **15:** 618-625

Yu F, Shi J, Zhou J, Gu J, Chen Q, Li J, Cheng W, Mao D, Tian L, Buchanan BB (2010) ANK6, a mitochondrial ankyrin repeat protein, is required for male-female gamete recognition in *Arabidopsis thaliana*. Proceedings of the National Academy of Sciences **107:** 22332-22337

Yuan X, Zhang S, Sun M, Liu S, Qi B, Li X (2013) Putative DHHC-cysteine-rich domain S-acyltransferase in plants. PLoS One **8**

Zdarska M, Dobisová T, Gelová Z, Pernisová M, Dabravolski S, Hejátko J (2015) Illuminating light, cytokinin, and ethylene signalling crosstalk in plant

development. Journal of Experimental Botany**:** erv261

Zeevaart J, Creelman R (1988) Metabolism and physiology of abscisic acid. Annual Review of Plant Physiology and Plant Molecular Biology **39:** 439-473

Zeidman R, Jackson CS, Magee AI (2009) Protein acyl thioesterases (Review). Molecular Membrane Biology **26:** 32-41

Zeng Q, Chen JG, Ellis BE (2011) AtMPK4 is required for male-specific meiotic cytokinesis in Arabidopsis. The Plant Journal **67:** 895-906

Zeng Q, Wang X, Running MP (2007) Dual lipid modification of Arabidopsis Gγ-subunits is required for efficient plasma membrane targeting. Plant Physiology **143:** 1119-1131

Zhang C, Shapiro A (2002) Two pathways act in an additive rather than obligatorily synergistic fashion to induce systemic acquired resistance and PR gene expression. BMC Plant Biology **2:** 9

Zhang J, Planey SL, Ceballos C, Stevens SM, Keay SK, Zacharias DA (2008) Identification of CKAP4/p63 as a major substrate of the palmitoyl acyltransferase DHHC2, a putative tumor suppressor, using a novel proteomics method. Molecular & Cellular Proteomics **7:** 1378-1388

Zhang MM, Wu P-YJ, Kelly FD, Nurse P, Hang HC (2013) Quantitative control of protein S-palmitoylation regulates meiotic entry in fission yeast. PLoS Biology **11:** e1001597

Zhang Y, He J (2015) Sugar-induced plant growth is dependent on brassinosteroids. Plant Signaling & Behavior **10:** e1082700

Zhang Y, Liu Z, Wang J, Chen Y, Bi Y, He J (2015) Brassinosteroid is required for sugar promotion of hypocotyl elongation in Arabidopsis in darkness. Planta **242:** 881-893

Zhang Y, Liu Z, Wang L, Zheng S, Xie J, Bi Y (2010) Sucrose-induced hypocotyl elongation of Arabidopsis seedlings in darkness depends on the presence of gibberellins. Journal of Plant Physiology **167:** 1130-1136

Zhao X, Yu X, Foo E, Symons GM, Lopez J, Bendehakkalu KT, Xiang J, Weller JL, Liu X, Reid JB (2007) A study of gibberellin homeostasis and cryptochrome-mediated blue light inhibition of hypocotyl elongation. Plant Physiology **145:** 106-118

Zhao XY, Wang JG, Song SJ, Wang Q, Kang H, Zhang Y, Li S (2016) Precocious leaf senescence by functional loss of PROTEIN S-ACYL TRANSFERASE14 involves the NPR1-dependent salicylic acid signaling. Scientific reports **6**

Zhou B, Liu L, Reddivari M, Zhang XA (2004) The palmitoylation of metastasis suppressor KAI1/CD82 is important for its motility-and invasiveness-inhibitory activity. Cancer Research **64:** 7455-7463

Zhou F, Xue Y, Yao X, Xu Y (2006) CSS-Palm: palmitoylation site prediction with a clustering and scoring strategy (CSS). Bioinformatics **22:** 894-896

Zhou LZ, Li S, Feng QN, Zhang YL, Zhao X, Zeng YL, Wang H, Jiang L, Zhang Y (2013) PROTEIN S-ACYL TRANSFERASE10 is critical for development and salt tolerance in Arabidopsis. The Plant Cell **25:** 1093-1107

Zhou S, Wang Y, Li W, Zhao Z, Ren Y, Wang Y, Gu S, Lin Q, Wang D, Jiang L (2011)

POLLEN SEMI-STERILITY1 encodes a kinesin-1–like protein important for male meiosis, anther dehiscence, and fertility in rice. The Plant Cell **23**: 111-129

Zolman BK, Martinez N, Millius A, Adham AR, Bartel B (2008) Identification and characterization of Arabidopsis indole-3-butyric acid response mutants defective in novel peroxisomal enzymes. Genetics **180:** 237-251

Zolman BK, Silva ID, Bartel B (2001) The Arabidopsis *pxa1* mutant is defective in an ATP-binding cassette transporter-like protein required for peroxisomal fatty acid β-oxidation. Plant Physiology **127:** 1266-1278

Zurcher T, Luo G, Palese P (1994) Mutations at palmitylation sites of the influenza virus hemagglutinin affect virus formation. Journal of Virology **68**: 5748-5754

Appendix

A. Supplemental tables

Table S1. Primers used for RT-PCR and cloning

Primers	Sequences (5'-3')
GAPc-F	CACTTGAAGGGTGGTGCCAAG
GAPc-R	CCTGTTGTCGCCAACGAAGTC
PAT21RT-F	ATGGCGAGAAGACATGGATG
PAT21RT-R	GTAGGAGCTGAGTTTAGGGGG
attB1	GGGGACAAGTTTGTACAAAAAAGCAGGCT
attB2	GGGGACCACTTTGTACAAGAAAGCTGGGT
PAT14Beg	CAAAAAAGCAGGCTCCACCATGCATAGATCTGGTACAAC
PAT14EndNS	CAAGAAAGCTGGGTCCTGGGAATCAAAGTCG
PAT14DHHC-SFor	GATGGATCACCATTCTGTTTGGGTTGTTAAC
PAT14DHHC-SRev	GTTAACAACCCAAACAGAATGGTGATCCATC
PAT21Beg	CAAAAAAGCAGGCTCCACCATGGCGAGAAGACATGGATG
PAT21EndNS	CAAGAAAGCTGGGTCATGGAATCTAGTAGATAAATG
PAT21DHHC-SFor	GGTTTGATCACCATTCCCGGTGGCTGAATAAC
PAT21DHHC-SRev	GTTATTCAGCCACCGGAATGGTGATCAAACC
Ppat21attB1	CAAAAAAGCAGGCTCCACCTTTCTTCTTCTCTCTCTCAAAAGTTGACC
pPAT21attB2	CAAGAAAGCTGGGTCCATTGCAATGAAGAAACCCACAA

Table S2. Primers used for quantitative real-time PCR

Primers	Sequences (5'-3')
qEF-1α F	TGAGCACGCTCTTCTTGCTTTCA
qEF-1α R	GGTGGTGGCATCCATCTTGTTACA
qICLF	TATTGTTGGCAGTTCATA
qICLR	GTATCCTCTCCACATAAG
qMLSF	ATACTTAGCCGCATGGTTA
qMLSR	CTTATCTCAGCCGTAGCA
qKAT2F	CTTCTCTATCTGCTTCTG
qKAT2R	GACAACATCATCTCCATA
qPCK1F	TAACGGAAATGCTACTAACG
qPCK1R	TACCTCTCTTTGCTGCTC
AHK3F	TCCTCCAATAGTGATAGT
AHK3R	GGTTCTCTGATTCCAATA
CRE1F	GCAGATACGGTAATAATG
CRE1R	GGATGTTGTTGTCTTGTT
GA20ox1F	GAAGGTGTATCAAGAGTAT
GA20ox1R	GGTAGTAATTCAGTCTCAT
GA3ox1F	GGTTATCTGTAGCATTCC
GA3ox1R	GTATAGAGGCGATTCAAC
GA2ox1F	AGAAACGCATTGGAAGAG
GA2ox1R	GGTGGATAGTGATTAAGTCT

Table S3. Primers used for gentyping T-NDA insertion lines

Primers	Sequences (5'-3')
LBb1	GCGTGGACCGCTTGCTGCAACT
SALK016521LP	TGGGCCATATATTAGACACGG
SALK016521RP	GCTTGCAGGTGAAGGATACTG

B. Supplemental figures

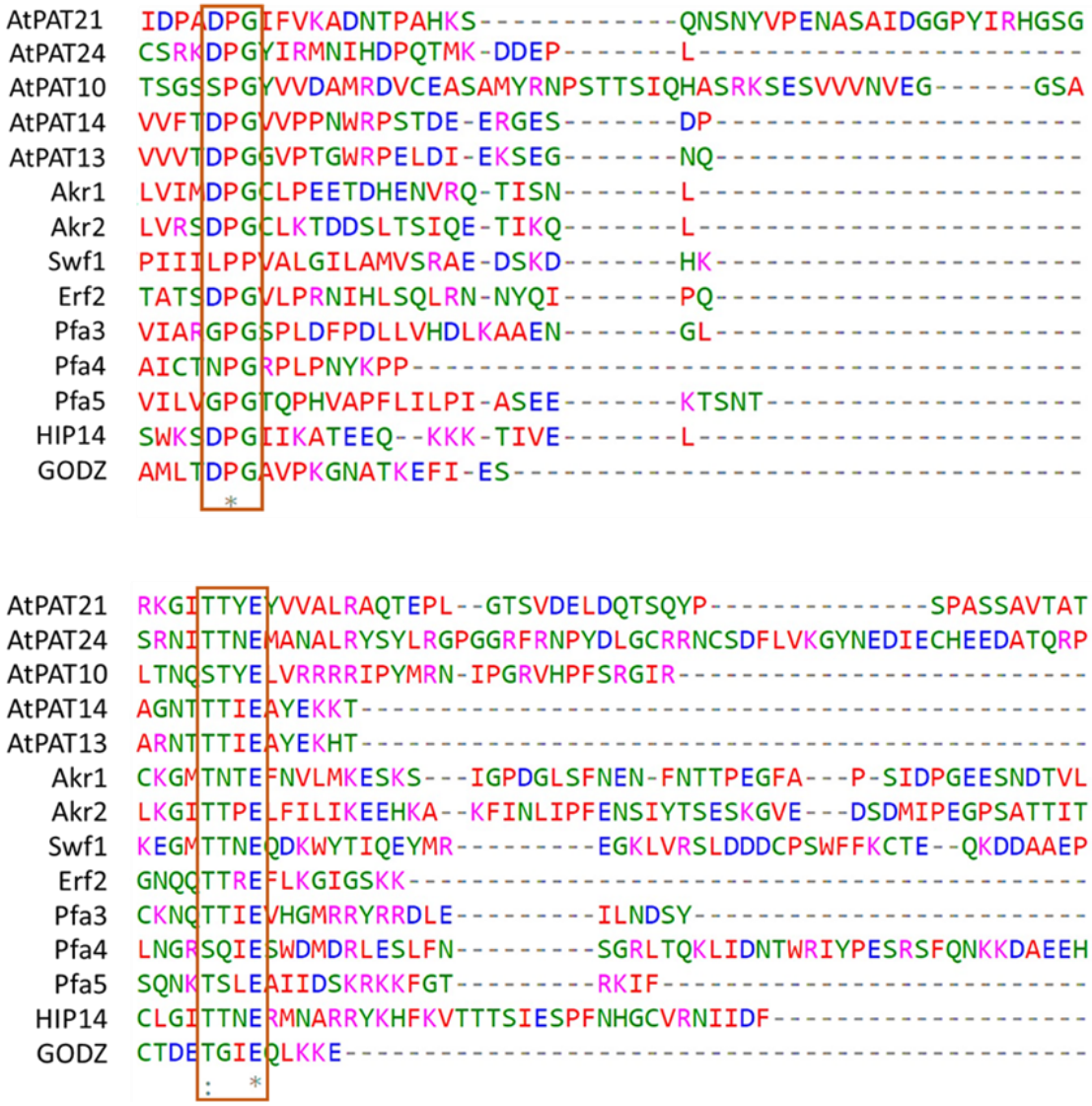

Figure S1. Conserved DPG and TTxE domains in AtPAT21. The conserved domains are boxed.